The Dissertation Committee for Daniel James Strohecker Certifies that this is the approved version of the following dissertation:

Novel *bis*(pyrazol-1-yl)pyridine Derivatives and Lanthanide(III) Complexes for Emissive Materials

Committee:

Richard A. Jones, Supervisor

Eric V. Anslyn

John G. Ekerdt

Jonathan L. Sessler

Emily L. Que

Novel *bis*-(pyrazol-1-yl)pyridine Derivatives and Lanthanide(III) Complexes for Emissive Materials

by

Daniel James Strohecker, B.S.

Dissertation

Presented to the Faculty of the Graduate School of

The University of Texas at Austin

in Partial Fulfillment

of the Requirements

for the Degree of

Doctor of Philosophy

The University of Texas at Austin

May 2017

Dedication

I dedicate this work to my father John, my mother Rae Ann, my step-mother Carmen, my brothers Sam and Mike, and all of my family and friends who have freely given their love and support while I worked towards this goal. Your encouragement assured me that I actually could do this. Your love gave me the incentive to get back to what really matters; I can't wait.

Acknowledgements

I would foremost like to thank my advisor, Rich Jones, for broadening my imagination with regard to the possibilities of the work I was pursuing, for encouraging me to put words on bits of paper, and always approaching these works with the fresh, healthy curiosity that I've come to know as the mark of a true scientist. I would also like to thank my previous advisor, Brad Holliday, for providing me with a rigorous research challenge to grow with and teaching me to never stop questioning myself.

I am very thankful for the great amount of help from Leander Cinninger and Dr. Vince Lynch in acquiring and processing the single-crystal X-ray crystallography data in this work. I would also like to thank Ty Davis for his creative and synthetic efforts towards the imine and amide oligomers described in Chapter 4 of this work. I would like to thank Dr. Alisha Bohnsack and Tyler King for synthesizing the materials that are the subject of the photophysical studies in Chapter 5.

I am also very grateful for the input of my peers, both past and present, including Dr. Minh Nguyen, Dr. Kory Mueller, Yawei Liang, Claudina Camack, and Ty Davis, which has proven fruitful many times over.

Novel *bis*-(pyrazol-1-yl)pyridine Derivatives and Lanthanide(III) Complexes for Emissive Materials

Daniel James Strohecker, Ph.D.

The University of Texas at Austin, 2017

Supervisor: Richard A. Jones

The electromagnetic emissions of the lanthanide series have served as inspiration for intense research in numerous fields, including emissive materials for lighting, displays, bioimaging, biomarkers, photodynamic cancer therapy, and laser material purposes. 2,6-bis(pyrazol-1-yl)pyridine (bppy) has been shown to effectively sensitize lanthanide emission, particularly when incorporated into a complex with europium tris(2-thenoyltrifluoroacetonate) ($Eu(tta)_3$). However, the majority of synthetic modification of this complex involves functionalization of the 4- position of the pyridine ring, or catalytic coupling of bppy species bearing halogen substituents at the 4- positions of the pyrazole rings.

The unifying focus of this work is the development of novel syntheses to functionalize bppy at the 4- positions of the bppy pyrazole rings with functional groups other than halogen coupling products, such as nitro groups, amines, amides, imines, azides, azo- compounds, thiols, sulfides and sulfonate derivatives. The driving force of the synthesis of these novel functionalized ligands is the adaptation of the highly-luminescent $Eu(tta)_3$bppy complex for a variety of specific applications.

Targeted synthesis of diarylamido-bppy derivatives was performed as an investigation into the development of a conjugation-interrupted metallopolymer for efficient emissive layers in OLED devices with the goal of preserving efficient Eu(III) ion sensitization while incorporating 3,4-ethylenedioxythiophene (EDOT) substituents which are readily electropolymerized. These new ligands and associated complexes were investigated by analytical techniques such as cyclic voltammetry, UV-vis absorption spectroscopy and spectrofluorimetry to quantitatively characterize the electronic energies which are vital to the light emission process from lanthanide ions. Analysis of these data gave insight into properties such as quantum yield, polymerization, and triplet-state energies to qualitatively assess emissive material performance.

Additionally, synthetic routes to imino-, azo-, azido-, triazolyl-, mercapto-, sulfido- and sulfonic acid-bppy derivatives were pursued as means to broaden the scope of applications of this ligand system.

Finally, the structural and spectroscopic properties of several novel lanthanide(III) species are reported and discussed.

Ultimate conclusions, outlooks and further directions of each of these studies are also disclosed herein.

Table of Contents

List of Tables

List of Figures

List of Schemes

Chapter 1: Introduction

2,6-BIS(PYRAZOL-1-YL)PYRIDINE LIGANDS

Origin and Ligand Characteristics

The 2,6-*bis*(pyrazol-1-yl)pyridine (bppy) ligand was first reported by Jameson *et al.* in 1989 detailing the electronic properties of the $[Ru(bppy)_2]Cl_2$ complex.[1] The authors examined this complex using a combination of absorbance spectroscopy and cyclic voltammetry monitoring the Ru^{II}/Ru^{III} redox couple to infer characteristics of this ligand, which were then compared to those of the well-known 2,6-*bis*(2-pyridyl)pyridine (terpy) tridentate nitrogen-donor ligand (Figure 1.1).

The authors found that bppy is a weaker σ-donor than terpy, owing to the lesser basicity of the binding pyrazole N atoms with regard to the pyridine N atoms that participate in bonding in terpy. Bppy is a weaker π-acceptor than terpy as well on account of a greater π^* energy of the aromatic system. Overall, these two phenomena result in lessened ligand binding strength. It was also shown that substituting methyl groups on the 3- and 5-positions of one (Me_2-bppy) or both (Me_4-bppy) resulted in consistent decreases in the Ru^{II}/Ru^{III} redox couple potential apparent in the analogous Ru complexes. This

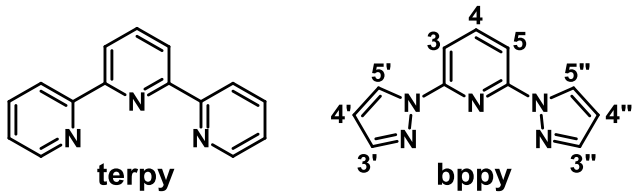

Figure 1.1: Depiction of tridentate N-donor ligands terpy and bppy.

indicates that facile control of ligand binding strength and metal center oxidation state can be achieved through synthetic modification of the ligand. This variation in electronic behavior in a ligand that is otherwise structurally similar to terpy, along with the ease with which bppy may be derivatized on the 4-position of pyridine, as well as the 3- and 5-positions of the pyrazole rings, has lent to the increasing popularity of bppy as a complementary platform for research into new *d*- and *f*-block metal complexes.

Synthesis and Derivatization

The methodology of the first-reported synthetic route to bppy-type ligands is still the synthetic path most followed (Figure 1.2.a);[1–3] this entails the substitution of a 2,6-dihalopyridine with the desired pyrazolate nucleophile (usually the Na^+ or K^+ derivative). This nucleophilic aromatic substitution synthesis may be performed in one step using one nucleophilic species for symmetrically-substituted ligands, but the slow second addition of pyrazole substituent makes the mono-pyrazol-1-yl-halo-pyridine readily isolable. Subsequent reaction of the mono-substituted intermediate with a different pyrazolate easily affords an asymmetrically-substituted species.[2,3]

Nucleophilic substitution of the dihalopyridine with pyrazoles containing substituents at the 3-position results in a mixture of 3',3"-, 3',5"- and 5',5"-disubstituted bppy regioisomers. In these cases, it has been observed that the majority product is the 3',3"-substituted bppy, which is to be expected since it minimizes steric hindrance between the two reactants during the substitution.[2,4–6]

As this nucleophilic synthesis calls for rather demanding conditions, owing to the "sluggish" nature of the second halogen displacement, made more difficult by the first displacement, there has been some interest in catalyzing this reaction to increase reaction rate and product yields, though only to modest effect.[2,7,8]

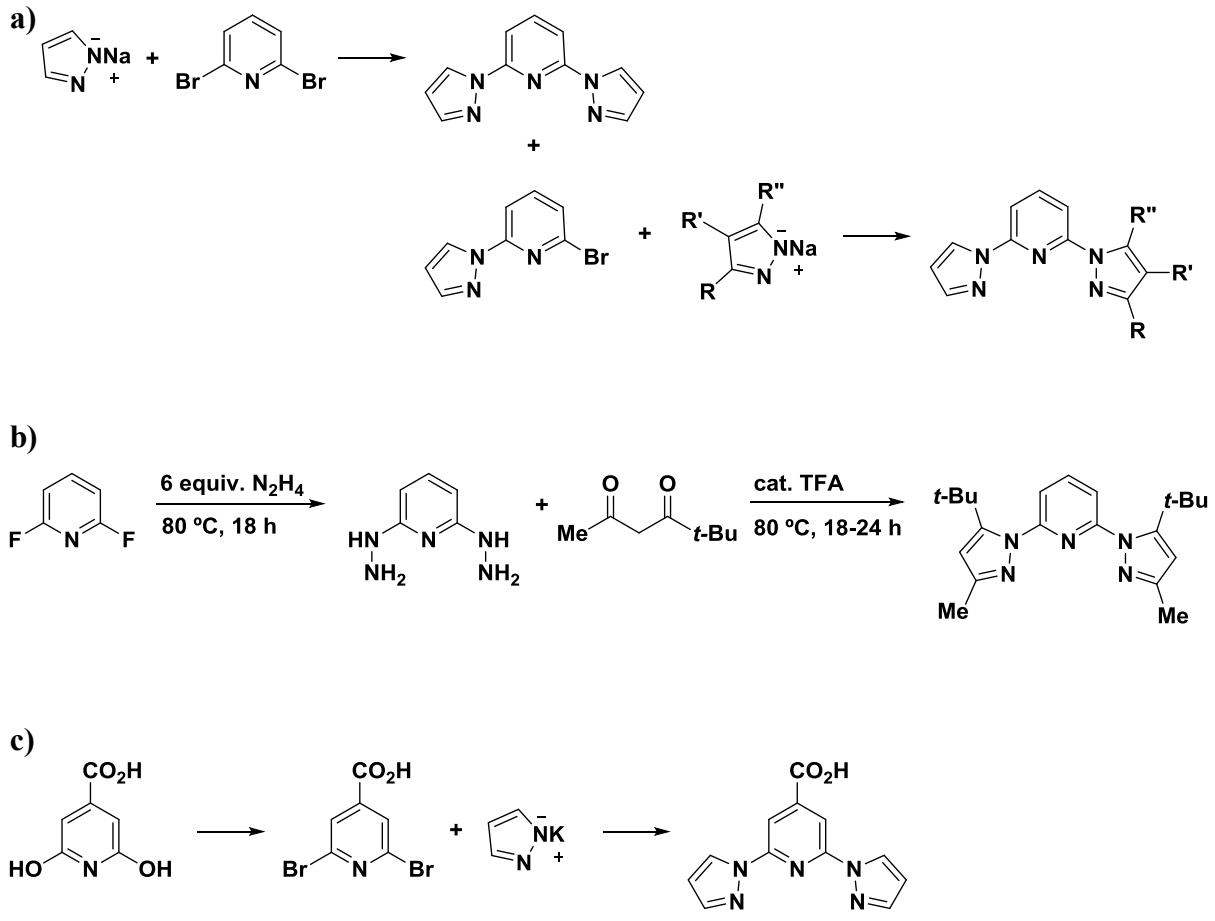

Figure 1.2: Synthetic routes for the formation of bppy derivatives. a) Commonplace nucleophilic substitution of 2,6-dihalopyridine to generate symmetric and asymmetric bppy derivatives. b) Condensation of *β*-diketones with BHP to form sterically-hindered 5',5"-regioisomers of bppy. c) Synthesis of 4-carboxylic acid derivatized bppy from citrazinic acid.

The preference for less-hindered substitution products can be reversed, however, if the ligand is synthesized via condensation reactions between 2,6-bis-hydrazinopyridine (BHP) and *β*-diketone derivatives.[4] Garner *et al.* reported such a synthesis (Figure 1.2.b) and found that upon condensation between BHP and 2,2-dimethyl-3,5-hexanedione, the positioning of the *t*-butyl substituents in the 5', 5"-pattern was preferable over the 5', 3"-regioisomer with a ratio of 98:2. The 3', 3"-substituted species was present in negligible

quantities. These findings are rationalized by the favorability of an initial reaction of the $–NH_2$ group with the less-hindered carbonyl of the dione, followed by cyclization of the pyrazole ring.

The same group uncovered interesting results in condensation reactions between BHP and 1,3-diaryl-1,3-diketones substituted with an electron-donating group on one aryl ring and an electron-withdrawing group on the other aryl ring, with all steric environments equal; the resulting product mixture indicates placement of the electron-withdrawing aryl substituents at the 3-position of the resulting pyrazole rings and the electron-donating aryl substituents at the 5-position.[9] This is proposed to be result of the increased electrophilicity of the carbonyl adjacent to the electron-withdrawing aryl ring, which favors condensation between the carbonyl and the $–NH_2$ group first.

A third synthetic route that has been described is a slightly longer synthesis beginning with citrazinic acid, but has the advantage of utilizing an inexpensive chemical feedstock and, more importantly, installs a synthetic handle in the form of a carboxylic acid on the 4-position of the pyridine ring (Figure 1.2.c).[10] It is worth noting that the nucleophilic substitution with the pyrazolate is tolerant of the pyridine 4-carboxylic acid.

Multiple groups have taken advantage of the synthetic utility of the carboxylic acid on the 4-position of the pyridine ring to create a plethora of bppy ligands appended with a wide range of functional groups, including but not limited to esters, alcohols, amines, halogens, alkanes, alkynes, arenes, tetrahydropyrans, tethered bppy ligands to form 4-4 dimers, and nucleic acids (Figure 1.3).[10–12] Chandrasekar *et al.* combined this citrazinic acid synthesis with regioselective halogenation methodologies to develop pathways to brominate and/or iodinate on every C atom of bppy. These methodologies are also compatible with that are aminated on C4 to give amines that are also halogenated

on C3', C5', C3, C5, C3" and C5", creating symmetric and asymmetric bppy derivatives that are truly remarkable in their synthetic versatility.[13]

Other common sites of derivatization of these ligands are the pyrazole 3- and 5-positions. Normally, these functionalizations occur by simply performing the nucleophilic substitution with the appropriate 3,5-substituted commercially-available pyrazole, though exceptionally bulky and/or electron-deficient pyrazolates react poorly

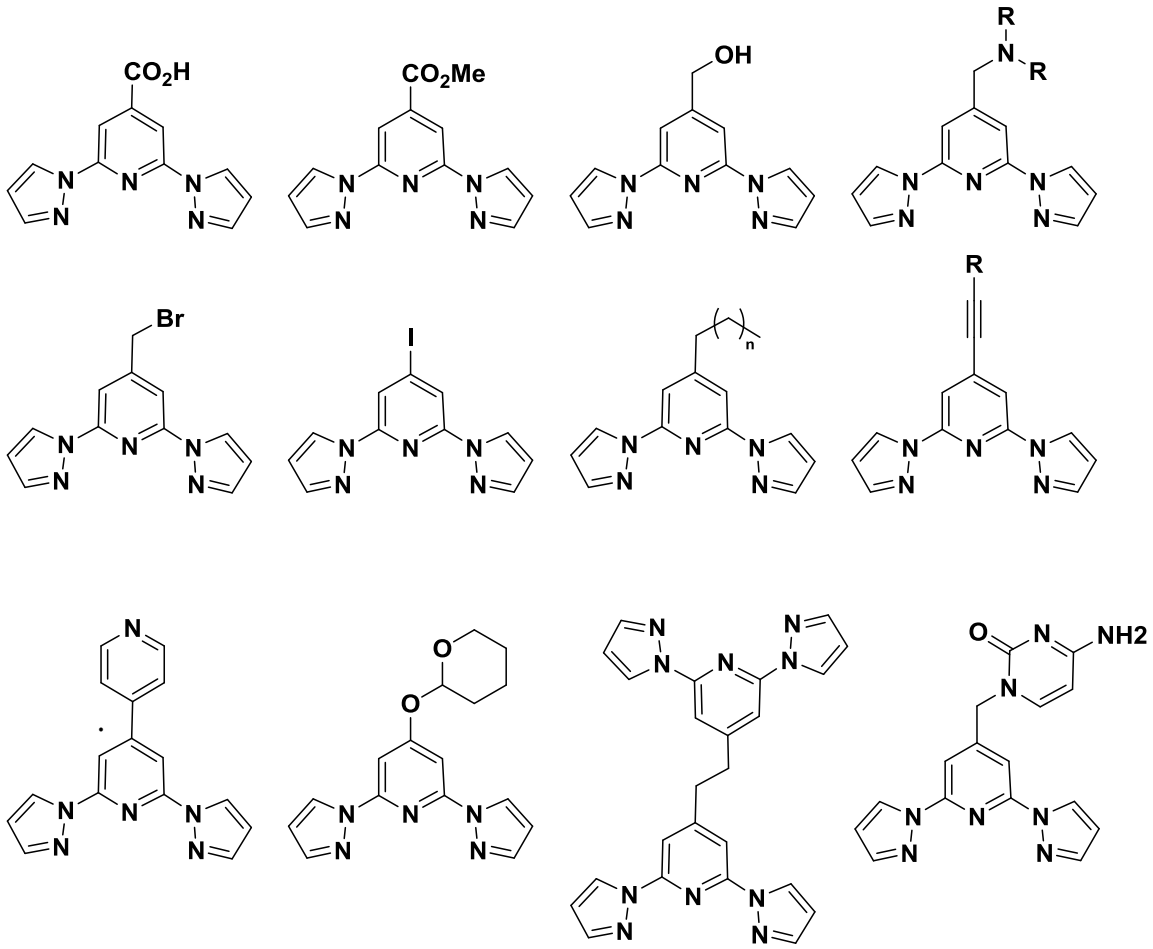

Figure 1.3: Some representative derivatives of bppy substituted at the pyridine 4-position via syntheses utilizing citrazinic acid starting materials. All structures are reported in references 8 – 10.

with this method.[2,3,9,14,15] With the advent of bppy synthesis using BHP (Figure 1.2.b), creating ligands functionalized on the pyrazole C-atoms adjacent to the N-atoms is as simple as condensing the bis-hydrazine with the appropriate β-diketone.

As Zoppellaro and Baumgarten observed in 2005, bppy derivatives substituted on the 4-position of the pyrazole ring are relatively rare, owing to unwieldy synthetic routes involving non-selective lithiations coupled with protection/deprotection steps.[16,17] They subsequently developed methods to generate selectively halogenated bppy at the 4-positions (X = Br, I), which have proved to be versatile synthons. As a result of this work, a modest number of carbon-coupling reaction products, including a variety of conjugated copolymers, of these compounds have been reported, in addition to carbonyl-containing ligands stemming from either the formylation of said bis(4-halopyrazol-1-yl)pyridines or nucleophilic substitution of 2,6-dibromopyridine with ethyl pyrazole-4-carboxylate (Figure 1.4).[18–20,13,21–24,16,25]

Apart from the aforementioned types of compounds, Chapter 2 of this dissertation describes the synthesis of bppy ligands that are mono-and di-substituted with nitro- and amino- groups,[26] which have then been subsequently used to synthesize secondary and tertiary bis-4',4"-diaryl-bppy ligands (Chapter 3) along with dimeric and oligomeric bppy units linked by *bis*-imines at the 4-position of the pyrazoles (Chapter 4). Chapter 4 also describes the synthesis of azo, azido, and triazolylbppy derivatives appended at the 4' positions as well as attempts to functionalize this position with thiols, sulfides and sulfonates.

This outline meant to provide a sampling of the functional possibilities enabled by the synthetic routes outlined in Figure 1.2. For more thorough reviews which encompass the synthetic endeavors of groups pursuing novel bppy derivatives, the reader is directed to the works of Halcrow.[3,27,28]

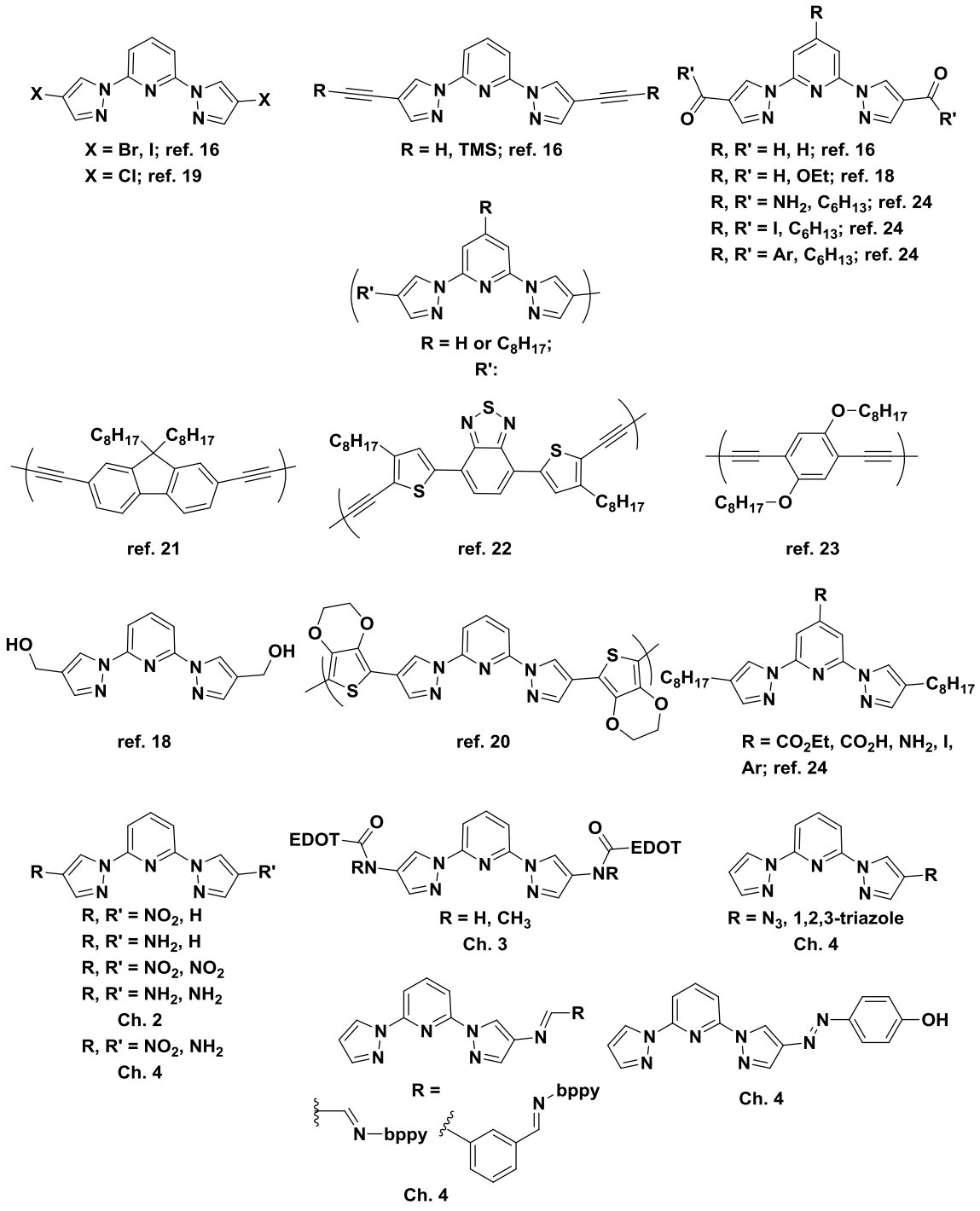

Figure 1.4: Some representative derivatives of bppy substituted at the pyrazole 4-positions.

Applications and Examples of Bppy in Literature

Catalysis

Although catalytic synthesis of bppy has met with limited success, reports of metal complexes that *utilize* bppy derivatives as a ligand in catalytic reactions have been steadily increasing, especially over the past decade. A survey of the literature shows the seminal report of a catalyst involving bppy demonstrating a variety of $[Ru(bppy)(bpy)OH_2]^{2+}$ catalysts for the successful oxidation of a variety of olefins, albeit with only modest selectivity for carbonyl products over epoxides or alcohols.[29] Catalysts which employ bppy-type ligands have since been developed for a variety of reactions.

For example, olefin polymerization catalysts have been pursued that utilize bppy ligands and Fe(III), Fe(II), Co(II), Ni(II), and Cr(III) metal centers combined with methylaluminoxane (MAO) and modified methylaluminoxane (MMAO) cocatalysts.[30–33] All of these studies indicate that catalytic activity and trans-selectivity decreases with alkylation of the pyrazole rings, likely due to steric restriction of the metal coordination site.

These ligands have also been used in Ni-catalyzed cross-coupling and aldoxime dehydrations with great success, featuring high yields and tolerance of broad scope of substrates.[34–38]

Additionally, an even broader scope of reactions such as ring-opening polymerization, transfer hydrogenation, borylation, and cycloadditions can be performed using bppy or one of the alkylated derivatives thereof.[39–44]

Spin-crossover Materials

Arguably the area of research which utilizes bppy the most is that of spin-crossover (SCO) materials. Spin-crossover was first explicitly reported in

$Fe(phen)_2(NCX)_2$ (X = S, Se)[45] and has since been heavily investigated for the intriguing switching behavior in color and magnetic properties they exhibit. Bppy and bis(1H-pyrazol-3-yl)pyridine (3-bppy) are among the most widely-used ligands in Fe SCO systems, and reviews have been written that cover SCO developments which utilize each of them.[27,46,47] Bppy was first incorporated in a SCO material upon being reacted with $[Fe(BF_4)_2 \bullet 6H_2O$ to yield the homoleptic $Fe(bppy)_2(BF_4)_2$ complex, which exhibits an Fe(II) center coordinated in a "terpyridine embrace" motif.[48,49] It features a reversible low-to-high-spin transition centered at 260 K with a hysteresis width of 4 K.

Modulation of the steric and electronic environment of the ligands by substitution at the 3', 3", 4, 4' and 4" positions, as well as varying the complex counter-ion, have shown to drastically change properties such as SCO transition T and range, as well as magnitude of hysteresis (see Figure 1.5) [18,25,46,50–53]

Luminescent Materials

Another area of focused bppy research involves the utilization of metal complexes and metallopolymers for luminescence applications. Though bppy has been clearly demonstrated to bind numerous main-group metals, there is a surprising dearth of bppy-containing d-block luminescent materials. Although the initial $[Ru(bppy)_2]^{2+}$ reported by Jameson and Goldsby was not emissive, subsequent reports that employ mixed-ligand systems have been shown to luminesce.[1] Two heteroleptic terpy-bppy-type binding motifs were first reported, wherein one *para*-phenylene linked bppy dimer "**L**" was coordinated to one or two $[Ru(terpy)](PF_6)_2$ units to create mono- or bi-nuclear complexes, which exhibited red emission from the ^{3}MLCT at low ($T \leq 100$ K) temperatures in a 10:1 v:v ACN:DMF solvent glass (Figure 1.6).[54]

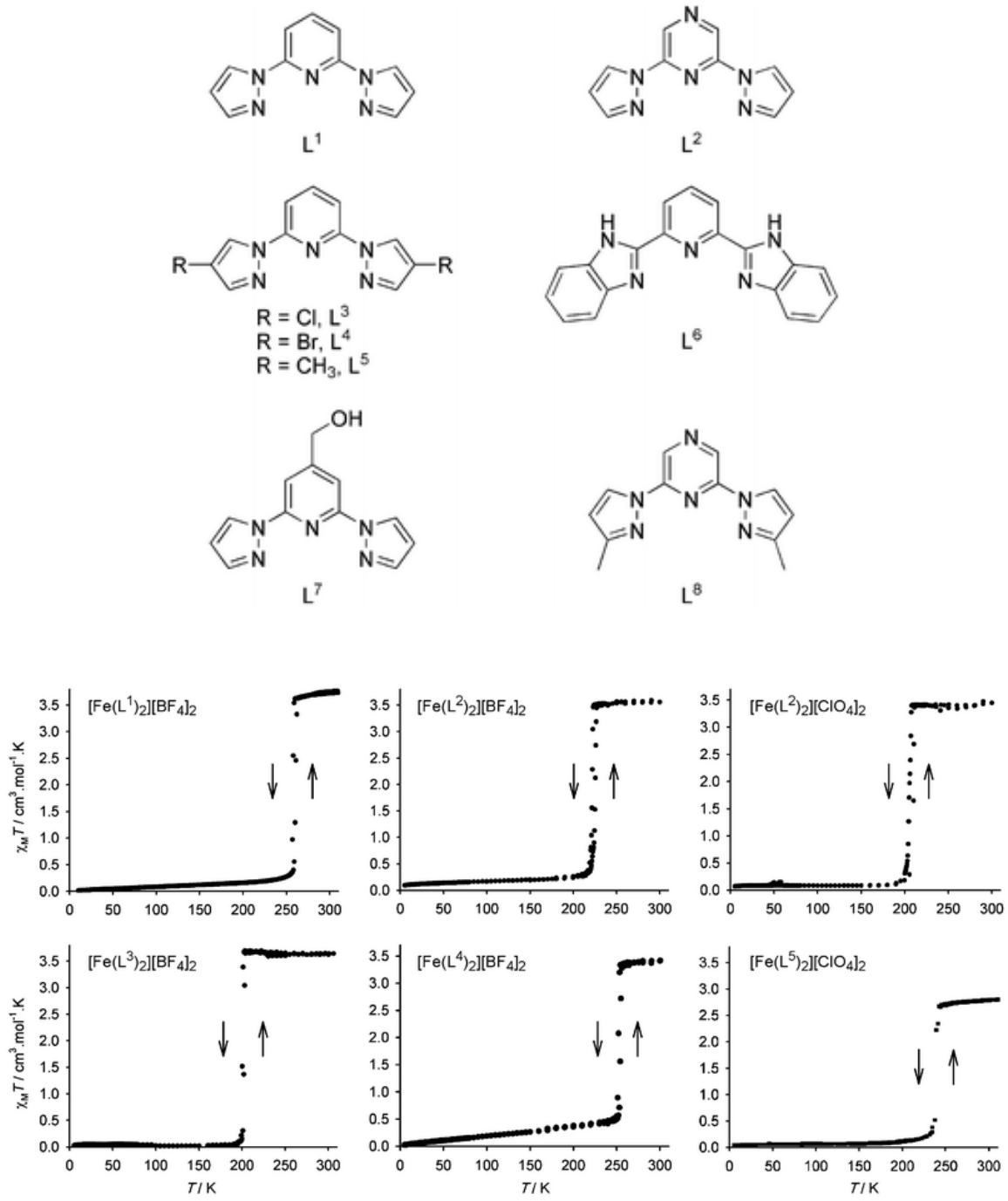

Figure 1.5: Ligands and temperature-dependent magnetic behavior of substituted $[Fe(bppy)_2]^{2+}$-type complexes. Reproduced with permission from ref. 50.

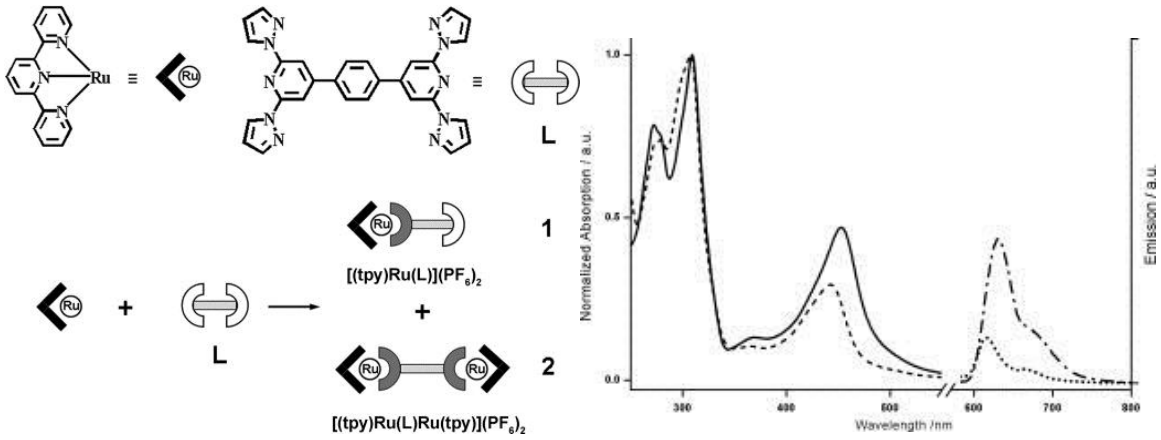

Figure 1.6: Structure (left) and spectroscopy (right) of mono- (**[tpy)Ru(L)](PF$_6$)$_2$**) and bi-nuclear(**[tpy)Ru(L)Ru(tpy)](PF$_6$)$_4$**) terpy-Ru-L complexes. Room temperature absorption spectra (**[tpy)Ru(L)](PF$_6$)$_2$** – dashed; **[tpy)Ru(L)Ru(tpy)](PF$_6$)$_4$** – solid) are on the left and 100 K emission (**[tpy)Ru(L)](PF$_6$)$_2$** – dotted; **[tpy)Ru(L)Ru(tpy)](PF$_6$)$_4$** – dash-dotted) spectra are on the right. Images adapted from reference 54.

A similar mixed-ligand [Ru(terpy)(EDOT$_2$bppy)](PF$_6$)$_2$ complex has been synthesized that also demonstrates weak luminescence at 77 K. This complex was able to be electropolymerized by oxidation of the EDOT groups to generate a metallopolymer film, which was subsequently studied by spectroelectrochemistry.[20]

Bppy and Me$_4$-bppy have been used to synthesize square planar [Pt(bppy)Cl]Cl•H$_2$O, Pt(Me$_4$-bppy)Cl]Cl•H$_2$O, [Pt(bppy)Ph](PF$_6$) and [Pt(Me$_4$-bppy)Ph](PF$_6$) complexes.[55] Of these, only [Pt(bppy)Ph](PF$_6$) displays an intense emission peak centered at 640 nm. The authors noted that weak emissions from Pt(II) and Ru(II) complexes in the literature are likely due to low-lying triplet ligand field energy levels which favor rapid non-radiative decay.

The vast majority of bppy derivatives employed in luminescent materials are incorporated into metal complexes or materials which contain luminescent lanthanide(III) (Ln(III)) ions. The unique properties of the light emitted from these ions has led to the development of Ln(III) materials for a number of different applications, which will be expanded upon in the following sections.

LANTHANIDE(III) ION LUMINESCENCE

Characteristics and Origins

The lanthanides first became industrially relevant with the development of the gas mantle by Carl Auer von Welsbach, which utilized various oxides of lanthanum, cerium and yttrium.[56] Although even as late as the 1970s it was stated that "*Lanthanum has only one important oxidation state in aqueous solution, the 3+ state. With few exceptions, this tells the whole boring story about the other 14 lanthanides,*"[57] in present day, the 4*f* elements have expanded into numerous other applications that take advantage of their unique coordinative and luminescent properties. These include catalysis,[58–65] electronic materials,[66–71] sensors and bioprobes,[64,72–80] luminescent materials,[21,22,81–90] and imaging contrast agents.[74,91–96] Much of this interest can be attributed to properties which arise from the electronic *f-f* transitions undergone by these ions.

The 4*f* orbitals where the *f-f* transitions originate are shielded from the electronic environment outside of the core by the filled outer 5*s* and 5*p* orbitals of the Ln(III). As a result, Ln(III) ions act as Lewis acids and exhibit "hard" interactions with coordinating species such as O-, N- and S-containing ligands. Additionally, the energies of these electronic transitions of these ions exhibit very little dependence on the coordination environment of the ion; each Ln(III) has its own signature emission spectrum with characteristically narrow peaks corresponding to specific transition between 4*f* orbital

energy levels (Figure 1.7).[97,98] The numerous peaks observed in a given Ln(III) spectrum arise from coulombic and spin-orbit coupling interactions between the 4*f* electrons, which break the degeneracy of the orbital energies (Figure 1.8).[99]

These unique electronic transitions are forbidden by Laporte selection rules ($\Delta J = 0, \pm 1$, but not $J = 0 \rightarrow J = 0$) and as such require the use of an "antenna" ligand to transfer energy to the excited state of the Ln(III).[98,100] Weissman first demonstrated this phenomenon, commonly known as the antenna effect, in 1942.[101] This energy transfer is in part responsible for the long (μs to ms) lifetimes (τ_{obs}) and large Stokes shifts of Ln(III) emissions, which are highly desirable in time-gated luminescence experiments. A representation of this sensitization process is shown in Figure 1.9. The predominant mechanism of this energy transfer process entails excitation of the ligand chromophore to the S_1 excited state, inter-system crossing to the ligand T_1 excited state, then energy transfer to the Ln(III) excited state followed by radiative decay.

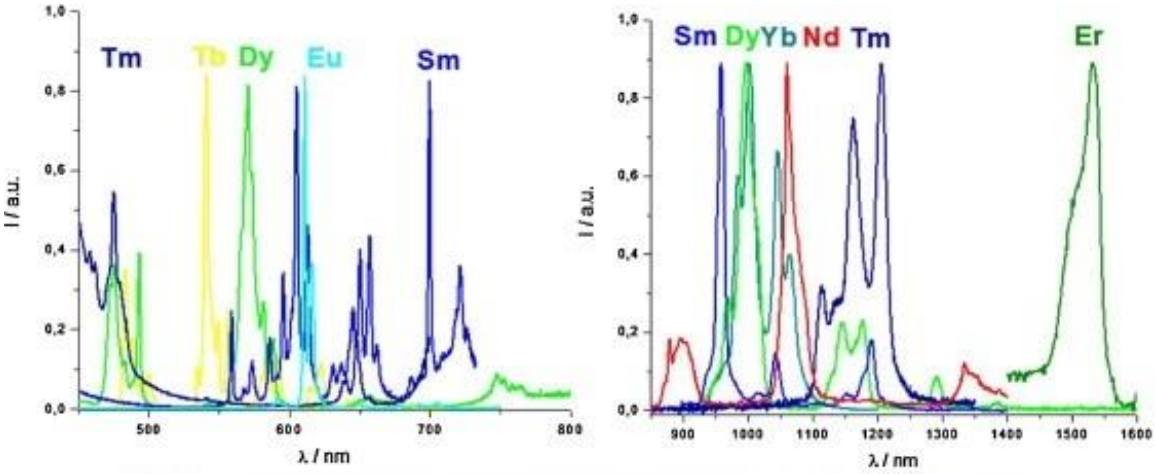

Figure 1.7: Some visible and NIR emission spectra of the lanthanides. Image adapted with from ref. 97.

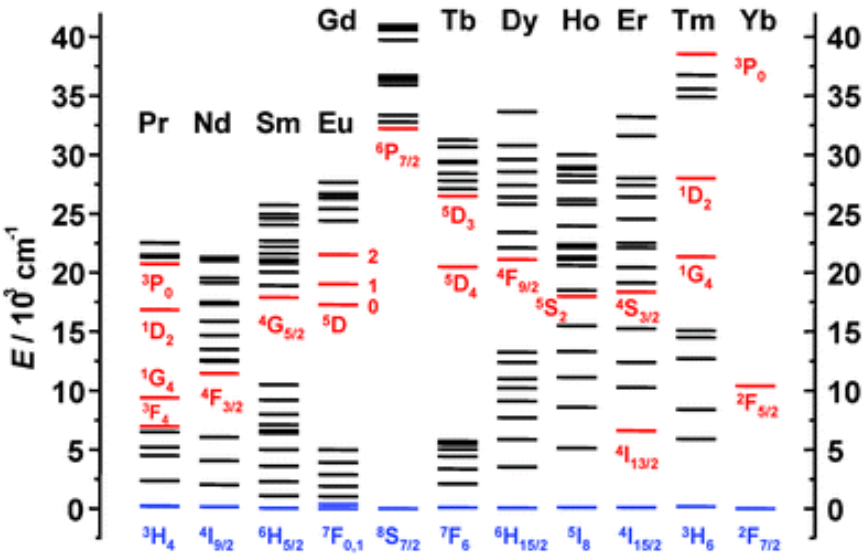

Figure 1.8: Energy diagram of luminescent lanthanide ions. Main emissive levels are in red and ground electronic states are in blue; reproduced from ref. 98.

Though the most common sensitization pathway involves energy transfer from the ligand T_1 excited state, other donor states such as the S_1 excited state and ligand- and metal-centered charge-transfer states have also been observed.[98,102–104]

As seen in Figure 1.9, there are numerous competing pathways in the Ln(III) sensitization process, so careful consideration of ligand and metal center donor and acceptor excited state energy levels must be taken into consideration in order to create a thermodynamically-favorable and efficient energy sensitization process.[102,105,106] Competing processes such as ligand luminescence and internal conversion are detrimental to sensitization and can result in lessened Ln(III) luminescence quantum yields (Φ_{Ln}^{L}).

Two of the largest detractors of Ln(III) luminescence efficiency are coupling between the excited states and vibronic oscillations of either the ligand system or the solvent molecules themselves, which results in non-radiative decay processes.[107] O–H

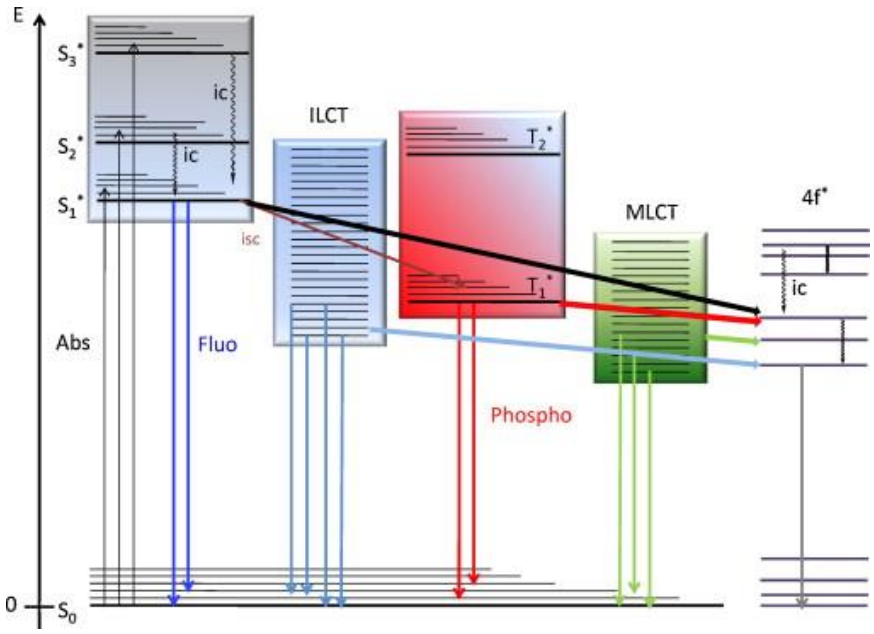

Figure 1.9: Energy diagram detailing the energy transfer process of the antenna effect. Abs: absorbance; Fluo: fluorescence; Phospho: phosphorescence; S: singlet state; ILCT: intra-ligand charge transfer; T: triplet excited state; MLCT: metal-to-ligand charge transfer; ic: internal conversion; isc: inter-system crossing; 4f*: Ln(III) excited state. Image reproduced with permission from ref. 97.

and N–H oscillators are well-known to quench Ln(III) luminescence, especially in the case of Eu(III).[105,108–110]

The number of water molecules coordinated to the inner sphere (as well as the outer sphere, but to a lesser extent) of a Ln(III), q, can be experimentally determined by observing the emissive lifetime in H_2O and D_2O solutions, and applying those values to the following equations:[111]

$$q = A(\tau_{H_2O}^{-1} - \tau_{D_2O}^{-1} - k_{XH}) \quad (1)$$

$$k_{XH} = \alpha + \beta n_{OH} + \gamma n_{NH} + \delta n_{O=CNH} \quad (2)$$

A is an empirically-determined constant with units of water molecules · ms, τ is the lifetime in H_2O or D_2O, n are the numbers of X–H oscillators in the first coordination sphere of the complex, α is a constant which accounts for second coordination sphere water molecule quenching, and the terms β, γ, and δ are contribution factors of the respective types of oscillators to excited state quenching. Luminescent lifetimes are longer in D_2O than in H_2O, owing to the lessened likelihood for non-radiative decay to occur via the energetically weaker O–D oscillators.

The luminescence quantum yield of a given complex can either be determined by direct measurement through the use of an integrating sphere that collects all light emitted by a sample to be measured by a detector capable of a photon counting mode (absolute quantum yield), or indirectly by comparing relative intensities of emissions between a solution of interest and that of a suitable reference (reference quantum yield).[81] Measurement of Φ_{Ln}^{L} in conjunction with τ_{obs} can be combined to reveal information regarding the radiative lifetime (τ_{rad}) in the absence of non-radiative processes, efficiency of the sensitization of Ln(III) (η_{sens}), and the intrinsic quantum yield, Φ_{Ln}^{Ln}, which describes the efficiency of light emission from the lanthanide. This is separate from the Φ_{Ln}^{L}, which accounts for radiative and non-radiative processes in the sensitization mechanism as well.[112] These quantities are related by equations 3 and 4:

$$\Phi_{Ln}^{Ln} = \tau_{obs}/\tau_{rad} \tag{3}$$

$$\eta_{sens} = \Phi_{Ln}^{L} / \Phi_{Ln}^{Ln} \tag{4}$$

The Φ_{Ln}^{Ln}, τ_{rad}, and η_{sens} of a species cannot be directly measured, but must be calculated using experimentally-determined Φ_{Ln}^{L} and τ_{obs} values. However, calculation of τ_{rad} is

remarkably complicated in the case of most Ln(III) ions, with the exception of Eu(III). This is because Eu(III) emissions feature one purely magnetic-dipole electronic transition, $^5D_0 \rightarrow {}^7F_1$, the intensity of which is almost totally independent of the chemical environment. This attribute allows the determination of τ_{rad} to be simplified to equation 5:

$$1/\tau_{rad} = A_{MD,0} n^3 (I_{tot}/I_{MD}) \quad (5)$$

where $A_{MD,0}$ is a constant that defines the strength of the MD transition (14.65 s^{-1}), *n* is the refractive index of the solvent, and *I* indicates the intensity of either the entire Eu(III) emission spectrum or the intensity of the MD transition, respectively. By determining Φ_{Ln}^{Ln}, τ_{rad}, and η_{sens}, valuable information about the sensitization process of the Ln(III) center can be achieved.

Ln(III)bppy–type Complexes

Lanthanides have been incorporated into an extensive number of bppy-containing metal complexes for luminescent applications, as alluded to earlier in this chapter. An extraordinarily-well explored motif are nona-dentate podand-type ligands with methylaminodiacetate moieties appended to the 3' and 3" positions to yield anionic Ln(III) complexes.[113] These ligands chelate in a 1:1 ratio with various Ln(III) ions to produce complexes which are not only stable in aqueous media, but are also highly luminescent in the case of Tb(III).[114] Charbonniere *et al*. have considerably expanded the use of this podand scaffold by functionalizing the 4-position of the pyridine ring in order to investigate the consequences of tuning the podand electronics on Ln(III) luminescence (Figure 1.10).[115,116]

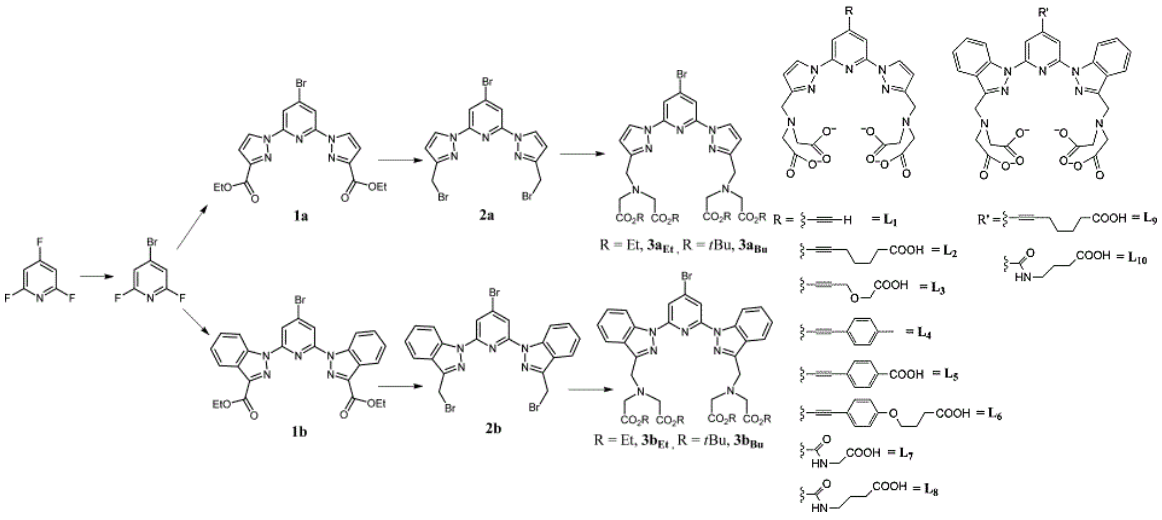

Figure 1.10: Synthetic scheme and derivatives of bppy-podand type ligands. Images adapted from ref. 116.

Lanthanide compounds containing *β*-diketonato ligands have been extensively studied owing to the commercial availability of a large number of *β*-diketones, as well as the ease of synthesis and interesting luminescence of the resulting Ln(III) complexes.[81,106,117] Ln(III) ions usually coordinate three diketonate ligands to generate a neutral eight-coordinate di-aquo species, but the *tetrakis*-diketonato anionic complexes have also been reported.[96,118–120] The two inner-sphere H_2O ligands of the *tris*(*β*-diketonato) Ln(III) complexes may be displaced by a Lewis basic ligand, such as bppy, to generate nona-coordinate Ln(*β*-diketonato)$_3$bppy complexes. A variety of bppy derivatives have been used to successfully synthesize a number of complexes and materials whose luminescent properties have subsequently been investigated.

Chandrasekar *et al*. have synthesized a number of alternating bppy copolymers utilizing a variety of conjugated co-monomers. They achieved the polymerization via

Sonogashira cross-coupling bis(4-iodopyrazol-1-yl)pyridine with the co-monomer, then introduced Tb and/or Eu β-diketonato precursors to form RGB color-tunable metallopolymers and self-assembly structures (Figure 1.11).[21–24,82] Similarly, Holliday *et al*. have appended electropolymerizable thiophene-based moieties to the 4' and 4" positions of bppy and incorporated it into a $Eu(tta)_3$ (tta = 2-thenoylacetonate) complex.[19] Unfortunately, no electropolymeric film growth was achieved upon oxidation of the complex.

Interestingly, only one report has detailed the synthesis and photophysical characterization of simple Ln(β-diketonato)$_3$bppy derivatives has appeared.[121] Four Ln(III) ions were treated with bppy and four different β-diketonate ligands to yield 16 different lanthanide complexes, which were investigated by absorption and emission spectroscopies (Figure 1.12). Surprisingly, the simple $Eu(tta)_3$bppy complex achieved a Φ_{Ln}^{L} of 60%in dichloromethane solution and 93% in the solid state, which is greater than any Eu(III) solid state Φ_{Ln}^{L} previously reported.

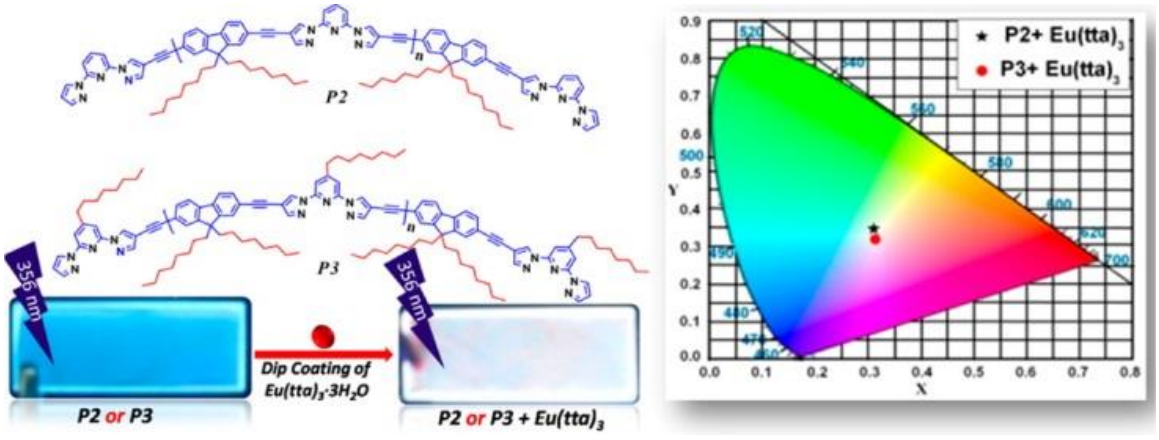

Figure 1.11: Representative scheme of $Eu(tta)_3$bppy copolymer with alternating conjugated co-monomers. Image reproduced with permission from ref. 23.

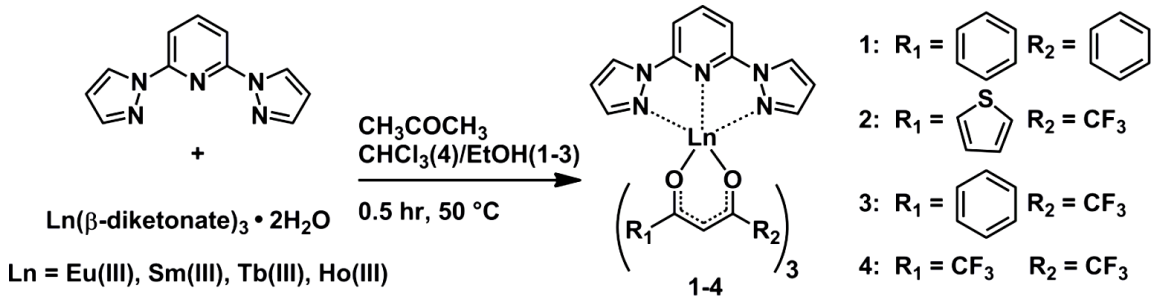

Figure 1.12: Synthesis of Ln(β-diketonato)$_3$bppy complexes, including the highly-luminescent complex, **Eu2**. Image reproduced from ref. 121.

Given the remarkable potential of both bppy ligands and luminescent Ln(III) complexes for targeted materials applications, the shortage of synthetic variety available to functionalize the 4' and 4" position of bppy, and the promising luminescence properties of the Eu(tta)$_3$bppy complex outlined in this introduction, this dissertation concerns itself efforts in functionalizing bppy for applications in Eu(III) luminescence.

CHAPTER REFERENCES

(1) Jameson, D. L.; Blaho, J. K.; Kruger, K. T.; Goldsby, K. A. *Inorg. Chem.* 1989, 28 (24), 4312–4314.

(2) Jameson, D. L.; Goldsby, K. A. *J. Org. Chem.* 1990, 55 (17), 4992–4994.

(3) Halcrow, M. A. *New J. Chem.* 2014, 38 (5), 1868–1882.

(4) Brien, K. A.; Garner, C. M.; Pinney, K. G. *Tetrahedron* 2006, 62 (15), 3663–3666.

(5) Christenson, D. L.; Tokar, C. J.; Tolman, W. B. *Organometallics* 1995, 14 (5), 2148–2150.

(6) Watson, A. A.; House, D. A.; Steel, P. J. *J. Org. Chem.* 1991, 56 (12), 4072–4074.

(7) Sun; Yu; Wu; Xiao, W.-J. *Organometallics* 2005, 24 (12), 2959–2963.

(8) Wang, L.; Liu, N.; Dai, B.; Hu, H. *Eur. J. Org. Chem.* 2014, 2014 (29), 6493–6500.

(9) Duncan, N. C.; Garner, C. M.; Nguyen, T.; Hung, F.; Klausmeyer, K. *Tetrahedron Lett.* 2008, 49 (40), 5766–5769.

(10) Vermonden, T.; Branowska, D.; Marcelis, A. T. M.; Sudhölter, E. J. R. *Tetrahedron* 2003, 59 (27), 5039–5045.

(11) Rajadurai, C.; Schramm, F.; Brink, S.; Fuhr, O.; Ghafari, M.; Kruk, R.; Ruben, M. *Inorg. Chem.* 2006, 45 (25), 10019–10021.

(12) Elhaïk, J.; Pask, C. M.; Kilner, C. A.; Halcrow, M. A. *Tetrahedron* 2007, 63 (2), 291–298.

(13) Basak, S.; Hui, P.; Chandrasekar, R. *Synthesis* 2009, 2009 (23), 4042–4048.

(14) Mohammed, R.; Chastanet, G.; Tuna, F.; Malkin, T. L.; Barrett, S. A.; Kilner, C. A.; Létard, J.-F.; Halcrow, M. A. *Eur. J. Inorg. Chem.* 2013, 2013 (5–6), 819–831.

(15) Du, W.; Wang, Q.; Wang, L.; Yu, Z. *Organometallics* 2014, 33 (4), 974–982.

(16) Zoppellaro, G.; Baumgarten, M. *Eur. J. Org. Chem.* 2005, 2005 (14), 2888–2892.

(17) Grimmett, M.; Iddon, B. *Heterocycles* 1994, 37 (3), 2087–2147.

(18) Pritchard, R.; Lazar, H.; Barrett, S. A.; Kilner, C. A.; Asthana, S.; Carbonera, C.; Létard, J.-F.; Halcrow, M. A. *Dalton Trans.* 2009, No. 33, 6656–6666.

(19) Stanley, J. M.; Zhu, X.; Yang, X.; Holliday, B. *J. Inorg. Chem.* 2010, 49 (5), 2035–2037.

(20) Zhu, X. J.; Holliday, B. J. *Macromol. Rapid Commun.* 2010, 31 (9–10), 904–909.

(21) Basak, S.; Narayana, Y. S. L. V.; Baumgarten, M.; Müllen, K.; Chandrasekar, R. *Macromolecules* 2013, 46 (2), 362–369.

(22) Narayana, Y. S. L. V.; Venkatakrishnarao, D.; Biswas, A.; Mohiddon, M. A.; Viswanathan, N.; Chandrasekar, R. *ACS Appl. Mater. Interfaces* 2016, 8 (1), 952–958.

(23) Narayana, Y. S. L. V.; Basak, S.; Baumgarten, M.; Müllen, K.; Chandrasekar, R. *Adv. Funct. Mater.* 2013, 23 (47), 5875–5880.

(24) Basak, S.; Hui, P.; Boodida, S.; Chandrasekar, R. *J. Org. Chem.* 2012, 77 (7), 3620–3626.

(25) Pritchard, R.; Kilner, C. A.; Barrett, S. A.; Halcrow, M. A. *Inorganica Chim. Acta* 2009, 362 (12), 4365–4371.

(26) Strohecker, D. J.; Lynch, V. M.; Holliday, B. J.; Jones, R. A. *Dalton Trans.*, submitted.

(27) Halcrow, M. A. *Coord. Chem. Rev.* 2009, 253 (21–22), 2493–2514.

(28) Halcrow, M. A. *Coord. Chem. Rev.* 2005, 249 (24), 2880–2908.

(29) Jo, D.-H.; Yeo, H.-J. *Bull. Korean Chem. Soc.* 1993, 14 (6), 682–686.

(30) Karam, A. R.; Catarí, E. L.; López-Linares, F.; Agrifoglio, G.; Albano, C. L.; Díaz-Barrios, A.; Lehmann, T. E.; Pekerar, S. V.; Albornoz, L. A.; Atencio, R.; González, T.; Ortega, H. B.; Joskowics, P. *Appl. Catal. Gen.* 2005, 280 (2), 165–173.

(31) Gong, D.; Jia, X.; Wang, B.; Zhang, X.; Jiang, L. *J. Organomet. Chem.* 2012, 702, 10–18.

(32) Nyamato, G. S.; Alam, M. G.; Ojwach, S. O.; Akerman, M. P. *Appl. Organomet. Chem.* 2016, 30 (2), 89–94.

(33) Gong, D.; Jia, X.; Wang, B.; Zhang, X.; Huang, K.-W. *J. Organomet. Chem.* 2014, 766, 79–85.

(34) Jones, G. D.; Martin, J. L.; McFarland, C.; Allen, O. R.; Hall, R. E.; Haley, A. D.; Brandon, R. J.; Konovalova, T.; Desrochers, P. J.; Pulay, P.; Vicic, D. A. *J. Am. Chem. Soc.* 2006, 128 (40), 13175–13183.

(35) Smith, S. W.; Fu, G. C. *Angew. Chem. Int. Ed.* 2008, 47 (48), 9334–9336.

(36) Arendt, K. M.; Doyle, A. G. *Angew. Chem. Int. Ed.* 2015, 54 (34), 9876–9880.

(37) Erickson, L. W.; Lucas, E. L.; Tollefson, E. J.; Jarvo, E. R. *J. Am. Chem. Soc*. 2016, 138 (42), 14006–14011.

(38) Li, Y.-T.; Liao, B.-S.; Chen, H.-P.; Liu, S.-T. *Synthesis* 2011, 2011 (16), 2639–2643.

(39) Zikode, M.; Ojwach, S. O.; Akerman, M. P. *Appl. Organomet. Chem.* 2017, 31 (2), e3556.

(40) Magubane, M. N.; Nyamato, G. S.; Ojwach, S. O.; Munro, O. Q. *RSC Adv.* 2016, 6 (69), 65205–65221.

(41) Ghoochany, L. T.; Farsadpour, S.; Sun, Y.; Thiel, W. R. *Eur. J. Inorg. Chem.* 2011, 2011 (23), 3421–3424.

(42) Jin, W.; Wang, L.; Yu, Z. *Organometallics* 2012, 31 (15), 5664–5667.

(43) Liu, S.; Zeng, X.; Xu, B. *Tetrahedron Lett.* 2016, 57 (33), 3706–3710.

(44) Shin, M. S.; Oh, B. J.; Ryu, J. Y.; Park, M. H.; Kim, M.; Lee, J.; Kim, Y. *Polyhedron* 2017, 125, 101–106.

(45) König, E.; Madeja, K. *Chem. Commun.* Lond. 1966, No. 3, 61–62.

(46) Kershaw Cook, L. J.; Mohammed, R.; Sherborne, G.; Roberts, T. D.; Alvarez, S.; Halcrow, M. A. *Coord. Chem. Rev.* 2015, 289–290, 2–12.

(47) Craig, G. A.; Roubeau, O.; Aromí, G. *Coord. Chem. Rev.* 2014, 269, 13–31.

(48) Holland, J. M.; McAllister, J. A.; Lu, Z.; Kilner, C. A.; Thornton-Pett, M.; Halcrow, M. A. *Chem. Commun.* 2001, No. 6, 577–578.

(49) Scudder, M. L.; Goodwin, H. A.; Dance, I. G. *New J. Chem.* 1999, 23 (7), 695–705.

(50) Pritchard, R.; Kilner, C. A.; Halcrow, M. A. *Chem. Commun.* 2007, No. 6, 577–579.

(51) Elhaïk, J.; Evans, D. J.; Kilner, C. A.; Halcrow, M. A. *Dalton Trans.* 2005, No. 9, 1693–1700.

(52) Pelascini, F.; Wesolek, M.; Peruch, F.; Cian, A. D.; Kyritsakas, N.; Lutz, P. J.; Kress, J. *Polyhedron* 2004, 23 (18), 3193–3199.

(53) Money, V. A.; Carbonera, C.; Elhaïk, J.; Halcrow, M. A.; Howard, J. A. K.; Létard, J.-F. *Chem. – Eur. J.* 2007, 13 (19), 5503–5514.

(54) Schramm, F.; Chandrasekar, R.; Zevaco, T. A.; Rudolph, M.; Görls, H.; Poppitz, W.; Ruben, M. *Eur. J. Inorg. Chem.* 2009, 2009 (1), 53–61.

(55) Willison, S. A.; Jude, H.; Antonelli, R. M.; Rennekamp, J. M.; Eckert, N. A.; Krause Bauer, J. A.; Connick, W. B. *Inorg. Chem.* 2004, 43 (8), 2548–2555.

(56) Stock, J. T. *J. Chem. Educ.* 1991, 68 (10), 801.

(57) Pimentel, G. C.; Spratley, R. D. Understanding Chemistry; Holden-Day, Inc.: San Francisco, CA, USA, 1971.

(58) Cirera, B.; Björk, J.; Otero, R.; Gallego, J. M.; Miranda, R.; Ecija, D. *J. Phys. Chem. C* 2017, 121 (14), 8033–8041.

(59) Dochain, S.; Vetica, F.; Puttreddy, R.; Rissanen, K.; Enders, D. *Angew. Chem. Int. Ed.* 2016, 55 (52), 16153–16155.

(60) Chen, D.; Yu, L.; Wang, P. G. *Tetrahedron Lett.* 1996, 37 (26), 4467–4470.

(61) Yu, L.; Chen, D.; Wang, P. G. *Tetrahedron Lett.* 1996, 37 (13), 2169–2172.

(62) Kobayashi, S.; Hachiya, I.; Takahori, T.; Araki, M.; Ishitani, H. *Tetrahedron Lett.* 1992, 33 (45), 6815–6818.

(63) Dissanayake, P.; Allen, M. J. *J. Am. Chem. Soc.* 2009, 131 (18), 6342–6343.

(64) Wu, P.; Wang, J.; Li, Y.; He, C.; Xie, Z.; Duan, C. *Adv. Funct. Mater.* 2011, 21 (14), 2788–2794.

(65) Ward, B. D.; Gade, L. H. *Chem. Commun.* 2012, 48 (86), 10587–10599.

(66) Ende, B. M. van der; Aarts, L.; Meijerink, A. *Phys. Chem. Chem. Phys.* 2009, 11 (47), 11081–11095.

(67) Méndez-Blas, A.; López-Cruz, E.; Palestino, G.; Calixto, M. E. *MRS Adv.* 2017, 2 (3), 147–152.

(68) Jeng, J.-T.; Li, Y.-L. *J. Vac. Sci. Technol. B Nanotechnol. Microelectron. Mater. Process. Meas. Phenom.* 2017, 35 (2), 022203.

(69) Bethencourt, M.; Botana, F. J.; Calvino, J. J.; Marcos, M.; RodrÍguez-Chacón, M. A. *Corros. Sci.* 1998, 40 (11), 1803–1819.

(70) Tiwari, B.; Ram, S.; Banerji, P. *MRS Adv.* 2017, 2 (3), 141–146.

(71) Bomberger, C. C.; Lewis, M. R. *J. Vac. Sci. Technol. B Nanotechnol. Microelectron. Mater. Process. Meas. Phenom.* 2017, 35 (3), 030801.

(72) Chow, C.-F. *J. Fluoresc.* 2012, 22 (6), 1539–1546.

(73) Sessler, J. L.; Dow, W. C.; O'Connor, D.; Harriman, A.; Hemmi, G.; Mody, T. D.; Miller, R. A.; Qing, F.; Springs, S.; Woodburn, K.; Young, S. W. *J. Alloys Compd.* 1997, 249 (1–2), 146–152.

(74) Rocha, J.; Carlos, L. D.; Paz, F. A. A.; Ananias, D. *Chem. Soc. Rev.* 2011, 40 (2), 926–940.

(75) Wang, Y.-F.; Liu, G.-Y.; Sun, L.-D.; Xiao, J.-W.; Zhou, J.-C.; Yan, C.-H. *ACS Nano* 2013, 7 (8), 7200–7206.

(76) Hanaoka, K.; Kikuchi, K.; Kojima, H.; Urano, Y.; Nagano, T. *J. Am. Chem. Soc.* 2004, 126 (39), 12470–12476.

(77) Liu, Y.; Tu, D.; Zhu, H.; Chen, X. *Chem. Soc. Rev.* 2013, 42 (16), 6924–6958.

(78) Cheng, L.; Yang, K.; Li, Y.; Chen, J.; Wang, C.; Shao, M.; Lee, S.-T.; Liu, Z. *Angew. Chem. Int. Ed.* 2011, 50 (32), 7385–7390.

(79) Wang, M.; Chen, Z.; Zheng, W.; Zhu, H.; Lu, S.; Ma, E.; Tu, D.; Zhou, S.; Huang, M.; Chen, X. *Nanoscale* 2014, 6 (14), 8274–8282.

(80) Moore, E. G.; Samuel, A. P. S.; Raymond, K. N. *Acc. Chem. Res.* 2009, 42 (4), 542–552.

(81) Binnemans, K. *Chem. Rev.* 2009, 109 (9), 4283–4374.

(82) Basak, S.; Mohiddon, M. A.; Baumgarten, M.; Müllen, K.; Chandrasekar, R. *Sci. Rep.* 2015, 5, 8406.

(83) Chen, X.-Y.; Yang, X.; Holliday, B. J. *J. Am. Chem. Soc.* 2008, 130 (5), 1546–1547.

(84) de Hatten, X.; Asil, D.; Friend, R. H.; Nitschke, J. R. *J. Am. Chem. Soc.* 2012, 134 (46), 19170–19178.

(85) Hasegawa, Y.; Kawai, H.; Nakamura, K.; Yasuda, N.; Wada, Y.; Yanagida, S. *J. Alloys Compd.* 2006, 408–412, 669–674.

(86) Carlos, L. D.; Ferreira, R. A. S.; Bermudez, V. de Z.; Ribeiro, S. J. L. *Adv. Mater.* 2009, 21 (5), 509–534.

(87) Ma, M.-L.; Ji, C.; Zang, S.-Q. *Dalton Trans.* 2013, 42 (29), 10579–10586.

(88) Armelao, L.; Quici, S.; Barigelletti, F.; Accorsi, G.; Bottaro, G.; Cavazzini, M.; Tondello, E. *Coord. Chem. Rev.* 2010, 254 (5–6), 487–505.

(89) Carlos, L. D.; Ferreira, R. A. S.; Bermudez, V. de Z.; Julián-López, B.; Escribano, P. *Chem. Soc. Rev.* 2011, 40 (2), 536–549.

(90) Bettencourt-Dias, A. de. *Dalton Trans.* 2007, No. 22, 2229–2241.

(91) Aime, S.; Botta, M.; Fasano, M.; Terreno, E. *Chem. Soc. Rev*. 1998, 27 (1), 19–29.

(92) Peters, J. A.; Huskens, J.; Raber, D. *J. Prog. Nucl. Magn. Reson. Spectrosc.* 1996, 28 (3–4), 283–350.

(93) Aspinall, H. C. *Chem. Rev.* 2002, 102 (6), 1807–1850.

(94) Aime, S.; Barge, A.; Delli Castelli, D.; Fedeli, F.; Mortillaro, A.; Nielsen, F. U.; Terreno, E. *Magn. Reson. Med.* 2002, 47 (4), 639–648.

(95) Aime, S.; Castelli, D. D.; Crich, S. G.; Gianolio, E.; Terreno, E. *Acc. Chem. Res.* 2009, 42 (7), 822–831.

(96) Wenzel, T. J.; Zaia, J. *J. Org. Chem.* 1985, 50 (8), 1322–1324.

(97) Bünzli, J.-C. G. *J. Coord. Chem.* 2014, 67 (23/24), 3706–3733.

(98) D'Aléo, A.; Pointillart, F.; Ouahab, L.; Andraud, C.; Maury, O. *Coord. Chem. Rev.* 2012, 256 (15–16), 1604–1620.

(99) Bünzli, J.-C. G.; Piguet, *C. Chem. Soc. Rev.* 2005, 34 (12), 1048–1077.

(100) Vleck, J. H. V. *J. Phys. Chem.* 1937, 41 (1), 67–80.

(101) Weissman, S. I. *J. Chem. Phys.* 1942, 10 (4), 214–217.

(102) Latva, M.; Takalo, H.; Mukkala, V.-M.; Matachescu, C.; Rodríguez-Ubis, J. C.; Kankare, J. *J. Lumin.* 1997, 75 (2), 149–169.

(103) Fu, L.-M.; Ai, X.-C.; Li, M.-Y.; Wen, X.-F.; Hao, R.; Wu, Y.-S.; Wang, Y.; Zhang, J.-P. *J. Phys. Chem. A* 2010, 114 (13), 4494–4500.

(104) Narayana, Y. S. L. V.; Chandrasekar, R. *ChemPhysChem* 2011, 12 (13), 2391–2396.

(105) Bünzli, J.-C. G. Coord. Chem. Rev. 2015, 293–294, 19–47.

(106) Sato, S.; Wada, M. *Bull. Chem. Soc. Jpn.* 1970, 43 (7), 1955–1962.

(107) Whan, R. E.; Crosby, G. A. *J. Mol. Spectrosc.* 1962, 8 (1), 315–327.

(108) Binnemans, K. *Coord. Chem. Rev.* 2015, 295, 1–45.

(109) Haas, Y.; Stein, G. *J. Phys. Chem.* 1971, 75 (24), 3677–3681.

(110) Haas, Y.; Stein, G. *J. Phys. Chem.* 1971, 75 (24), 3668–3677.

(111) Supkowski, R. M.; Horrocks Jr., W. D. *Inorganica Chim. Acta* 2002, 340, 44–48.

(112) Werts, M. H. V.; Jukes, R. T. F.; Verhoeven, J. W. *Phys. Chem. Chem. Phys.* 2002, 4 (9), 1542–1548.

(113) Remuiñán, M. J.; Román, H.; Alonso, M. T.; Rodríguez-Ubis, J. C. *J. Chem. Soc. Perkin Trans. 2* 1993, No. 6, 1099–1102.

(114) Brunet, E.; Juanes, O.; Sedano, R.; Rodríguez-Ubis, J.-C. *Photochem. Photobiol. Sci.* 2002, 1 (8), 613–618.

(115) Kadjane, P.; Starck, M.; Camerel, F.; Hill, D.; Hildebrandt, N.; Ziessel, R.; Charbonnière, L. *J. Inorg. Chem.* 2009, 48 (11), 4601–4603.

(116) Starck, M.; Kadjane, P.; Bois, E.; Darbouret, B.; Incamps, A.; Ziessel, R.; Charbonnière, L. J. *Chem. – Eur. J.* 2011, 17 (33), 9164–9179.

(117) Sager, W. F.; Filipescu, N.; Serafin, F. A. *J. Phys. Chem.* 1965, 69 (4), 1092–1100.

(118) Pereira, C. C. L.; Coutinho, J. T.; Pereira, L. C. J.; Leal, J. P.; Laia, C. A. T.; Monteiro, B. *Polyhedron* 2015, 91, 42–46.

(119) Martins, J. P.; Martín-Ramos, P.; Coya, C.; Álvarez, A. L.; Pereira, L. C.; Díaz, R.; Martín-Gil, J.; Ramos Silva, M. Mater. Chem. Phys. 2014, 147 (3), 1157–1164.

(120) Binnemans, K.; Bex, C.; Venard, A.; De Leebeeck, H.; Görller-Walrand, C. *J. Mol. Liq.* 1999, 83 (1–3), 283–294.

(121) Wilkerson, J. M. Luminescent lanthanide-containing materials: from small molecules to conducting metallopolymers, The University of Texas at Austin: Austin, TX, 2012.

Chapter 2: Synthesis and Electronic Investigation of Mono- and Di-substituted 4-Nitro- and 4-Amino-pyrazol-1-yl Bis(pyrazol-1-yl)pyridine-type Ligands and Luminescent Eu(III) Derivatives

INTRODUCTION

Lanthanide complexes continue to be of significant interest for potential applications in magnetism, optoelectronics and as probes in biological systems.[1–4] The useful photophysical properties of certain lanthanide complexes include large pseudo-Stokes shifts, discreet emission wavelengths and long lifetimes. Due to their ease of synthesis and favourable emissive properties lanthanide complexes of multidentate ligands containing pyridyl or pyrazolyl groups, or both, are now well established. Two of the most important ligands of this class are, 2,6-bis(pyrazol-1-yl)pyridine (bppy) and 2,6-bis(2-pyridyl)pyridine (terpy) (Figure 2.1). First reported in the pioneering work by Jameson *et al.* in 1989, bppy has been shown to serve as a versatile analogue to the well-known tridentate nitrogen-donor terpy.[5] With respect to terpy, bppy is a weaker σ-donor as well as a weaker π-acceptor, owing to the lesser basicity of pyrazole in addition to a higher π* energy of the aromatic system, resulting in lessened ligand binding strength.[5] This deviation in electronic behavior in a ligand that is otherwise structurally similar to terpy, along with the synthetic ease with which bppy may be derivatized on the 4-position of pyridine, as well as the 3- and 5-positions of the pyrazole rings, has led to the increasing popularity of bppy as a complementary platform for research into new d- and f-block metal complexes. Halcrow published an especially thorough review of such ligands and complexes as they pertain to catalysis, dye-sensitized solar cells, spin-

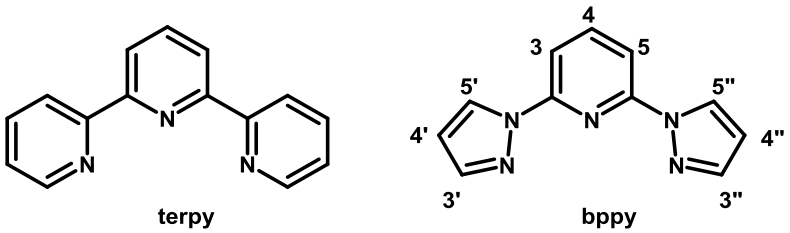

Figure 2.1: Depiction of tridentate N-donor ligands terpy and bppy.

crossover materials, and emissive materials for LEDs and biomarkers, with a special interest taken on spin-crossover and luminescent lanthanide complexes.[6]

As Zoppellaro and Baumgarten reported in 2005, bppy derivatives substituted on the 4-position of the pyrazole ring are relatively rare, due to unwieldy synthetic routes involving non-selective lithiations or protection/deprotection steps.[7] There are consequently few examples of this type of substitution, being limited to a handful of (4-halopyrazol-1-yl)pyridines, a modest number of carbon-coupling reaction products of these compounds, and some carbonyl-derived ligands, either stemming from the formylation of said (4-halopyrazol-1-yl)pyridines or nucleophilic substitution of 2,6-dibromopyridine with ethyl pyrazole-4-carboxylate.[7–15]

Herein, we report the synthesis and electronic properties of the 4,4" symmetrically substituted di-nitro and di-amino derivatives $(NO_2)_2$bppy (**2.1**), $(NH_2)_2$bppy) (**2.2**), the 4-mono-substituted NO_2bppy (**2.5**) and NH_2bppy (**2.6**) compounds as well as the synthesis and spectroscopic characterization of two Eu(III) derivatives of the amino substituted ligands, $Eu(tta)_3(NH_2)_2$bppy (**2.7**) and $Eu(tta)_3NH_2$bppy (**2.8**) (tta = 2-thenoylacetonate) (Scheme 2.1).

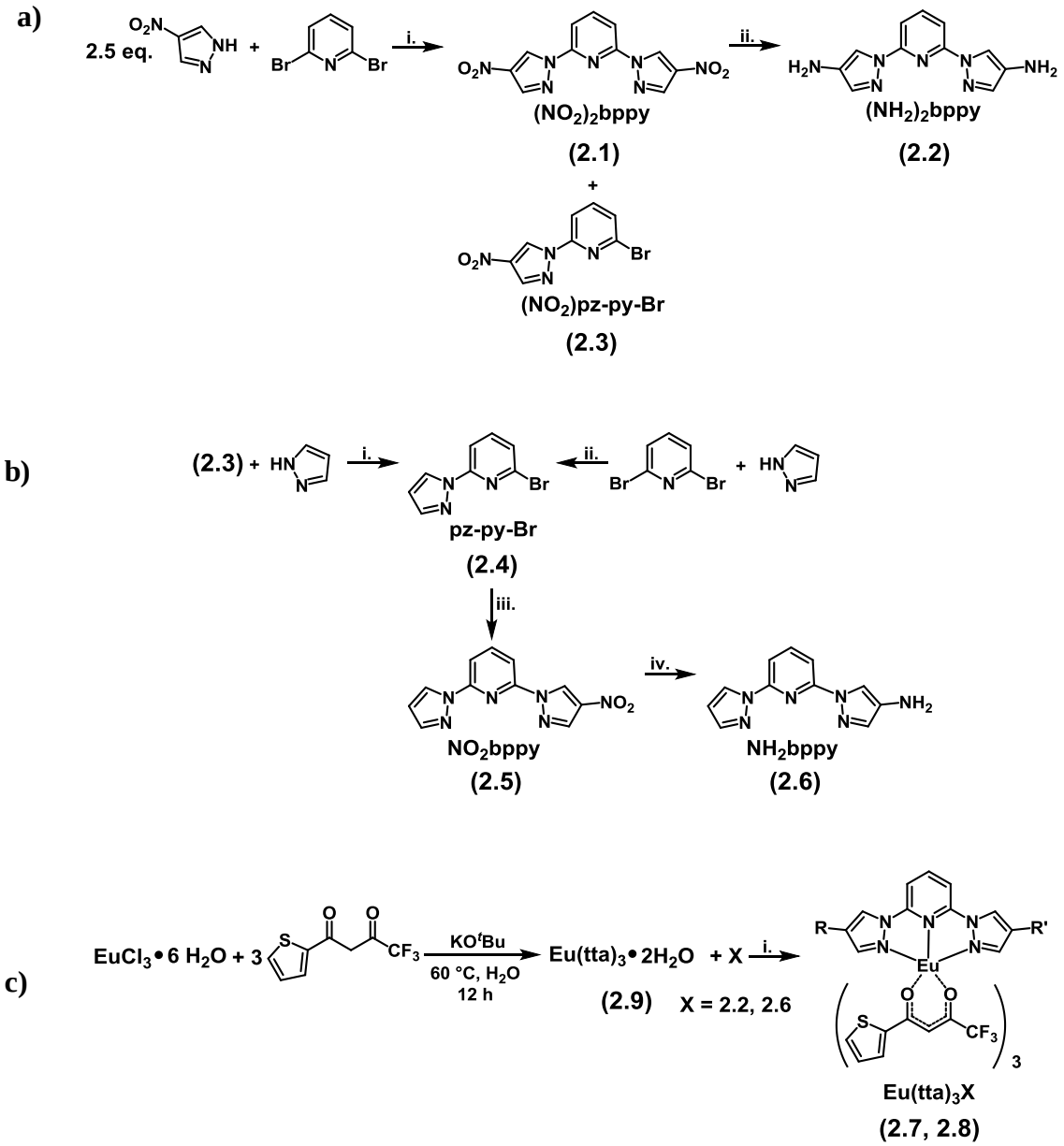

Scheme 2.1: a) Synthesis of **2.1** and **2.2**. i. NaH, N_2, 120 °C, 7 d; yield = 93% ii. 20% PtO_2, 2:3 EtOH: ethyl acetate, H_2 3 d; yield = 81% b) Synthesis of **2.5** and **2.6**. i. NaH, N_2, 110 °C, 3 d ii. NaH, N_2, 70 °C, 2 d; yield = 50% iii. NaH, N_2, 120 °C 4 d; yield = 89% iv. 10% PtO_2, 1:1 EtOH: ethyl acetate, 25 – 45°C H_2 2 d; yield = 70% c) Synthesis of **2.7** and **2.8**. i. refluxing acetone, 1 d; 2.7: R = R'= NH_2, yield = 76 %; 2.8: R = H, R' = NH_2, yield = 46.0%.

RESULTS AND DISCUSSION

Synthesis

The synthesis of the mono- and disubstituted nitro- ligands **2.1** and **2.5** was achieved via the established nucleophilic substitution of 2,6-dibromopyridine affording satisfactory yields. The synthesis of the di-substituted species **2.1** was achieved by reacting excess of the pyrazolate of 4-nitropyrazole and 2,6-dibromopyridine, followed by hydrogenation to yield **2.2**. Although it has been noted that this procedure may be expected to result in the decomposition of the 4-nitropyrazolate rather than the desired substitution,[16] we have found that by limiting the reaction temperature to 120 °C and increasing the reaction time to 7 days in diglyme yields **2.1** in high yield (92.6%). Initial attempts to form **2.1** using stoichiometric amounts of 4-nitropyrazole and reaction temperatures above 130 °C gave low yields and formation of the expected mono-substitution product, **2.3**, in yields of approximately 30%. Reaction of **2.3** with an additional equivalent of 4-nitropyrazole can be employed to further improve the yield of **2.1**. Optimization of reaction conditions such as introducing one extra equivalent of the pyrazole and NaH each, as well as extending reaction times to 7 days eventually yielded **1** in excellent yield with minimal mono-substitution by-products.

The subsequent reduction to form **2.2** was problematic due to the poor solubility of **2.1**. Limited success was achieved by reducing with $SnCl_2$ in basic media as per the literature,[17] however higher catalytic loading of Adams's catalyst and careful adjustment of the volumetric ratio of EtOH: EtOAc (2:3 was found to be optimal) enabled the desired reduction to **2.2** in consistent satisfactory yields in the range of 80%.

Synthesis of the asymmetrically-substituted derivatives was also performed with similar nucleophilic substitutions followed by nitro- group reduction, but careful

consideration was required when choosing the order of pyrazolate nucleophilic substitution. Attempts to synthesize **2.5** by treating **2.3** with pyrazole and NaH resulted in low yields, with large by-product formation of **2.4** and 4-nitropyrazole as well as bppy, indicating competition between substitution of the 4-nitropyrazole and bromine with pyrazolate. Step-wise formation of **2.4** via nucleophilic substitution of 2-6-dibromopyridine with pyrazole, followed by substitution with 4-nitropyrazole proved to be effective in synthesizing the mono-substituted **2.5**. Nucleophilic aromatic substitution using 4-aminopyrazole to directly produce **2.2** is undesirable, as the amine would necessitate a longer synthetic route entailing protection and deprotection steps; additionally the cost of this reactant is quite high.

Ligand Crystallography

In order to unequivocally establish the identities of **2.5** and **2.6** single crystal X-ray structures were obtained (Figure 2.2). In the solid state structure of **2.6**, a slight distortion from co-planarity with regard to the pyridine ring is apparent for the pyrazole ring bearing the primary amine, with a dihedral angle of 12.40 ° between the two

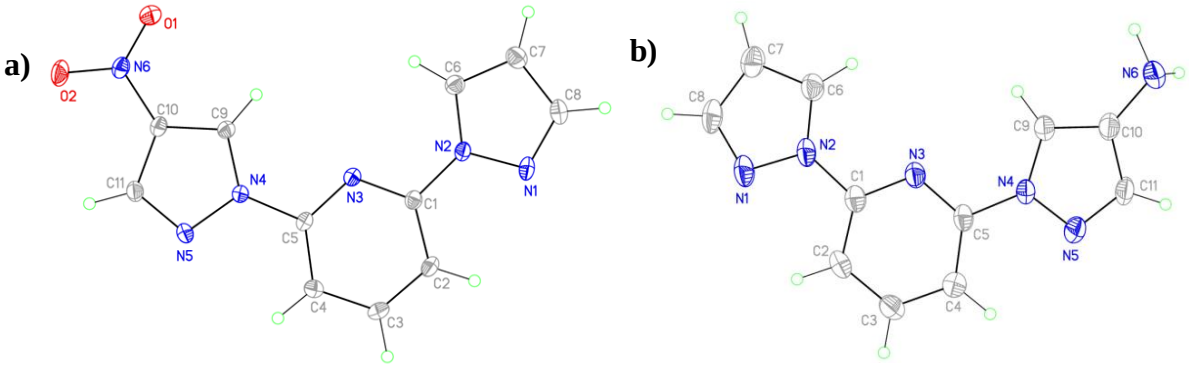

Figure 2.2: a) Single crystal structure of **2.5**. b) Single crystal structure of **2.6**. Displacement ellipsoids are scaled to the 50% probability level.

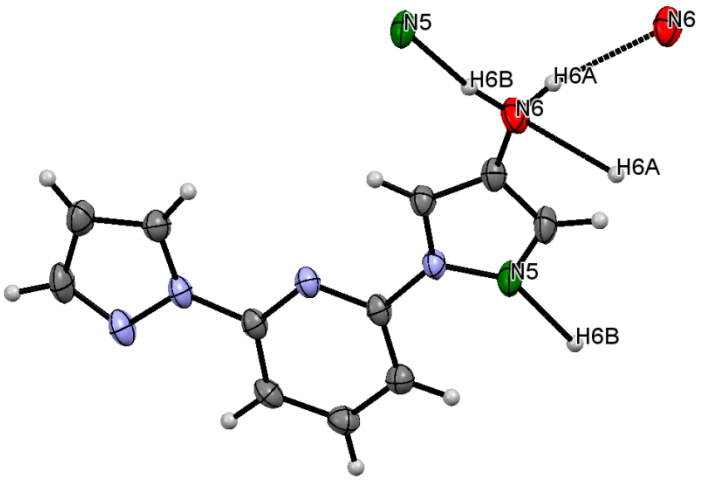

Figure 2.3: Solid-state structure of **2.6** showing H-bonding interactions. All atoms participating in H- bonding are labeled; atoms N5 and N6 are colored green and red, respectively, for clarity.

heterocycles. The primary amine N–H bond distances are 0.963 Å and 0.880 Å. The difference in bond lengths arise from two distinct H-bonding interactions involving the separate H atoms, one involving an adjacent primary amine N6 (2.312 Å) and the other involving the pyrazole imine N5 atom of an adjacent 4-aminopyrazole ring (2.143 Å) (Figure 2.3). **2.5** was isolated as three polymorphs and is discussed further in Appendix A.

Ligand Spectroscopy

The results of UV-Vis absorption spectroscopy are summarized in Table 2.1. The absorption spectra of all ligands are characterized by two $\pi \rightarrow \pi^*$ transitions in the UV region in the range of 260 nm – 317 nm, with the exception of **2.2** (Figure 2.4.a). The bathochromic shift of the low-energy transition seen in **2.2** (327 nm) suggests a lower energy $n \rightarrow \pi^*$ transition combining with or completely covering the expected $\pi \rightarrow \pi^*$ transition.

Table 2.1: UV-Vis absorbances of ligands and complexes

λ (nm); ε ($M^{-1}cm^{-1}$)	**2.1**	**2.2**	**2.5**	**2.6**	**2.7**	**2.8**
	--	--	259; 12,499	248; 18,073	266; 49,402	---
	289; 19,489	279; 5,638	276; 13,114	--	--	276; 27,902
	317; 18,397	327; 14,571	312; 14,503	314; 22,017	338; 84,565	340; 51,415

Fluorescence spectroscopy of these molecules reveals excitation profiles that closely resemble the respective absorbance spectra, with excitation λ_{max} being closely associated with the λ_{max} of absorption in all cases. At room temperature, **2.2** and **2.6** exhibit broad emission peaks centered at 404 nm and 414 nm, respectively (Figure 2.4.b); **2.1** and **2.5** can be seen to emit very faintly in the UV region. Observation of **2.2**, **2.5** and **2.6** in a 2:2:1:1 volumetric ratio of ethyl iodide: diethyl ether: ethanol: toluene (EEET) solvent glass upon cooling to 77 K permitted the phosphorescence of these molecules to be observed; in the case of **2.2** and **2.6**, emission from the T_1 manifold appears as an additional shoulder in the emission spectrum of **2.2** centered at 486 nm and a resolved phosphorescence manifold in **2.6** (Figure 2.4.c). Identification of the blue edges of phosphorescence allowed for the determination of the T_1 energy of 25,381 cm^{-1} for **2.2** and 26,201 cm^{-1} for **2.6**. This information is of key importance in the consideration of this molecule as a sensitizing ligand for lanthanide luminescence. The blue edge of phosphorescence from **2.2** was determined by fitting the 77 K emission spectrum to a multi-peak Gaussian distribution model and extrapolating the resultant phosphorescence curve (Figure 2.5). In the case of **2.5** there appears to be significant overlap between fluorescence and phosphorescence processes, making determination of the T_1 energy

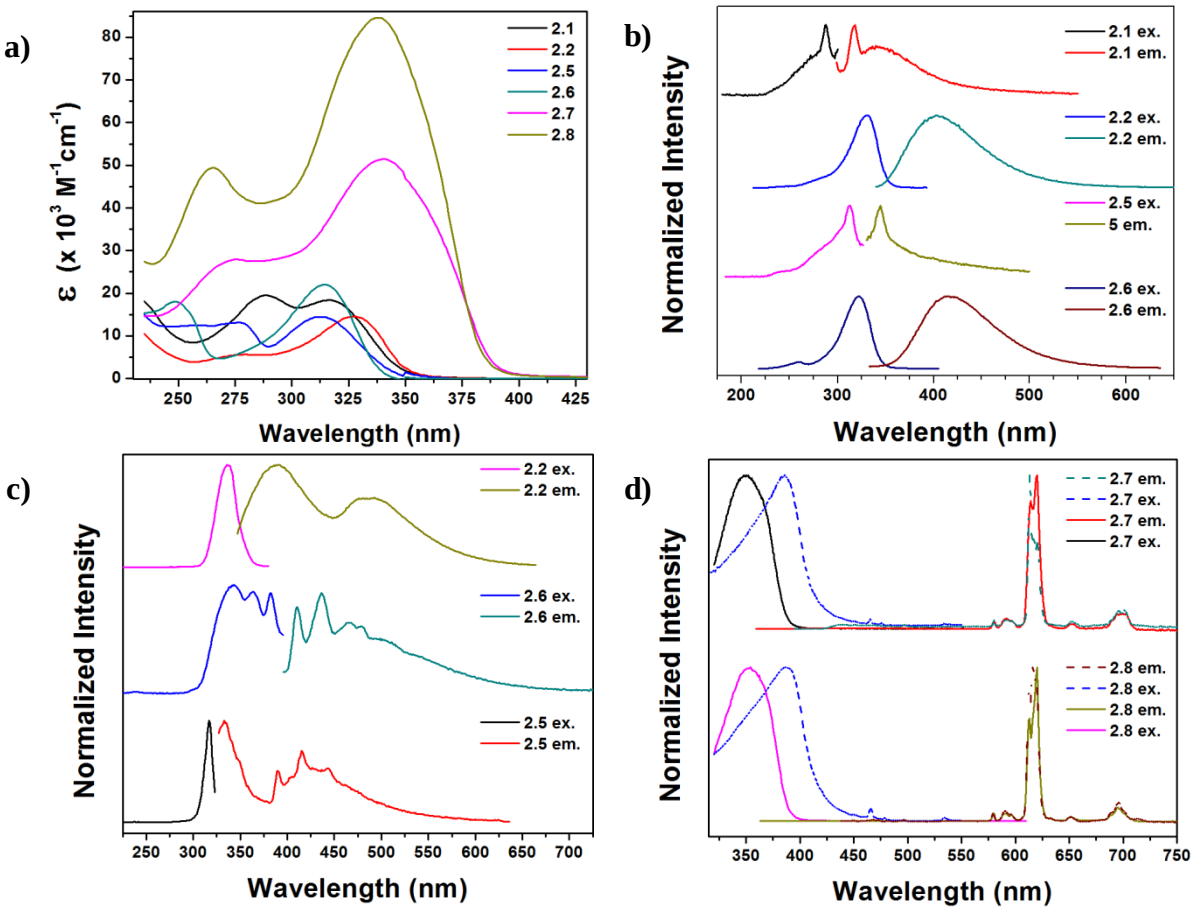

Figure 2.4: a) Absorption spectra of ligands and complexes b) Room-temperature excitation and emission spectra of ligands c) 77 K excitation and emission spectra of **2.2**, **2.5**, and **2.6** d) solution (solid lines) and solid-state (dashed lines) excitation and emission spectra of **2.7** and **2.8**.

level difficult; the shape and range of the 77 K emission spectrum of **2.5** changes drastically depending on the chosen excitation wavelength, and attempts to determine emission lifetimes for phosphorescence peak identification were not possible with our current instrumentation. Excitation with the lowest-energy excitation wavelength that was discrete from the 77 K emission profile of **2.5** is shown in Figure 2.3.c, as this wave-

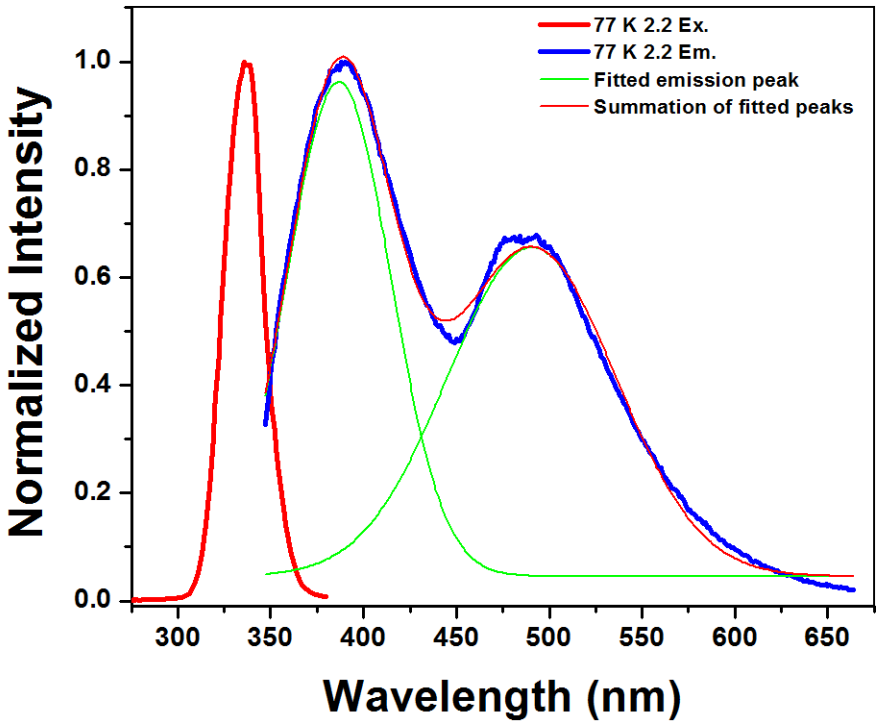

Figure 2.5: 77 K excitation and emission spectra of **2.2** in EEET with fitting of emission spectrum peaks.

length should maximize the phosphorescence character of the emission. This emission appears as a well-resolved manifold, though we hesitate to assign a ligand T_1 energy using the emission edge. Unfortunately no phosphorescence could be observed from **2.1.**

Cyclic Voltammetry

Cyclic voltammetry (CV) was performed to determine the electrochemical behavior as well as energies of the HOMO (E_{HOMO}), LUMO (E_{LUMO}), and HOMO-LUMO gap (ΔE) of these species by identifying the onset potential of each initial reductive and oxidative event of the ligands. The resultant voltammograms are shown with that of bppy under identical conditions in Figure 2.6; redox event peak potentials and frontier orbital energy values are reported in Table 2.2. Electrochemical energy levels

were calculated utilizing onsets of oxidation and reduction according to equations 1 and 2:[18]

$$E_{HOMO} = -\left(E_{onset,ox.vs.Fc/Fc^{+}} + 5.1\right)(eV) \quad (1)$$

$$E_{LUMO} = -\left(E_{onset,red.vs.Fc/Fc^{+}} + 5.1\right)(eV) \quad (2)$$

To the best of our knowledge, the electrochemical behavior of the parent bppy ligand has not been reported until now. Electrochemistry of bppy reveals two irreversible oxidative events at relatively high potentials; this suggests that the irreversible oxidative events

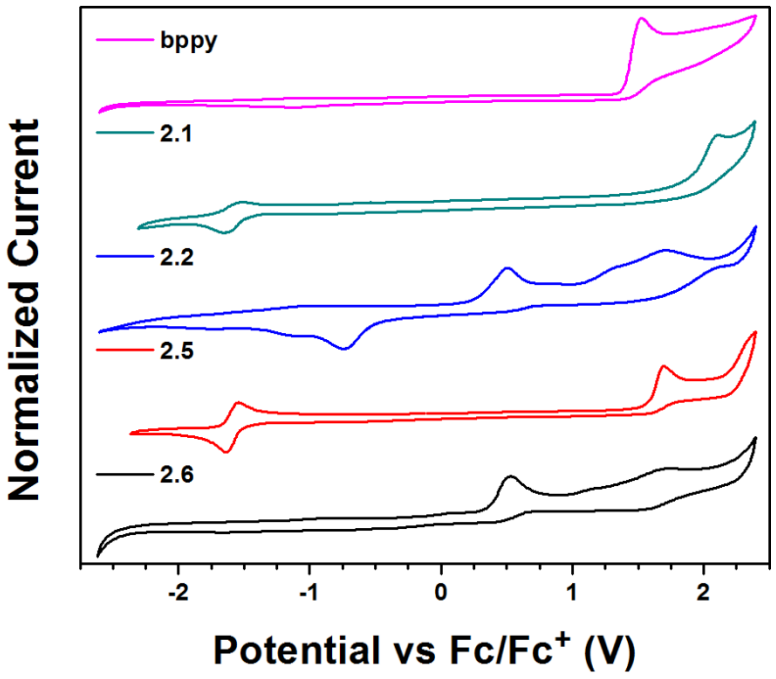

Figure 2.6: Cyclic voltammograms of bppy and substituted bppy derivatives.

Table 2.2: Cyclic voltammetry redox potentials and HOMO/LUMO energy levels

Ligand	E_{red} (V)	E_{ox} (V)	$E_{1/2}$ (V)	E_{HOMO} (eV)	E_{LUMO} (eV)	ΔE (eV)
bppy	---	1.53, 2.06	---	–6.18	–2.35	3.83
2.1	–1.64	–1.52, 2.11	–1.58	–7.04	–3.64	3.54
2.2	–1.12, –0.74	0.51, 0.86, 1.34, 1.71	---	–5.35	–1.82	3.53
2.5	1.64	–1.54, 1.70	–1.59	–6.68	–3.59	3.01
2.6	---	0.48, 1.16, 1.72	---	–5.46	–1.80	3.66

seen in all of these ligands which take place at approximately 1.1 V and greater are due to the oxidation of the aromatic system; this is corroborated by the presence of similar irreversible oxidative signals in each of the rest of the series. The electron-rich or deficient nature of the amino- and nitro-bppy derivatives are reflected in the potentials at which the aromatic system is oxidized, with larger potentials being required for the molecules bearing NO_2- groups and lesser potentials required for the NH_2-bearing molecules. **2.1** and **2.5** each exhibit only one irreversible oxidative peak at positive potentials, and a reversible nitro-group redox couple upon sweeping to negative potentials. **2.2** and **2.6** undergo multiple irreversible oxidative events, and **2.2** can be seen to undergo two irreversible reductive events. Performing negative potential sweeps of **2.2** from 0 V to -2.5 V yields no reductive current, indicating coupling between the two reductive events and the oxidative events which correspond to neither bppy oxidation nor

reduction of the oxidized residue; we therefore attribute these signals to redox processes undergone by the amine functionalities.

Since the reductive events evident in the voltammograms of **2.2** are coupled to these initial oxidative peaks and no reductive events are discernible in **2.6** or bppy, the E_{LUMO} of these three ligands cannot be determined electrochemically. Therefore, the E_{LUMO} and ΔE of these molecules were calculated by combining optical measurement data with E_{HOMO} values obtained from CV studies. The energy of the red edge of the UV-Vis absorption spectra, corresponding to the $0 - 0$ $S_0 \rightarrow S_1$ electronic transition, was assigned the ΔE of these ligands. The assignment of frontier orbital energies for these ligands allows for empirical LUMO energy determination and comparison across the series (Figure 2.7). As expected, the electron-deficient NO_2-containing ligands exhibit lowered E_{HOMO} values and raised E_{LUMO} values, whereas the electron-rich NH_2- ligands exhibit the opposite.[19–21] Interestingly, the disparity in ΔE is greatest with the mono-substituted bppy ligands whereas the di-substituted ligands exhibit nearly identical ΔE values but at different energies. In addition to serving as versatile synthetic intermediates, characterization of the electronics of these ligands indicate that they offer a means of tuning energy levels and binding strengths of bppy ligands.

Eu(III) Complex Synthesis and Spectroscopy

The new compounds were also investigated as ligands for sensitizing Eu(III) luminescence, owing to the highly-luminescent nature of the parent bppy complex.[22] Presently, all attempts at forming lanthanide complexes with **2.1** and **2.5** have failed, presumably due to the exceedingly electron-deficient nature of the ligands. However, metalation of **2.2** and **2.6** upon refluxing with $Eu(tta)_3 \bullet 2H_2O$ in acetone yielded

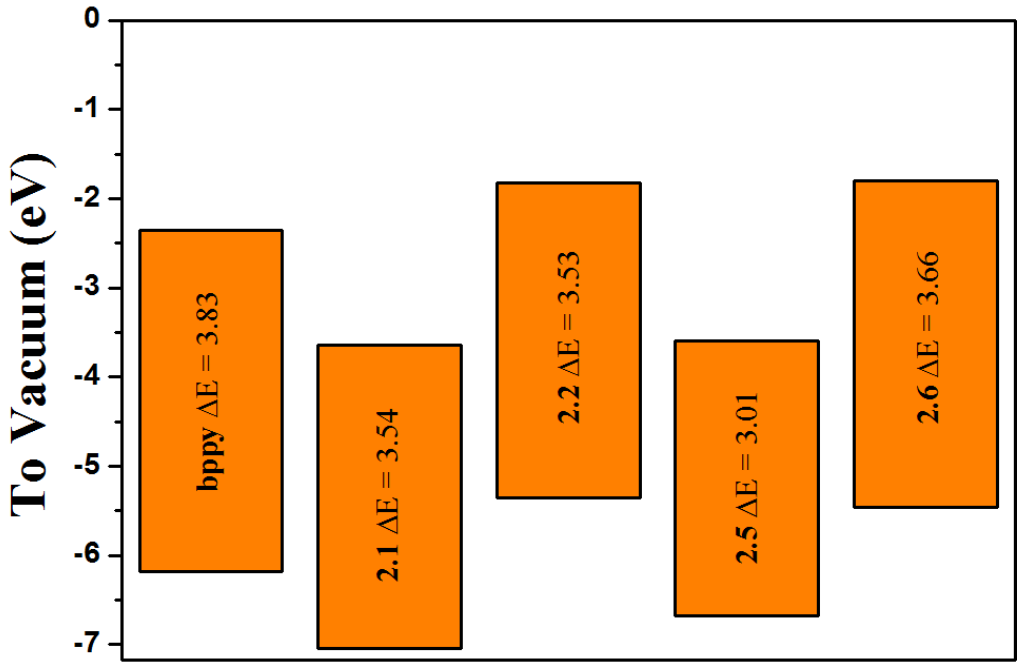

Figure 2.7: HOMO-LUMO gaps of the ligands described in this chapter.

complexes $Eu(tta)_3(NH_2)_2bppy$ (**2.7**) and $Eu(tta)_3NH_2bppy$ (**2.8**) (tta = 2-thenoylacetonate) (Scheme 2.1.c). The absorption profiles of these complexes (Figure 2.4.a) are primarily dominated by absorption of the tta moieties, and feature greatly enhanced absorptivity values with respect to the ligands themselves. Solution and solid-state excitation and emission spectra of these complexes are shown in Figure 2.4.d. The excitation spectra indicate that population of the tta chromophore excited states is responsible for sensitization of Eu(III) luminescence; the $^5D_0 \leftarrow {}^7F_0$ absorption feature of the Eu(III) ion can be seen in the excitation spectra of the solid samples.

Luminescent lifetimes (τ_{obs}) and absolute quantum yields (Φ_{Eu}^{L}) were also measured. Attempts to model τ_{obs} of **2.7** and **2.8** reveals two components of luminescent relaxation in both solution and solid phases; in solution the longer-lived component

Table 2.3. Emissive τ_{obs} components of **2.7** and **2.8** and respective contributions of each

Complex	Solvent	τ_1 (μs)	Contribution (%)	τ_2 (μs)	Contribution (%)	χ^2
2.7	CH_2Cl_2	160 ± 20	20 ± 3	490 ± 10	80 ± 3	1.029
	Solid	41 ± 3	34 ± 2	361 ± 6	66 ± 2	1.030
2.8	CH_2Cl_2	66 ± 9	13 ± 1	380 ± 10	87.4 ± 0.5	0.994
	Solid	60 ± 2	52.7 ± 0.9	212 ± 2	47.3 ± 0.9	1.056

appears to have a much greater contribution to the luminescence decay, whereas in the solid state, the shorter-lived decay component exhibits an increased involvement in the decay process (Table 2.3). The greatly-increased contribution of the shorter lifetime in the solid state is consistent with the decreased quantum yield. By combining the weighted contributions of these components into an averaged lifetime measurement ($\tau_{obs,avg}$) and calculating the radiative lifetime (τ_{rad}), it is possible to obtain an approximation of sensitization efficiency (η_{sens}) and intrinsic quantum yield (Φ_{Eu}^{Eu}) (Equations 3 – 5); these data are reported in Table 2.4.[23,24]

$$1/\tau_{rad} = A_{MD,0} n^3 (I_{tot}/I_{MD}) \quad (3)$$

$$\Phi_{Eu}^{Eu} = \tau_{obs}/\tau_{rad} \quad (4)$$

$$\eta_{sens} = \Phi_{Eu}^{L} / \Phi_{Eu}^{Eu} \quad (5)$$

The absence of any observable ligand luminescence in all of the luminescence emission spectra is indicative of optimal intra-complex energy matching and minimal energy loss to radiative processes (Figure 2.4.d). One trend that holds true for both complexes is the

Table 2.4: Photophysical characterization of Eu(III) emission of **2.7** and **2.8**

Complex	**Solvent**	λ_{ex} **(nm)**	τ_{obs} **(μs)**	$\tau_{obs,avg}$ **(μs)**	Φ_{Eu}^{L} **(%)**	τ_{rad} **(μs)**	Φ_{Eu}^{Eu} **(%)**	η_{sens} **(%)**
2.7	CH_2Cl_2	350	66 ± 9; 380 ± 10	339	24.2 ± 0.8	1,150	29	82
	solid	386	60 ± 2; 212 ± 2	132	1.1 ± 0.2	615	21	5
2.8	CH_2Cl_2	353	160 ± 20; 490 ± 10	424	30 ± 2	821	52	58
	solid	386	41 ± 3; 361 ± 6	252	10.2 ± 0.1	726	35	29

decrease of τ, Φ, and η_{sens} in solid-state measurements with respect to solution measurements. This is not surprising, as decreased distances between lanthanide complexes give rise to greater opportunity for N–H oscillators of the primary amino-groups to non-radiatively quench energy absorbed by the chromophores. We also attribute the difference in emission efficiencies of **2.7** and **2.8** to quenching involving the amine groups, as the 820 cm^{-1} difference in T_1 levels of the differing bppy ligands is unlikely to affect Eu(III) sensitization to a large extent; this is especially likely since the excitation spectra of all of these complexes are suggestive of Eu(III) luminescence occurring at wavelengths corresponding with light absorption of the tta moieties. Current research is underway to improve the luminescent efficiency of the amino-bppy complexes by synthetic modifications to remove the amine N–H oscillators in an effort to minimize excited-state quenching.[25]

CONCLUSIONS

This chapter describes four new nitro- or amino-substituted derivatives of bppy, their electronic properties, and have successfully demonstrated the utility of two of these ligands in sensitizing lanthanide luminescence.

The synthesis and characterization of the bppy derivatives described in this work should allow for further expansion of the library of possible ligands with an even larger range of electronic and chemical environments. Future studies will be focused on 4-pyrazolyl- hydroxylamines,[26,27] secondary or tertiary amines, amides, imines, nitroamines, azoxy compounds,[28] and diazonium salts.[29]Additionally, **2.2** and **2.6** lend themselves well to the formation of products resulting from a wealth of diazonium substitution chemistry, such as *bis*- aryl-, azido-,[30] azo-,[31] cyano-, fluoro-, hydroxyl-,[32]and mercapto- substituted bppy species, as well as those made possible by Buchwald-Hartwig amination conditions. The formation of **2.3** also presents the opportunity for asymmetric syntheses of bppy derivatives containing different substituents at either 4-position of the pyrazole rings, as is common in nucleophilic aryl substitution synthetic routes. Additionally, with established synthetic routes to form both mono- and di-substituted terminal amino-bppy ligands (**2.2** and **2.6**), condensation polymerization of bppy for Wolf Type II metallopolymer syntheses, and numerous other supramolecular structures that avoid the use of expensive metal catalysts are now possible.[33–36]

EXPERIMENTAL

Materials and Methods

All reagents were purchased from commercial sources and used without further purification. Dry diglyme was obtained from Sigma-Aldrich in Sure/Seal™ bottles and used without further drying. Compound **2.9** was synthesized via a literature procedure and the crystalline product was characterized by LRMS and melting-point determination.[37] Dry acetonitrile (MeCN) for electrochemical measurements was obtained using an Innovative Technology PureSolv 400 solvent purifier with a double

purifying column and stored in Schlenk storage flasks over 3 Å molecular sieves under nitrogen atmosphere.

Single-crystals for X-ray diffraction studies on **2.3**, **2.5,** and **2.6** were grown by slow evaporation of saturated dichloromethane solutions. X-ray diffraction data acquisition and analysis were performed by Dr. Vincent M. Lynch. Diffraction data for **2.5** were collected on a Rigaku AFC12 diffractometer with a Saturn 724+ CCD using a graphite monochromator with MoKα radiation (λ = 0.71073Å) at 100 K with the use of a Rigaku XStream low temperature device. Diffraction data for **2.3** and **2.6** data were collected on an Agilent Technologies SuperNova Dual Source diffractometer using a μ-focus Cu Kα radiation source (λ = 1.5418Å) with collimating mirror monochromators at 100 K (**2.4**) and 173 K (**2.6**) with the use of an Oxford Cryostream low temperature device. X-ray powder diffraction data of **2.4** was obtained on the same Agilent Technologies instrument, but powder diffraction data of **2.5** and **2.6** were collected on a Rigaku R-Axis Spider diffractometer with an image plate detector utilizing a graphite monochrometer, CuKα radiation (λ = 1.5418 Å) and Rigaku RINT RAPID control software for system automation. Further information regarding crystal structure data including powder diffraction data, refinement details, and tables of select bond lengths and angles is provided in the following X-ray Crystallography section.

NMR spectroscopy was performed using an Agilent MR 400 spectrometer; spectra were referenced to residual solvent peaks, with chemical shifts reported in ppm and coupling constants measured in Hz. Mass spectrometry was carried out using Micromass Autospec Ultima HRMS and Agilent 6530 QTOF instruments.IR spectra were recorded with a Thermo Nicolet Smart Performer ATR accessory on a Nicolet Avatar 330 FT-IR spectrophotometer. Elemental analysis was performed by Midwest

Micro Lab, LLC. Melting points were recorded on a Stanford Research Systems MP100 OptiMelt in open capillaries and are reported uncorrected.

UV-Vis absorption spectrophotometry and fluorescence spectroscopy excitation/emission measurements were performed in Starna quartz fluorometer cells with 1.0 cm path lengths. All room-temperature solution absorption, excitation and emission spectra were obtained in dichloromethane (DCM) solvent. Luminescence measurements were recorded on a Photon Technology International QuantaMaster 4 spectrofluorometer equipped with a calibrated 6-in. diameter K Sphere-B integrating sphere used for absolute quantum yield (Φ^{L}_{Eu}) measurements. Absolute quantum yields were calculated by dividing the area under the emission peak of the complex by the ddifference between the area under the excitation peak of the sample and that of either a solvent blank or solid $BaSO_4$ sample. 77 K luminescence measurements were performed by dissolving **2.2** in 2:2:1:1 diethyl ether: ethyl iodide: ethanol: toluene solvent mixture, then cooling to a solid glass in a quartz liquid nitrogen bath. The spectrum in Figure 2.5 was modeled using a two-peak polynomial fitting function in order to extrapolate the blue edge of phosphorescence for T_1 determination ($R^2 = 0.9963$).

Electrochemical experiments were carried out in a dry box under a nitrogen atmosphere using a GPES system from Eco. Chemie B. V. in 0.1 M solutions of tetrabutylammonium hexafluorophosphate in dry MeCN at a scan rate of 0.100 $V \cdot s^{-1}$. The electrochemical cell consisted of a 1.6 mm-diameter Pt button working electrode, Pt wire counter electrode and $Ag/AgNO_3$ reference electrode. All potentials were externally referenced to the ferrocene/ferrocenium (Fc/Fc^{+}) redox couple.

Synthesis

2,6-*bis*(4-nitropyrazol-1-yl)pyridine (2.1): In a dry box, 4-nitropyrazole (1.798 g, 15.90 mmol) was dissolved in dry diglyme (15 mL). To this solution NaH (0.520 g, 21.67 mmol) was added in small portions and stirred until H_2 (g) evolution ceased. 2,6-dibromopyridine (1.502 g, 6.34 mmol) was then added in one portion with stirring, and additional dry diglyme (50 mL) was added to the mixture. The resulting solution was removed from the dry box and heated in a 120 °C oil bath for 7 d under an N_2 atmosphere using standard Schlenk techniques. After cooling to room temperature, the reaction was quenched with H_2O (10 mL) and solvent was removed under vacuum to give a light brown solid. The solid was washed with deionized ice water (three x 50 mL portions), vacuum-filtered and then subjected to silica column chromatography using dichloromethane eluent. The product (R_f = 0.45) was isolated as a lustrous white needle-like crystalline solid (yield: 1.768g, 92.6%). ^{1}H-NMR (500 MHz, *d*-DMSO, 130 °C): 9.99 (s, 2H), 8.506 (s, 2H), 8.316 (t, 1H *J* = 1.5) 8.058 (d, 2H *J* = 6.0). ^{13}C{^{1}H}-NMR (100 MHz, *d*-DMSO, 130 °C): 148.0, 142.8, 137.1, 137.0, 127.6, 111.6. HR-MS (CI^+): calcd for $C_{11}H_7N_7O_4$ *m/*z 301.0560, found 301.0557. IR ($\bar{\nu}$, cm^{-1}): 3,162 (s, C – H), 3,148 (m, C – H), 1,615 (m, N – O), 1,405 (s, N – O). M.P.: 344.16 – 346.10 °C. Elemental Analysis: calcd C 43.86% H 2.34% N 32.55%, found C 43.73% H 2.28% N 32.32%.

2-bromo-6-(4-nitropyrazol-1-yl)pyridine (2.3) was formed as a yellow crystalline solid by-product in the previous reaction and isolated as the R_f = 0.8 band with silica column chromatography using dichloromethane eluent. ^{1}H NMR (400 MHz, $CDCl_3$): 9.24 (s,1H), 8.25 (s, 1H), 7.98 (d, 1H *J* = 8.0), 7.73 (t, 1H *J* = 7.9), 7.52 (d, 1H *J* = 7.8). ^{13}C{^{1}H}-NMR (100 MHz, $CDCl_3$): 149.8, 141.3, 140.6, 137.74, 137.65, 127.8, 126.4, 111.6. HR-MS (ESI^+): calcd for $C_8H_6BrN_4O_2$ $(M + H)^+$ *m/z* 270.96490, found

270.96520. IR ($\bar{\nu}$, cm^{-1}): 2,921 (m, C – H), 1,566 (m, N – O), 1,501 (m, N – O), 1,038 m, C – Br). M.P. 136.1 – 137.5 °C. Elemental Analysis: calcd C 35.71% H 1.87% N 20.82%, found C 34.89% H 1.73% N 20.13%.

2,6-*bis*(4-aminopyrazol-1-yl)pyridine (2.2): $PtO_2 \bullet H_2O$ (0.0811 g, 20% catalyst loading) was suspended in a 2:3 mixture of EtOH: ethyl acetate (EtOAc) (500 mL). H_2 gas was sparged through this mixture for 1 h. **1** (0.497 g, 1.65 mmol) was then added to this mixture in one portion and the stirred suspension was sparged with H_2 gas for an additional hour then sealed under a H_2 atmosphere. The sealed reaction mixture was stirred an additional 3 d at room temperature with 1 h H_2 sparge cycles every 24 h. The reaction was then vacuum-filtered through Celite and concentrated under vacuum to yield a brown solid. The solid was subjected to silica column chromatography using a 5% v: v methanol: dichloromethane eluent. The last band (R_f = 0.15) was isolated and concentrated to give a yellow solid (yield: 0.320 g, 80.5%). ^{1}H-NMR (400 MHz, *d*-DMSO): 7.93 (d, 2H J = 1.0), 7.92 (t, 1H *J* = 8.0), 7.54 (d, 2H *J* = 8.0), 7.38 (d, 2H *J* = 0.98), 4.41 (s, 4H). $^{13}C\{^1H\}$-NMR (100 MHz, *d*-DMSO): 150.1, 141.5, 135.1, 134.1, 111.09, 106.54. HR-MS (CI^+): calcd for $C_{11}H_{11}N_7$ *m/z* 241.1076, found 241.1075. IR ($\bar{\nu}$, cm^{-1}): 3,310 (b, N – H), 2,962 (m, C – H), 1,603 (s, N – H), 1,577 (s, N – H), 1,259 (s, C – N amine). M.P. 168.19 – 213.16 °C (decomp.). Elemental Analysis: calcd C 54.76% H 4.60% N 40.64%, found C 54.93% H 4.41% N 38.24%

2-bromo-6-(pyrazole-1-yl)pyridine (2.4): This compound was prepared following a slightly-modified literature procedure.[38] In a dry box, 1-H-pyrazole (0.657 g, 9.75 mmol) was dissolved in dry diglyme (15 mL). To this solution NaH (60 % in oil, 0.458 g, 11.41 mmol) was added in small portions and stirred until H_2 (g) evolution ceased. 2,6-dibromopyridine (2.457 g, 10.37 mmol) was then added in one portion with

stirring, and additional dry diglyme (20 mL) was added to the mixture. The resulting solution was removed from the dry box and heated in a 70 °C oil bath for 2 d under an N_2 atmosphere using standard Schlenk techniques. After cooling to room temperature, the reaction was quenched with H_2O and solvent was removed to give a light brown solid. The solid was extracted with DCM, washed with H_2O then subjected to silica column chromatography using DCM eluent. The product (R_f = 0.65) was isolated as a white crystalline solid (1.17 g, 50.2% yield). ^{1}H-NMR (400 MHz, $CDCl_3$): 8.31 (d, 1H *J* = 2.6), 7.93 (d, 1H *J* = 8.0), 7.73 (s, 1H), 7.65 (td, 1H *J* = 7.8, 1.2), 7.35 (d, 1H *J* = 7.72, 0.8), 6.46 (m, 1H).

2-(4-nitropyrazol-1-yl)-6-(pyrazol-1-yl)pyridine (2.5): In a dry box, 4-nitropyrazole (0.505 g, 4.46 mmol) was dissolved in dry diglyme (15 mL). To this solution NaH (60% wt. in oil, 0.156 g, 3.90 mmol) was added in small portions and stirred until H_2 (g) evolution ceased. **4** (0.500 g, 2.23 mmol) was then added in one portion with stirring, and additional dry diglyme (5 mL) was added to the mixture. The resulting solution was removed from the dry box and heated in a 120 °C oil bath for 4 d under an N_2 atmosphere using standard Schlenk techniques. After cooling to room temperature, the reaction was quenched with H_2O (10 mL) and solvent was removed under vacuum to give a canary-yellow solid. This solid was dissolved in DCM, washed with H_2O then subjected to silica column chromatography using DCM eluent. The product (R_f = 0.5) was isolated as a white crystalline solid (0.509 g, 89.0% yield). ^{1}H-NMR (400 MHz, $CDCl_3$): 9.25 (d, 1H *J* = 0.72), 8.58 (dd, 1H *J* = 2.6, 0.7), 8.29 (d, 1H *J* = 0.5), 8.04 (d, 1H *J* = 1.3), 8.07 – 7.99 (m, 2H), 7.94 – 7.87 (m, 1H), 7.82 – 7.77 (m, 1H), 6.55 (dd, 1H J = 2.6, 1.7). ^{13}C{^{1}H}-NMR (100 MHz, $CDCl_3$): 151.6, 143.1, 142.7, 137.6, 127.3, 125.9, 112.0, 110.0, 108.8. HR-MS (ESI^+): calcd for $C_{11}H_8N_6O_2$ ($[M+Na]^+$)

m/z 279.0610, found 279.03090. IR ($\bar{\nu}$, cm^{-1}): 3,175 (s, C – H), 3,130 (m, C – H), 2,922 (m, C – H), 1,605 (m, N – O), 1,397 (s, N – O). M.P. 167.0 °C (decomp.). Elemental Analysis: calcd C 51.56% H 3.15% N 32.80%, found C 51.88% H 3.12% N 32.68%.

2-(4-aminopyrazol-1-yl)-6-(pyrazol-1-yl)pyridine (2.6): PtO_2•H_2O (0.0074 g, 5% catalyst loading) was suspended in a 1:1 mixture of EtOH: EtOAc (100 mL). H_2 gas was sparged through this mixture for 20 min. **5** (0.154 g, 0.599 mmol) was then added to this mixture in one portion and the stirring suspension was sparged with H_2 gas for an additional hour then sealed under a H_2 atmosphere. The sealed reaction mixture was stirred an additional 1 d at room temperature and reaction progress was monitored via TLC (5% v/v MeOH/DCM on silica). After 1 d an additional 0.007 g (5% cat. loading) PtO_2•H_2O was added to the stirring reaction accompanied by a 30 min sparge with H_2. The reaction was allowed to proceed for an additional day in a 45 °C oil bath. The reaction was then vacuum-filtered through Celite and concentrated to yield a yellow oil. This oil was subjected to silica column chromatography using a 2% v: v methanol: dichloromethane eluent. The last band (R_f = 0.10) was isolated and concentrated to give a brown crystalline solid (0.095 g, 70.4% yield). ^{1}H-NMR (400MHz, $CDCl_3$): 8.53 (d, 1H *J* = 2.64), 8.08 (d, 1H *J* = 0.96), 7.85 (t, 1H *J* = 8.0), 7.77-7.68 (m, 3H), 7.43 (d, 1H *J* = 1.0), 6.47 (dd, 1H *J* = 1.6, 0.7), 3.12 (s, 2H). ^{13}C{^{1}H}-NMR (100 MHz, $CDCl_3$): 142.4, 141.2, 135.4, 131.4, 127.1, 114.0, 110.5, 108.7, 108.5, 108.0, HR-MS (ESI^+): calcd for $C_{11}H_{10}N_6$ ($[M+Na]^+$) *m/z* 279.0610, found 279.03090. IR ($\bar{\nu}$, cm^{-1}): 3,347 (m, CN – H), 3,203 (m, N – H), 2,922 (m, C – H), 2852 (m, C – H) 1,602 (s, N – H), 1,578 (s, N – H). M.P. 150.2 – 158.4 °C. Elemental Analysis: calcd C 58.40% H 4.46% N 37.15%, found C 57.75% H 4.15% N 35.64%

$Eu(tta)_3X$ (complexes 2.7 and 2.8): Both complexes were synthesized following the same procedure; the synthesis of complex **2.7** is described as a general example: Ligand **2.7** (0.025 g, 0.104 mmol) was combined with **2.9** (0.088 g, 0.104 mmol) and dissolved in acetone (20 mL). The solution was refluxed for 30 min, stirred at room temperature overnight and then concentrated under vacuum to give a pale brown solid. The solid was washed with hexanes, dried under vacuum and collected. We have, so far, been unable to obtain single crystals suitable for X-ray diffraction studies; bulk purity was assessed by elemental analysis and confirmed by the absence of splitting in the $5D_0 \rightarrow 7F_0$ Eu(III) ion emission spectra (indicative of one emissive species in the sample).[39]

$Eu(tta)(NH_2)_2bppy$ (2.7): (83.4 mg, 76.2% yield) HR-MS ($MALDI^+$): calcd for $C_{27}H_{19}EuF_6N_7O_4S_2$ ($[M\text{-}tta]^+$) *m/z* 836.00509, found 836.0045. . IR ($\bar{\nu}$, cm^{-1}): 3,105 (b, N – H), 2,962 (m, C – H). M.P. 104.1°C (decomp.). Elemental Analysis: calcd C 39.78% H 2.19% N 9.28%, found C 40.19% H 2.37% N 8.71%.

$Eu(tta)NH_2bppy$ (2.8): (32.2 mg, 46.0% yield) HR-MS (ESI^+): calcd for $C_{35}H_{22}EuF_9N_6O_6S_3$ ($[M+Na]^+$) *m/z* 1064.97210, found 1064.97290. IR ($\bar{\nu}$, cm^{-1}): 3,131 (b, N – H), 2,926 (w, C – H). M.P. 99.2 – 145.4 °C (decomp.). Elemental Analysis: calcd C 40.35% H 2.13% N 8.07%, found C 40.59% H 2.22% N 7.01%.

X-ray Crystallography

X-ray Experimental for $C_{11}H_8N_6O_2$ (2.5): Crystals grew as large, colorless prisms by slow evaporation from dichloromethane. The data crystal was cut from a larger crystal and had approximate dimensions; 0.62 x 0.42 x 0.30 mm. The data were collected on a Rigaku AFC12 diffractometer with a Saturn 724+ CCD using a graphite monochromator with MoKα radiation (λ = 0.71073Å). A total of 1138 frames of data were collected using ω-scans with a scan range of 0.5° and a counting time of 15 seconds

per frame. The data were collected at 100 K using a Rigaku XStream low temperature device. Details of crystal data, data collection and structure refinement are listed in Table 2.4. Data reduction were performed using the Rigaku Americas Corporation's Crystal Clear version 1.40.[40] The structure was solved by direct methods using SIR2004[41] and refined by full-matrix least-squares on F^2 with anisotropic displacement parameters for the non-H atoms using SHELXL-2014/7.[42] Structure analysis was aided by use of the programs PLATON98[43] and WinGX.[44] The hydrogen atoms on carbon were calculated in ideal positions with isotropic displacement parameters set to 1.2xUeq of the attached atom (1.5xUeq for methyl hydrogen atoms).

The function, $\Sigma w(|F_o|^2 - |F_c|^2)^2$, was minimized, where $w = 1/[(\sigma(F_o))^2 + (0.0457*P)^2 + (0.2349*P)]$ and $P = (|F_o|^2 + 2|F_c|^2)/3$. $R_w(F^2)$ refined to 0.0919, with R(F) equal to 0.0332 and a goodness of fit, S, = 1.06. Definitions used for calculating R(F), $R_w(F^2)$ and the goodness of fit, S, are given below.[45] The data were checked for secondary extinction effects but no correction was necessary. Neutral atom scattering factors and values used to calculate the linear absorption coefficient are from the International Tables for X-ray Crystallography (1992).[46] Figure 2.2 was generated using SHELXTL/PC.[47] Tables of positional and thermal parameters, bond lengths and angles, torsion angles and figures are found below.

Table 2.5: Crystal data and structure refinement for **2.5**.

Empirical formula	$C_{11}H_8N_6O_2$	
Formula weight	256.23	
Temperature	100(2) K	
Wavelength	0.71073 Å	
Crystal system	triclinic	
Space group	P -1	
Unit cell dimensions	a = 6.0442(17) Å	α = 72.362(7) °
	b = 8.393(2) Å	β = 89.297(7) °
	c = 11.447(3) Å	γ = 78.103(7) °
Volume	540.7(3) $Å^3$	
Z	2	
Density (calculated)	1.574 Mg/m^3	
Absorption coefficient	0.116 mm^{-1}	
F(000)	264	
Crystal size	0.620 x 0.420 x 0.300 mm^3	
θ range for data collection	3.450 to 27.484°.	
Index ranges	-7<=h<=7, -10<=k<=10, -14<=l<=13	
Reflections collected	7034	
Independent reflections	2419 [R(int) = 0.0191]	
Completeness to θ = 25.242°	99.2 %	
Absorption correction	Semi-empirical from equivalents	
Max. and min. transmission	1.00 and 0.901	
Refinement method	Full-matrix least-squares on F^2	
Data/restraints/parameters	2419 / 0 / 172	
Goodness-of-fit on F^2	1.057	
Final R indices [I>2σ(I)]	R1 = 0.0332, wR2 = 0.0904	
R indices (all data)	R1 = 0.0357, wR2 = 0.0919	
Extinction coefficient	n/a	
Largest diff. peak and hole	0.295 and -0.273 $e.Å^{-3}$	

Table 2.6: Atomic coordinates (x 10^4) and equivalent isotropic displacement parameters ($Å^2$ x 10^3) for **2.5**. U(eq) is defined as one third of the trace of the orthogonalized U^{ij} tensor.

	x	y	z	U(eq)
C1	10732(2)	9866(1)	1921(1)	14(1)
C2	12688(2)	10157(1)	2389(1)	16(1)
C3	14079(2)	8766(2)	3223(1)	18(1)
C4	13517(2)	7163(2)	3566(1)	17(1)
C5	11506(2)	7064(1)	3047(1)	13(1)
C6	7192(2)	11144(1)	587(1)	17(1)
C7	6317(2)	12751(2)	-189(1)	20(1)
C8	7963(2)	13714(2)	-153(1)	19(1)
C9	8910(2)	5228(1)	2847(1)	14(1)
C10	8849(2)	3548(1)	3435(1)	15(1)
C11	10735(2)	2870(1)	4279(1)	16(1)
N1	9740(2)	12786(1)	593(1)	18(1)
N2	9241(2)	11200(1)	1046(1)	14(1)
N3	10108(2)	8363(1)	2250(1)	13(1)
N4	10759(2)	5489(1)	3349(1)	14(1)
N5	11906(2)	4059(1)	4235(1)	16(1)
N6	7151(2)	2692(1)	3219(1)	16(1)
O1	5585(1)	3512(1)	2456(1)	20(1)
O2	7352(2)	1166(1)	3819(1)	25(1)

Table 2.7: Bond lengths [Å] and angles [°] for **2.5**.

C1-N3	1.3338(14)	C7-C8	1.4130(17)
C1-C2	1.3999(15)	C7-H7	0.95
C1-N2	1.4123(14)	C8-N1	1.3287(15)
C2-C3	1.3861(16)	C8-H8	0.95
C2-H2	0.95	C9-N4	1.3490(14)
C3-C4	1.3944(16)	C9-C10	1.3743(15)
C3-H3	0.95	C9-H9	0.95
C4-C5	1.3882(15)	C10-C11	1.4080(15)
C4-H4	0.95	C10-N6	1.4314(14)
C5-N3	1.3304(14)	C11-N5	1.3268(15)
C5-N4	1.4271(14)	C11-H11	0.95
C6-N2	1.3662(15)	N1-N2	1.3694(13)
C6-C7	1.3710(16)	N4-N5	1.3735(13)
C6-H6	0.95	N6-O1	1.2330(13)
N6-O2	1.2374(13)		
N3-C1-C2	124.32(10)	C2-C3-H3	119.8
N3-C1-N2	114.86(10)	C4-C3-H3	119.8
C2-C1-N2	120.82(10)	C5-C4-C3	116.49(10)
C3-C2-C1	116.91(10)	C5-C4-H4	121.8
C3-C2-H2	121.5	C3-C4-H4	121.8
C1-C2-H2	121.5	N3-C5-C4	125.26(10)
C2-C3-C4	120.49(10)	N3-C5-N4	113.77(9)
C4-C5-N4	120.97(10)	C6-C7-C8	105.08(10)
N2-C6-C7	106.59(10)	C6-C7-H7	127.5
N2-C6-H6	126.7	C8-C7-H7	127.5
C7-C6-H6	126.7	N1-C8-C7	112.02(10)
N1-C8-H8	124.0	C11-C10-N6	127.68(10)
C7-C8-H8	124.0	N5-C11-C10	110.39(10)
N4-C9-C10	105.06(9)	N5-C11-H11	124.8
N4-C9-H9	127.5	C10-C11-H11	124.8
C10-C9-H9	127.5	C8-N1-N2	104.20(9)
C9-C10-C11	106.93(10)	C6-N2-N1	112.12(9)
C9-C10-N6	125.39(10)	C6-N2-C1	127.30(10)
N1-N2-C1	120.54(9)	C9-N4-C5	125.79(9)
C5-N3-C1	116.49(10)	N5-N4-C5	121.11(9)
C9-N4-N5	113.10(9)	C11-N5-N4	104.51(9)
O1-N6-O2	124.16(10)	O2-N6-C10	117.42(10)
O1-N6-C10	118.42(10)		

Table 2.8: Anisotropic displacement parameters ($Å^2$ x 10^3) for **2.5**. The anisotropic displacement factor exponent takes the form: $-2\pi^2[h^2 a^{*2}U^{11} + ... + 2 h k a^* b^* U^{12}]$.

	U11	U22	U33	U23	U13	U12
C1	14(1)	13(1)	15(1)	-5(1)	2(1)	-3(1)
C2	17(1)	14(1)	21(1)	-6(1)	3(1)	-7(1)
C3	15(1)	21(1)	22(1)	-7(1)	-1(1)	-7(1)
C4	15(1)	17(1)	17(1)	-3(1)	-1(1)	-4(1)
C5	15(1)	12(1)	14(1)	-5(1)	3(1)	-5(1)
C6	17(1)	17(1)	17(1)	-6(1)	1(1)	-4(1)
C7	21(1)	19(1)	18(1)	-5(1)	-1(1)	-1(1)
C8	26(1)	13(1)	18(1)	-3(1)	3(1)	-2(1)
C9	15(1)	14(1)	14(1)	-4(1)	0(1)	-4(1)
C10	18(1)	13(1)	15(1)	-5(1)	2(1)	-5(1)
C11	20(1)	12(1)	16(1)	-2(1)	0(1)	-4(1)
N1	22(1)	11(1)	21(1)	-3(1)	4(1)	-6(1)
N2	16(1)	11(1)	16(1)	-3(1)	1(1)	-4(1)
N3	14(1)	13(1)	15(1)	-5(1)	1(1)	-4(1)
N4	14(1)	12(1)	14(1)	-3(1)	-1(1)	-4(1)
N5	18(1)	12(1)	16(1)	-1(1)	-2(1)	-2(1)
N6	20(1)	14(1)	16(1)	-6(1)	2(1)	-7(1)
O1	20(1)	21(1)	21(1)	-6(1)	-2(1)	-7(1)
O2	34(1)	14(1)	28(1)	-3(1)	-1(1)	-12(1)

Table 2.9: Hydrogen coordinates (x 10^4) and isotropic displacement parameters ($Å^2$ x 10^3) for **2.5**.

	x	y	z	U(eq)
H2	13046	11258	2146	20
H3	15425	8905	3564	22
H4	14461	6190	4125	20
H6	6508	10180	770	20
H7	4909	13134	-651	24
H8	7815	14887	-609	23
H9	7875	6031	2222	17
H11	11116	1723	4804	20

Table 2.10: Torsion angles [°] for **2.5**.

N3-C1-C2-C3	1.87(17)	C6-C7-C8-N1	-0.19(13)
N2-C1-C2-C3	178.62(10)	N4-C9-C10-C11	-0.42(12)
C1-C2-C3-C4	-0.04(17)	N4-C9-C10-N6	178.96(10)
C2-C3-C4-C5	-1.10(17)	C9-C10-C11-N5	0.65(13)
C3-C4-C5-N3	0.64(17)	N6-C10-C11-N5	178.71(10)
C3-C4-C5-N4	179.11(10)	C7-C8-N1-N2	0.03(12)
N2-C6-C7-C8	0.26(12)	C7-C6-N2-N1	-0.26(13)
C7-C6-N2-C1	177.36(10)	C2-C1-N3-C5	-2.32(16)
C8-N1-N2-C6	0.14(12)	N2-C1-N3-C5	178.14(9)
C8-N1-N2-C1	-177.66(9)	C10-C9-N4-N5	0.07(12)
N3-C1-N2-C6	5.42(16)	C10-C9-N4-C5	178.82(10)
C2-C1-N2-C6	174.14(10)	N3-C5-N4-C9	4.37(15)
N3-C1-N2-N1	-177.15(9)	C4-C5-N4-C9	175.86(10)
C2-C1-N2-N1	3.29(15)	N3-C5-N4-N5	-174.44(9)
C4-C5-N3-C1	1.02(16)	C4-C5-N4-N5	5.34(15)
N4-C5-N3-C1	-179.22(9)	C10-C11-N5-N4	-0.58(12)
C9-N4-N5-C11	0.32(12)	C11-C10-N6-O1	178.37(10)
C5-N4-N5-C11	179.27(9)	C9-C10-N6-O2	179.38(11)
C9-C10-N6-O1	-0.88(16)	C11-C10-N6-O2	-1.38(17)

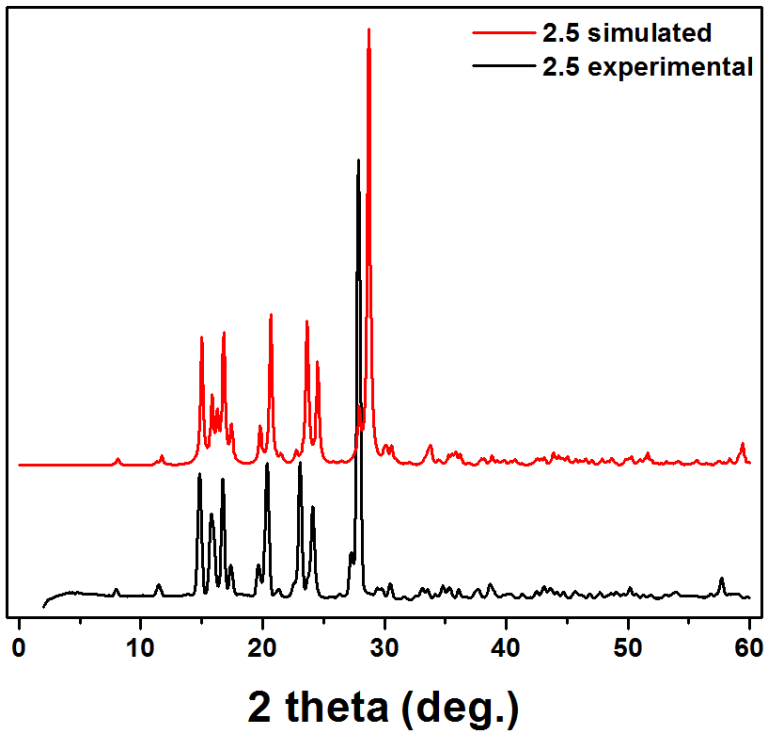

Figure 2.8: Experimental and simulated X-ray powder diffraction patterns of **2.5**.

X-ray Experimental for $C_{12}H_{11}N_5$ (2.6): Crystals grew as pale yellow plates by slow evaporation from dichloromethane. The data crystal had approximate dimensions; 0.18 x 0.06 x 0.06 mm. The data were collected on an Agilent Technologies SuperNova Dual Source diffractometer using a μ-focus Cu Kα radiation source (λ = 1.5418Å) with collimating mirror monochromators. A total of 965 frames of data were collected using ω-scans with a scan range of 1° and a counting time of 15 seconds per frame with a detector offset of +/- 41.9° and 48 seconds per frame with a detector offset of +/- 111.0°. The data were collected at 173 K using an Oxford Cryostream low temperature device. Details of crystal data, data collection and structure refinement are listed in Table 2.10. Data collection, unit cell refinement and data reduction were performed using Agilent Technologies CrysAlisPro V 1.171.37.31.[48] The structure was solved by direct methods

using SHELXT[49] and refined by full-matrix least-squares on F^2 with anisotropic displacement parameters for the non-H atoms using SHELXL-2016/6.[47] Structure analysis was aided by use of the programs PLATON98[43] and WinGX.[44] The hydrogen atoms were calculated in ideal positions with isotropic displacement parameters set to 1.2xUeq of the attached atom. The hydrogen atoms on the amine nitrogen, N6, were observed in a ΔF map and refined with isotropic displacement parameters.

The function, $\Sigma w(|F_o|^2 - |F_c|^2)^2$, was minimized, where $w = 1/[(\sigma(F_o))^2 + (0.1058*P)^2 + (0.3513*P)]$ and $P = (|F_o|^2 + 2|F_c|^2)/3$. $Rw(F^2)$ refined to 0.214, with R(F) equal to 0.0670 and a goodness of fit, S, = 1.05. Definitions used for calculating R(F), $Rw(F^2)$ and the goodness of fit, S, are given below.[45] The data were checked for secondary extinction effects but no correction was necessary. Neutral atom scattering factors and values used to calculate the linear absorption coefficient are from the International Tables for X-ray Crystallography (1992).[46] All figures were generated using SHELXTL/PC.[47] Tables of positional and thermal parameters, bond lengths and angles, torsion angles and figures are found below.

Table 2.11: Crystal data and structure refinement for **2.6**.

Empirical formula	$C_{12}H_{11}N_5$
Formula weight	225.26
Temperature	173(2) K
Wavelength	1.54184 Å
Crystal system	monoclinic
Space group	P 21/c
Unit cell dimensions	a = 22.9809(16) Å α = 90°
	b = 3.7881(3) Å β = 104.812(7)°
	c = 12.2183(9) Å γ = 90°
Volume	1028.31(14) $Å^3$
Z	4
Density (calculated)	1.455 Mg/m^3
Absorption coefficient	0.759 mm^{-1}
F(000)	472
Crystal size	0.180 x 0.060 x 0.060 mm^3
θ range for data collection	3.979 to 75.692°.
Index ranges	-19<=h<=28, -4<=k<=3, -15<=l<=15
Reflections collected	5061
Independent reflections	2060 [R(int) = 0.0500]
Completeness to θ= 67.684°	99.3 %
Absorption correction	Semi-empirical from equivalents
Max. and min. transmission	1.00 and 0.485
Refinement method	Full-matrix least-squares on F^2
Data/restraints/parameters	2060 / 0 / 162
Goodness-of-fit on F^2	1.050
Final R indices [I>2σ(I)]	R1 = 0.0670, wR2 = 0.1865
R indices (all data)	R1 = 0.0803, wR2 = 0.2137
Extinction coefficient	n/a
Largest diff. peak and hole	0.340 and -0.358 $e.Å^{-3}$

Table 2.12: Atomic coordinates (x 10^4) and equivalent isotropic displacement parameters ($Å^2$ x 10^3) for **2.6**. U(eq) is defined as one third of the trace of the orthogonalized U^{ij} tensor.

	x	y	z	U(eq)
C1	6872(1)	5198(6)	3314(2)	25(1)
C2	6825(1)	6797(6)	4314(2)	29(1)
C3	7360(1)	7520(6)	5113(2)	30(1)
C4	7904(1)	6685(6)	4906(2)	29(1)
C5	7895(1)	5066(6)	3874(2)	24(1)
C6	6319(1)	2818(6)	1442(2)	30(1)
C7	5726(1)	2497(7)	897(2)	35(1)
C8	5421(1)	3842(7)	1681(2)	38(1)
C9	8515(1)	2872(6)	2611(2)	26(1)
C10	9113(1)	2104(6)	2793(2)	28(1)
C11	9360(1)	2816(7)	3952(2)	32(1)
N1	5796(1)	4941(6)	2632(2)	34(1)
N2	6351(1)	4305(5)	2470(2)	28(1)
N3	7391(1)	4342(5)	3081(2)	25(1)
N4	8432(1)	4027(5)	3627(2)	25(1)
N5	8951(1)	3970(6)	4457(2)	34(1)
N6	9446(1)	1071(7)	2035(2)	36(1)

Table 2.13: Bond lengths [Å] and angles [°] for **2.6**.

C1-N3	1.334(3)	C5-N4	1.401(3)
C1-C2	1.393(3)	C6-C7	1.360(3)
C1-N2	1.408(3)	C6-N2	1.361(3)
C2-C3	1.386(3)	C6-H6	0.95
C2-H2	0.95	C7-C8	1.418(4)
C3-C4	1.376(3)	C7-H7	0.95
C3-H3	0.95	C8-N1	1.324(3)
C4-C5	1.397(3)	C8-H8	0.95
C4-H4	0.95	C9-C10	1.368(3)
C5-N3	1.335(3)	C9-N4	1.373(3)
C9-H9	0.95	C10-N6	1.399(3)

Table 2.13 Continued:

C10-C11	1.411(3)	N4-N5	1.354(2)
C11-N5	1.323(3)	N6-H6A	0.90(4)
C11-H11	0.95	N6-H6B	1.04(4)
N1-N2	1.361(3)		
N3-C1-C2	124.5(2)	N3-C1-N2	115.1(2)
C2-C1-N2	120.4(2)	C4-C3-C2	120.6(2)
C3-C2-C1	116.8(2)	C4-C3-H3	119.7
C3-C2-H2	121.6	C2-C3-H3	119.7
C1-C2-H2	121.6	C3-C4-C5	117.5(2)
C3-C4-H4	121.2	N3-C5-N4	115.81(19)
C5-C4-H4	121.2	C4-C5-N4	120.44(19)
N3-C5-C4	123.7(2)	C7-C6-N2	107.5(2)
C7-C6-H6	126.3	N4-C9-H9	126.7
N2-C6-H6	126.3	C9-C10-N6	130.5(2)
C6-C7-C8	104.0(2)	C9-C10-C11	104.6(2)
C6-C7-H7	128.0	N6-C10-C11	124.7(2)
C8-C7-H7	128.0	N5-C11-C10	112.3(2)
N1-C8-C7	112.5(2)	N5-C11-H11	123.9
N1-C8-H8	123.7	C10-C11-H11	123.9
C7-C8-H8	123.7	C8-N1-N2	103.9(2)
C10-C9-N4	106.60(19)	C6-N2-N1	112.07(19)
C10-C9-H9	126.7	C6-N2-C1	127.6(2)
N1-N2-C1	120.3(2)	C11-N5-N4	104.53(18)
C1-N3-C5	116.9(2)	C10-N6-H6A	119(3)
N5-N4-C9	111.94(18)	C10-N6-H6B	114(2)
N5-N4-C5	119.97(18)	H6A-N6-H6B	113(3)
C9-N4-C5	128.06(18)		

Table 2.14: Anisotropic displacement parameters ($Å^2$ x 10^3) for **2.6**. The anisotropic displacement factor exponent takes the form: $-2\pi^2[h^2 a^{*2} U^{11} + ... + 2 h k a^* b^* U^{12}]$

	U11	U22	U33	U23	U13	U12
C1	20(1)	26(1)	30(1)	4(1)	9(1)	0(1)
C2	24(1)	32(1)	34(1)	1(1)	14(1)	5(1)
C3	31(1)	32(1)	30(1)	-3(1)	13(1)	2(1)
C4	25(1)	31(1)	30(1)	-2(1)	6(1)	-1(1)
C5	18(1)	28(1)	29(1)	5(1)	9(1)	-1(1)
C6	22(1)	33(1)	35(1)	-2(1)	9(1)	-2(1)
C7	23(1)	37(1)	43(1)	-1(1)	6(1)	-6(1)
C8	16(1)	47(2)	50(1)	4(1)	7(1)	-2(1)
C9	19(1)	34(1)	26(1)	0(1)	7(1)	0(1)
C10	19(1)	34(1)	31(1)	2(1)	6(1)	-1(1)
C11	15(1)	50(1)	32(1)	1(1)	4(1)	-2(1)
N1	18(1)	44(1)	44(1)	2(1)	12(1)	2(1)
N2	16(1)	34(1)	35(1)	3(1)	9(1)	1(1)
N3	19(1)	30(1)	28(1)	2(1)	8(1)	1(1)
N4	16(1)	34(1)	26(1)	-1(1)	5(1)	1(1)
N5	20(1)	50(1)	28(1)	-1(1)	1(1)	2(1)
N6	22(1)	54(1)	34(1)	-2(1)	10(1)	5(1)

Table 2.15: Hydrogen coordinates (x 10^4) and isotropic displacement parameters ($Å^2$ x 10^3) for **2.6**.

	x	y	z	U(eq)		
H2	6446	7365	4443	35		
H3	7350	8603	5809	36		
H4	8273	7190	5444	35		
H6	6649	2130	1158	36		
H7	5555	1583	160	42		
H8	4995	3943	1539	45		
H9	8214	2649	1918	32		
H11	9773	2501	4328	39		
H6A	9716(18)		-690(120)		2240(40)	84(14)
H6B	9189(15)		830(100)		1210(30)	67(11)

Table 2.16: Torsion angles [°] for **2.6**.

N3-C1-C2-C3	-0.1(4)	C3-C4-C5-N4	-177.6(2)
N2-C1-C2-C3	178.6(2)	N2-C6-C7-C8	-0.8(3)
C1-C2-C3-C4	0.2(4)	C6-C7-C8-N1	0.6(3)
C2-C3-C4-C5	-0.6(4)	N4-C9-C10-N6	-175.0(2)
C3-C4-C5-N3	1.0(3)	N4-C9-C10-C11	1.0(3)
C9-C10-C11-N5	-0.6(3)	C7-C8-N1-N2	-0.1(3)
N6-C10-C11-N5	175.7(2)	C7-C6-N2-N1	0.9(3)
C7-C6-N2-C1	-178.7(2)	C8-N1-N2-C1	179.1(2)
C8-N1-N2-C6	-0.5(3)	N3-C1-N2-C6	-2.8(3)
C2-C1-N2-C6	178.4(2)	C10-C9-N4-C5	-178.8(2)
N3-C1-N2-N1	177.72(18)	N3-C5-N4-N5	166.33(19)
C2-C1-N2-N1	-1.2(3)	C4-C5-N4-N5	12.4(3)
C2-C1-N3-C5	0.5(3)	N3-C5-N4-C9	11.2(3)
N2-C1-N3-C5	178.34(17)	C4-C5-N4-C9	-170.1(2)
C4-C5-N3-C1	-0.9(3)	C10-C11-N5-N4	-0.1(3)
N4-C5-N3-C1	177.76(18)	C9-N4-N5-C11	0.8(3)
C10-C9-N4-N5	-1.1(3)	C5-N4-N5-C11	178.7(2)

Table 2.17: Hydrogen bonds for **2.6** [Å and °].

D-H...A	d(D-H)	d(H...A)	d(D...A)	<(DHA)
N6-H6A...N6#1	0.90(4)	2.27(4)	3.144(3)	165(4)
N6-H6B...N5#2	1.04(4)	2.07(4)	3.064(3)	160(3)

Symmetry transformations used to generate equivalent atoms:

#1 -x+2,y-1/2,-z+1/2 #2 x,-y+1/2,z-1/2

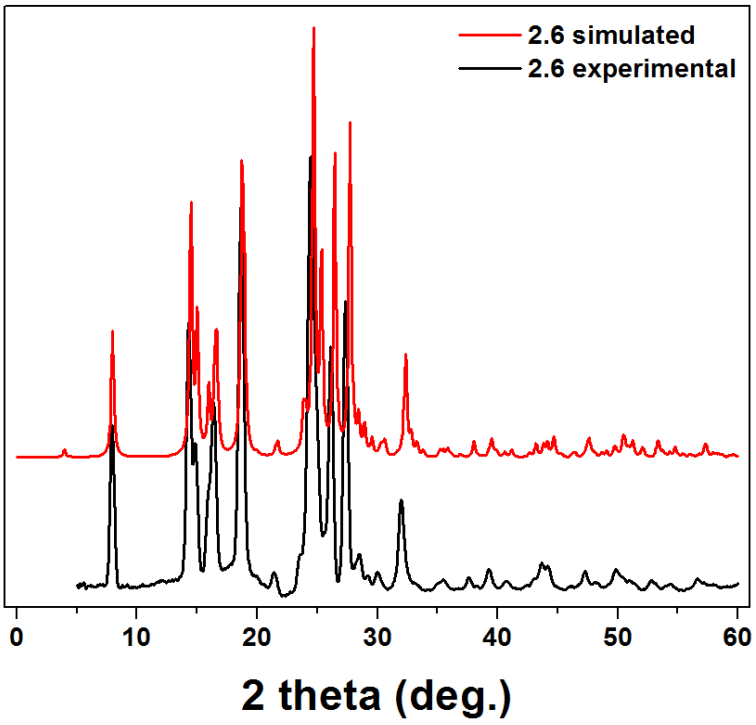

Figure 2.9: Experimental and simulated X-ray powder diffraction patterns of **2.6**.

X-ray Experimental for $C_8H_5N_4O_2Br$ (2.3): Crystals grew as colorless prisms by slow evaporation from dichloromethane. The data crystal had approximate dimensions; 0.39 x 0.18 x 0.046 mm. The data were collected on a Rigaku AFC12 diffractometer with a Saturn 724+ CCD using a graphite monochromator with MoKα radiation (λ = 0.71073Å). A total of 1299 frames of data were collected using ω-scans with a scan range of 0.5° and a counting time of 20 seconds per frame. The data were collected at 100 K using an Rigaku XStream low temperature device. Details of crystal data, data collection and structure refinement are listed in Table 2.17. Data reduction were performed using the Rigaku Americas Corporation's Crystal Clear version 1.40.[40] The structure was solved by direct methods using SIR2004[41] and refined by full-matrix least-squares on F^2 with anisotropic displacement parameters for the non-H atoms using

SHELXL-2016/6.[42] Structure analysis was aided by use of the programs PLATON98[43] and WinGX.[44] The hydrogen atoms on carbon were located in a ΔF map and refined with isotropic displacement parameters.

The function, $\Sigma w(|F_o|^2 - |F_c|^2)^2$, was minimized, where $w = 1/[(\sigma(F_o))^2 + (0.0328*P)^2 + (0.275*P)]$ and $P = (|F_o|^2 + 2|F_c|^2)/3$. $Rw(F^2)$ refined to 0.0680, with R(F) equal to 0.0269 and a goodness of fit, S, = 1.10. Definitions used for calculating R(F), $Rw(F^2)$ and the goodness of fit, S, are given below.[45] The data were checked for secondary extinction effects but no correction was necessary. Neutral atom scattering factors and values used to calculate the linear absorption coefficient are from the International Tables for X-ray Crystallography (1992).[46] All figures were generated using SHELXTL/PC.[47] Tables of positional and thermal parameters, bond lengths and angles, torsion angles and figures are found below.

Table 2.18: Crystal data and structure refinement for **2.3**.

Empirical formula	$C_8H_5BrN_4O_2$	
Formula weight	269.07	
Temperature	100(2) K	
Wavelength	0.71073 Å	
Crystal system	triclinic	
Space group	P -1	
Unit cell dimensions	a = 5.1820(14) Å	α = 77.698(7)°
	b = 8.556(3) Å	β = 81.398(7)°
	c = 11.285(3) Å	γ = 75.758(7)°
Volume	471.3(2) $Å^3$	
Z	2	
Density (calculated)	1.896 Mg/m^3	
Absorption coefficient	4.344 mm^{-1}	
F(000)	264	
Crystal size	0.390 x 0.180 x 0.046 mm^3	
θ range for data collection	3.377 to 27.367°.	
Index ranges	-6<=h<=6, -11<=k<=10, -14<=l<=14	
Reflections collected	6902	
Independent reflections	2125 [R(int) = 0.0408]	
Completeness to θ= 25.242°	99.6 %	
Absorption correction	Semi-empirical from equivalents	
Max. and min. transmission	1.00 and 0.576	
Refinement method	Full-matrix least-squares on F^2	
Data/restraints/parameters	2125 / 0 / 156	
Goodness-of-fit on F^2	1.096	
Final R indices [I>2σ(I)]	R1 = 0.0269, wR2 = 0.0666	
R indices (all data)	R1 = 0.0288, wR2 = 0.0680	
Extinction coefficient	n/a	
Largest diff. peak and hole	0.662 and -0.446 $e.Å^{-3}$	

Table 2.19: Atomic coordinates (x 10^4) and equivalent isotropic displacement parameters ($Å^2$ x 10^3) for **2.3**. U(eq) is defined as one third of the trace of the orthogonalized U^{ij} tensor.

	x	y	z	U(eq)
C1	4769(4)	7291(3)	3689(2)	16(1)
C2	6689(4)	8200(3)	3185(2)	18(1)
C3	8305(4)	7763(3)	2159(2)	19(1)
C4	7966(4)	6464(3)	1674(2)	16(1)
C5	5981(4)	5664(2)	2279(2)	14(1)
C6	3538(4)	3485(3)	2338(2)	14(1)
C7	3819(4)	2339(2)	1611(2)	14(1)
C8	5993(4)	2543(3)	720(2)	17(1)
Br1	2457(1)	7866(1)	5082(1)	20(1)
N1	4360(3)	6056(2)	3261(2)	16(1)
N2	5472(3)	4314(2)	1861(2)	14(1)
N3	7025(4)	3744(2)	874(2)	17(1)
N4	2168(3)	1181(2)	1736(2)	15(1)
O1	2461(3)	395(2)	910(2)	22(1)
O2	544(3)	1039(2)	2646(1)	21(1)

Table 2.20: Bond lengths [Å] and angles [°] for **2.3**.

C1-N1	1.324(3)	C1-Br1	1.904(2)
C1-C2	1.393(3)	C2-C3	1.386(3)
C2-H2	0.93(3)	C6-H6	0.91(3)
C3-C4	1.397(3)	C7-C8	1.412(3)
C3-H3	0.93(3)	C7-N4	1.434(3)
C4-C5	1.389(3)	C8-N3	1.321(3)
C4-H4	0.93(3)	C8-H8	0.97(3)
C5-N1	1.337(3)	N2-N3	1.377(2)
C5-N2	1.430(3)	N4-O2	1.232(2)
C6-N2	1.350(3)	N4-O1	1.232(2)
C6-C7	1.376(3)		
N1-C1-C2	125.2(2)	C3-C2-H2	120.0(17)
N1-C1-Br1	116.03(16)	C1-C2-H2	122.9(17)
C2-C1-Br1	118.77(16)	C2-C3-C4	120.1(2)
C3-C2-C1	117.1(2)	C2-C3-H3	118.7(18)
C4-C3-H3	121.2(19)	N2-C6-C7	104.66(18)
C5-C4-C3	116.4(2)	N2-C6-H6	121.1(18)
C5-C4-H4	116.5(17)	C7-C6-H6	134.2(18)
C3-C4-H4	127.1(17)	C6-C7-C8	107.12(18)
N1-C5-C4	125.50(19)	C6-C7-N4	125.84(19)
N1-C5-N2	113.51(18)	C8-C7-N4	127.04(19)
C4-C5-N2	120.98(18)	N3-C8-C7	110.38(19)
N3-C8-H8	119.1(19)	N3-N2-C5	120.17(17)
C7-C8-H8	130.5(19)	C8-N3-N2	104.49(17)
C1-N1-C5	115.75(18)	O2-N4-O1	124.15(18)
C6-N2-N3	113.33(17)	O2-N4-C7	118.60(17)
C6-N2-C5	126.49(18)	O1-N4-C7	117.25(18)

Table 2.21: Anisotropic displacement parameters ($Å^2$ x 10^3) for **2.3**. The anisotropic displacement factor exponent takes the form: $-2\pi^2[h^2 a^{*2} U^{11} + ... + 2 h k a^* b^* U^{12}]$

	U11	U22	U33	U23	U13	U12
C1	15(1)	15(1)	18(1)	-5(1)	-4(1)	-1(1)
C2	21(1)	15(1)	22(1)	-6(1)	-5(1)	-5(1)
C3	19(1)	17(1)	26(1)	-4(1)	-5(1)	-7(1)
C4	17(1)	16(1)	18(1)	-6(1)	-3(1)	-5(1)
C5	14(1)	11(1)	18(1)	-5(1)	-6(1)	-1(1)
C6	13(1)	16(1)	14(1)	-4(1)	-2(1)	-4(1)
C7	14(1)	12(1)	18(1)	-4(1)	-2(1)	-3(1)
C8	16(1)	17(1)	18(1)	-7(1)	0(1)	-4(1)
Br1	24(1)	18(1)	18(1)	-8(1)	-1(1)	-2(1)
N1	16(1)	14(1)	17(1)	-4(1)	-2(1)	-2(1)
N2	14(1)	14(1)	15(1)	-6(1)	-2(1)	-3(1)
N3	15(1)	18(1)	18(1)	-9(1)	2(1)	-3(1)
N4	16(1)	14(1)	18(1)	-5(1)	-3(1)	-4(1)
O1	25(1)	23(1)	24(1)	-15(1)	3(1)	-10(1)
O2	23(1)	22(1)	19(1)	-7(1)	5(1)	-10(1)

Table 2.22: Hydrogen coordinates (x 10^4) and isotropic displacement parameters ($Å^2$ x 10^3) for **2.3**.

	x	y	z	U(eq)
H2	6920(50)	9060(30)	3510(20)	19(6)
H3	9590(60)	8360(40)	1800(30)	26(7)
H4	8920(50)	6080(40)	990(30)	24(7)
H6	2370(50)	3770(30)	2990(30)	17(6)
H8	6780(60)	1950(40)	70(30)	30(8)

Table 2.23: Torsion angles [°] for **2.3**.

N1-C1-C2-C3	-0.4(3)	C2-C3-C4-C5	-0.6(3)
Br1-C1-C2-C3	178.97(16)	C3-C4-C5-N1	1.3(3)
C1-C2-C3-C4	0.2(3)	C3-C4-C5-N2	179.78(19)
N2-C6-C7-C8	0.7(2)	C4-C5-N1-C1	-1.6(3)
N2-C6-C7-N4	178.44(19)	N2-C5-N1-C1	179.48(18)
C6-C7-C8-N3	0.0(3)	C7-C6-N2-N3	-1.1(2)
N4-C7-C8-N3	179.1(2)	C7-C6-N2-C5	178.57(19)
C2-C1-N1-C5	1.1(3)	N1-C5-N2-C6	1.9(3)
Br1-C1-N1-C5	179.65(14)	C4-C5-N2-C6	-177.1(2)
N1-C5-N2-N3	178.41(17)	C6-C7-N4-O2	-9.2(3)
C4-C5-N2-N3	2.6(3)	C8-C7-N4-O2	171.9(2)
C7-C8-N3-N2	-0.6(2)	C6-C7-N4-O1	170.3(2)
C6-N2-N3-C8	1.1(2)	C8-C7-N4-O1	-8.6(3)
C5-N2-N3-C8	178.60(19)		

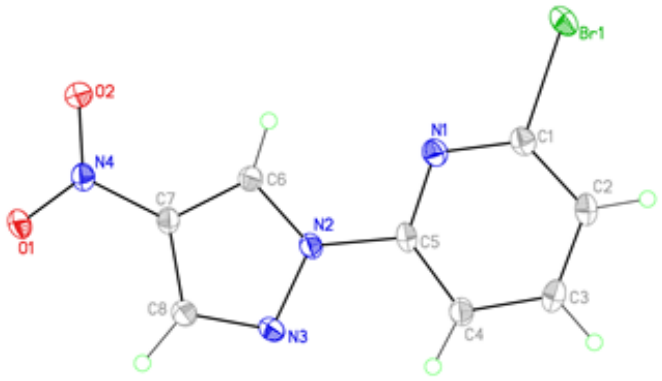

Figure 2.10: Single crystal structure of **2.3**. Displacement ellipsoids are scaled to the 50% probability level.

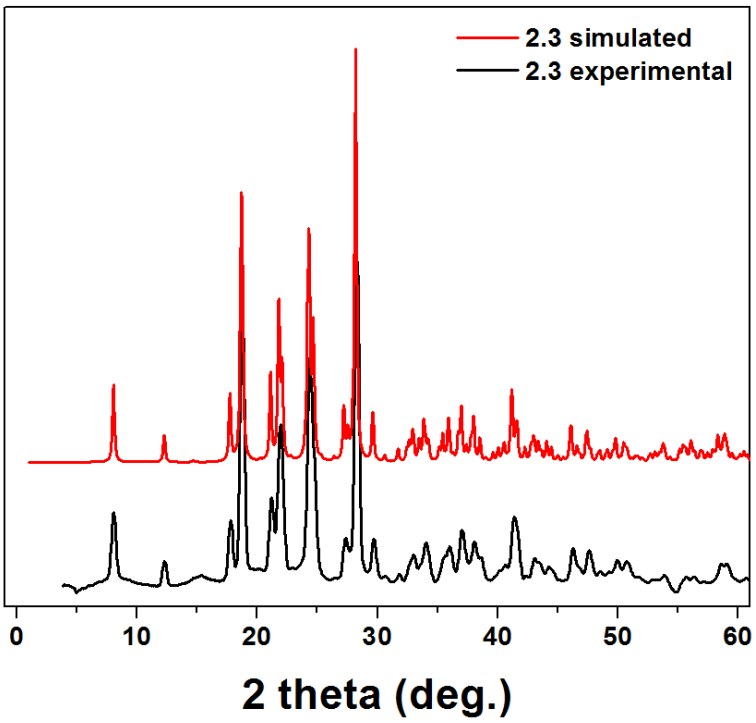

Figure 2.11: Experimental and simulated X-ray powder diffraction patterns of **2.3**.

CHAPTER NOTES AND REFERENCES

(1) Halcrow, M. A. *Coord. Chem. Rev.* **2009**, *253* (21–22), 2493–2514.

(2) Carlos, L. D.; Ferreira, R. A. S.; Bermudez, V. de Z.; Ribeiro, S. J. L. *Adv. Mater.* **2009**, *21* (5), 509–534.

(3) Wang, X.; Chang, H.; Xie, J.; Zhao, B.; Liu, B.; Xu, S.; Pei, W.; Ren, N.; Huang, L.; Huang, W. *Coord. Chem. Rev.* **2014**, *273–274*, 201–212.

(4) Fernández-Moreira, V.; Song, B.; Sivagnanam, V.; Chauvin, A.-S.; Vandevyver, C. D. B.; Gijs, M.; Hemmilä, I.; Lehr, H.-A.; Bünzli, J.-C. G. *Analyst* **2009**, *135* (1), 42–52.

(5) Jameson, D. L.; Blaho, J. K.; Kruger, K. T.; Goldsby, K. A. *Inorg. Chem.* **1989**, *28* (24), 4312–4314.

(6) Halcrow, M. A. *New J. Chem.* **2014**, *38* (5), 1868–1882.

(7) Zoppellaro, G.; Baumgarten, M. *Eur. J. Org. Chem.* **2005**, *2005* (14), 2888–2892.

(8) Zhu, X. J.; Holliday, B. J. *Macromol. Rapid Commun.* **2010**, *31* (9–10), 904–909.

(9) Basak, S.; Hui, P.; Chandrasekar, R. *Synthesis* **2009**, *2009* (23), 4042–4048.

(10) Basak, S.; Narayana, Y. S. L. V.; Baumgarten, M.; Müllen, K.; Chandrasekar, R. *Macromolecules* **2013**, *46* (2), 362–369.

(11) Narayana, Y. S. L. V.; Venkatakrishnarao, D.; Biswas, A.; Mohiddon, M. A.; Viswanathan, N.; Chandrasekar, R. *ACS Appl. Mater. Interfaces* **2016**, *8* (1), 952–958.

(12) Narayana, Y. S. L. V.; Basak, S.; Baumgarten, M.; Müllen, K.; Chandrasekar, R. *Adv. Funct. Mater.* **2013**, *23* (47), 5875–5880.

(13) Narayana, Y. S. L. V.; Baumgarten, M.; Müllen, K.; Chandrasekar, R. *Macromolecules* **2015**, *48* (14), 4801–4812.

(14) Basak, S.; Hui, P.; Boodida, S.; Chandrasekar, R. *J. Org. Chem.* **2012**, *77* (7), 3620–3626.

(15) Pritchard, R.; Kilner, C. A.; Barrett, S. A.; Halcrow, M. A. *Inorganica Chim. Acta* **2009**, *362* (12), 4365–4371.

(16) Mohammed, R.; Chastanet, G.; Tuna, F.; Malkin, T. L.; Barrett, S. A.; Kilner, C. A.; Létard, J.-F.; Halcrow, M. A. *Eur. J. Inorg. Chem.* **2013**, *2013* (5–6), 819–831.

(17) Govor, E. V.; Lysenko, A. B.; Quiñonero, D.; Rusanov, E. B.; Chernega, A. N.; Moellmer, J.; Staudt, R.; Krautscheid, H.; Frontera, A.; Domasevitch, K. V. *Chem. Commun.* **2011**, *47* (6), 1764–1766.

(18) Cardona, C. M.; Li, W.; Kaifer, A. E.; Stockdale, D.; Bazan, G. C. *Adv. Mater.* **2011**, *23* (20), 2367–2371.

(19) Huang, Y.; Zhang, M.; Ye, L.; Guo, X.; Han, C. C.; Li, Y.; Hou, J. *J. Mater. Chem.* **2012**, *22* (12), 5700–5705.

(20) Krumova, K.; Cosa, G. *J. Am. Chem. Soc.* **2010**, *132* (49), 17560–17569.

(21) Al-Anber, M.; Milde, B.; Alhalasah, W.; Lang, H.; Holze, R. *Electrochimica Acta* **2008**, *53* (20), 6038–6047.

(22) Wilkerson, J. M. Luminescent lanthanide-containing materials: from small molecules to conducting metallopolymers, The University of Texas at Austin: Austin, TX, 2012.

(23) Binnemans, K. *Coord. Chem. Rev.* **2015**, *295*, 1–45.

(24) Werts, M. H. V.; Jukes, R. T. F.; Verhoeven, J. W. *Phys. Chem. Chem. Phys.* **2002**, *4* (9), 1542–1548.

(25) Bünzli, J.-C. G. *Coord. Chem. Rev.* **2015**, *293–294*, 19–47.

(26) Tallec, A.; Hazard, R.; SuwiNski, J.; Wagner, P. *Pol. J. Chem.* **2000**, *47* (8), 1177–1183.

(27) Cuadrado, P.; González-Nogal, A. M.; Martínez, S. *Tetrahedron* **1997**, *53* (25), 8585–8598.

(28) Suwiński, J.; Wagner, P. *Pol. J. Chem.* **2000**, *74* (11), 1575–1580.

(29) Yin, P.; Zhang, J.; Parrish, D. A.; Shreeve, J. M. *Chem. - Eur. J.* **2014**, *20* (50), 16529–16536.

(30) Fevig, J. M.; Cacciola, J.; Buriak Jr., J.; Rossi, K. A.; Knabb, R. M.; Luettgen, J. M.; Wong, P. C.; Bai, S. A.; Wexler, R. R.; Lam, P. Y. S. *Bioorg. Med. Chem. Lett.* **2006**, *16* (14), 3755–3760.

(31) Kumar, R.; Joshi, Y. C.; Joshi, P. *Heterocycl. Commun.* **2005**, *11* (3–4), 361–364.

(32) De Sio, F. *Heterocycles* **1984**, *22* (10), 2309–2311.

(33) Wolf, M. O. *Adv. Mater.* **2001**, *13* (8), 545–553.

(34) de Hatten, X.; Asil, D.; Friend, R. H.; Nitschke, J. R. *J. Am. Chem. Soc.* **2012**, *134* (46), 19170–19178.

(35) Chow, C.-F. *J. Fluoresc.* **2012**, *22* (6), 1539–1546.

(36) Tennyson, A. G.; Norris, B.; Bielawski, C. W. *Macromolecules* **2010**, *43* (17), 6923–6935.

(37) De Silva, C. R.; Maeyer, J. R.; Wang, R.; Nichol, G. S.; Zheng, Z. *Inorganica Chim. Acta* **2007**, *360* (11), 3543–3552.

(38) Kumar, K. S.; Schäfer, B.; Lebedkin, S.; Karmazin, L.; Kappes, M. M.; Ruben, M. *Dalton Trans.* **2015**, *44* (35), 15611–15619.

(39) Horrocks, W. D.; Albin, M. In *Progress in Inorganic Chemistry*; Lippard, S. J., Ed.; John Wiley & Sons, Inc.: Hoboken, NJ, USA, 1984; Vol. 31, pp 1–104.

(40) *CrystalClear*; Rigaku Americas Corporation: The Woodlands, Texas, USA, 2008.

(41) Burla, M. C.; Caliandro, R.; Camalli, M.; Carrozzini, B.; Cascarano, G. L.; De Caro, L.; Giacovazzo, C.; Polidori, G.; Spagna, R. *J. Appl. Crystallogr.* **2005**, *38* (2), 381–388.

(42) Sheldrick, G. M. *Acta Crystallogr. Sect. C Struct. Chem.* **2015**, *71* (1), 3–8.

(43) Spek, A. L. *PLATON98*; Utrecht University: Padualaan 8, 3584 CH Utrecht, The Netherlands, 1998.

(44) Farrugia, L. J. *J. Appl. Crystallogr.* **1999**, *32* (4), 837–838.

(45) $R_w(F^2) = \{S_w(|F_o|^2 - |F_c|^2)^2/S_w(|F_o|)^4\}^{1/2}$ where w is the weight given each reflection. $R(F) = S(|F_o| - |F_c|)/S|F_o|\}$ for reflections with $F_o > 4(s(F_o))$. $S = [S_w(|F_o|^2 - |F_c|^2)^2/(n - p)]^{1/2}$, where n is the number of reflections and p is the number of refined parameters.

(46) *International Tables for X-ray Crystallography*; Kluwer Academic Press: Boston, MA, USA, 1992; Vol. C.

(47) Sheldrick, G. M. *SHELXLT/PC*; Siemens Analytical X-ray Instruments, Inc.: Madison, WI, USA, 1994.

(48) *CrysAlisPro*; Agilent Technologies UK Ltd.: Oxford, UK, 2013.

(49) Sheldrick, G. M. *Acta Crystallogr. Sect. A* **2015**, *71* (1), 3–8.

Chapter 3: Modification of EDOT-substituted *Bis*-2,6(pyrazole-1-yl)pyridine Ligands Towards Improved Europium(III) Luminescent Materials

INTRODUCTION

Light emission by lanthanide (III) ions has garnered much attention in numerous areas of research due to distinguishing features they exhibit. These features include large Stokes shifts, extremely long radiative lifetimes, and characteristically narrow emission profiles arising from the shielded nature of the 4*f* orbitals where these electronic transitions occur. These characteristic properties have helped Ln(III) luminescence find numerous applications in areas such as biomarkers and bioimaging,[1–4] emissive materials for lighting and displays,[5–9] security tags,[8,10,11] photodynamic cancer treatments,[4,12,13] and laser materials.[14,15] The spin-and parity-forbidden nature of these transitions necessitate the use of antennae ligands for appreciable emission intensities to be achieved. Among the various lanthanide emissive species, Eu (III) is a prominent and well-utilized luminophor, perhaps due to the desirable visible-light emission it produces, or simply the length of time it has been studied, having been examined in the seminal work of Weissman (reported in 1942) which described the first investigation of Ln (III) luminescence utilizing the antenna effect.[16]

2,6-*Bis*(pyrazol-1-yl)pyridine (bppy) has been shown to exceptionally facilitate Eu (III) emission when incorporated into a $Eu(tta)_3bppy$ complex (tta: 2-thenoyltrifluoroacetonate) (Φ_{solid} = 93 ± 3%).[17] Additionally, this class of molecule is attractive for its ease of synthetic modification on all heteroaromatic rings; substitution of the pyridine ring primarily occurs at the 4- position, and the pyrazole rings can readily be

modified at the 3-, 4-, and 5- positions, providing a facile path to tailoring metal complexes utilizing these ligands for a broad range of applications.[18–20] Notably, bppy Ln (III) complexes have been successfully incorporated into numerous metallopolymers via catalytic C-C coupling to give several lanthanide-containing color-tuned emissive materials.[21–26] The incorporation of sulfur-containing thiophene and 3,4-(ethylenedioxy)thiophene (EDOT) derivatives into luminescent complexes may be beneficial by virtue of increased conjugation across the ligand, which in turn lowers the T_1 donor energy level;[27] in many cases, these moieties have also served as a route to metallopolymer fabrication via electropolymerization.[27–32]

Incorporation of emissive metal centers directly into the conductive backbone of metallopolymer emissive layers for lighting applications is highly advantageous, as such a structural motif mitigates the problems of ligand-metal electronic communication, non-uniform emitter dispersion, phase separation and concentration quenching.[33,34] Attachment of EDOT substituents to the 4-positions of the pyrazole rings of bppy has been used to create a poly[Ru[$(EDOT)_2$bppy](terpy)$(PF_6)_2$] conducting metallopolymer,[29] as well as an emissive Eu$(tta)_3(EDOT)_2$bppy complex;[27] however, fluorimetry of this complex revealed a lower quantum yield with respect to Eu$(tta)_3$bppy, presumably as a result of less-efficient Eu(III) sensitization owing to a decreased ligand T_1 donor energy level which is caused by the extended conjugation of the sensitizing ligand upon appending the EDOT groups.[17] Additionally, Eu$(tta)_3(EDOT)_2$bppy was found to be not readily electropolymerized.

In order to retain the high quantum yield of Eu$(tta)_3$bppy while incorporating this complex into uniform electropolymerizable metallopolymer films, the central sensitizing portion of the ligand must not be conjugated with the rest of the polymer. Amides have been employed as spacers that limit π-conjugation between otherwise-conjugated

systems,[35,36] and with newly-developed synthetic methods, it is now feasible to append these groups in an analogous manner to the 4-position of the pyrazole rings of bppy.[37] This chapter details efforts to separate electronic communication between the central bppy core and the EDOT substituents by incorporating amide spacers between the two moieties in order to raise the ligand T_1 donor level, improve electropolymerization and retain the heavy-atom effect imparted by the EDOT substituents.

SYNTHESIS

The synthesis of amide ligands **3.2** and **3.3** began with the previously reported synthesis of **$(NH_2)_2$bppy** (**2.2**) via reduction of **$(NO_2)_2$bppy** (**2.1**) (Scheme 3.1).[37] EDOT was treated with *n*-BuLi, followed by CO_2 (g) and excess HCl to give the 2-carboxylic acid (**3.1**). This was converted to the acid chloride then condensed with **2.2** without further purification in the presence of a suitable trapping base to give the secondary amide **3.2**. Deprotonation of the amide functionalities with sodium hydride and subsequent methylation using methyl iodide yielded the tertiary amide **3.3**. Metalation was achieved by refluxing ligands **3.2** and **3.3** with **$Eu(tta)_3 \cdot 2H_2O$** (**2.9**) to give complexes **3.5** and **3.6**.

CRYSTAL STRUCTURES OF COMPOUNDS 3.2 AND 3.3

Examination of the crystal structures and key angles of **3.2** and **3.3** (Figure 3.1) obtained by single-crystal X-ray diffraction studies suggest conjugation between the bppy and EDOT portions of the molecules is decreased, if not interrupted completely. The torsion angles between the planes of the conjugated portions of the EDOT and bppy moieties of the previously reported $(EDOT)_2$bppy ligand are 6.32 and 13.25°; analogous measurements of the same rings in ligand **3.2** and ligand **3.3** exhibit moderate and drastic decreases in planarity across the molecules, respectively.[29] These angles are indicative of

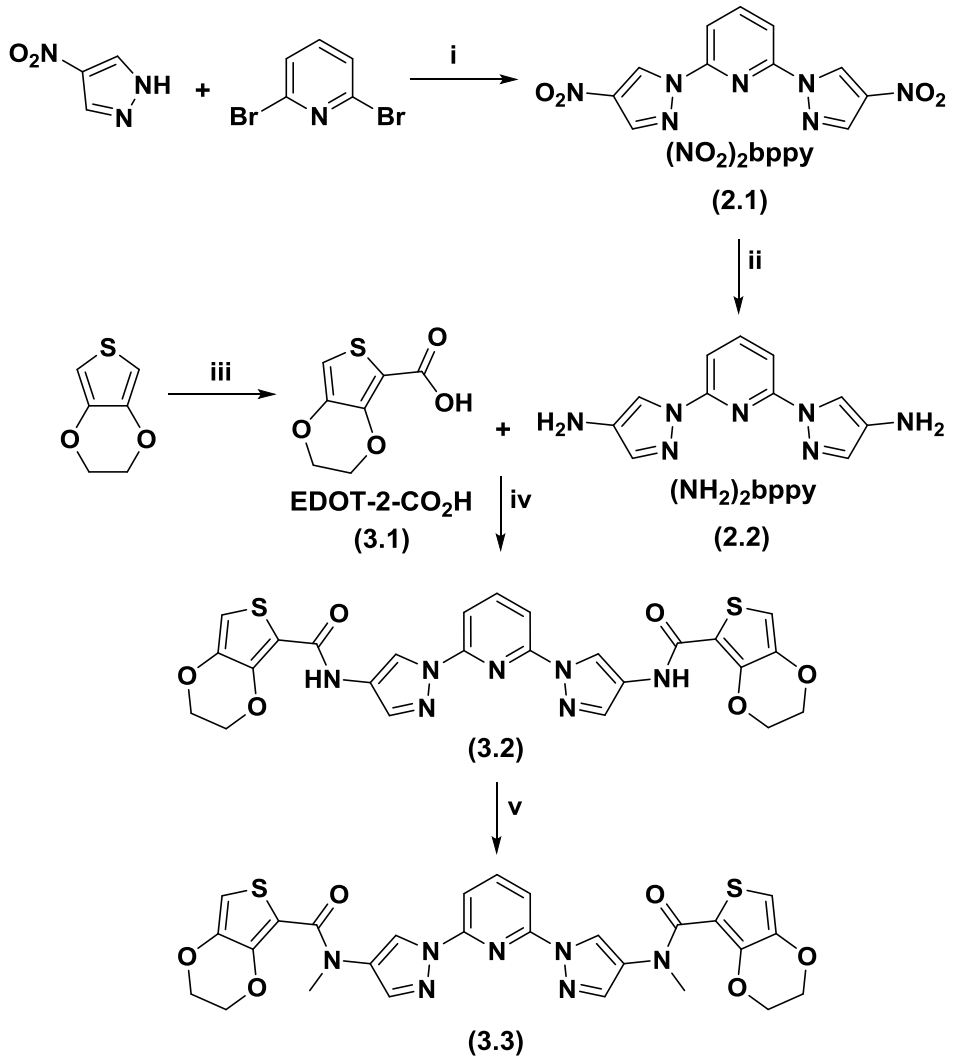

Scheme 3.1: Synthesis of amide-linked EDOT-bppy ligands **3.2** and **3.3**. i) NaH, dry diglyme, 120 °C 7 d; yield = 93% ii) 0.2 eq. $PtO_2 \bullet H_2O$, H_2 (g), 1:1 ethyl acetate: ethanol, 36 h; yield = quantitative iii) 1. n-BuLi, THF, -78 °C 2. CO_2 (g) 3. Excess HCl; yield = 89% iv) 1. $SOCl_2$ (neat), 90 °C 2. Proton-sponge®, dry DCM, 50 °C 18h; yield =98% v) MeI, NaH, DMF; yield = 74%.

decreased π-orbital overlap between the bppy portion and the EDOT portions of the ligands.

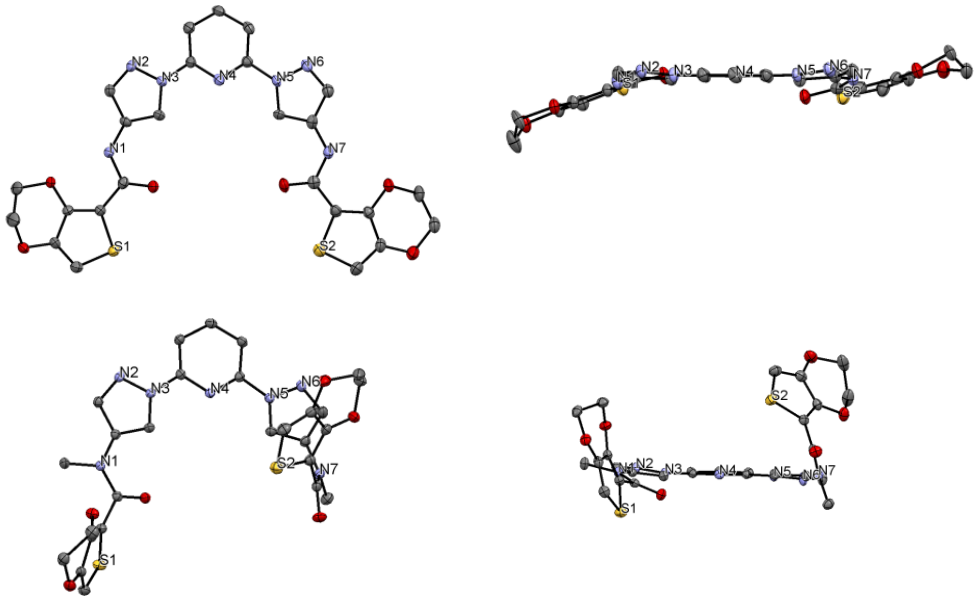

Ligand	S1-N2 angle	S2-N5 angle	N2-N4 angle	N6-N4 angle
3.2	9.16	23.06	9.03	6.16
3.3	65.68	58.85	7.72	7.08

Figure 3.1: Crystal structures of **3.2** (top) and **3.3** (middle), as viewed facing (left) and parallel to (right) the plane of the bppy moieties of each ligand. Select angles between planes of the aromatic rings are in the bottom table; angles are measured in degrees and rings are denoted by the labeled heteroatoms they contain. Hydrogen atoms are omitted for clarity.

ABSORPTION AND EMISSION SPECTROSCOPY OF 3.2, 3.3, 3.5 AND 3.6

UV-vis absorption spectroscopy of these ligands and their corresponding Eu(III) complexes in dichloromethane (DCM) was performed and the resulting spectra are shown in Figure 3.2. The molar absorptivities of **3.2** and **3.3** were determined as 27,143 M^{-1} cm^{-1} and 30,741 $M^{-1}cm^{-1}$ respectively. **3.2** exhibits familiar $\pi \rightarrow \pi^*$ transitions characteristic of bppy with very little shift in wavelengths, which is also indicative of conjugation interruption between the EDOT and central bppy portions of the molecule.

Additionally, a new absorption is seen to appear in the spectra of both **3.2** and **3.3** at approximately 325 nm, which we assign to $n \rightarrow \pi^*$ transitions of the amide linkers themselves. UV-vis spectra of the Eu(III) complexes, **3.5** and **3.6**, show absorption features of both the diketonate and bppy ligands, but are largely dominated by tta absorbance features.

Fluorimetry of these molecules and the associated $Eu(tta)_3$ complexes was performed both at room temperature and at 77 K. (Figure 3.3). At room temperature, both ligands exhibit broad featureless emission profiles, similar in energy and shape to that of bppy, indicating similar electronic transitions as well as a limiting of the electronic communication between the EDOT and bppy.[17] In addition, the metalated species exhibit very desirable pure Eu(III) emissions with no detectable ligand fluorescence. Fluorimetry measurements of **3.2** and **3.3** were performed at 77 K to determine the energy of the T_1 excited state by assigning the blue edge of phosphorescence as the $0-0$ $T_1 \rightarrow S_0$

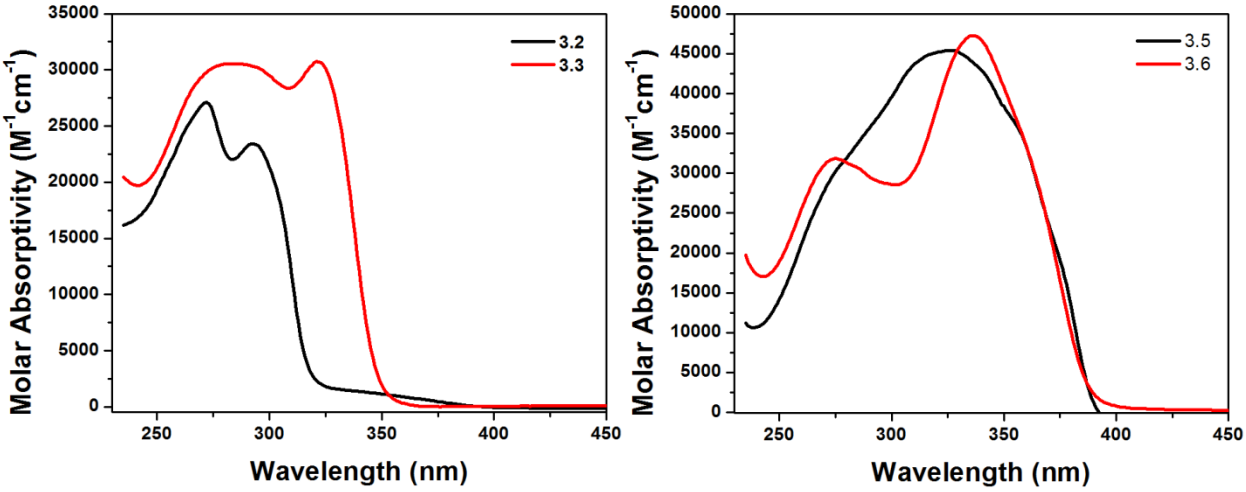

Figure 3.2: UV-vis absorption spectra of **3.2** and **3.3** (left) and **3.5** and **3.6** (right).

transition;[38] the T_1 of the sensitizing ligand is generally considered the primary donor energy level involved in lanthanide luminescence.[8,39] Efforts to determine the bound-state ligand energy by performing fluorimetry of ligands metalated with $Gd(tta)_3$ were unsuccessful, as the 77 K emission profiles were largely dominated by phosphorescence from the diketonate moieties.

Compared to that of **$(EDOT)_2$bppy**, the T_1 of both **3.2** and **3.3** are larger, which was expected to result in greater absolute quantum yields (Φ_{abs}) for the Eu complexes. However, Φ_{abs} measurements revealed decreased values for Eu (III) complexes involving both ligand systems (Table 3.1); when viewed in conjunction with the structural and photophysical evidence of lessened ligand conjugation, the presence of a new emission deactivation mechanism appears highly probable. Such deactivation may arise from the $n \rightarrow \pi^*$ transitions in the absorption spectra, PET quenching involving the amides,[3,8] or in the case of **3.5**, the presence of N-H oscillators which have been shown to non-radiatively quench Eu (III) luminescence;[8] this is supported by the larger Φ_{abs} of **3.6** than that of **3.5**. Though the solid-state structures of these complexes differ drastically, the T_1 energy levels of **3.2** and **3.3** only differ by 431 cm^{-1}, supporting the notion that methylation of the amide is of little consequence to the electronic environment of the ligands.

Table 3.1: Φ_{abs} and T_1 Energy of bppy Ligands

	bppy[17]	**$(EDOT)_2$bppy**[27]	**3.2**	**3.3**
Φ_{abs}	0.60 ± .05	0.28 ± .01	0.126 ± .005	0.17± .02
T_1 (cm^{-1})	26,000	21,473	23,041	23,474

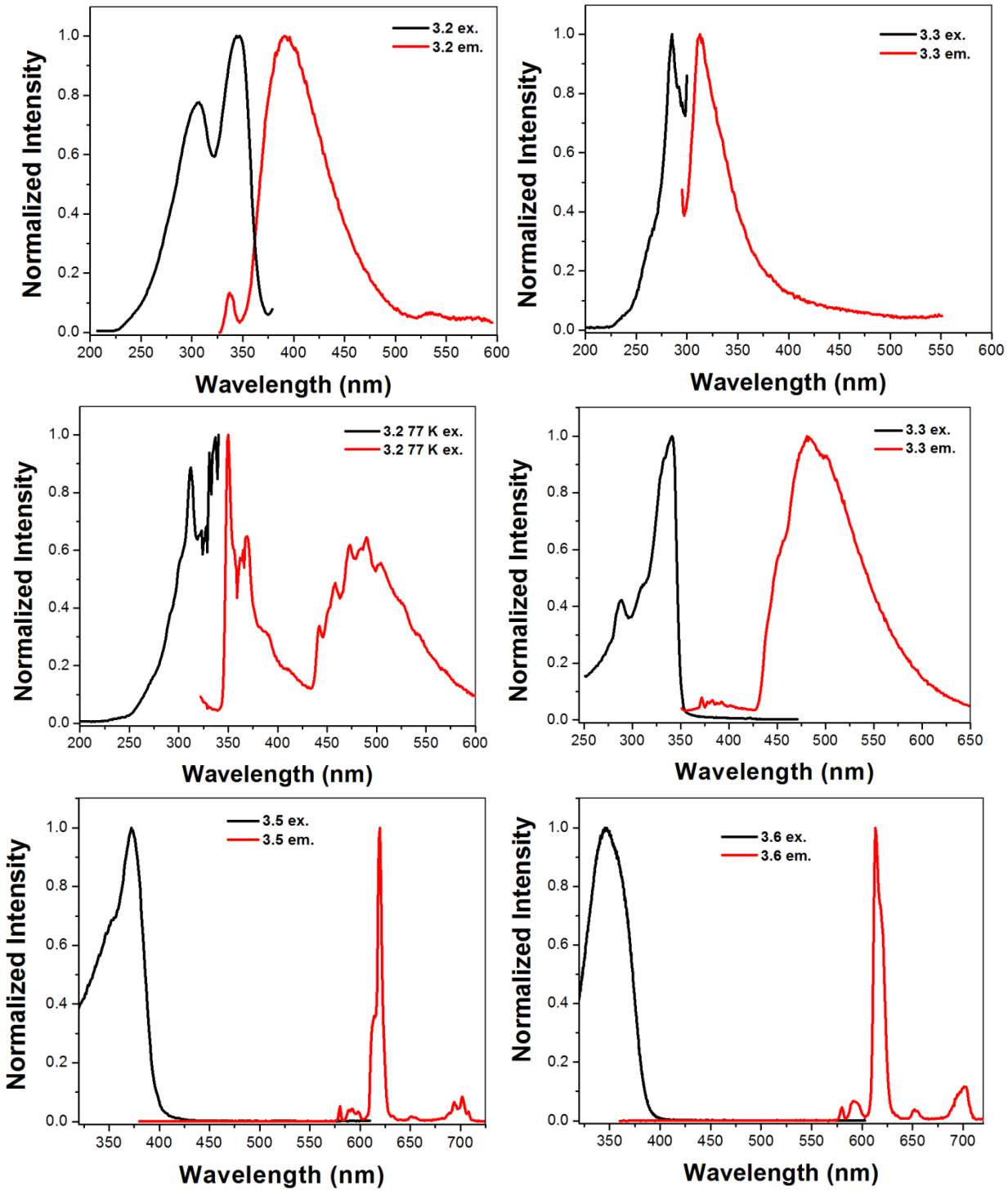

Figure 3.3: RT ligand (top), 77 K ligand (center), and RT **Eu(tta)$_3$X** (bottom) excitation and emission spectra of **3.2** (left) and **3.3** (right).

ELECTROCHEMISTRY OF 3.2, 3.3 AND 3.4

Cyclic voltammetry (CV) was also performed on these ligands in attempts to form conductive polymers as well as to determine electrochemical bandgaps; representative voltammograms are seen in Figure 3.4.

Although variations in ligand concentration, solvent and working electrodes were employed, no polymer films of either **3.2** or **3.3** could be obtained. The oxidative event seen at approximately 1.0 V was initially attributed to the oxidation of the EDOT moieties, and those peaks at more cathodic potentials as oxidation of the bppy core of the molecules.[40] To confirm this assumption, a model ligand, **3.4**, was synthesized by condensation of compound **2.2** with benzoyl chloride, thereby substituting the EDOT portions for phenyl groups, then subjecting this molecule to CV studies. The presence of

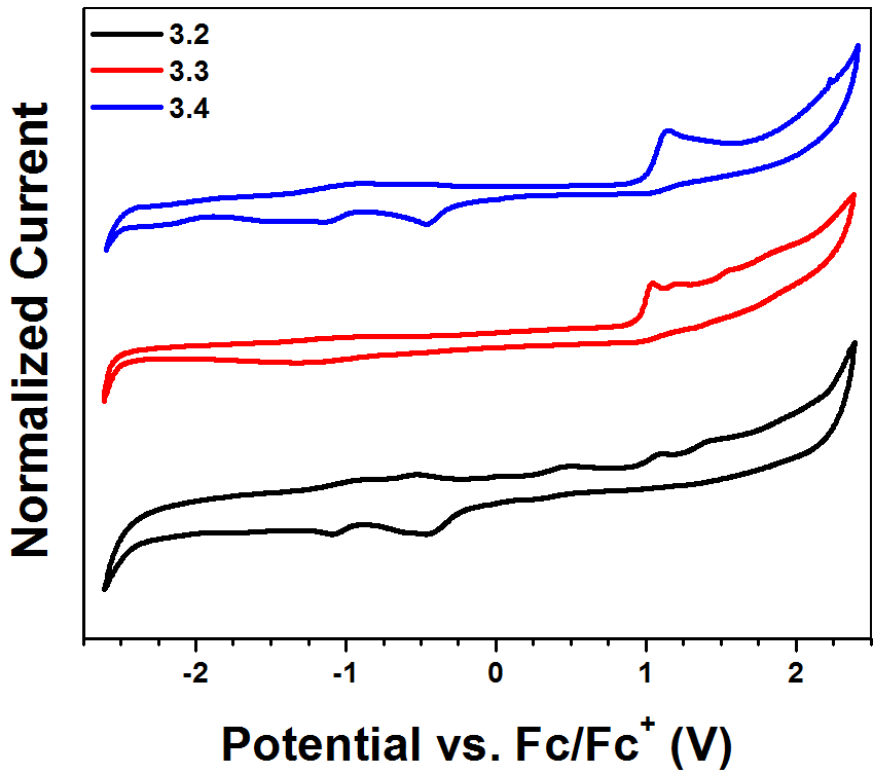

Figure 3.4: Cyclic voltammograms of amide ligands and bppy.

a similar oxidative peak with an onset around 1.0 V in the CV of **3.4** suggests the first oxidative event in all three of the amide-containing molecules actually indicates oxidation of the amide functionalities themselves, as has been reported in the literature.[41,42] This is supported by the irreversible nature of the oxidation signals in the CV of all four species.

LC-MS of Oxidized Ligands

Electrochemical amide bond cleavage similar to that seen in previous studies concerning oxidation of amide functionalities was detected by mass spectrometry. Solutions of **3.2**, **3.3**, and **3.4** in 0.1 M TBAPF were subjected to 20 CV oxidation cycles (0 V – 1.5 V), then analyzed by LC-MS in order to detect oligomer formation and/or amide fragmentation. Unfortunately, no EDOT-EDOT coupling products were detected, though amide cleavage by-products were. Bond cleavage was observed between the amide N and C4 of one of the pyrazole rings as well as between the amide N and the carbonyl C (Figure 3.5). The complementary fragment arising from amide N – pyrazole C bond cleavage was only observed for **3.3**; the analogous species for **3.2** and **3.4** are suspected to have co-eluted with the *tert*-butylammonium electrolyte.

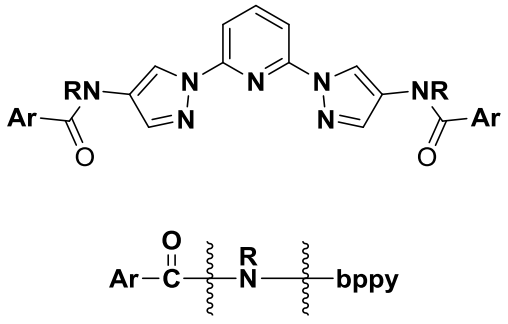

Figure 3.5: Amide bond cleavage of ligands based on LC-MS analysis of CV solutions. R: **3.2**, **3.4** = H; **3.3** = $–CH_3$. Ar: **3.2**, **3.3** = EDOT; **3.4** = C_6H_5.

CONCLUSIONS

In summary, incorporation of amide spacers into a known electropolymerizable ligand has demonstrated disruption of π-conjugation between separate portions of a previously-conjugated molecule as evidenced by crystallographic and spectroscopic analyses. These new ligands could not be polymerized, however, and exhibit lessened Φ_{abs} of $Eu(tta)_3$ complexes. Evidence gathered in these studies suggests two viable paths for the improvement of highly-emissive electropolymerizable metallopolymers: the substitution of EDOT with electropolymerizable groups which undergo oxidation at lower anodic potentials such as oligothiophene derivatives, or the employment of inert, rigid, aliphatic spacers such as bicyclo[2.2.2]octane derivatives to achieve conjugation interruption while avoiding incorporation of possible excited-state quenchers. This class of substituents have been shown to effectively limit conjugation along polymer chains and may avoid possible quenching pathways of Eu (III) emission by the omission of O–H and N–H bonds .[43,44]

EXPERIMENTAL

General Considerations

All chemicals were used as received from commercial suppliers without further purification. Air- and moisture-sensitive reactions were performed in flame-dried glassware using standard Schlenk techniques under an inert nitrogen atmosphere. Column chromatography was performed using Silicycle Silica Flash® F60 silica gel.

NMR spectroscopy was performed using an Agilent MR 400 spectrometer. Spectra were referenced to residual solvent peaks, with chemical shifts reported in ppm and coupling constants measured in Hz. Mass spectrometry was carried out using Micromass Autospec Ultima HRMS and Agilent 6530 QTOF instruments. IR spectra

were recorded with a Thermo Nicolet Smart Performer ATR accessory on a Nicolet Avatar 330 FT-IR spectrophotometer. Elemental analysis was performed by Midwest Micro Lab, LLC. Melting points were recorded on a Stanford Research Systems MP100 OptiMelt in open capillaries and are reported uncorrected.

UV-Vis absorption spectrophotometry was performed using a Varian Cary 6000i UV-Vis-NIR spectrophotometer in Starna quartz cells with 1.0 cm path lengths. Luminescence measurements were recorded on a Photon Technology International QM 4 spectrophotometer equipped with a calibrated 6 ″ diameter K Sphere-B integrating sphere used for absolute quantum yield measurements. Absolute quantum yields were calculated by dividing the area under the emission peak of the complex by the difference between the area under the excitation peak of the sample and that of either a solvent blank or solid $BaSO_4$ sample. Luminescence lifetime instrument response function (IRF) measurements were obtained using a suspension of powdered coffee creamer in H_2O[45] and determined as single-exponential decays using the 1 – 4 exponential lifetime fitting function of PTI Felix32 software. Electrochemical experiments were carried out in a dry box under a nitrogen atmosphere using a GPES system from Eco. Chemie B. V. OriginPro 8.0 SR0 software was used to plot electrochemistry and spectroscopy data.

Synthesis

Compounds **2.1**, **2.2**, **2.9**, and **3.1** were prepared as described previously.[37,46,47]

N,N'-(pyridine-2,6-diylbis(1H-pyrazole-1,4-diyl))bis(2,3-dihydrothieno[3,4-b][1,4]dioxine-5-carboxamide) (3.2): A short-path distillation apparatus, reflux condenser, and septum with copper wire were assembled onto a flame-dried three-neck flask containing a stir bar. After purging the assembly with N_2, **3.1** (0.0250 g, 0.134 mmol) was added to the flask under positive N_2 pressure, followed by $SOCl_2$ (10 mL).

This solution was heated to reflux in a 90 °C oil bath for 1 h under N_2. The solution was cooled to room temperature and $SOCl_2$ was removed by vacuum distillation into the apparatus attached to the flask. The resulting acid chloride appeared as a pale purple solid and was reacted *in situ* owing to its moisture-sensitive nature. In a separate flame-dried flask, **2.2** (0.0107 g, 0.0444 mmol) and 1,8-bis(dimethylamino)naphthalene (Proton-sponge®) (0.0248 g, 0.1157 mmol) were dried using vacuum/N_2 and dissolved in dry DCM with stirring. The diamine-trapping base solution was transferred to the three-neck flask containing the acid chloride via cannula transfer and the reaction solution was heated to reflux in a 50 °C oil bath for 24 h under a N_2 atmosphere, then concentrated under vacuum. The collected yellow solid was dissolved in DCM (125 mL) and washed with three portions of DI H_2O (3 x 25 mL). The organic phase was concentrated via rotovap and purified via silica column chromatography (5% v/v MeOH/DCM) to give a yellow solid (0.0181 g, 70.7% yield). ^{1}H-NMR (400 MHz, d-DMSO): 9.52 (s, 2H), 8.98 (s, 2H), 8.14 (s, 2H), 8.12 (t, 1H J = 8.0), 7.80 (d, 2H J = 8.4), 4.48 (m, 4H), 4.31 (m, 4H). ^{13}C{^{1}H}-NMR (100 MHz, d-DMSO): 157.9, 149.6, 142.3, 142.0, 135.7, 123.8, 117.0, 112.0, 108.3, 106.7, 66.6, 64.0. HR-MS (CI^+): calcd for $C_{25}H_{19}N_7O_6S_2$ m/z 577.0830, found 577.0832. IR ($\bar{\nu}$, cm^{-1}): 3,368 (m, N – H), 2,962 (m, C – H), 1,644 (m, C = O). M.P. 184.51 – 230.03 °C (decomp.). Elemental Analysis: calcd C 51.99% H 3.32% N 16.98%, found C 51.60% H 3.74% N 15.26%.

N,N'-(pyridine-2,6-diylbis(1H-pyrazole-1,4-diyl))bis(N-methyl-2,3-dihydrothieno[3,4-b][1,4]dioxine-5-carboxamide) (3.3): **L** (0.0300 g, 0.05194 mmol) was dissolved in dry DMF in a N_2 atmosphere, and CH_3I (9.75 μL, 0.156 mmol) was added to this solution via syringe. After 2 min. stirring, NaH (0.0046 g, 0.1917 mmol) was added to the reaction under positive N_2 pressure. The reaction solution was left to stir at ambient temperature for 12 h, then H_2O (1 mL) was added and the solution was

evaporated under N_2 flow to give a pale yellow solid. The residue was dissolved in DCM, washed with H_2O (3 x 25 mL), and subjected to silica column chromatography (5% v/v MeOH/DCM). The product was isolated as a waxy yellow solid (0.0232 g, 74.0% yield). ^{1}H-NMR (400 MHz, d-DMSO): 9.00 (s, 2H), 8.13 (t, J = 8.0 Hz, 1H), 7.98 (s, 2H), 7.81 (s, 2H), 6.87 (s, 2H) 4.15 (s, 8H), 3.43 (s, 6H). ^{13}C{^{1}H}-NMR (100 MHz, d-DMSO): 161.78, 149.42, 142.58, 140.56, 140.53, 129.10, 111.19, 108.64, 103.95, 76.57, 64.69, 63.92, 55.33, 54.92. HR-MS (ESI$^+$): calcd for $C_{27}H_{23}N_7O_6S_2Na^+$ $(M + Na)^+$ m/z 628.10430, found 628.10330. IR ($\bar{\nu}$, cm^{-1}): 3,109 (w, C – H), 2,921 (m, C – H), 1,605 (m, C = O). Elemental Analysis: calcd C 53.55% H 3.83% N 16.19%, found C 48.78% H 4.02% N 12.82%.

N,N'-(pyridine-2,6-diylbis(1H-pyrazole-1,4-diyl))dibenzamide (3.4): In a flame-dried flask, **2.2** (0.0306g, 0.143 mmol) and 1,8-bis(dimethylamino)naphthalene (Proton-sponge®) (0.0857 g, 0.355 mmol) dried using vacuum/N_2 and dissolved in dry DCM with stirring. Benzoyl chloride (0.042 mL, 0.362 mmol) was added to the solution via syringe and the reaction was heated to reflux in a 50°C oil bath for 18 h. The reaction was then allowed to cool to room temperature, concentrated under a N_2 stream and washed with H_2O (3 x 15 mL)and evaporated. The resulting residue was subjected to column chromatography using a silica stationary phase (2% v/v MeOH/DCM) and the product was concentrated to give a yellow solid (0.011 g, 17.4% yield). ^{1}H-NMR (400 MHz, d-DMSO): 10.80 (s, 2H), 9.04 (s, 2H), 8.14 (t, J = 8.0 Hz, 1H), 8.12 – 8.09 (m, 3H), 8.07 – 7.98 (m, 4H), 7.82 (d, J = 8.0 Hz, 2H), 7.65 – 7.52 (m, 5H). ^{13}C{^{1}H}-NMR (100 MHz, d-DMSO): 164.02, 149.65, 142.34, 135.29, 133.71, 131.81, 128.58, 127.47, 124.57, 116.56, 108.37. HR-MS (ESI$^+$): calcd for $C_{25}H_{20}N_7O_2$ $(M + H)^+$ m/z 450.16730, found 450.16700. IR ($\bar{\nu}$, cm^{-1}): 3,292 (m, N – H), 2,923 (w, C – H), 1,640 (m, C = O).

Elemental Analysis: calcd C 66.81% H 4.26% N 21.81%, found C 64.97% H 4.56% N 19.68%.

Eu(tta)$_3$X (**3.5**, **3.6**): Both complexes were synthesized following the same procedure. The synthesis of **3.5** is described as a general example. Ligand **3.2** (0.0146 g, 0.0253 mmol) was combined with **2.9** (0.0214 g, 0.0251 mmol) and dissolved in 10 mL acetone. This solution was refluxed for 30 min and concentrated to approximately 2 mL in volume. Boiling hexanes (15 mL) were added to the reaction in one portion and the resulting precipitate was collected via vacuum filtration, washed with hexanes, dried under vacuum and collected. As single-crystal growth of these species proved to be exceptionally difficult, bulk purity was confirmed by the absence of splitting in the $^5D_0 \rightarrow {}^7F_0$ Eu(III) ion emission spectra (indicative of one emissive species in the sample).[48]

(**3.5**): 0.0173 g, 49.1%;. HR-MS (ESI$^+$): calcd for $C_{49}H_{31}EuF_9N_7O_{12}S_5$ $(M + Na)^+$ m/z 1413.95810, found 1413.95670. IR ($\bar{\nu}$, cm^{-1}): 3,369 (w, N – H), 2,962 (m, C – H), 1,648 (m, C = O), 1,608 (m, C = O). Elemental Analysis: calcd C 42.25% H 2.24% N 3.77%, found C 43.52% H 3.77% N 3.99%.

(**3.6**): 0.0294 g, 42.1%; . HR-MS (ESI$^+$): calcd for $C_{51}H_{35}EuF_9N_7O_{12}S_5$ $(M + Na)^+$ m/z 1441.98940, found 1441.98670. IR ($\bar{\nu}$, cm^{-1}): 3,107 (w, C – H), 2,922 (m, C – H), 1,646 (m, C = O), 1,600 (m, C = O). Elemental Analysis: calcd C 53.55% H 3.83% N 16.19%, found C 48.78% H 4.02% N 12.82%.

Single Crystal X-ray Crystallography

Suitable single crystals of **3.2** and **3.3** were obtained via slow evaporation of an acetone solution and subsequently analyzed by Leander M. Cinninger. The single crystals were removed from their respective vials, covered with Paratone, and mounted separately on nylon thread loops. The single crystal X-ray diffraction data for **L** was collected using

a Rigaku AFC12 Saturn 724+ CCD diffractometer equipped with a graphite-monochromated Mo Kα radiation source (λ = 0.71073 Å) and a Rigaku XStream low temperature device that was operated at 100 K. Data collection, unit cell refinement, and data reduction were performed using the Rigaku CrystalClear program.[49] The single crystal X-ray diffraction data for **3.3** was collected using an Agilent Technologies SuperNova Dual Source diffractometer equipped with a collimating mirror-monochromated μ-focus Cu Kα radiation source (λ = 1.5418 Å) and an Oxford Cryostream 700 low temperature device that was operated at 100 K. Data collection, unit cell refinement, and data reduction were performed using the Agilent Technologies CrysAlisPro program.[50] Both structures were solved by direct methods using the SIR2014[51] program and refined by full-matrix least-squares on F^2 with anisotropic displacement parameters for all non-H atoms using SHELXL-2016.[52] The structural analyses were performed using the PLATON98[53] and WinGX[54] programs. The hydrogen atoms were placed in fixed, calculated positions with isotropic displacement parameters set to 1.2 x U_{eq} with respect to the attached atom. The POV-Ray images were created using the Mercury version 3.8 program.

Table 3.2: Crystal data and structure refinement for **3.2**.

Empirical formula	$C_{25}H_{19}N_7O_6S_2$	
Formula weight	577.59	
Temperature	100(2) K	
Wavelength	0.71075 Å	
Crystal system	Triclinic	
Space group	P -1	
Unit cell dimensions	a = 8.799(4) Å	α = 72.358(12)°
	b = 11.773(4) Å	β = 87.606(14)°
	c = 12.579(5) Å	γ = 85.694(18)°
Volume	1238.1(9) $Å^3$	
Z	2	
Density (calculated)	1.549 Mg/m^3	
Absorption coefficient	0.274 mm^{-1}	
F(000)	596	
Crystal size	0.1560 x 0.0410 x 0.0350 mm^3	
θ range for data collection	1.699 to 25.022°.	
Index ranges	-10<=h<=10, -14<=k<=13, -14<=l<=14	
Reflections collected	16517	
Independent reflections	4370 [R(int) = 0.0842]	
Completeness to θ = 25.022°	100.0 %	
Absorption correction	Semi-empirical from equivalents	
Max. and min. transmission	1.0000 and 0.7723	
Refinement method	Full-matrix least-squares on F^2	
Data / restraints / parameters	4370 / 0 / 369	
Goodness-of-fit on F^2	1.225	
Final R indices [I>2σ(I)]	R1 = 0.0855, wR2 = 0.1456	
R indices (all data)	R1 = 0.1050, wR2 = 0.1540	
Extinction coefficient	n/a	
Largest diff. peak and hole	0.669 and -0.342 e.$Å^{-3}$	

Table 3.3: Atomic coordinates (x 10^4) and equivalent isotropic displacement parameters ($Å^2$ x 10^3) for **3.2**. U(eq) is defined as one third of the trace of the orthogonalized U^{ij} tensor.

	x	y	z	U(eq)
C(1)	307(5)	7961(4)	-1171(4)	28(1)
C(2)	-872(5)	8178(4)	-520(4)	23(1)
C(3)	-3270(5)	7917(5)	325(4)	48(2)
C(4)	-2994(5)	8726(5)	948(4)	36(1)

Table 3.3 Continued:

C(5)	-412(5)	8456(4)	439(3)	21(1)
C(6)	1148(5)	8409(4)	514(3)	21(1)
C(7)	2079(5)	8539(4)	1397(4)	24(1)
C(8)	1859(5)	9030(4)	3168(3)	20(1)
C(9)	3246(5)	8613(4)	3661(3)	23(1)
C(10)	1046(5)	9574(4)	3901(4)	26(1)
C(11)	4315(5)	8641(4)	5461(4)	23(1)
C(12)	4032(5)	8903(4)	6460(4)	27(1)
C(13)	5201(5)	8627(4)	7210(4)	29(1)
C(14)	6585(5)	8117(4)	6958(4)	26(1)
C(15)	6736(5)	7923(4)	5932(4)	23(1)
C(16)	8391(5)	7063(4)	4671(4)	24(1)
C(17)	10464(5)	6853(4)	5655(4)	29(1)
C(18)	9895(5)	6673(4)	4688(4)	25(1)
C(19)	10188(5)	5913(4)	3078(4)	26(1)
C(20)	11327(5)	5480(4)	2385(4)	25(1)
C(21)	12886(5)	5321(4)	2472(4)	24(1)
C(22)	15294(5)	5568(4)	3049(4)	34(1)
C(23)	15897(5)	4625(4)	2526(4)	34(1)
C(24)	13598(5)	4946(4)	1597(4)	29(1)
C(25)	12582(5)	4819(4)	853(4)	34(1)
N(1)	1275(4)	8919(3)	2192(3)	22(1)
N(2)	1843(4)	9499(3)	4794(3)	22(1)
N(3)	3188(4)	8907(3)	4635(3)	22(1)
N(4)	5628(4)	8158(3)	5174(3)	22(1)
N(5)	8123(4)	7447(3)	5584(3)	23(1)
N(6)	9405(4)	7310(3)	6209(3)	27(1)
N(7)	10764(4)	6205(3)	3946(3)	26(1)
O(1)	-2401(3)	8131(3)	-706(2)	29(1)
O(2)	-1399(3)	8728(3)	1204(2)	24(1)
O(3)	3484(3)	8328(3)	1432(3)	30(1)
O(4)	8804(3)	6025(3)	2876(3)	30(1)
O(5)	13677(3)	5476(3)	3328(3)	30(1)
O(6)	15167(3)	4769(3)	1489(3)	37(1)
S(1)	2023(1)	8046(1)	-614(1)	26(1)
S(2)	10747(1)	5155(1)	1224(1)	31(1)

Table 3.4: Bond lengths (Å) and angles (°) for **3.2**.

C(1)-C(2)	1.352(6)	C(3)-H(3B)	0.9900
C(1)-S(1)	1.713(4)	C(4)-O(2)	1.453(5)
C(1)-H(1)	0.9500	C(4)-H(4A)	0.9900
C(2)-O(1)	1.382(5)	C(4)-H(4B)	0.9900
C(2)-C(5)	1.424(6)	C(5)-O(2)	1.362(5)
C(3)-O(1)	1.441(5)	C(5)-C(6)	1.375(5)
C(3)-C(4)	1.444(6)	C(6)-C(7)	1.459(6)
C(3)-H(3A)	0.9900	C(6)-S(1)	1.737(4)
C(7)-O(3)	1.242(5)	C(8)-C(9)	1.380(6)
C(7)-N(1)	1.366(5)	C(8)-N(1)	1.396(5)
C(8)-C(10)	1.417(6)	C(12)-C(13)	1.377(6)
C(9)-N(3)	1.369(5)	C(12)-H(12)	0.9500
C(9)-H(9)	0.9500	C(13)-C(14)	1.385(6)
C(10)-N(2)	1.325(5)	C(13)-H(13)	0.9500
C(10)-H(10)	0.9500	C(14)-C(15)	1.377(6)
C(11)-N(4)	1.334(5)	C(14)-H(14)	0.9500
C(11)-C(12)	1.391(6)	C(15)-N(4)	1.347(5)
C(11)-N(3)	1.415(5)	C(15)-N(5)	1.413(5)
C(16)-N(5)	1.362(5)	C(17)-N(6)	1.320(5)
C(16)-C(18)	1.366(6)	C(17)-C(18)	1.414(6)
C(16)-H(16)	0.9500	C(17)-H(17)	0.9500
C(18)-N(7)	1.396(6)	C(19)-N(7)	1.366(6)
C(19)-O(4)	1.244(5)	C(19)-C(20)	1.464(6)
C(20)-C(21)	1.376(6)	N(5)-N(6)	1.373(5)
C(20)-S(2)	1.723(4)	N(7)-H(7N)	0.84(5)
C(21)-O(5)	1.370(5)	C(2)-C(1)-S(1)	111.4(3)
C(21)-C(24)	1.412(6)	C(2)-C(1)-H(1)	124.3
C(22)-O(5)	1.455(5)	S(1)-C(1)-H(1)	124.3
C(22)-C(23)	1.507(6)	C(1)-C(2)-O(1)	126.1(4)
C(22)-H(22A)	0.9900	C(1)-C(2)-C(5)	113.6(4)
C(22)-H(22B)	0.9900	O(1)-C(2)-C(5)	120.3(4)
C(23)-O(6)	1.437(5)	O(1)-C(3)-C(4)	113.6(4)
C(23)-H(23A)	0.9900	O(1)-C(3)-H(3A)	108.8
C(23)-H(23B)	0.9900	C(4)-C(3)-H(3A)	108.8
C(24)-C(25)	1.369(6)	O(1)-C(3)-H(3B)	108.8
C(24)-O(6)	1.387(5)	C(4)-C(3)-H(3B)	108.8
C(25)-S(2)	1.714(5)	H(3A)-C(3)-H(3B)	107.7
C(25)-H(25)	0.9500	C(3)-C(4)-O(2)	113.5(4)
N(1)-H(1N)	0.90(5)	C(3)-C(4)-H(4A)	108.9
N(2)-N(3)	1.365(4)	O(2)-C(4)-H(4A)	108.9

Table 3.4 Continued:

C(3)-C(4)-H(4B)	108.9	O(2)-C(5)-C(6)	123.7(4)
O(2)-C(4)-H(4B)	108.9	O(2)-C(5)-C(2)	124.1(4)
H(4A)-C(4)-H(4B)	107.7		
C(6)-C(5)-C(2)	112.3(4)	C(7)-C(6)-S(1)	119.6(3)
C(5)-C(6)-C(7)	129.9(4)	O(3)-C(7)-N(1)	122.3(4)
C(5)-C(6)-S(1)	110.4(3)	O(3)-C(7)-C(6)	123.5(4)
N(1)-C(7)-C(6)	114.2(4)	C(9)-C(8)-C(10)	105.4(4)
C(9)-C(8)-N(1)	129.9(4)	N(1)-C(8)-C(10)	124.6(4)
N(3)-C(9)-C(8)	105.5(4)	N(2)-C(10)-C(8)	111.9(4)
N(3)-C(9)-H(9)	127.3	N(2)-C(10)-H(10)	124.0
C(8)-C(9)-H(9)	127.3	C(8)-C(10)-H(10)	124.0
N(4)-C(11)-C(12)	125.0(4)	C(12)-C(13)-H(13)	119.8
N(4)-C(11)-N(3)	114.1(4)	C(14)-C(13)-H(13)	119.8
C(12)-C(11)-N(3)	120.9(4)	C(15)-C(14)-C(13)	117.1(4)
C(13)-C(12)-C(11)	116.9(4)	C(15)-C(14)-H(14)	121.4
C(13)-C(12)-H(12)	121.5	C(13)-C(14)-H(14)	121.4
C(11)-C(12)-H(12)	121.5	N(4)-C(15)-C(14)	125.0(4)
C(12)-C(13)-C(14)	120.5(4)	N(4)-C(15)-N(5)	113.8(4)
C(14)-C(15)-N(5)	121.3(4)	O(4)-C(19)-N(7)	122.7(4)
N(5)-C(16)-C(18)	106.8(4)	O(4)-C(19)-C(20)	122.3(4)
N(5)-C(16)-H(16)	126.6	N(7)-C(19)-C(20)	115.0(4)
C(18)-C(16)-H(16)	126.6	C(21)-C(20)-C(19)	130.0(4)
N(6)-C(17)-C(18)	112.4(4)	C(21)-C(20)-S(2)	110.7(3)
N(6)-C(17)-H(17)	123.8	C(19)-C(20)-S(2)	119.2(3)
C(18)-C(17)-H(17)	123.8	O(5)-C(21)-C(20)	124.1(4)
C(16)-C(18)-N(7)	130.5(4)	O(5)-C(21)-C(24)	123.0(4)
C(16)-C(18)-C(17)	104.8(4)	C(20)-C(21)-C(24)	112.9(4)
N(7)-C(18)-C(17)	124.7(4)	O(5)-C(22)-C(23)	111.5(4)
O(5)-C(22)-H(22A)	109.3	C(23)-C(22)-H(22B)	109.3
C(23)-C(22)-H(22A)	109.3	H(22A)-C(22)-H(22B)	108.0
O(5)-C(22)-H(22B)	109.3	O(6)-C(23)-C(22)	111.2(4)
O(6)-C(23)-H(23A)	109.4	O(6)-C(23)-H(23B)	109.4
C(22)-C(23)-H(23A)	109.4	C(22)-C(23)-H(23B)	109.4
H(23A)-C(23)-H(23B)	108.0	C(7)-N(1)-H(1N)	118(3)
C(25)-C(24)-O(6)	123.9(4)	C(8)-N(1)-H(1N)	115(3)
C(25)-C(24)-C(21)	112.9(4)	C(10)-N(2)-N(3)	104.1(3)
O(6)-C(24)-C(21)	123.2(4)	N(2)-N(3)-C(9)	113.0(3)
C(24)-C(25)-S(2)	111.2(4)	N(2)-N(3)-C(11)	119.4(3)
C(24)-C(25)-H(25)	124.4	C(9)-N(3)-C(11)	127.6(4)
S(2)-C(25)-H(25)	124.4	C(11)-N(4)-C(15)	115.4(4)
C(7)-N(1)-C(8)	126.1(4)	C(16)-N(5)-N(6)	112.1(3)

Table 3.4 Continued:

C(16)-N(5)-C(15)	128.0(3)	C(17)-N(6)-N(5)	103.9(4)
N(6)-N(5)-C(15)	119.9(3)	C(19)-N(7)-C(18)	124.7(4)
C(19)-N(7)-H(7N)	116(4)	C(21)-O(5)-C(22)	111.3(3)
C(18)-N(7)-H(7N)	119(4)	C(24)-O(6)-C(23)	111.0(3)
C(2)-O(1)-C(3)	110.5(3)	C(1)-S(1)-C(6)	92.3(2)
C(5)-O(2)-C(4)	113.8(3)	C(25)-S(2)-C(20)	92.3(2)

Table 3.5: Anisotropic displacement parameters ($Å^2$ x 10^3) for **3.2**. The anisotropic displacement factor exponent takes the form: $-2\pi^2[h^2a^{*2}U^{11} + ... + 2\ h\ k\ a^*\ b^*\ U^{12}]$.

	U11	U22	U33	U23	U13	U12
C(1)	27(2)	36(3)	24(3)	-12(2)	-1(2)	-2(2)
C(2)	20(2)	28(2)	23(2)	-10(2)	-5(2)	0(2)
C(3)	22(3)	88(4)	41(3)	-29(3)	6(2)	-11(3)
C(4)	14(2)	61(3)	43(3)	-29(3)	5(2)	-9(2)
C(5)	20(2)	26(2)	19(2)	-8(2)	2(2)	0(2)
C(6)	20(2)	24(2)	21(2)	-9(2)	-2(2)	-1(2)
C(7)	19(2)	24(2)	28(3)	-8(2)	1(2)	-2(2)
C(8)	22(2)	22(2)	20(2)	-8(2)	-2(2)	-7(2)
C(9)	23(2)	26(2)	21(2)	-11(2)	-2(2)	-2(2)
C(10)	21(2)	28(2)	28(3)	-9(2)	-5(2)	3(2)
C(11)	17(2)	29(2)	23(2)	-9(2)	0(2)	-3(2)
C(12)	22(2)	32(3)	26(3)	-10(2)	2(2)	-2(2)
C(13)	28(2)	42(3)	20(2)	-13(2)	-1(2)	-7(2)
C(14)	22(2)	33(3)	22(2)	-4(2)	-5(2)	-6(2)
C(15)	22(2)	25(2)	23(2)	-8(2)	-1(2)	-3(2)
C(16)	25(2)	29(2)	23(2)	-14(2)	-5(2)	1(2)
C(17)	24(2)	32(3)	29(3)	-6(2)	-4(2)	0(2)
C(18)	20(2)	21(2)	32(3)	-5(2)	-1(2)	-1(2)
C(19)	25(2)	21(2)	29(3)	-5(2)	-1(2)	-4(2)
C(20)	25(2)	23(2)	28(3)	-9(2)	-5(2)	-1(2)
C(21)	25(2)	23(2)	24(2)	-4(2)	-5(2)	1(2)
C(22)	16(2)	42(3)	44(3)	-11(2)	-1(2)	-6(2)
C(23)	22(2)	39(3)	38(3)	-5(2)	-5(2)	3(2)
C(24)	20(2)	32(3)	34(3)	-7(2)	-3(2)	4(2)
C(25)	31(3)	35(3)	37(3)	-15(2)	-2(2)	6(2)
N(1)	16(2)	31(2)	24(2)	-14(2)	-1(2)	1(2)

Table 3.5 Continued:

N(2)	16(2)	27(2)	25(2)	-10(2)	2(2)	0(2)
N(3)	19(2)	31(2)	19(2)	-12(2)	-5(2)	1(2)
N(4)	21(2)	25(2)	20(2)	-5(2)	0(2)	-6(2)
N(5)	17(2)	30(2)	22(2)	-8(2)	-8(2)	-1(2)
N(6)	22(2)	36(2)	21(2)	-6(2)	-4(2)	-5(2)
N(7)	18(2)	28(2)	30(2)	-8(2)	-4(2)	1(2)
O(1)	22(2)	46(2)	22(2)	-13(2)	-3(1)	-2(2)
O(2)	16(2)	34(2)	23(2)	-12(1)	-2(1)	2(1)
O(3)	18(2)	45(2)	32(2)	-19(2)	-1(1)	-1(1)
O(4)	19(2)	35(2)	37(2)	-11(2)	-9(1)	0(1)
O(5)	18(2)	40(2)	33(2)	-13(2)	-4(1)	-3(1)
O(6)	26(2)	48(2)	34(2)	-11(2)	1(2)	4(2)
S(1)	22(1)	36(1)	25(1)	-14(1)	3(1)	-2(1)
S(2)	29(1)	34(1)	32(1)	-13(1)	-7(1)	1(1)

Table 3.6: Crystal data and structure refinement for **3.3**.

Empirical formula	$C_{27}H_{23}N_7O_6S_2$
Formula weight	605.64
Temperature	100 K
Wavelength	1.54184 Å
Crystal system	Monoclinic
Space group	P 21/n
Unit cell dimensions	a = 7.0155(4) Å α = 90°
	b = 18.3245(9) Å β = 90.333(3)°
	c = 20.4611(12) Å γ = 90°
Volume	2630.3(3) $Å^3$
Z	4
Density (calculated)	1.529 Mg/m^3
Absorption coefficient	2.345 mm^{-1}
F(000) 1256	
Crystal size	0.220 x 0.106 x 0.027 mm^3
θ range for data collection	3.238 to 75.932°.
Index ranges	-7<=h<=8, -21<=k<=22, -22<=l<=25
Reflections collected	14439
Independent reflections	5279 [R(int) = 0.0249]
Completeness to θ = 67.684°	99.1 %
Absorption correction	Gaussian
Max. and min. transmission	0.940 and 0.755
Refinement method	Full-matrix least-squares on F^2
Data / restraints / parameters	5279 / 0 / 381
Goodness-of-fit on F^2	1.035
Final R indices [I>2σ(I)]	R1 = 0.0323, wR2 = 0.0803
R indices (all data)	R1 = 0.0366, wR2 = 0.0830
Extinction coefficient	n/a
Largest diff. peak and hole	0.359 and -0.329 $e.Å^{-3}$

Table 3.7: Atomic coordinates (x 10^4) and equivalent isotropic displacement parameters ($Å^2$ x 10^3) for **3.3**. U(eq) is defined as one third of the trace of the orthogonalized U^{ij} tensor.

	x	y	z	U(eq)
C(1)	-148(2)	1205(1)	1140(1)	24(1)
C(2)	1121(2)	1253(1)	1737(1)	25(1)
C(3)	2521(2)	1603(1)	565(1)	19(1)
C(4)	3124(2)	1990(1)	1137(1)	18(1)
C(5)	3659(2)	1728(1)	46(1)	22(1)
C(6)	4673(2)	2423(1)	1030(1)	18(1)
C(7)	5859(2)	2852(1)	1498(1)	16(1)
C(8)	2978(2)	3580(1)	1794(1)	21(1)
C(9)	6006(2)	3731(1)	2366(1)	16(1)
C(10)	7797(2)	3592(1)	2613(1)	17(1)
C(11)	5354(2)	4350(1)	2714(1)	18(1)
C(12)	9738(2)	4153(1)	3489(1)	16(1)
C(13)	9998(2)	4724(1)	3927(1)	18(1)
C(14)	11618(2)	4696(1)	4323(1)	20(1)
C(15)	12911(2)	4129(1)	4268(1)	18(1)
C(16)	12490(2)	3598(1)	3803(1)	16(1)
C(17)	13365(2)	2406(1)	3314(1)	18(1)
C(18)	16166(2)	2329(1)	3812(1)	23(1)
C(19)	14917(2)	1959(1)	3381(1)	19(1)
C(20)	16436(2)	1241(1)	2508(1)	24(1)
C(21)	13934(2)	712(1)	3161(1)	19(1)
C(22)	12716(2)	750(1)	3750(1)	20(1)
C(23)	9910(2)	751(1)	4486(1)	28(1)
C(24)	13188(2)	877(1)	4391(1)	21(1)
C(25)	11579(2)	867(1)	4811(1)	24(1)
C(26)	15025(3)	1279(1)	5269(1)	36(1)
C(27)	13666(3)	867(1)	5697(1)	37(1)
N(1)	4960(2)	3345(1)	1886(1)	16(1)
N(2)	6634(2)	4578(1)	3148(1)	18(1)
N(3)	8117(2)	4109(1)	3080(1)	16(1)
N(4)	10946(2)	3597(1)	3423(1)	16(1)
N(5)	13712(2)	2997(1)	3702(1)	17(1)
N(6)	15441(2)	2958(1)	4008(1)	23(1)
N(7)	15184(2)	1271(1)	3076(1)	19(1)
O(1)	982(2)	1144(1)	556(1)	23(1)

Table 3.7 Continued:

O(2)	2247(2)	1915(1)	1727(1)	22(1)
O(3)	7592(1)	2748(1)	1526(1)	21(1)
O(4)	13813(2)	202(1)	2774(1)	24(1)
O(5)	15005(2)	985(1)	4611(1)	27(1)
O(6)	11732(2)	972(1)	5473(1)	30(1)
S(1)	5461(1)	2325(1)	236(1)	22(1)
S(2)	10286(1)	618(1)	3666(1)	24(1)

Table 3.8: Bond lengths (Å) and angles (°) for **3.3**.

C(1)-O(1)	1.442(2)	C(2)-H(2A)	0.9700
C(1)-C(2)	1.511(2)	C(2)-H(2B)	0.9700
C(1)-H(1A)	0.9700	C(3)-C(5)	1.352(2)
C(1)-H(1B)	0.9700	C(3)-O(1)	1.3690(17)
C(2)-O(2)	1.4477(18)	C(3)-C(4)	1.4307(19)
C(4)-C(6)	1.364(2)	C(6)-S(1)	1.7279(14)
C(4)-O(2)	1.3653(18)	C(7)-O(3)	1.2314(18)
C(5)-S(1)	1.7147(15)	C(7)-N(1)	1.3606(18)
C(5)-H(5)	0.9300	C(8)-N(1)	1.4672(18)
C(6)-C(7)	1.4886(19)	C(8)-H(8A)	0.9600
C(8)-H(8B)	0.9600	C(12)-N(3)	1.4111(18)
C(8)-H(8C)	0.9600	C(13)-C(14)	1.392(2)
C(9)-C(10)	1.3757(19)	C(13)-H(13)	0.9300
C(9)-N(1)	1.4122(17)	C(14)-C(15)	1.384(2)
C(9)-C(11)	1.4163(19)	C(14)-H(14)	0.9300
C(10)-N(3)	1.3628(17)	C(15)-C(16)	1.3907(19)
C(10)-H(10)	0.9300	C(15)-H(15)	0.9300
C(11)-N(2)	1.3263(19)	C(16)-N(4)	1.3297(18)
C(11)-H(11)	0.9300	C(16)-N(5)	1.4127(18)
C(12)-N(4)	1.3330(18)	C(17)-N(5)	1.3639(18)
C(12)-C(13)	1.3877(19)	C(17)-C(19)	1.368(2)
C(17)-H(17)	0.9300	C(18)-C(19)	1.413(2)
C(18)-N(6)	1.323(2)	C(18)-H(18)	0.9300
C(19)-N(7)	1.4192(18)	C(20)-H(20B)	0.9600
C(20)-N(7)	1.463(2)	C(20)-H(20C)	0.9600
C(20)-H(20A)	0.9600	C(21)-O(4)	1.2274(18)

Table 3.8 Continued:

C(21)-N(7)	1.3608(19)	C(21)-C(22)	1.483(2)
C(22)-C(24)	1.371(2)	C(24)-O(5)	1.3639(19)
C(22)-S(2)	1.7291(15)	C(24)-C(25)	1.423(2)
C(23)-C(25)	1.360(2)	C(25)-O(6)	1.371(2)
C(23)-S(2)	1.7185(17)	C(26)-O(5)	1.4505(19)
C(23)-H(23)	0.9300	C(26)-C(27)	1.502(3)
C(26)-H(26A)	0.9700	O(1)-C(1)-H(1B)	109.5
C(26)-H(26B)	0.9700	C(2)-C(1)-H(1B)	109.5
C(27)-O(6)	1.443(2)	H(1A)-C(1)-H(1B)	108.1
C(27)-H(27A)	0.9700	O(2)-C(2)-C(1)	110.82(12)
C(27)-H(27B)	0.9700	O(2)-C(2)-H(2A)	109.5
N(2)-N(3)	1.3578(16)	C(1)-C(2)-H(2A)	109.5
N(5)-N(6)	1.3633(17)	O(2)-C(2)-H(2B)	109.5
		C(1)-C(2)-H(2B)	109.5
O(1)-C(1)-C(2)	110.51(12)	H(2A)-C(2)-H(2B)	108.1
O(1)-C(1)-H(1A)	109.5	C(5)-C(3)-O(1)	124.29(13)
C(2)-C(1)-H(1A)	109.5	C(5)-C(3)-C(4)	112.68(13)
O(1)-C(3)-C(4)	123.01(14)	C(6)-C(4)-C(3)	112.92(13)
C(6)-C(4)-O(2)	124.34(13)	O(2)-C(4)-C(3)	122.73(13)
C(3)-C(5)-S(1)	111.54(11)	C(7)-C(6)-S(1)	118.64(10)
C(3)-C(5)-H(5)	124.2	O(3)-C(7)-N(1)	122.43(13)
S(1)-C(5)-H(5)	124.2	O(3)-C(7)-C(6)	119.77(13)
C(4)-C(6)-C(7)	130.26(13)	N(1)-C(7)-C(6)	117.80(12)
C(4)-C(6)-S(1)	110.43(10)	N(1)-C(8)-H(8A)	109.5
N(1)-C(8)-H(8B)	109.5	H(8B)-C(8)-H(8C)	109.5
H(8A)-C(8)-H(8B)	109.5	C(10)-C(9)-N(1)	129.24(12)
N(1)-C(8)-H(8C)	109.5	C(10)-C(9)-C(11)	105.07(12)
H(8A)-C(8)-H(8C)	109.5	N(1)-C(9)-C(11)	125.66(12)
N(3)-C(10)-C(9)	105.97(12)	C(14)-C(13)-H(13)	121.6
N(3)-C(10)-H(10)	127.0	C(15)-C(14)-C(13)	120.88(13)
C(9)-C(10)-H(10)	127.0	C(15)-C(14)-H(14)	119.6
N(2)-C(11)-C(9)	111.74(12)	C(13)-C(14)-H(14)	119.6
N(2)-C(11)-H(11)	124.1	C(14)-C(15)-C(16)	116.33(13)
C(9)-C(11)-H(11)	124.1	C(14)-C(15)-H(15)	121.8
N(4)-C(12)-C(13)	124.06(13)	C(16)-C(15)-H(15)	121.8
N(4)-C(12)-N(3)	113.99(12)	N(4)-C(16)-C(15)	124.77(13)
C(13)-C(12)-N(3)	121.94(12)	N(4)-C(16)-N(5)	113.96(12)
C(12)-C(13)-C(14)	116.85(13)	C(15)-C(16)-N(5)	121.27(13)
C(12)-C(13)-H(13)	121.6	N(5)-C(17)-C(19)	106.14(12)
N(5)-C(17)-H(17)	126.9	C(19)-C(17)-H(17)	126.9

Table 3.8 Continued:

N(6)-C(18)-C(19)	111.68(13)	N(6)-C(18)-H(18)	124.2
C(19)-C(18)-H(18)	124.2	H(20A)-C(20)-H(20B)	109.5
C(17)-C(19)-C(18)	105.39(13)	N(7)-C(20)-H(20C)	109.5
C(17)-C(19)-N(7)	126.47(13)	H(20A)-C(20)-H(20C)	109.5
C(18)-C(19)-N(7)	128.14(13)	H(20B)-C(20)-H(20C)	109.5
N(7)-C(20)-H(20A)	109.5	O(4)-C(21)-N(7)	122.21(14)
N(7)-C(20)-H(20B)	109.5	O(4)-C(21)-C(22)	121.47(13)
N(7)-C(21)-C(22)	116.31(12)	C(21)-C(22)-S(2)	119.00(11)
C(24)-C(22)-C(21)	130.43(14)	C(25)-C(23)-S(2)	111.28(12)
C(24)-C(22)-S(2)	110.57(12)	C(25)-C(23)-H(23)	124.4
S(2)-C(23)-H(23)	124.4	C(27)-C(26)-H(26B)	109.5
O(5)-C(24)-C(22)	124.12(14)	H(26A)-C(26)-H(26B)	108.1
O(5)-C(24)-C(25)	123.02(14)	O(6)-C(27)-C(26)	110.27(14)
C(22)-C(24)-C(25)	112.84(14)	O(6)-C(27)-H(27A)	109.6
C(23)-C(25)-O(6)	124.54(15)	C(26)-C(27)-H(27A)	109.6
C(23)-C(25)-C(24)	112.97(15)	O(6)-C(27)-H(27B)	109.6
O(6)-C(25)-C(24)	122.49(15)	C(26)-C(27)-H(27B)	109.6
O(5)-C(26)-C(27)	110.58(15)	H(27A)-C(27)-H(27B)	108.1
O(5)-C(26)-H(26A)	109.5	C(7)-N(1)-C(9)	119.83(12)
C(27)-C(26)-H(26A)	109.5	C(7)-N(1)-C(8)	124.23(12)
O(5)-C(26)-H(26B)	109.5	C(9)-N(1)-C(8)	115.51(11)
C(11)-N(2)-N(3)	104.32(11)	N(2)-N(3)-C(12)	121.21(11)
N(2)-N(3)-C(10)	112.90(11)	C(10)-N(3)-C(12)	125.80(12)
C(16)-N(4)-C(12)	117.09(12)	C(3)-O(1)-C(1)	112.27(11)
N(6)-N(5)-C(17)	112.41(11)	C(4)-O(2)-C(2)	110.29(11)
N(6)-N(5)-C(16)	120.85(11)	C(24)-O(5)-C(26)	111.42(13)
C(17)-N(5)-C(16)	126.75(12)	C(25)-O(6)-C(27)	111.31(13)
C(18)-N(6)-N(5)	104.38(12)	C(5)-S(1)-C(6)	92.36(7)
C(21)-N(7)-C(19)	121.76(12)	C(23)-S(2)-C(22)	92.29(8)
C(21)-N(7)-C(20)	117.59(12)		
C(19)-N(7)-C(20)	117.70(12)		

Table 3.9: Anisotropic displacement parameters ($Å^2$ x 10^3) for **3.3**. The anisotropic displacement factor exponent takes the form: $-2\pi^2[h^2a^{*2}U^{11} + ... + 2\ h\ k\ a^*\ b^*\ U^{12}]$.

	U11	U22	U33	U23	U13	U12
C(1)	18(1)	22(1)	33(1)	-2(1)	0(1)	-3(1)
C(2)	23(1)	25(1)	27(1)	2(1)	2(1)	-5(1)
C(3)	19(1)	15(1)	23(1)	-1(1)	-5(1)	0(1)
C(4)	18(1)	17(1)	17(1)	0(1)	-2(1)	2(1)
C(5)	26(1)	20(1)	20(1)	-4(1)	-3(1)	-1(1)
C(6)	20(1)	17(1)	15(1)	-2(1)	-1(1)	1(1)
C(7)	18(1)	16(1)	15(1)	1(1)	0(1)	-1(1)
C(8)	17(1)	21(1)	24(1)	-4(1)	-5(1)	4(1)
C(9)	17(1)	15(1)	15(1)	1(1)	0(1)	0(1)
C(10)	18(1)	15(1)	17(1)	-2(1)	-1(1)	1(1)
C(11)	17(1)	15(1)	20(1)	1(1)	-1(1)	1(1)
C(12)	16(1)	16(1)	16(1)	1(1)	0(1)	-1(1)
C(13)	21(1)	15(1)	19(1)	-1(1)	-1(1)	1(1)
C(14)	24(1)	17(1)	18(1)	-3(1)	-1(1)	-2(1)
C(15)	19(1)	18(1)	18(1)	0(1)	-3(1)	-2(1)
C(16)	18(1)	15(1)	17(1)	1(1)	0(1)	0(1)
C(17)	19(1)	16(1)	19(1)	-2(1)	-2(1)	-1(1)
C(18)	19(1)	20(1)	32(1)	-2(1)	-6(1)	3(1)
C(19)	19(1)	15(1)	23(1)	-1(1)	-1(1)	0(1)
C(20)	22(1)	22(1)	28(1)	-1(1)	4(1)	1(1)
C(21)	18(1)	17(1)	20(1)	0(1)	-3(1)	2(1)
C(22)	21(1)	16(1)	22(1)	-1(1)	-1(1)	0(1)
C(23)	28(1)	28(1)	28(1)	-1(1)	7(1)	0(1)
C(24)	25(1)	17(1)	23(1)	-2(1)	-2(1)	4(1)
C(25)	33(1)	19(1)	22(1)	-1(1)	3(1)	5(1)
C(26)	31(1)	50(1)	28(1)	-18(1)	-8(1)	12(1)
C(27)	45(1)	43(1)	21(1)	-7(1)	-5(1)	23(1)
N(1)	15(1)	16(1)	18(1)	-2(1)	-3(1)	1(1)
N(2)	18(1)	15(1)	20(1)	-1(1)	-1(1)	3(1)
N(3)	16(1)	14(1)	17(1)	-1(1)	-1(1)	2(1)
N(4)	17(1)	15(1)	17(1)	0(1)	-1(1)	0(1)
N(5)	16(1)	16(1)	20(1)	-1(1)	-4(1)	1(1)
N(6)	19(1)	21(1)	27(1)	-3(1)	-9(1)	2(1)
N(7)	19(1)	15(1)	24(1)	-3(1)	1(1)	1(1)

Table 3.9 Continued:

O(1)	21(1)	20(1)	26(1)	-3(1)	-4(1)	-4(1)
O(2)	21(1)	24(1)	20(1)	-2(1)	2(1)	-5(1)
O(3)	17(1)	22(1)	22(1)	-4(1)	-2(1)	2(1)
O(4)	28(1)	20(1)	24(1)	-7(1)	1(1)	-4(1)
O(5)	25(1)	35(1)	22(1)	-7(1)	-6(1)	6(1)
O(6)	40(1)	31(1)	21(1)	-3(1)	3(1)	9(1)
S(1)	25(1)	24(1)	17(1)	-3(1)	2(1)	-5(1)
S(2)	21(1)	27(1)	25(1)	-3(1)	1(1)	-3(1)

CHAPTER REFERENCES

(1) Fernández-Moreira, V.; Song, B.; Sivagnanam, V.; Chauvin, A.-S.; Vandevyver, C. D. B.; Gijs, M.; Hemmilä, I.; Lehr, H.-A.; Bünzli, J.-C. G. *Analyst* **2009**, *135* (1), 42–52.

(2) Wang, X.; Chang, H.; Xie, J.; Zhao, B.; Liu, B.; Xu, S.; Pei, W.; Ren, N.; Huang, L.; Huang, W. *Coord. Chem. Rev.* **2014**, *273–274*, 201–212.

(3) Terai, T.; Kikuchi, K.; Iwasawa, S.; Kawabe, T.; Hirata, Y.; Urano, Y.; Nagano, T. *J. Am. Chem. Soc.* **2006**, *128* (21), 6938–6946.

(4) Park, Y. I.; Kim, H. M.; Kim, J. H.; Moon, K. C.; Yoo, B.; Lee, K. T.; Lee, N.; Choi, Y.; Park, W.; Ling, D.; Na, K.; Moon, W. K.; Choi, S. H.; Park, H. S.; Yoon, S.-Y.; Suh, Y. D.; Lee, S. H.; Hyeon, T. *Adv. Mater.* **2012**, *24* (42), 5755–5761.

(5) Kanazawa, K.; Nakamura, K.; Kobayashi, N. *Jpn. J. Appl. Phys.* **2013**, *52* (5S1), 05DA14.

(6) Carlos, L. D.; Ferreira, R. A. S.; Bermudez, V. de Z.; Ribeiro, S. J. L. *Adv. Mater.* **2009**, *21* (5), 509–534.

(7) Qiao, Y.; Lin, Y.; Zhang, S.; Huang, J. *Chem. – Eur. J.* **2011**, *17* (18), 5180–5187.

(8) Bünzli, J.-C. G. *Coord. Chem. Rev.* **2015**, *293–294*, 19–47.

(9) Ma, M.-L.; Ji, C.; Zang, S.-Q. *Dalton Trans.* **2013**, *42* (29), 10579–10586.

(10) Meruga, J. M.; Cross, W. M.; May, P. S.; Luu, Q.; Crawford, G. A.; Kellar, J. J. *Nanotechnology* **2012**, *23* (39), 395201.

(11) Gupta, B. K.; Haranath, D.; Saini, S.; Singh, V. N.; Shanker, V. *Nanotechnology* **2010**, *21* (5), 055607.

(12) Sessler, J. L.; Dow, W. C.; O'Connor, D.; Harriman, A.; Hemmi, G.; Mody, T. D.; Miller, R. A.; Qing, F.; Springs, S.; Woodburn, K.; Young, S. W. *J. Alloys Compd.* **1997**, *249* (1–2), 146–152.

(13) Wang, M.; Chen, Z.; Zheng, W.; Zhu, H.; Lu, S.; Ma, E.; Tu, D.; Zhou, S.; Huang, M.; Chen, X. *Nanoscale* **2014**, *6* (14), 8274–8282.

(14) Rogin, P.; Hulliger, J. *J. Cryst. Growth* **1997**, *172* (1–2), 200–208.

(15) Hasegawa, Y.; Kawai, H.; Nakamura, K.; Yasuda, N.; Wada, Y.; Yanagida, S. *J. Alloys Compd.* **2006**, *408–412*, 669–674.

(16) Weissman, S. I. *J. Chem. Phys.* **1942**, *10* (4), 214–217.

(17) Wilkerson, J. M. Luminescent lanthanide-containing materials: from small molecules to conducting metallopolymers, The University of Texas at Austin: Austin, TX, 2012.

(18) Jameson, D. L.; Goldsby, K. A. *J. Org. Chem.* **1990**, *55* (17), 4992–4994.

(19) Halcrow, M. A. *New J. Chem.* **2014**, *38* (5), 1868–1882.

(20) Zoppellaro, G.; Baumgarten, M. *Eur. J. Org. Chem.* **2005**, *2005* (14), 2888–2892.

(21) Basak, S.; Mohiddon, M. A.; Baumgarten, M.; Müllen, K.; Chandrasekar, R. *Sci. Rep.* **2015**, *5*, 8406.

(22) Basak, S.; Hui, P.; Boodida, S.; Chandrasekar, R. *J. Org. Chem.* **2012**, *77* (7), 3620–3626.

(23) Narayana, Y. S. L. V.; Baumgarten, M.; Müllen, K.; Chandrasekar, R. *Macromolecules* **2015**, *48* (14), 4801–4812.

(24) Narayana, Y. S. L. V.; Venkatakrishnarao, D.; Biswas, A.; Mohiddon, M. A.; Viswanathan, N.; Chandrasekar, R. *ACS Appl. Mater. Interfaces* **2016**, *8* (1), 952–958.

(25) Narayana, Y. S. L. V.; Basak, S.; Baumgarten, M.; Müllen, K.; Chandrasekar, R. *Adv. Funct. Mater.* **2013**, *23* (47), 5875–5880.

(26) Basak, S.; Narayana, Y. S. L. V.; Baumgarten, M.; Müllen, K.; Chandrasekar, R. *Macromolecules* **2013**, *46* (2), 362–369.

(27) Stanley, J. M.; Zhu, X.; Yang, X.; Holliday, B. J. *Inorg. Chem.* **2010**, *49* (5), 2035–2037.

(28) Chen, X.-Y.; Yang, X.; Holliday, B. J. *J. Am. Chem. Soc.* **2008**, *130* (5), 1546–1547.

(29) Zhu, X. J.; Holliday, B. J. *Macromol. Rapid Commun.* **2010**, *31* (9–10), 904–909.

(30) Milum, K. M.; Kim, Y. N.; Holliday, B. J. *Chem. Mater.* **2010**, *22* (8), 2414–2416.

(31) Friebe, C.; Görls, H.; Jäger, M.; Schubert, U. S. *Eur. J. Inorg. Chem.* **2013**, *2013* (24), 4191–4202.

(32) Caraway, J. D.; Nguyen, M. T.; Mitchell, L. A.; Holliday, B. J. *Macromol. Rapid Commun.* **2015**, *36* (7), 665–670.

(33) Wolf, M. O. *J. Inorg. Organomet. Polym. Mater.* **2006**, *16* (3), 189–199.

(34) Stanley, J. M.; Holliday, B. J. *Coord. Chem. Rev.* **2012**, *256* (15–16), 1520–1530.

(35) Grutzmacher, H.-F. *Eur. Mass Spectrom.* **1998**, *4* (5), 349–357.

(36) Tagle, L. H.; Terraza, C. A.; Ortiz, P.; Rodríguez, M. J.; Tundidor-Camba, A.; Leiva, A.; González-Henríquez, C.; Cabrera, A. L.; Volkmann, U. G.; Ramos-Moore, E. *J. Macromol. Sci. Part A* **2012**, *49* (7), 562–570.

(37) Strohecker, D. J.; Lynch, V. M.; Holliday, B. J.; Jones, R. A. *Dalton Trans.*

(38) Sato, S.; Wada, M. *Bull. Chem. Soc. Jpn.* **1970**, *43* (7), 1955–1962.

(39) Latva, M.; Takalo, H.; Mukkala, V.-M.; Matachescu, C.; Rodríguez-Ubis, J. C.; Kankare, J. *J. Lumin.* **1997**, *75* (2), 149–169.

(40) Chen, J. H.; Dai, C.-A.; Chiu, W.-Y. *J. Polym. Sci. Part Polym. Chem.* **2008**, *46* (5), 1662–1673.

(41) Golub, T.; Becker, J. Y. *Org. Biomol. Chem.* **2012**, *10* (19), 3906–3912.

(42) Xu, H.-C.; Campbell, J. M.; Moeller, K. D. *J. Org. Chem.* **2014**, *79* (1), 379–391.

(43) Zimmerman, H. E.; McKelvey, R. D. *J. Am. Chem. Soc.* **1971**, *93* (15), 3638–3645.

(44) Vives, G.; Gonzalez, A.; Jaud, J.; Launay, J.-P.; Rapenne, G. *Chem. – Eur. J.* **2007**, *13* (19), 5622–5631.

(45) *Rev. Sci. Instrum.* **1996**, *67* (10), 3722–3731.

(46) Pepitone, M. F.; Hardaker, S. S.; Gregory, R. V. *Chem. Mater.* **2003**, *15* (2), 557–563.

(47) De Silva, C. R.; Maeyer, J. R.; Wang, R.; Nichol, G. S.; Zheng, Z. *Inorganica Chim. Acta* **2007**, *360* (11), 3543–3552.

(48) Horrocks, W. D.; Albin, M. In *Progress in Inorganic Chemistry*; Lippard, S. J., Ed.; John Wiley & Sons, Inc.: Hoboken, NJ, USA, 1984; Vol. 31, pp 1–104.

(49) *CrystalClear*; Rigaku Americas Corporation: The Woodlands, Texas, USA, 2008.

(50) *CrysAlisPro*; Agilent Technologies UK Ltd.: Oxford, UK, 2013.

(51) Altomare, A.; Burla, M. C.; Camalli, M.; Cascarano, G. L.; Giacovazzo, C.; Guagliardi, A.; Moliterni, A. G. G.; Polidori, G.; Spagna, R. *J. Appl. Crystallogr.* **1999**, *32* (1), 115–119.

(52) Sheldrick, G. M. *Acta Crystallogr. Sect. A* **2008**, *64* (1), 112–122.

(53) Spek, A. L. *J. Appl. Crystallogr.* **2003**, *36* (1), 7–13.

(54) Farrugia, L. J. *J. Appl. Crystallogr.* **1999**, *32* (4), 837–838.

Chapter 4: Exploiting the Synthetic Utility of 2-(4-Aminopyrazol-1-yl)-6-(pyrazol-1-yl)pyridine

INTRODUCTION

First reported in the pioneering work by Jameson *et al.* in 1989, 2,6-bis(pyrazole-1-yl)pyridine (bppy) has been shown to serve as a versatile analogue to the well-known tridentate nitrogen-donor terpy (Figure 4.1).[1] This has led to the increasing popularity of bppy as a complementary platform for research into new *d*- and *f*-block metal complexes, in part owing to the relative ease of derivatizing the 4-position of the pyridine ring as well as the 3- and 5-positions of the pyrazole rings. Halcrow has published an especially thorough review covering the many roles in functional materials these modified ligands have assumed, with a focus on spin-crossover, supramolecular self-assembly materials and luminescent lanthanide areas.[2]

Notably, however, bppy derivatives substituted on the 4'- and 4"-positions of the pyrazole ring are comparatively rare due to unwieldy synthetic routes involving harsh, non-selective lithiations or protection/deprotection steps.[3] Though there is a growing number of examples of this type of substitution, the scope of reactions undergone by bppy derivatives at the pyrazole 4-position in the literature are largely confined to carbon

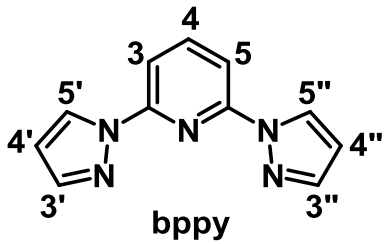

Figure 4.1: Structure and labelled positions of bppy.

coupling reactions stemming from bis(4-halopyrazol-1-yl)pyridines along with some carbonyl-derived ligands resulting from the formylation of bis(4-halopyrazol-1-yl)pyridines or nucleophilic substitution of 2,6-dibromopyridine with ethyl pyrazole-4-carboxylate.[3–11]

The synthesis and characterization of the nitro- and amino- derivatives described in Chapter 2 of this work allows for further expansion of possible ligand motifs with an even larger range of structural, electronic, and chemical environments, including 4-pyrazolyl- hydroxylamines,[12,13] secondary or tertiary amines, amides, imines, nitroamines, and azoxy compounds.[14] Additionally, 2,6-bis(4-aminopyrazol-1-yl)pyridine **(2.2)** and 2-(4-aminopyrazol-1-yl)-6-(pyrazol-1-yl)pyridine **(2.6)** discussed in Chapter 2 lend themselves well to the formation of products resulting from a wealth of diazonium substitution chemistry,[15] such as *bis*- aryl-, azido-,[16] azo-,[17] cyano-, fluoro-, hydroxyl-,[18] and mercapto- substituted bppy species, as well as those made possible by Buchwald-Hartwig amination conditions (Scheme 4.1).[19] Having explored the synthesis of 4-amido-pyrazol-1-yl bppy derivatives in Chapter 3, this chapter details efforts taken to synthesize novel monomeric and oligomeric bppy derivatives, including imines, diazotization products, azo compounds, thiols and alkylated amines.

RESULTS AND DISCUSSION

As shown in Scheme 4.1, there is great potential for derivatization upon appending nitro- and amino- groups to the pyrazole 4-position, and synthetic control of mono- or di-substitution allows for the controlled stepwise design of monomeric, oligomeric or polymeric materials of organic or organometallic (Wolf types I or III) materials.[20] Of these two newly-created bppy compounds, however, the greater expansion

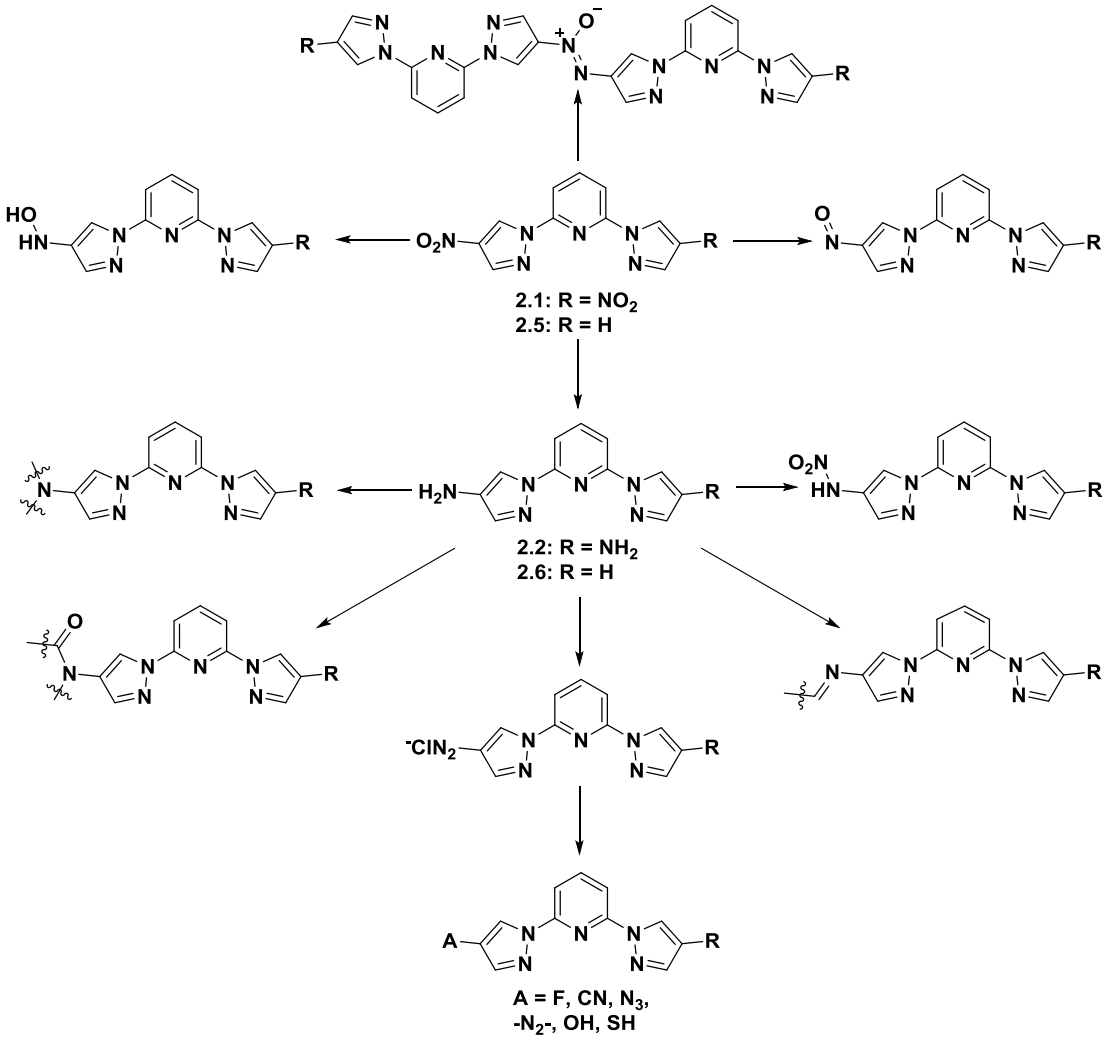

Scheme 4.1: Possible routes for functionalization of bppy ligands derived from 4-nitro- and 4-aminopyrazole compounds **2.1**, **2.2**, **2.5** and **2.6**. **R** denotes either H atoms or the matching functionality of the other pyrazole 4-position.

of synthetic utility arguably lies in the exploration of the reactivity of the amino-derivatives, which may undergo reaction with a number of electrophilic species, or be substituted with other functional groups via a diazonium intermediate. For similar reasons, pre-existing halogenated species such as 2,6-bis(4-iodopyrazol-1-yl)pyridine (**I_2-bppy**) were also explored for potential substitution reactions.[3]

In an effort to simplify reaction workup, test reactions were performed with the solubility of the synthons in mind, and thus only the easily-made and readily-soluble **I_2-bppy** halogen derivative (**4.1)** and soluble mono-amino- species, **2.6**, were explored for reactivity. Compound **2.6** further simplified reaction workups by eliminating the possibility of mono- vs. di-substitution products of each reaction. The di-substituted amine **2.2** (see Chapter 2) should undergo the same transformations as those pursued with **2.6**, but adjustment of reaction conditions, or even functionalization of the pyridyl ring may be required on account of the lessened solubility of the compound.

Imine Oligomers

Though Chapter 3 describes the establishment of a synthetic route to 4',4"-bisamides, it is advantageous to demonstrate the capacity of the mono-substituted amine**2.6** to form imines, as amide formation required harsh conditions to convert the carboxylic acid to the reactive acid chloride for condensation, whereas imines do not. Two new bisimine-linked dimeric bppy species, **4.2** and **4.3** were synthesized (Scheme 4.2); these represent interesting possibilities for the incorporation of bppy units in Schiff base ligands and cavitands, as well as structurally-dynamic functional polyimine materials.[21–25] Compound **4.2** was formed by refluxing **2.6** with the isophthalaldehyde linker, and compound **4.3** was formed by room temperature reaction of **2.6** and glyoxal in the presence of a catalytic amount of formic acid. Compound **2.6** was also reacted with 2,6-bis(pyrazol-1-yl-4-carbaldehyde)pyridine (**$(CHO)_2$bppy**) to form a bisimine-linked bppy trimer,[26] however it was not possible to isolate a pure product in this case, either by crystallization or column chromatography due to issues with solubility and product hydrolysis. This avenue could be further pursued with the addition of solubilizing groups on the pyrazole or pyridine rings.

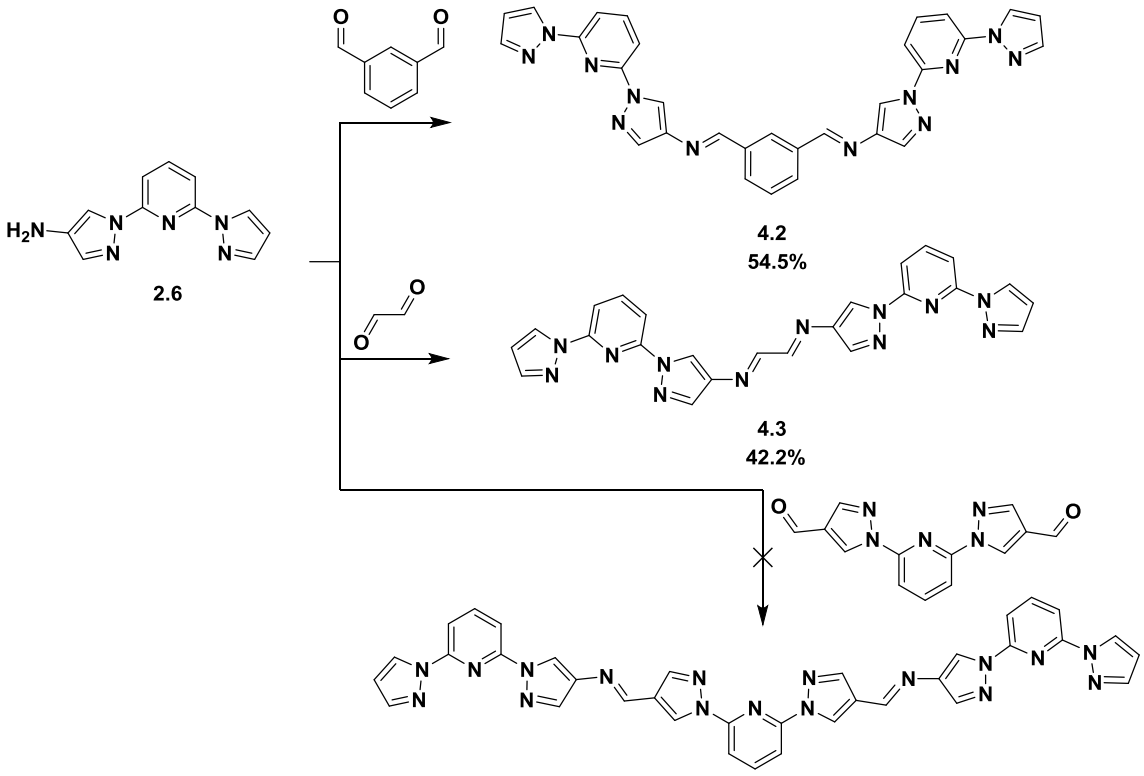

Scheme 4.2: Synthesis of imine-linked bppy derivatives **4.2** and **4.3**.

Diazonium-derived Azo compounds, Azides and Triazoles

The formation of diazonium salts from primary amines has long been pursued for the ability to convert amines to other useful functional groups, such as halogens, thiols and sulfides, alcohols and ethers, nitriles, azides and azo-compounds.[27–29] As such, development of synthetic routes which take advantage of a diazonium intermediate represents a significant addition to the ability to adapt electronic properties and functionality of bppy by synthetic means. Scheme 4.3 demonstrates progress thus far in the synthesis of new bppy derivatives via diazotization.

Interestingly, **2.6** was shown to readily dissolve in 1.1 M HCl, and diazotized in the presence of $NaNO_2$. Unfortunately, the diazonium salt (**4.4**) could not be isolated owing to its reactive nature. However, diazotization was confirmed by the formation of

the azo- compound **4.5** in the presence of phenol, and the azide **4.6** upon addition of NaN_3 (Scheme 4.3). Though yields were modest, these were exciting results owing to the further possibilities for these two substrates. Both azo compounds and azides are the subject of intense research.

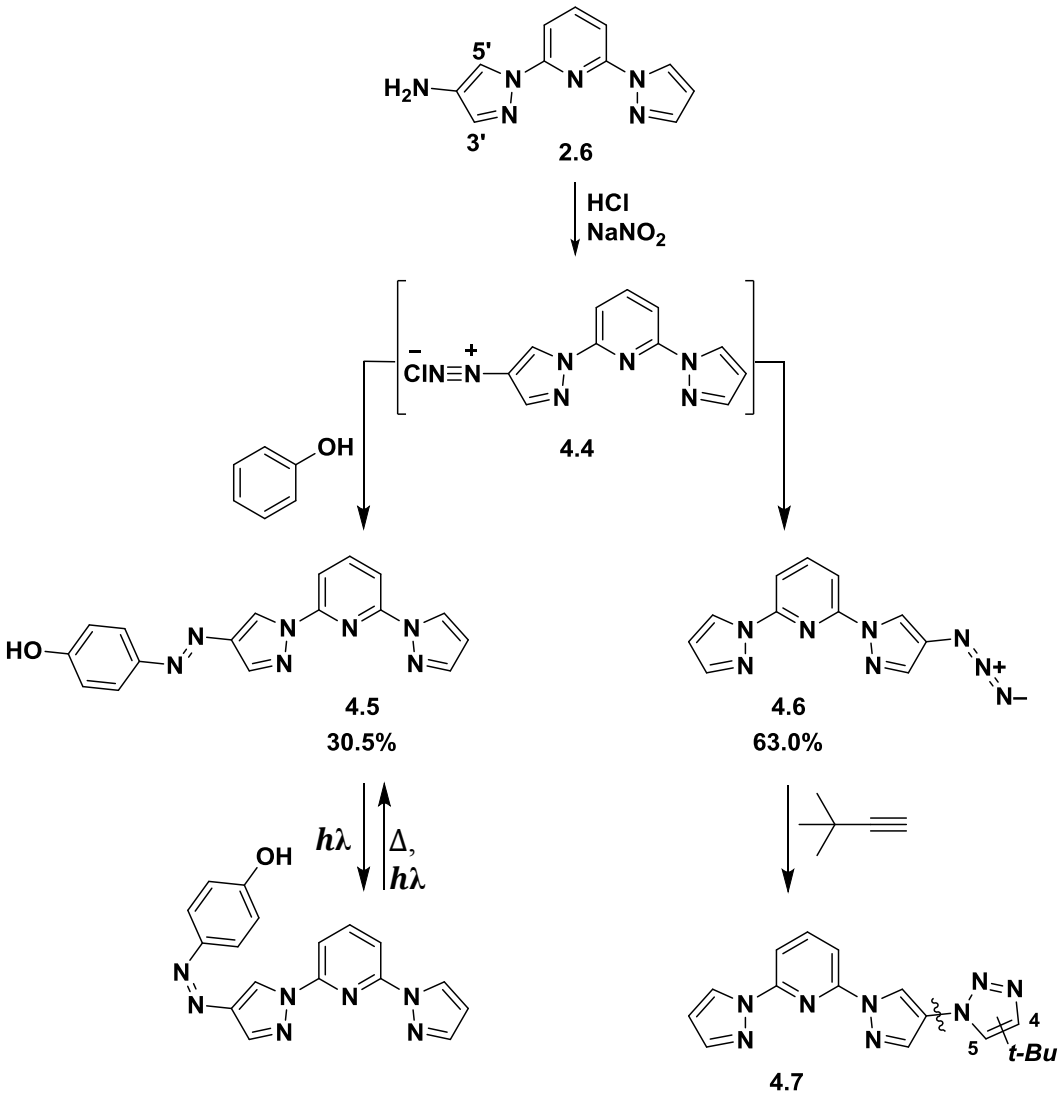

Scheme 4.3: Synthesis and additional reactivity of **4.3** and **4.4**.

Azo Compound 4.4 and Photoisomerization Investigation

It is well-known that azo compounds make up a majority of molecules used in the dye industry.[30] Additionally, these compounds are known to undergo photo-induced trans-cis isomerizations (Scheme 4.3). Azo compounds are readily formed by coupling electron-rich aryl electrophiles with diazonium salts in neutral to basic conditions. In the case of **4.5**, the crude product is a brilliant yellow solid which immediately forms upon neutralization of an acidic solution of diazonium salt **4.4** and phenol. Column chromatography of this residue yields two main fractions, both of which exhibit the characteristic coloration of the azo compound. NOESY NMR experiments indicate that these are a mixture of the expected *p*-substituted product (**4.5**, isolated 30.5%) as expected, as well *o*- and *m*- substitution by-products (approximately 7%) which proved difficult to separate by chromatography.

The UV-Vis absorption spectrum of **4.5** can be seen in Figure 4.2. A characteristic azo- absorption can be observed at approximately 435 nm, which contributes to the bright yellow color of the molecule. Two large absorbance bands can be seen centered at 350 nm and 244 nm, as well as multiple smaller features at 334, 316 and 287 nm. Irradiation of a solution of this compound with a 395 nm light source results in a drastic change in the absorption profile, which we attribute to the aforementioned photoisomerization behavior of the azo group (Figure 4.2). Namely, the peak at 350 nm decreases to approximately half of its initial intensity, and the shoulders at 316 and 287 nm increase in intensity. The presence of an isosbestic point at 327 nm also supports the existence of a trans-cis isomerization event and indicates this is an intramolecular process. The presence of the small shoulders at 316 nm and 287 nm in the spectrum of pre-irradiated solution suggests the presence of an equilibrium between the trans- and cis- isomers of this

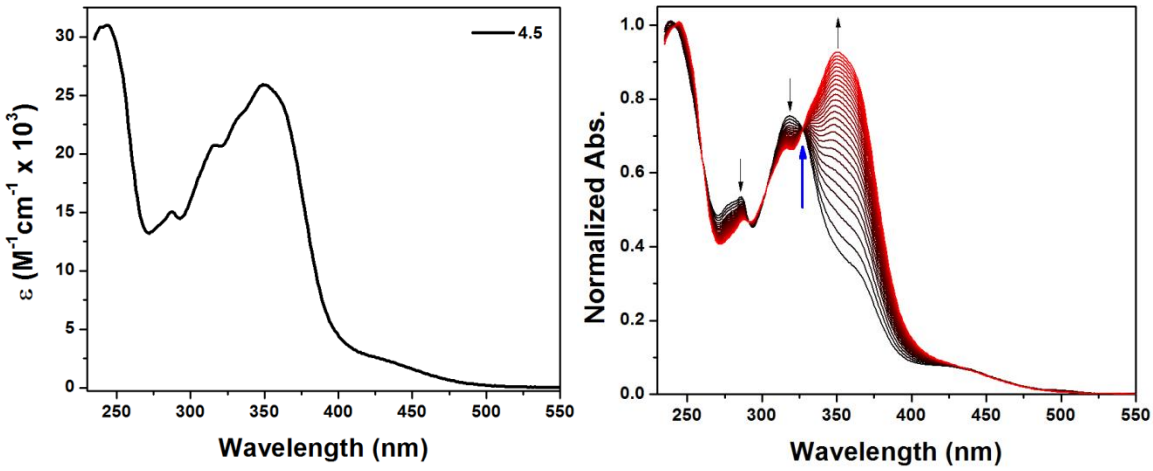

Figure 4.2: UV-Vis absorbance of **4.5** in dichloromethane solution before (left) and after (right) irradiation with a 395 nm light source. Traces in the right graph transition from black (0 min after irradiation) to red (25 min after irradiation) with isosbestic point indicated by blue arrow.

species. Subsequent absorption spectra of the irradiated sample at 1 minute intervals while it was stored in the dark indicate thermal reversibility of the photoisomerization. Full restoration of all original peak intensities was observed after 25 min.

This system could be investigated with temperature-, photoswitch cycling and concentration-dependence experiments, and the initial findings described here indicate that **4.5** is a promising precursor for a photoswitchable electronic bppy material. This is especially true when considering the ease of synthesis, the appreciable (60%) change in intensity of the 350 nm absorption peak and metal-binding capabilities of this ligand. Judicious choice of azo coupling partners may mitigate regioisomer byproduct formation in addition to proving useful in augmenting properties of the photoswitching process, such as visible-spectrum photochromism and photostability of the azo molecule in the future.

Azide Compound 4.6 and Cycloaddition with t-butylacetylene

With the synthesis of the azide-functionalized compound **4.6** (Scheme 4.3), several other types of reactions become possible. With a focus on materials chemistry, one of the most useful of these are the Huisgen 1,3-dipolar cycloaddition and the Cu(I)-catalyzed azide-alkyne cycloaddition (CuAAC), or "click" reaction which yield 1,2,3-triazoles.[31,32] These reactions are well-known to proceed cleanly and form stable products. However, the addition of asymmetric dipolarophiles by cycloaddition can lead to a mixture of products with the substituent attached to what is the 4- or 5- position of the triazole ring; research efforts have thus been focused on controlling the regioselectivity of this addition by employing various catalytic systems.[33–35]

Compound **4.6** was first isolated as a tan-colored solid after diazotization of **2.6** and *in situ* reaction of **4.4** with NaN_3. Immediately upon addition of the aqueous NaN_3 to the solution containing **4.4**, gas evolution (N_2) was seen to accompany the formation of a cream-colored flocculate. This was isolated by evaporating under a stream of air overnight (whereupon the color change to red-brown occurred), in order to prevent a potentially dangerous thermal decomposition of the azide functionality. This residue was purified by washing with ice water and the purity was determined by ^{1}H NMR.

Compound **4.6** was first subjected to simple reflux conditions in benzene with *t*-butylacetylene in lieu of CuAAC conditions to avoid Cu chelation by the tridentate N-donor binding pocket of the molecule and inadvertent formation of Cu-bppy derivatives.[2,36–38] A bulky dipolarophile was chosen in order to favor formation of the 4-substitution pattern of the resulting triazole ring (Scheme 4.3).

However, this reaction yielded a complex mixture of products, and consequently the desired product was not isolated. The formation of *t*-butyltriazole-substituted bppy

was confirmed by mass spectrometry, but no information regarding the stereochemistry of this species (4-substituted triazole vs. 5-substituted triazole) could be determined by NMR.

One possible explanation for the mixture of products from this reaction is that the azide decomposes at the elevated temperatures required for the uncatalyzed reaction. Upon melting point determination, solid **4.6** appears to change color and decompose at 78 °C, and upon further heating can be seen to expand in volume above 120 °C, indicating decomposition by gas evolution; This is suggestive of the presence of an impurity or degradation in **4.6** that is not detectable by ^{1}H NMR. Although one was not detected by NMR, the presence of an impurity may also be a plausible explanation for the cream – to – rust color change observed on prolonged exposure to ambient conditions in addition to the unexpected formation of multiple products when attempting the cycloaddition reaction.

It may also be plausible that instead of generating a preference for triazole 4-substitution as predicted, the cycloaddition gave rise to both 4-substituted and 5-substituted isomers. It is possible that triazole ring substitution at the 5-position with a bulky *t*-butyl group may distort the triazole ring out of co-planarity with the adjacent pyrazole ring, resulting in atropisomers as illustrated in Figure 4.3. Though undesirable

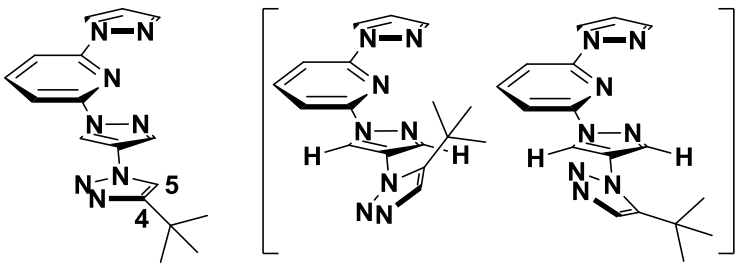

Figure 4.3: Possible stereoisomers of **4.7** resulting from 4-substitution of *tert*-butylacetylene (left) or 5-substitution (brackets) to generate atropisomers.

for the purposes of product isolation in this proof-of-concept experiment, this may be further pursued as a means to induce chirality into this bppy system. There have been a small number of examples of chiral bppy derivatives, and catalytic systems which employ them in cyclopropanation and Diels-Alder reactions showed little to moderate stereoselectivity.[39–41,37,42] As such, there is significant room for exploratory research in this area.

Compound **4.6** was then reacted with *t*-butylacetylene in the presence of a Cu(I) catalyst as described by Sharpless *et al*.[33] Subjecting the reagents to analogous conditions as described in reference 33 (3:1 volumetric ratio of *t*-butanol:water, five mole percent $CuSO_4 \bullet 5H_2O$, 50% sodium ascorbate) gave trace amounts of 4-(*t*-butyl)-triazolyl-bppy product (compound **4.7**) was isolated. Even after reacting for 36 h at room temperature, significant starting material **4.6** was present and column chromatography was necessary to purify the product. Although this reaction serves as a positive proof-of-concept for CuAAC coupling with bppy at the pyrazole 4-position, reaction conditions should be optimized in the future to improve the solubility of the **4.6** starting material.

Reaction of azide**s** and terminal alkynes under Ru-catalyzed azide-alkyne coupling (RuAAC) conditions have been shown to selectively form the 5-substituted triazole product.[43] Reaction of **4.6** and *t*-butylacetylene, or other sterically-demanding substrates may be performed using RuAAC catalysts in the future to investigate chiral atropisomers as displayed in Figure 4.3.

2-(4-Aminopyrazol-1-yl)-6-(4-nitropyrazol-1-yl)pyridine (4.8)

The reduction of dinitro-compound **2.1** to the corresponding amine **2.2** has only been achieved in reasonable yields by hydrogenation with the use of 20 mole percent PtO_2 precatalyst. Though yields in the 80% range for this reaction (reported in Chapter 2)

have been consistently achieved, the large amount of expensive catalyst required and the prolonged reaction time incentivized the search for a means to achieve the reduction of **2.1** to **2.2** using milder and more cost-effective conditions. Surprisingly, employing $HSiCl_3$ and trimethylamine as described by Benaglia *et al*. was mild enough to affect reduction of one nitro-group to form compound **4.8** in 15% yield (Scheme 4.4).[44] Unfortunately, this molecule decomposes in a matter of days under ambient storage conditions and subsequent metalation to give an analogous Ln(III) complex was not achieved.

Though the desired transformation to **2.2** was not achieved, compound **4.8** may be an interesting molecule worthy of investigation in its own right. Stepwise reactions of the amine followed by reduction of the nitro- group may serve as a route to asymmetric functionalization of amines on this ligand. Furthermore, a "push-pull" type of molecule such as **4.8** may give rise to interesting non-linear optical properties or unique binding motifs in metal complexes.[45–47]

Scheme 4.4: Synthesis of compound **4.8**.

Sulfonates, Thiols, and Thioethers

The synthesis of bppy derivatives functionalized with sulfur-containing groups may impart desirable properties such as water solubility and further synthetic possibilities. To this end, syntheses of bppy derivatives functionalized with free thiols,

benzyl sulfides and sulfonates appended at the pyrazole 4-positions were pursued. However, these attempts were met with little or no success (Scheme 4.5).

Initial attempts at direct sulfonation with fuming sulfuric acid gave intractable mixtures of poly-sulfonation products. Installation of a sulfonate on pyrazole, followed by nucleophilic substitution using the Ba^+ sulfonate (compound **4.9**) and generating the Na^+ pyrazolate with NaH gave no reaction. It is likely that this species is too poor of a nucleophile to undergo nucleophilic aromatic substitution, even upon heating at 140 °C; the 4-nitropyrazolate generated with NaH was able to undergo substitution at 120 °C.

Attempts to synthesize the free thiol were also unsuccessful. Substitution of **4.1** was attempted using multiple conditions with NaS, as well as ethanenedithiol in the presence of a Cu(II) catalyst source as per literature.[48] The Cu-catalyzed reaction did yield substantial amounts of bppy, and trace amounts of mono- and di-substitution products by MS, but no product in an isolable quantity was achieved. It is possible that the reaction progress was inhibited by chelation of the catalyst with the bppy substrate. However, the formation of bppy and the thiols of interest in small quantities suggest that

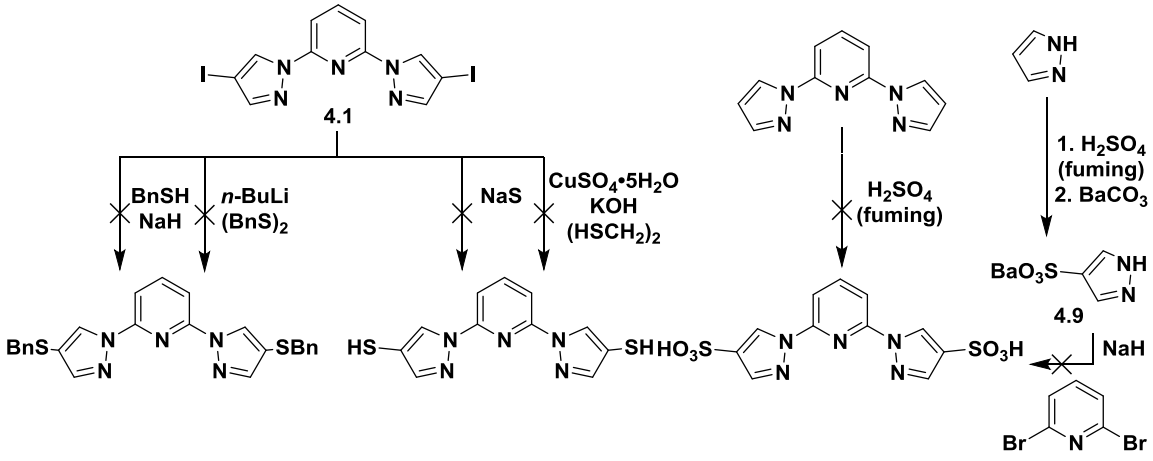

Scheme 4.5: Attempted syntheses of S-containing bppy derivatives.

further optimization of these conditions such as increasing catalyst loading, reaction temperature, or reaction time, may lead to appreciable yields of product.

Finally a bppy benzyl thioether was targeted as a protected thiol from which other sulfur-containing bppy ligands could be derived. Initial attempts at substitution of **4.1** with benzyl thiolate resulted in the formation of benzyl disulfide instead of nucleophilic attack of the halogenated species. Subsequent lithiations of **4.1** and treatment with benzyl disulfide also failed to produce any isolable amount of product, though the di-substituted species (formula $C_{25}H_{21}N_5S_2$) was detected by MS.

CONCLUSIONS

With established synthetic routes to form both mono- and di-substituted terminal imino-bppy ligands **4.2** and **4.3**, as well as amido-bppy ligands **3.2** – **3.4**, condensation polymerization of bppy for facile bulk functional materials syntheses, and numerous other derivatives and structures that avoid the use of expensive metal catalysts are now possible.[23,49–51]

The synthesis of diazotization products **4.5** and **4.6** are also particularly exciting, as they demonstrate the feasibility of diazonium chemistry at the pyrazole 4-position as a new tool for the synthetic modification of bppy. Additionally, these compounds open up opportunities for the incorporation of bppy in new classes of functional materials, such as azo- dyes,[30,38,52] photoswitchable systems,[46,53,54] surface-functionalized electronic materials[28] and click polymers.[23]

The reduction of one nitro- group of compound **2.1** to form the asymmetric compound **4.8** demonstrates a method of controlling the electronic nature of this ligand. Molecules with opposing electron-withdrawing and -donating substituents have been used in nonlinear optical materials.[36] This compound may be of interest for similar

reasons, in addition to the possibility for stepwise reaction of each amine group of the ligand by virtue of protecting one as a nitro group while reacting the other.

Finally, this chapter described unsuccessful attempts to prepare bppy derivatives with sulfur-containing functionalities at the pyrazole 4-position. Future efforts towards this goal may be well-served by attempting syntheses with a mono-iodinated bppy substrate to simplify workup, protection of the ligand binding pocket by forming N-oxides to prevent catalyst poisoning, or the employment of the diazotization described in this chapter to increase the driving force of the reaction by N_2 liberation.

EXPERIMENTAL

Materials and Methods

All reagents were purchased from commercial sources and used without further purification. Dry diglyme was obtained from Sigma-Aldrich in Sure/Seal™ bottles and used without further drying. Other dry solvents were obtained from an Innovative Technology PureSolv 400 solvent purifier with a double purifying column and stored in Schlenk storage flasks over 3 Å molecular sieves under nitrogen atmosphere.

NMR spectra were referenced to residual solvent peaks, with chemical shifts reported in ppm and coupling constants measured in Hz. Mass spectrometry was carried out using Micromass Autospec Ultima HRMS and Agilent 6530 QTOF instruments. IR spectra were recorded with a Thermo Nicolet Smart Performer ATR accessory on a Nicolet Avatar 330 FT-IR spectrophotometer. Melting points were recorded on a Stanford Research Systems MP100 OptiMelt in open capillaries and are reported uncorrected. UV-Vis absorption spectrophotometry measurements were performed in quartz fluorometer cells with 1.0 cm path lengths. All room-temperature UV-Vis absorption measurements were obtained with dichloromethane (DCM) solvent.

Synthesis

The synthesis of **2.2**, **2.6**, **4.1** and **4.9** were performed and characterized as reported elsewhere.[3,19,55] The insoluble nature of bisimines **3.1** and **3.2** prevented characterization by ^{13}C NMR in $CDCl_3$ or DMSO-d_6 solvents.

1,1'-(1,3-phenylene)*bis*(N-(1-(6-(1*H*-pyrazol-1-yl)pyridin-2-yl)-1*H*-pyrazol-4-yl)methanimine) (4.2): **2.6** (0.300 g, 0.133 mmol) and isophthalic dicarboxaldehyde (0.0107 g, 0.0798 mmol) were dissolved in ethanol (10 mL), then heated to reflux while stirring in an 85 °C oil bath for 12 h. The reaction mixture was placed in an ice bath for 30 min, then the white flocculate was washed with portions of cold ethanol (20 mL) and collected via vacuum filtration. The off-white solid product was dried under vacuum at 60 °C, then weighed (yield: 0.0199 g; 54.5%). ^1H NMR (400 MHz, $CDCl_3$) δ 8.77 (d, J = 6.9 Hz, 4H), 8.61 (dd, J = 2.6, 0.7 Hz, 2H), 8.42 (s, 1H), 8.06 – 7.94 (m, 6H), 7.92 – 7.84 (m, 4H), 7.81 – 7.77 (m, 2H), 7.61 (t, J = 7.7 Hz, 1H), 6.56 – 6.49 (m, 2H). M.P. 247.1 – 255.8 °C. HR-MS (ESI^+): calcd for $C_{30}H_{22}N_{12}$ $(M + H)^+$ *m/z* 551.21630, found 551.21730. IR ($\bar{\nu}$, cm^{-1}): 3,126 (w, C – H), 2,878 (m, C – H), 1,606 (m, C = N).

N,N'-*bis*(1-(6-(1*H*-pyrazol-1-yl)pyridin-2-yl)-1*H*-pyrazol-4-yl)ethane-1,2-diimine (4.3): **2.6** (0.0308 g, 0.136 mmol) was dissolved in methanol (10 mL) and stirred in an ice bath for 5 min to cool. Glyoxal (40% wt. in H_2O, 0.010 mL, 0.0870 mmoL) and formic acid (0.002 mL, 0.0530 mmol) were added to the stirred solution, and the reaction was removed from the ice bath to return to room temperature. The reaction mixture was allowed to evaporate under ambient conditions, and then washed with cold methanol (50 mL). The product was then collected by vacuum filtration to afford a light yellow solid. (yield: 0.0133 g, 42.2%). ^1H NMR (500 MHz, DMSO-d_6) δ 9.38 (s, 2H), 9.09 (d, J = 2.7 Hz, 2H), 8.74 (s, 2H), 8.31 (s, 2H), 8.18 (t, J = 8.0 Hz, 2H), 7.89 (s, 2H), 7.87 (d, J = 3.9 Hz, 2H), 7.85 (d, J = 3.8 Hz, 2H), 6.66 (dd, J = 2.6, 1.6 Hz, 2H). M.P. 228.4 °C

(decomp.). HR-MS (ESI^+): calcd for $C_{24}H_{18}N_{12}$ $(M + Na)^+$ *m/z* 497.16700, found 497.16830. IR ($\bar{\nu}$, cm^{-1}): 3,132 (w, C – H), 2,948 (w, C – H), 1,602 (m, C = N).

4-((1-(6-(1*H*-pyrazol-1-yl)pyridin-2-yl)-1*H*-pyrazol-4-yl)diazenyl)phenol (4.5): **2.6** (0.0251 g, 0.111 mmol) was suspended in H_2O (5 mL), cooled in an ice bath for 10 min, then dissolved via the addition of conc. HCl (12.1 M, 0.5 mL) in the presence of stirring. This solution was allowed to stir for an additional 10 min to cool, then a cold solution of $NaNO_2$ (0.0083 g, 0.120 mmol) in H_2O (2 mL) was added to the acidified amine solution at a rate of 1 drop/s with rapid stirring. The yellow solution was stirred for an additional 30 min, then a solution of phenol (0.0103 g, 0.109 mmol) in cold methanol (2 mL) was added at a rate of 1 drop/s. The reaction mixture was stirred in an ice bath for an additional 15 minutes, and then allowed to warm to room temperature for 12 h. The warmed solution was then neutralized to pH 7 with saturated $NaHCO_3$ (5.5 mL) and a bright yellow precipitate immediately formed. The solid was collected via vacuum filtration, then purified by column chromatography with silica and 2% v/v methanol/DCM. The product was collected then concentrated under vacuum to give a bright yellow solid (yield: 0.0112 g; 30.5%). ^1H NMR (499 MHz, $CDCl_3$) δ 9.12 (d, J = 0.7 Hz, 1H), 8.63 (dd, J = 2.6, 0.8 Hz, 1H), 8.23 (d, J = 0.7 Hz, 1H), 7.99 (t, J = 7.9 Hz, 1H), 7.92 (t, J = 8.3 Hz, 2H), 7.83 (d, J = 9.2 Hz, 2H), 7.79 (dd, J = 1.7, 0.8 Hz, 1H), 6.95 (d, J = 8.3 Hz, 2H), 6.53 (dd, J = 2.6, 1.6 Hz, 1H), 5.21 (s, 1H). ^{13}C NMR (126 MHz, $CDCl_3$) δ 142.61, 141.57, 135.29, 127.04, 124.56, 123.54, 115.87,109.61, 108.13, 78.09, 76.79, 76.58. M.P. 195.5 – 215.1 °C (decomp.). HR-MS (ESI^+): calcd for $C_{17}H_{13}N_7O$ $(M + Na)^+$ *m/z* 354.10740, found 354.10770. IR ($\bar{\nu}$, cm^{-1}): 3,316 (w, O – H), 3,120 (w, C – H) 2,925 (m, C – H), 1,439 (s, N = N).

2-(4-azido-1*H*-pyrazol-1-yl)-6-(1*H*-pyrazol-1-yl)pyridine (4.6): **2.6** (0.0252 g, 0.111 mmol) was suspended in H_2O (5 mL), cooled in an ice bath for 10 min, then

dissolved via the addition of conc. HCl (12.1 M, 0.5 mL) in the presence of stirring. The solution was allowed to stir for an additional 10 min to cool, then a cold solution of $NaNO_2$ (0.0083 g, 0.120 mmol) in H_2O (2 mL) was added to the acidified amine solution at a rate of 1 drop/s with rapid stirring. This yellow solution was stirred for an additional 30 min, then a solution of NaN_3 (0.0120 g, 0.185 mmol) in cold water (1 mL) was added to the rapidly stirred solution at a rate of 1 drop/s. A white precipitate immediately formed and gas evolution was observed. The reaction mixture was stirred in an ice bath for an additional 15 minutes, then removed and allowed to warm to room temperature for 12 h. The volatile materials were evaporated using a stream of N_2 overnight at room temperature to yield a rust-colored solid. The solid was suspended in and washed with ice water (50 mL), collected by vacuum filtration, washed with boiling hexanes (50 mL), then dried under ambient conditions for 1 d and collected as a tan solid (yield: 0.0177 g; 63.0%). ^{1}H NMR (500 MHz, $CDCl_3$) δ 8.56 (d, J = 2.6 Hz, 1H), 8.39 (d, J = 0.9 Hz, 1H), 7.94 (t, J = 8.0 Hz, 1H), 7.89 – 7.85 (m, 1H), 7.81 (dd, J = 7.9, 0.8 Hz, 1H), 7.77 (d, J = 1.6 Hz, 1H), 7.62 (d, J = 0.9 Hz, 1H), 6.51 (dd, J = 2.6, 1.7 Hz, 1H). ^{13}C NMR (126 MHz, $CDCl_3$): δ 150.24, 149.72, 142.69, 141.62, 134.87, 127.19, 125.50, 117.41, 109.88, 108.99, 108.29. M.P. 78.62 °C (decomp.). HR-MS (ESI^+): calcd for $C_{11}H_8N_8$ $(M + Na)^+$ *m/z* 275.07640, found 275.07630. IR ($\bar{\nu}$, cm^{-1}): 3,104 (w, C – H), 2,922 (w, C – H), 2,110 (s, N = N).

2-(4-(4-(tert-butyl)-1H-1,2,3-triazol-1-yl)-1H-pyrazol-1-yl)-6-(1H-pyrazol-1-yl)pyridine (**4.7**): **4.6** (0.020 g, 0.0793 mmol) and 3,3-dimethylbut-1-yne (0.010 mL, 0.0816 mmol) were suspended in a 3:1 v:v *t*-butanol: water (8 mL) solution with rapid stirring. Sodium ascorbate (0.008 g, 0.0404 mmol) and copper sulfate pentahydrate (0.001 g, 0.0048 mmol) were dissolved in H_2O (0.5 mL each) then added to the reaction mixture in that order. The reaction was stirred at room temperature and monitored by

TLC using 1% v/v methanol/DCM eluent. After 36 h, the reaction was vacuum-filtered and washed with cold H_2O (50 mL) to give a tan solid. The solid was subjected to silica column chromatography (1% methanol/DCM eluent) and the R_f = 0.1 band was isolated to give **4.7** as a yellow residue. The amount of product isolated was too small for chemical yield or characterization beyond ^{1}H NMR an HR-MS to be determined. ^{1}H NMR (500 MHz, $CDCl_3$) δ 8.96 (s, 1H), 8.59 (d, J = 2.6 Hz, 1H), 8.07 (s, 1H), 8.00 (t, J = 7.9 Hz, 1H), 7.95 (s, 1H), 7.90 (dd, J = 7.8, 1.0 Hz, 1H), 7.78 (d, J = 1.6 Hz, 1H), 7.61 (s, 1H), 6.56 – 6.52 (m, 1H), 1.44 (s, 9H). HR-MS (ESI^+): calcd for $C_{11}H_{18}N_8$ $(M + H)^+$ *m/z* 335.17270, found 335.17270.

2-(4-nitropyrazol-1-yl)-6-(4-aminopyrazol-1-yl)pyridine (4.8): **2.1** (0.1255 g, 0.417 mmol) and N,N-diisopropylethylamine (0.730 mL, 4.190 mmol) were suspended in dry DCM (300 mL) under a N_2 atmosphere, then immersed in an ice bath. A solution of trichlorosilane (0.350 mL, 3.46 mmol) in dry acetonitrile (5 mL) was added to the stirred reaction mixture at a rate of 0.5 drop/s. After addition of the silane, the reaction was allowed to warm to room temperature 12 h. The reaction mixture was then concentrated by heating under N_2 and then suspended in wet DCM (100 mL). The reaction was neutralized with saturated $NaHCO_3$ (20 mL), then washed with H_2O (50 mL x 3) and concentrated on a rotary evaporator. The resulting yellow solid was purified by column chromatography with silica and DCM. The product was concentrated under vacuum then collected as a brown solid (yield: 0.0179 g; 15.8%). Note: under ambient storage conditions, this product appears to decompose, as monitored by ^{1}H NMR; a ^{13}C NMR spectrum could not be obtained for this compound. ^{1}H NMR (400 MHz, DMSO-d_6): 9.81(s, 1H), 8.64 (s, 1H) 8.32 (s, 1H), 8.12 (t, J = 8.0, 1H), 7.83 (d, J = 8.0, 1H), 7.76 (d, J = 8.0, 1H), 7.43 (s, 1H). M.P. 72.36 °C (decomp.). HR-MS (ESI^+): calcd for $C_{11}H_9N_7O_2$

$(M + H)^+$ *m/z* 272.08900, found 272.08950. IR ($\bar{\nu}$, cm^{-1}): 3,334 (w, N – H), 3,121 (m, C – H), 2927 (m, C – H), 1608 (w, N – O) 1,473 (m, N – O).

CHAPTER REFERENCES

(1) Jameson, D. L.; Blaho, J. K.; Kruger, K. T.; Goldsby, K. A. *Inorg. Chem.* **1989**, *28* (24), 4312–4314.

(2) Halcrow, M. A. *New J. Chem.* **2014**, *38* (5), 1868–1882.

(3) Zoppellaro, G.; Baumgarten, M. *Eur. J. Org. Chem.* **2005**, *2005* (14), 2888–2892.

(4) Zhu, X. J.; Holliday, B. J. *Macromol. Rapid Commun.* **2010**, *31* (9–10), 904–909.

(5) Basak, S.; Hui, P.; Chandrasekar, R. *Synthesis* **2009**, *2009* (23), 4042–4048.

(6) Basak, S.; Narayana, Y. S. L. V.; Baumgarten, M.; Müllen, K.; Chandrasekar, R. *Macromolecules* **2013**, *46* (2), 362–369.

(7) Narayana, Y. S. L. V.; Venkatakrishnarao, D.; Biswas, A.; Mohiddon, M. A.; Viswanathan, N.; Chandrasekar, R. *ACS Appl. Mater. Interfaces* **2016**, *8* (1), 952–958.

(8) Narayana, Y. S. L. V.; Basak, S.; Baumgarten, M.; Müllen, K.; Chandrasekar, R. *Adv. Funct. Mater.* **2013**, *23* (47), 5875–5880.

(9) Narayana, Y. S. L. V.; Baumgarten, M.; Müllen, K.; Chandrasekar, R. *Macromolecules* **2015**, *48* (14), 4801–4812.

(10) Basak, S.; Hui, P.; Boodida, S.; Chandrasekar, R. *J. Org. Chem.* **2012**, *77* (7), 3620–3626.

(11) Pritchard, R.; Kilner, C. A.; Barrett, S. A.; Halcrow, M. A. *Inorganica Chim. Acta* **2009**, *362* (12), 4365–4371.

(12) Tallec, A.; Hazard, R.; SuwiNski, J.; Wagner, P. *Pol. J. Chem.* **2000**, *47* (8), 1177–1183.

(13) Cuadrado, P.; González-Nogal, A. M.; Martínez, S. *Tetrahedron* **1997**, *53* (25), 8585–8598.

(14) Suwiński, J.; Wagner, P. *Pol. J. Chem.* **2000**, *74* (11), 1575–1580.

(15) Yin, P.; Zhang, J.; Parrish, D. A.; Shreeve, J. M. *Chem. - Eur. J.* **2014**, *20* (50), 16529–16536.

(16) Fevig, J. M.; Cacciola, J.; Buriak Jr., J.; Rossi, K. A.; Knabb, R. M.; Luettgen, J. M.; Wong, P. C.; Bai, S. A.; Wexler, R. R.; Lam, P. Y. S. *Bioorg. Med. Chem. Lett.* **2006**, *16* (14), 3755–3760.

(17) Kumar, R.; Joshi, Y. C.; Joshi, P. *Heterocycl. Commun.* **2005**, *11* (3–4), 361–364.

(18) De Sio, F. *Heterocycles* **1984**, *22* (10), 2309–2311.

(19) Strohecker, D. J.; Lynch, V. M.; Holliday, B. J.; Jones, R. A. *Dalton Trans.*, submitted.

(20) Wolf, M. O. *Adv. Mater.* **2001**, *13* (8), 545–553.

(21) Frischmann, P. D.; MacLachlan, M. J. *Chem. Commun.* **2007**, No. 43, 4480–4482.

(22) Nagymihály, Z.; Kollár, L. *Tetrahedron* **2015**, *71* (17), 2555–2560.

(23) Tennyson, A. G.; Norris, B.; Bielawski, C. W. *Macromolecules* **2010**, *43* (17), 6923–6935.

(24) Chen, L.; Chen, Z.; Li, X.; Huang, W.; Li, X.; Liu, X. *Polymer* **2013**, *54* (7), 1739–1745.

(25) Huang, W.; Jiang, Y.; Li, X.; Li, X.; Wang, J.; Wu, Q.; Liu, X. *ACS Appl. Mater. Interfaces* **2013**, *5* (18), 8845–8849.

(26) Davis, T. I., unpublished work.

(27) Deadman, B. J.; Collins, S. G.; Maguire, A. R. *Chem. – Eur. J.* **2015**, *21* (6), 2298–2308.

(28) Mahouche-Chergui, S.; Gam-Derouich, S.; Mangeney, C.; Chehimi, M. M. *Chem. Soc. Rev.* **2011**, *40* (7), 4143–4166.

(29) Miras; C, M.; Acevedo, D. F.; Monge, N.; Frontera, E.; Rivarola, C. R.; Barbero, C. A. *Open Macromol. J.* **2008**, *2* (1).

(30) Yildiz, E.; Boztepe, H. *Turk. J. Chem.* **2002**, *26* (6), 897.

(31) Huisgen, R. *Angew. Chem. Int. Ed. Engl.* **1963**, *2* (10), 565–598.

(32) Zheng, Z.-J.; Wang, D.; Xu, Z.; Xu, L.-W. *Beilstein J. Org. Chem.* **2015**, *11* (1), 2557–2576.

(33) Rostovtsev, V. V.; Green, L. G.; Fokin, V. V.; Sharpless, K. B. *Angew. Chem. Int. Ed.* **2002**, *41* (14), 2596–2599.

(34) Zhang, L.; Chen, X.; Xue, P.; Sun, H. H. Y.; Williams, I. D.; Sharpless, K. B.; Fokin, V. V.; Jia, G. *J. Am. Chem. Soc.* **2005**, *127* (46), 15998–15999.

(35) Kumar, K.; Konar, D.; Goyal, S.; Gangar, M.; Chouhan, M.; Rawal, R. K.; Nair, V. A. *J. Org. Chem.* **2016**, *81* (20), 9757–9764.

(36) Zikode, M.; Ojwach, S. O.; Akerman, M. P. *Appl. Organomet. Chem.* **2017**, *31* (2), n/a-n/a.

(37) Christenson, D. L.; Tokar, C. J.; Tolman, W. B. *Organometallics* **1995**, *14* (5), 2148–2150.

(38) Hussain, G.; Ather, M.; Khan, M. U. A.; Saeed, A.; Saleem, R.; Shabir, G.; Channar, P. A. *Dyes Pigments* **2016**, *130*, 90–98.

(39) Watson, A. A.; House, D. A.; Steel, P. J. *J. Org. Chem.* **1991**, *56* (12), 4072–4074.

(40) LeCloux, D. D.; Tolman, W. B. *J. Am. Chem. Soc.* **1993**, *115* (3), 1153–1154.

(41) Kowalczyk, R.; Skarżewski, J. *Tetrahedron* **2005**, *61* (3), 623–628.

(42) Kashima, C.; Shibata, S.; Yokoyama, H.; Nishio, T. *J. Heterocycl. Chem.* **2003**, *40* (5), 773–782.

(43) Zhang, L.; Chen, X.; Xue, P.; Sun, H. H. Y.; Williams, I. D.; Sharpless, K. B.; Fokin, V. V.; Jia, G. *J. Am. Chem. Soc.* **2005**, *127* (46), 15998–15999.

(44) Orlandi, M.; Tosi, F.; Bonsignore, M.; Benaglia, M. *Org. Lett.* **2015**, *17* (16), 3941–3943.

(45) Cabral, B. J. C. *Chem. Phys. Lett.* **2017**, *667*, 332–336.

(45) Zhou, Y.; Liu, B.; Wang, X. *Polymer* **2017**, *111*, 229–238.

(47) Delaire, J. A.; Nakatani, K. *Chem. Rev.* **2000**, *100* (5), 1817–1846.

(48) Liu, Y.; Kim, J.; Seo, H.; Park, S.; Chae, J. *Adv. Synth. Catal.* **2015**, *357* (10), 2205–2212.

(49) Wolf, M. O. *J. Inorg. Organomet. Polym. Mater.* **2006**, *16* (3), 189–199.

(50) de Hatten, X.; Asil, D.; Friend, R. H.; Nitschke, J. R. *J. Am. Chem. Soc.* **2012**, *134* (46), 19170–19178.

(51) Chow, C.-F. *J. Fluoresc.* **2012**, *22* (6), 1539–1546.

(52) Wang, M.; Funabiki, K.; Matsui, M. *Dyes Pigments* **2003**, *57* (1), 77–86.

(53) Travieso-Puente, R.; Budzak, S.; Chen, J.; Stacko, P.; Jastrzebski, J. T. B. H.; Jacquemin, D.; Otten, E. *J. Am. Chem. Soc.* **2017**, *139* (9), 3328–3331.

(54) Weston, C. E.; Richardson, R. D.; Fuchter, M. J. *Chem. Commun.* **2016**, *52* (24), 4521–4524.

(55) Morgan, G. T.; Ackerman, I. *J. Chem. Soc., Trans.* **1923**, *123* (0), 1308–1318.

Chapter 5: Spectroscopic and Structural Characterization of Novel Lanthanide Materials

INTRODUCTION

Lanthanides possess several unique properties including the characteristic light emission and diversity of coordination environments of the ions of this series. Lanthanide(III) ions can accommodate up to twelve ligands, which can give rise to a number of unique binding motifs not found in the d- or p- blocks of the periodic table.[1–6]

Light emission from the lanthanide ions has garnered research interest in a range of applications such as bioimaging, solid-state lighting, security inks, colorimetric sensing and photodynamic therapy.[7–16] This is because of the unique nature of the light emitted from these ions; Ln(III) emissions exhibit long lifetimes, large Stokes shifts and characteristic narrow, discrete emission bands.[13,17,18] These characteristics are due to the spin- and parity-forbidden nature of the *f-f* electronic transitions responsible for Ln(III) luminescence, which necessitates the use of an ancillary ligand to transfer energy onto the metal center, deemed the "antenna effect."[19,20] The electronically-insulated nature of the *f* orbitals results in luminescence transitions that are nearly constant in energy and that only vary by the relative intensity of the emission peaks; the wavelength of light emission is dictated by the identity of the Ln(III) ion.

This chapter discusses the spectroscopic properties of two types of Ln-containing materials (Figure 5.1) and their respective ligands. The first type is a series of trivalent Ln(III)-containing (Ln = Eu, Tb, Dy; compounds **5.2** – **5.4**) phosphine coordination materials (PCMs) synthesized by Dr. Alisha Bohnsack, denoted **Ln-PCM-25**, which feature a network of eight-coordinate metal centers linked by tetrahedral zwitterionic

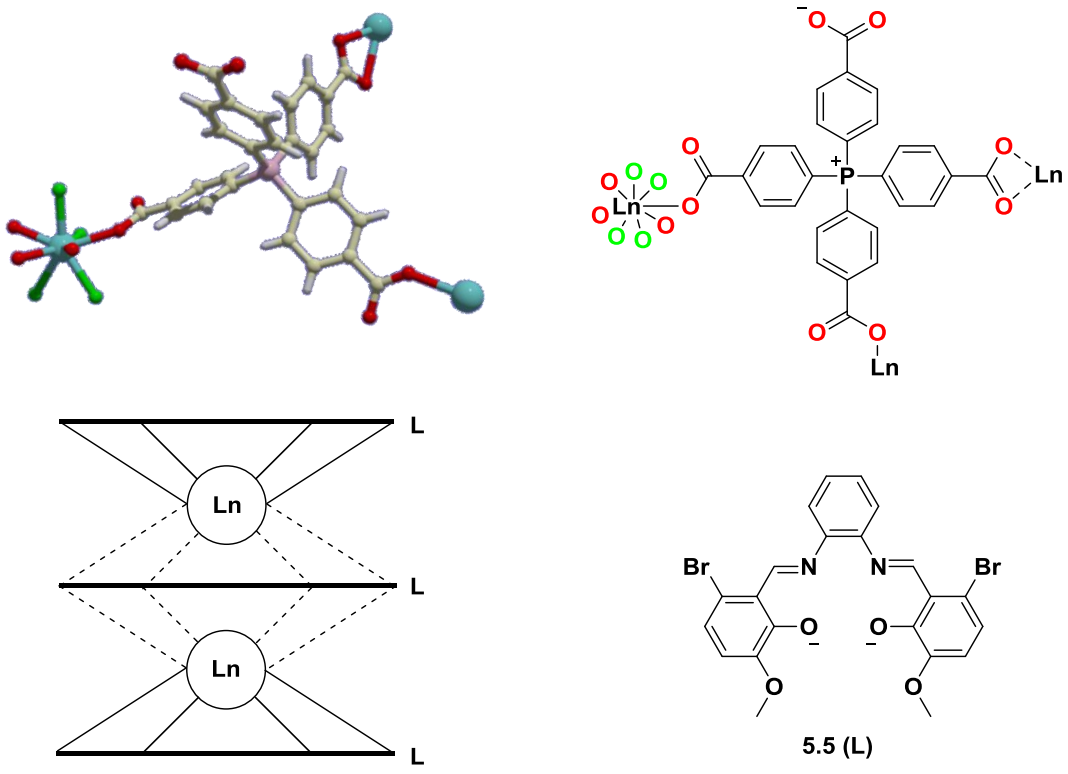

Figure 5.1: Depiction of **5.2** – **5.4** (Ln = Eu, Tb, Dy) (top, image adapted from ref. 21) and $\mathbf{Ln_2L_3}$ (bottom) tridecker complex and ligand structures.

tetrakis phosphonium(4-benzoate) ligands (denoted **5.1)**; these data have been reported previously.[21] The second is a series of $\mathbf{Ln_2L_3}$ "tridecker" complexes (Ln = Sm, Gd, Er, Yb; compounds **5.6** – **5.9**) synthesized by Tyler King that feature two eight-coordinate metal centers layered between three heteroleptic tetradentate Schiff-base ligands (denoted **5.5**).

This chapter also reports the single-crystal structures of several Ln(III) (Ln = Sm, Eu, Gd, Tb) complexes which all feature *tris*(*β*-diketonato) ligands (compounds **5.10** – **5.13**).

RESULTS AND DISCUSSION

Structure and Solid-State Luminescence of Ln-PCM-25 Materials[21]

All three PCMs are isostructural with the same interesting connectivity (Figure 5.1). Two carboxylate binding sites of ligand **5.1** coordinate to separate Ln(III) ions in a monodentate fashion and a third carboxylate binds to a third Ln(III) in an η^2 manner. The fourth deprotonated carboxylate of the zwitterionic ligand remains unbound. All Ln(III) nodes are eight-coordinate, binding four aquo ligands in addition to coordinating with the carboxylate ligands in the manner just described.

The T_1 energy level of ligand **5.1** was determined to be 22,222 cm^{-1} by quantifying the blue edge of the 77 K phosphorescence emission (Figure 5.2).

Luminescence spectra of the **Ln-PCM-25** materials are shown in Figure 5.3.

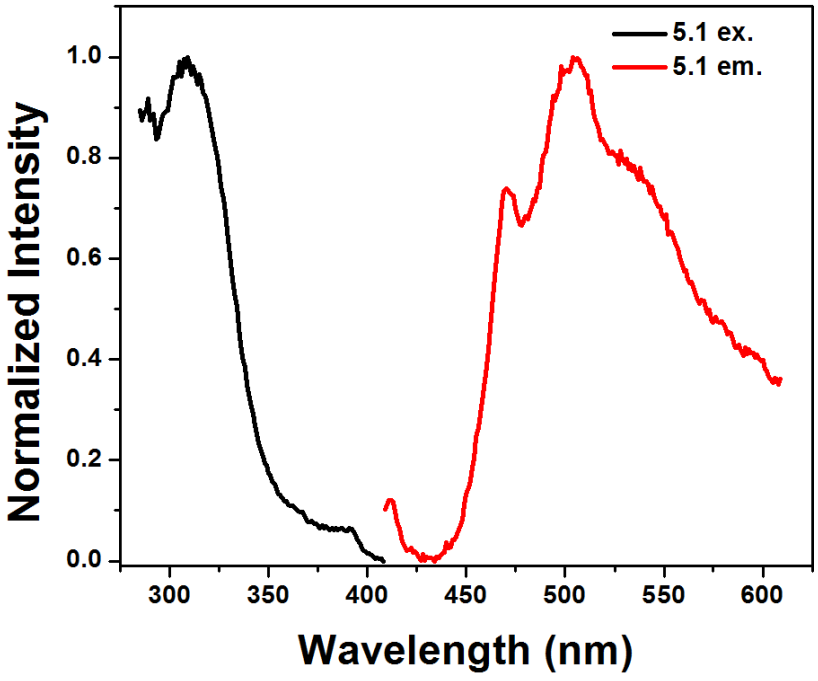

Figure 5.2: 77 K phosphorescence spectra of ligand **5.1**.

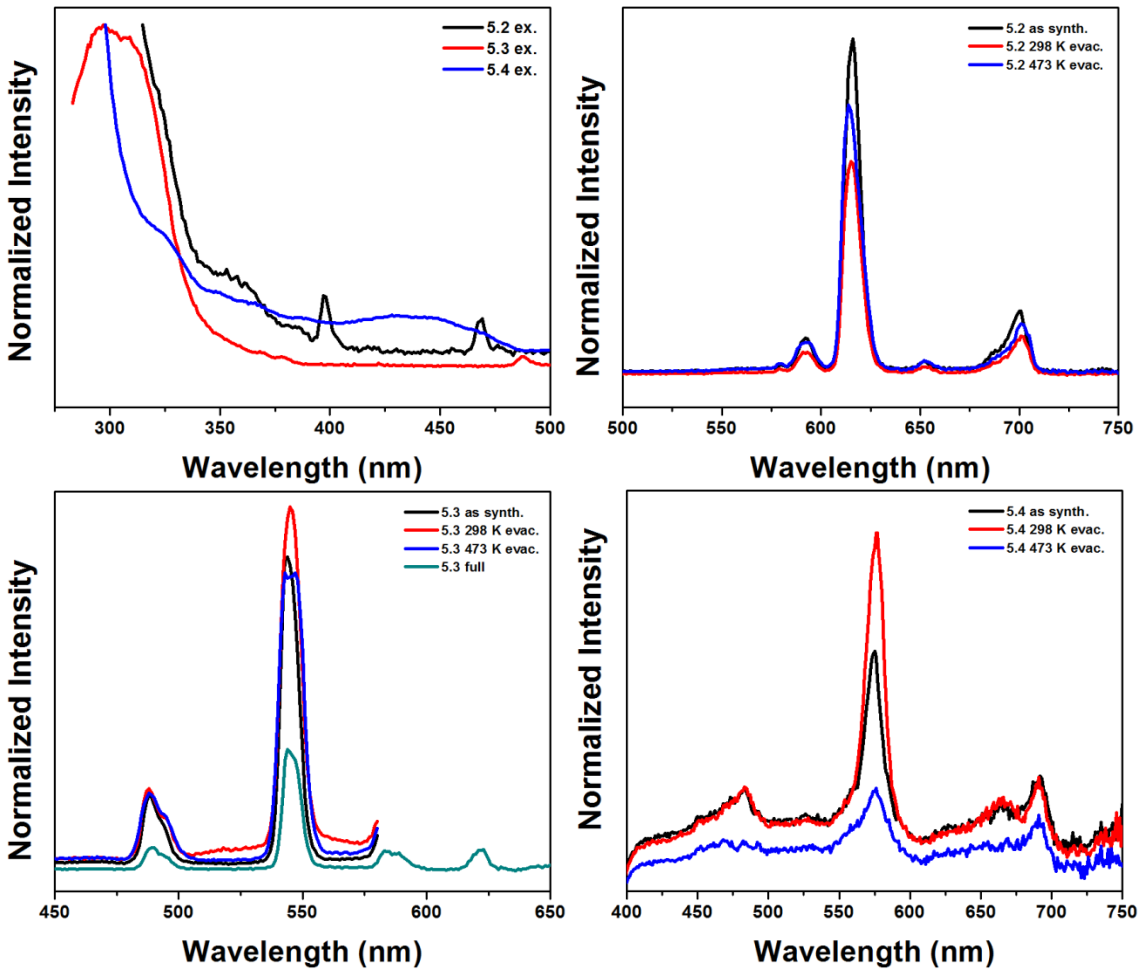

Figure 5.3: Excitation (top left) and overlays of as-synthesized and activated emission spectra of Eu (top right), Tb (lower left) and Dy (lower right) PCM-25 materials.

Three measurements were performed of as-synthesized materials as well as materials that had been "activated" by placing the materials under vacuum for 12 h at 298 K and 473 K for each different Ln(III)-containing material. Luminescence quantum yields (Φ_{abs}) and lifetime (τ_{obs}) of these materials were obtained in order to probe effects of activating these materials, as it was suspected this process would result in the removal of aquo ligands and increase the luminescence quantum yields.[13] In lieu of observing the expected trend of increased luminescence quantum yields and lifetimes in the presence of fewer

Table 5.1: Φ_{abs} and τ_{obs} of as-synthesized and activated **Ln-PCM-25** materials

PCM	Φ_{abs} As-synth. (%)	Φ_{abs} 298 K act. (%)	Φ_{abs} 473 K act. (%)	τ_{obs} As-synth. (μs)	τ_{obs} 298 K act. (μs)	τ_{obs} 473 K act. (μs)
5.2	8.4 ± 0.3	5.3± 0.4	6.5 ± 0.7	181 ± 3	79 ± 2	60 ± 2
5.3	3.7 ± 0.2	4.6 ± 0.5	5 ± 2	57 ± 2	20 ± 2	111 ± 1
5.4	0.94 ± 0.08	1.36 ± 0.07	0.41 ± 0.02	n/a	n/a	n/a

quenching O–H oscillators, these materials exhibited no discernable trend (table 5.1). This may be due to a suspected collapse of the ligand framework upon removal of H_2O ligands; **5.4** luminescence was too weak for τ_{obs} to be determined.

UV-Vis-NIR Spectroscopy of Ln_2L_3 Tridecker Complexes

The $\mathbf{Ln_2L_3}$ ligand **5.5** and complexes (Ln(III) = Sm, Gd, Er, Yb; complexes **5.6** – **5.9**) (Figure 5.1) were investigated by absorbance and emission optical spectroscopies. The absorbance spectra of these species are shown in Figure 5.4. As expected, the

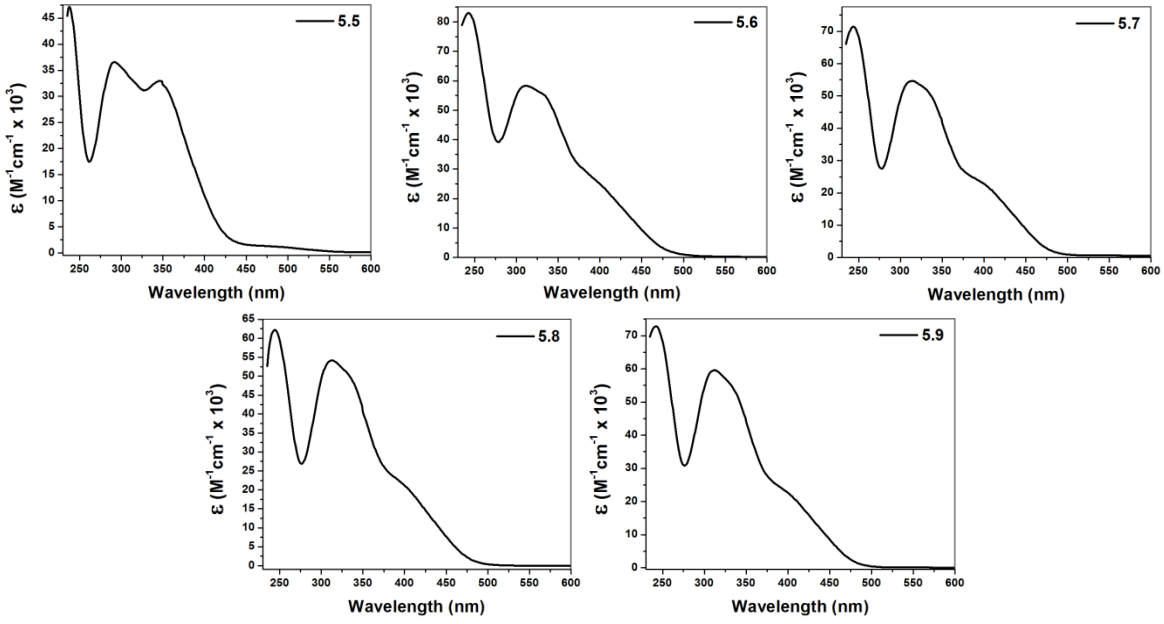

Figure 5.4: UV-Vis absorption spectra of **5.5** – **5.9**.

absorbance spectra of all species bear strong resemblance to the absorbance of the ligand, with little dependence on the identity of the lanthanide ion. The variation between the absorbance profiles of the complexes vs. that of the ligand is likely due to the protonation of the free ligand phenol groups vs the deprotonated nature of the ligand in the complexes.

Upon performing 77 K fluorimetry studies, **5.5** was seen to emit with well-separated S_1 and T_1 manifolds. Similar low-temperature bound-state studies of this ligand were performed in a solid solvent matrix with **5.7**, yielding similar results (Figure 5.5). The resulting T_1 energy levels assigned by measurement of the blue edges of these emission spectra are 26,911 cm^{-1} and 26,849 cm^{-1}, respectively. This similarity in energy is suggestive of little or no change in the nature of the ligand excited state regardless of whether it is free or bound.

Complexes **5.8** and **5.9** both exhibit near-infrared (NIR) luminescence spectra (Figure 5.6). The relative solution luminescence quantum yield (Φ_{Yb}^{L}) of **5.9** was determined to be 0.24% with the synthesis and photophysical measurement of a reference, **$Yb(tta)_3 \cdot 2H_2O$** (tta = thenoyltrifluoroacetonate).[22] Φ_{Yb}^{L} was calculated

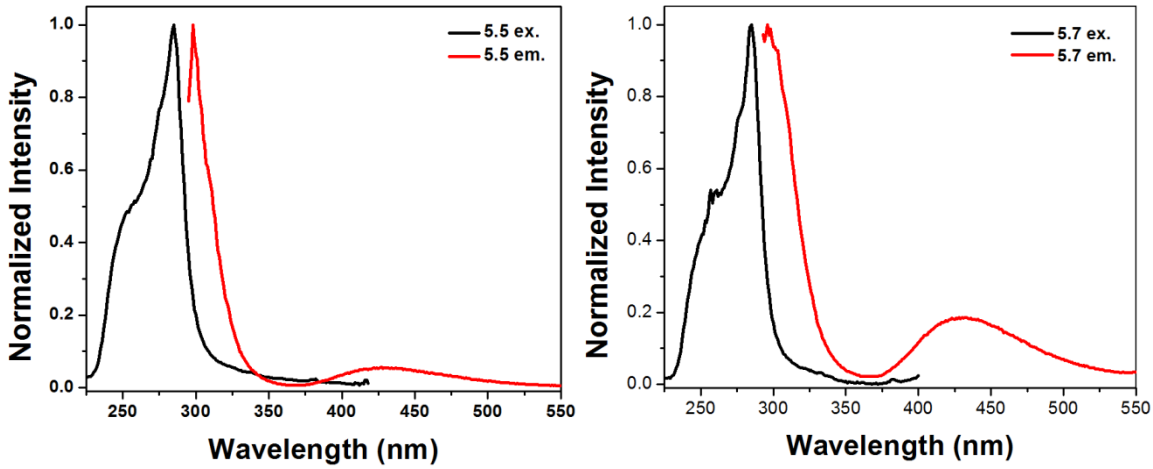

Figure 5.5: 77 K luminescence spectra of **L** (left) and **Gd_2L_3** (right).

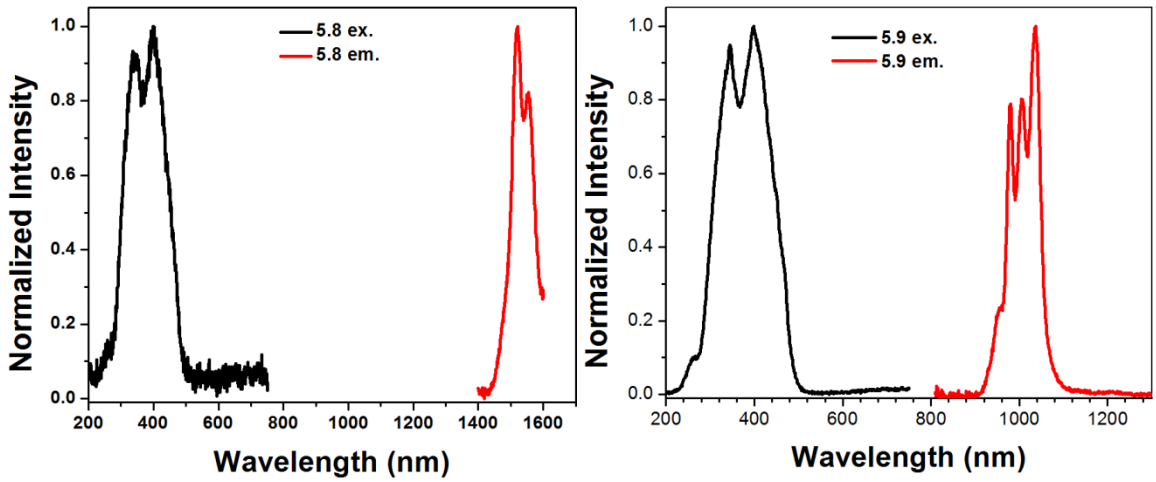

Figure 5.6: Luminescence spectra of **5.8** and **5.9**.

according to eq. 1.[13] Luminescence from **5.8** was too weak for Φ_{Er}^{L} determination. No luminescence from **5.6** was detected.

$$\Phi_{Yb}^{L} = \left(\frac{A_r}{A_x}\right)\left(\frac{E_x}{E_r}\right)\left(\frac{n_x}{n_r}\right)^2 \Phi_r \qquad (1)$$

A_r and A_x are the absorbance values of the reference and sample solutions at the excitation wavelength used, E is the area under the corrected emission spectrum, *n* is the refractive index of the solvent and Φ_r is the quantum yield of the reference solution. The $\left(\frac{n_x}{n_r}\right)^2$ term is simplified to 1 since the same solvent was used in both the reference and sample solutions.

Single-crystal X-ray Structures of Some Ln(III) Complexes

Eu(tta)$_3$ Diacetone Alcohol Dimer

In the work described in Chapter 2, attempts to metalate the mono-nitro-bppy ligand **2.5** with Eu(III) were unsuccessful, and no desired product was formed. However, crystals of a novel Eu dimer (**5.10**) were isolated and characterized (Figure 5.7). This

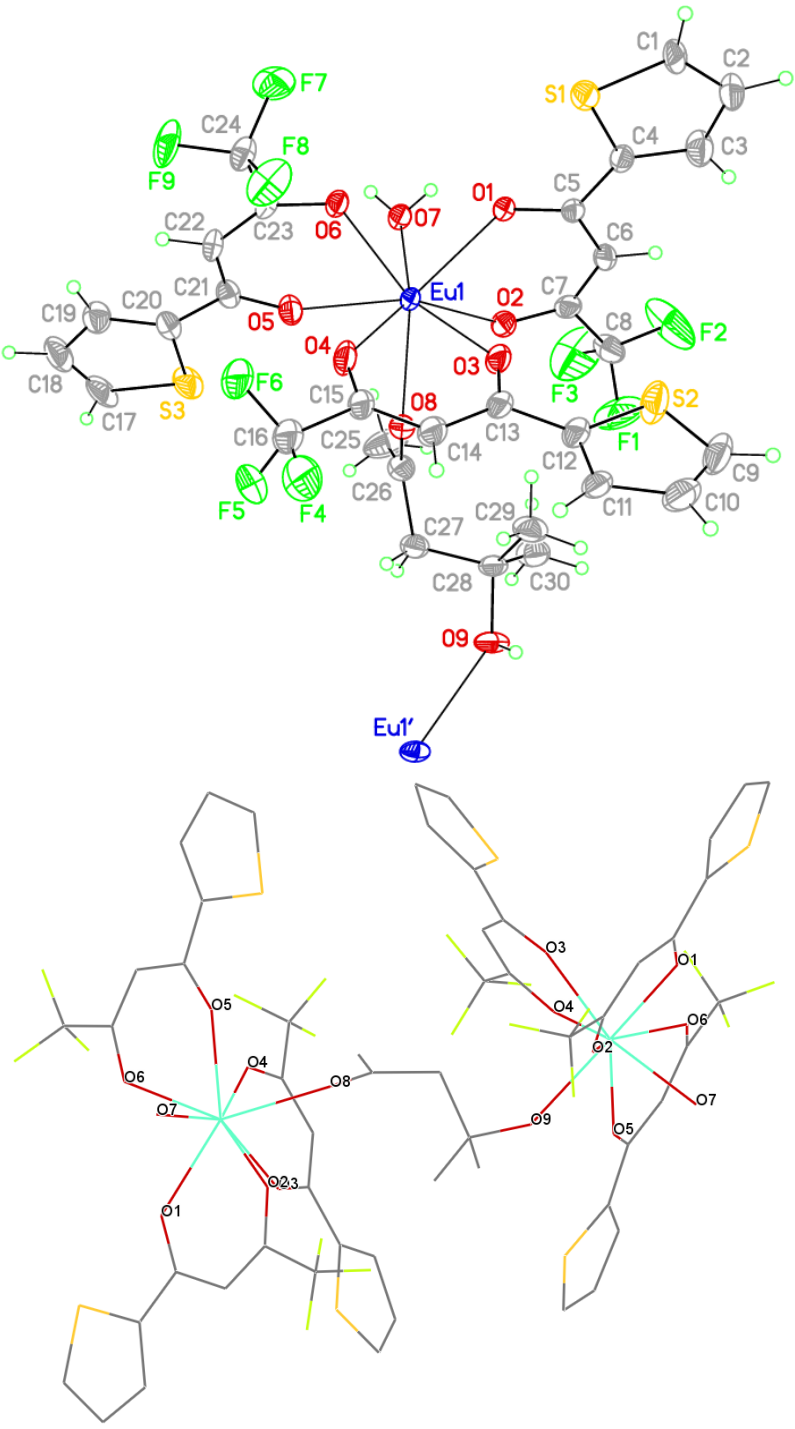

Figure 5.7: View of the asymmetric unit (top) and full structure (bottom) of **5.10**. Ellipsoids are scaled to the 50% probability level. H atoms are omitted in the full structure.

structure features a unique diacetone alcohol (4-hydroxy-4-methyl-2-pentanone) bridging ligand which is the condensation product of the initial reaction solvent, acetone. Unfortunately, repeated attempts to complex Eu(III) with **2.5** or by heating **Eu(tta)$_3$•2H$_2$O** for extended periods of time (1 – 2 d) gave variable yields. Crystals were grown from evaporation of a solution of the crude reaction mixture layered with hexanes at ambient temperature.

The complex crystallizes in the C 2/c space group and resides around a crystallographic two-fold rotation axis at ½, y, ¾. The two O atoms of the ketone and alcohol functionalities of the bridging molecule in compound **5.10** coordinate to separate eight-coordinate Eu(III) ions whose coordination spheres are completed by three tta ligands and one H_2O ligand each. There are few such instances of this molecule serving as such a bridge between metal ions.[23,24] The structure exhibits the common disorder of S atoms of the thiophene rings owing to differing orientations of the ring as a result of rotation about the C–C bond between the carbonyl C and the ring C. The lower occupancy atoms of the disordered thiophene rings have been omitted.

Ln(β-diketonato)$_3$bppy Complexes

Though Ln(III) complexes comprised of three *β*-diketonate and one *bis*(pyrazol-1-yl)pyridine (bppy) ligands have been reported before,[25] the three complexes described here have yet to be reported. The complexes were synthesized by heating the appropriate Ln(III) *tris*(*β*-diketonate) dihydrate salt with the corresponding bppy derivative, and crystals were grown through slow evaporation of acetone solutions to give **Eu(tta)$_3$I$_2$bppy** (**5.11**), **Gd(dbm)$_3$bppy** (dbm = dibenzoylmethanato) (**5.12**) and **Gd(tta)$_3$bppy** (**5.13**) (Figure 5.8).

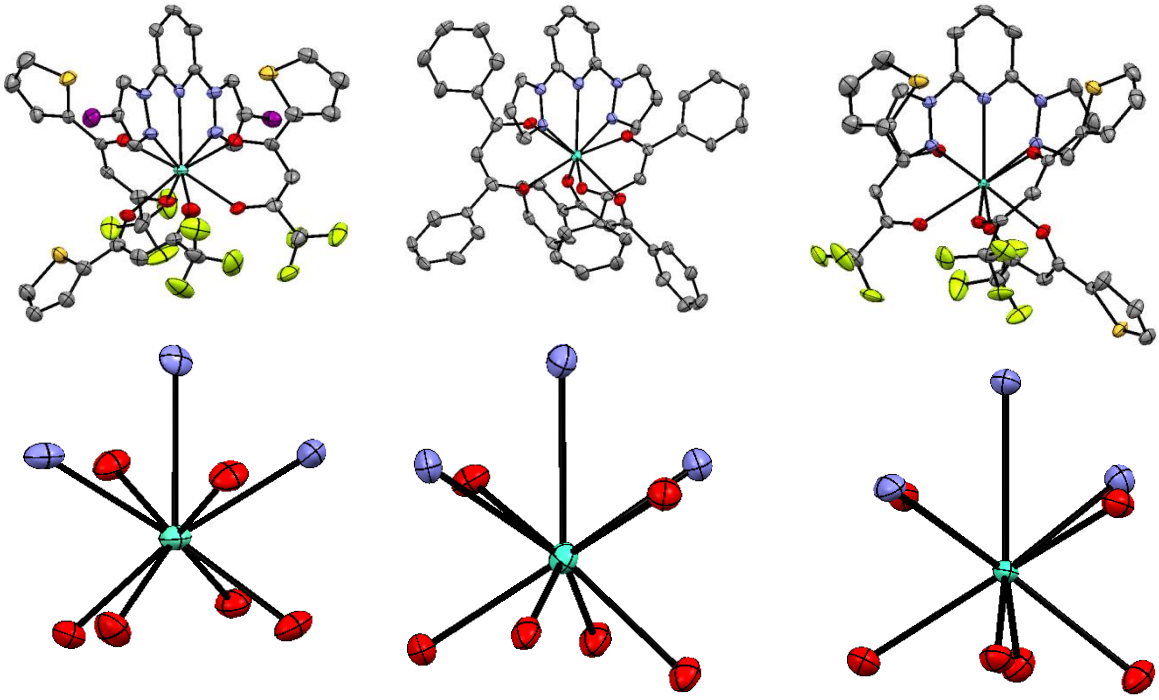

Figure 5.8: Solid-state structures (top) and metal center connectivity (bottom) of **5.11** – **5.13** (left to right).

All three structures form distorted tricapped prism geometries around the metal center, in keeping with similar structures containing bppy- and *β*-diketonate ligands previously reported.[25,26] However, **5.11** crystallizes in the Pba2 space group and contains four molecules per unit cell, whereas **5.12** and **5.13** each crystallize in the P-1 space group and contain two molecules per unit cell. Additionally, **5.12** contains two solvent acetone molecules in the unit cell. More detailed measurements of these structures are contained in the Experimental section of this chapter.

CONCLUSIONS

The materials and complexes described in this chapter are excellent examples of the coordinative and emissive properties of the lanthanides. Light emission in the 480 nm – 1600 nm range was observed in both bulk porous extended networks as well as a

unique tridecker dinuclear complex. In addition, the structures of four new Ln(III) complexes that feature eight- and nine-coordinate Ln(III) centers were determined. One of these structures was found to employ a rare diacetone alcohol bridging motif between two [Eu(tta)$_3$H$_2$O] centers.

EXPERIMENTAL

Materials and Methods

Compounds bppy,[27] I$_2$bppy,[28] Ln(β-diketonate)$_3$•2H$_2$O,[22,29] and **5.11** – **5.13**[25] were prepared as previously described. Compounds **5.1** – **5.4** were prepared by Dr. Alisha Bohnsack,[21] and compounds **5.5** – **5.9** were prepared by Tyler King. Reagents and solvents were purchased from commercial suppliers and used without purification. Dry diglyme was obtained from Sigma-Aldrich in Sure/Seal^{TM} bottles and used without further drying.

Spectroscopy

Room-temperature solution UV-Vis absorption spectrophotometry and fluorescence spectroscopy excitation/emission measurements were performed in Starna quartz fluorometer cells with 1.0 cm path lengths in dichloromethane (DCM) solvent. All solution-state spectroscopy was performed on solutions with absorbance values $A \leq 0.1$. UV-vis absorbance spectra and molar absorptivity (ε) values were obtained with a Varian Cary-6000i spectrophotometer. Luminescence measurements were recorded on a Photon Technology International QuantaMaster 4 spectrofluorometer equipped with a QM-InGaAs NIR enhancement detector system.

The as-synthesized absolute quantum yields of **5.2** – **5.4** were determined with the use of a calibrated 6-in. diameter K Sphere-B integrating sphere equipped with a powder sample holder and calculated by dividing the area under the emission peaks of the

materials by the difference between the area under the excitation peak of the sample and that of a $BaSO_4$ blank. Subsequent quantum yields of activated materials were determined by comparing the intensity of the main luminescent transition of each compound in a custom-built air-free quartz cell to that of the as-synthesized material; emission intensities were standardized to the λ_{em} = 575 nm emission intensity of an external perylene diimide reference utilizing λ_{ex} = 525 nm, which was stored in a sealed quartz tube. Luminescence lifetimes were determined by monitoring the main luminescent transition under excitation at the optimal wavelength inherent to each material, and utilized a quartz tube containing $BaSO_4$ to determine the instrument response function (IRF). Luminescence decays were modeled as single-exponential functions in all cases using FeliX32 Analysis software v. 1.2.[30]

77 K luminescence measurements of **5.1** were performed on a solid sample, whereas 77 K luminescence measurements of **5.5** and **5.7** were performed on 2-methyltetrahydrofuran solutions. In all cases, the samples were placed in a quartz tube and immersed in a dewar containing liquid nitrogen equipped with a quartz cold finger to cool.

X-RAY CRYSTALLOGRAPHY

Crystal structure data for complexes **5.11** and **5.12** were obtained and analyzed by Leander Cinninger; data for complexes **5.10** and **5.13** were obtained and analyzed by Dr. Vincent Lynch.

Data of compound **5.10** were collected at 123 K on a Nonius Kappa CCD diffractometer using a Bruker AXS Apex II detector and a graphite monochromator with MoKα radiation (λ = 0.71073Å). Reduced temperatures were maintained by use of an Oxford Cryosystems 700 low-temperature device. Data for complexes **5.11** –**5.13** were

collected on a Rigaku AFC12 diffractometer with a Saturn 724+ CCD using a graphite monochromator with MoKα radiation (λ = 0.71073Å). The data were collected at 100 K using a Rigaku XStream Cryostream low temperature device. Details of crystal data, data collection, positional and thermal parameters, bond lengths and angles, torsion angles and structure refinement are listed below.

X-ray Experimental for $[(C_8H_4O_2F_3S)_3Eu(H_2O)]_2C_6H_{12}O_2$ (**5.10**): Crystals grew as clusters of clear, pale yellow plates by slow evaporation from acetone. The data crystal was cut from a larger crystal and had approximate dimensions; 0.34 x 0.24 x 0.09 mm. A total of 1289 frames of data were collected using ω and ϕ-scans with a scan range of 0.7° and a counting time of 32 seconds per frame. Data reduction were performed using SAINT V8.27B.[31] The structure was solved by direct methods using SHELXT[32] and refined by full-matrix least-squares on F^2 with anisotropic displacement parameters for the non-H atoms using SHELXL-2014/7.[33] Structure analysis was aided by use of the programs PLATON98[34] and WinGX.[35] The hydrogen atoms bound to carbon atoms were calculated in idealized positions. The hydrogen atoms on the water molecule, O7, and the hydroxyl group, O9, were observed in a ΔF map and refined with isotropic displacement parameters.

The complex resides around a crystallographic two-fold rotation axis passing through ½, y, ¾. The Eu complex is bridged by a molecule of 4-hydroxy-4-methyl-2-pentanone. This molecule is disordered around the two-fold rotation axis. Two of the three thiophene rings are also disordered. Such disorder is commonly observed in thiophene rings and results from a nearly 180º rotation about the C-C bond to the remainder of the ligand. The disorder in these thiophene rings was modeled in the same manner for each. For one component of a disordered ring, the variable x was assigned to the site occupancy factors for the four atoms of the thiophene ring affected by the

disorder. The variable (1-x) was assigned to the atoms of the alternate component. A common isotropic displacement parameter was refined while refining x. The geometry of the two components was restrained to be equivalent throughout the refinement process. In this way, the site occupancy for the major component of the ring with S1 refined to 67(2)%. The site occupancy for the major component of the ring with S3 refined to 88(2)%. Except for the minor component of the ring with S3a, the non-H atoms were refined anisotropically in the final refinement model.

The function, $\Sigma w(|F_o|^2 - |F_c|^2)^2$, was minimized, where $w = 1/[(\sigma(F_o))^2 + (0.0199*P)^2 + (16.0503*P)]$ and $P = (|F_o|^2 + 2|F_c|^2)/3$. $R_w(F^2)$ refined to 0.0639, with R(F) equal to 0.0295 and a goodness of fit, S, = 1.03. Definitions used for calculating R(F),$R_w(F^2)$ and the goodness of fit, S, are given below.[36] The data were checked for secondary extinction but no correction was necessary. Neutral atom scattering factors and values used to calculate the linear absorption coefficient are from the International Tables for X-ray Crystallography (1992).[37] All figures were generated using SHELXTL/PC.[38]

Table 5.2: Crystal data and structure refinement for **5.10**.

Empirical formula	$C_{54}H_{40}Eu_2F_{18}O_{16}S_6$
Formula weight	1783.14
Temperature	123(2) K
Wavelength	0.71073 Å
Crystal system	monoclinic
Space group	C 2/c
Unit cell dimensions	a = 24.4026(18) Å α = 90°
	b = 12.5404(10) Å β = 106.177(4)°
	c = 22.2798(17) Å γ = 90°
Volume	6548.1(9) $Å^3$
Z	4
Density (calculated)	1.809 Mg/m^3
Absorption coefficient	2.204 mm^{-1}
F(000)	3504
Crystal size	0.340 x 0.240 x 0.090 mm^3
θ range for data collection	2.469 to 28.337°.
Index ranges	-32<=h<=32, -16<=k<=16, -27<=l<=29
Reflections collected	57014
Independent reflections	8137 [R(int) = 0.0554]
Completeness to θ = 25.242°	99.9 %
Absorption correction	Semi-empirical from equivalents
Max. and min. transmission	1.00 and 0.700
Refinement method	Full-matrix least-squares on F^2
Data / restraints / parameters	8137 / 672 / 534
Goodness-of-fit on F^2	1.027
Final R indices [I>2σ(I)]	R1 = 0.0295, wR2 = 0.0600
R indices (all data)	R1 = 0.0438, wR2 = 0.0639
Extinction coefficient	n/a
Largest diff. peak and hole	0.660 and -0.815 $e.Å^{-3}$

Table 5.3 Atomic coordinates (x 10^4) and equivalent isotropic displacement parameters ($Å^2$ x 10^3) for **5.10**. U(eq) is defined as one third of the trace of the orthogonalized U^{ij} tensor.

	x	y	z	U(eq)
Eu1	3549(1)	3092(1)	5917(1)	22(1)
O8	4281(2)	2888(3)	6917(2)	27(1)
O9	6057(2)	2428(4)	7984(2)	31(1)
C25	4109(3)	1470(6)	7533(4)	50(2)

Table 5.3 Continued:

C26	4466(7)	2331(10)	7370(6)	28(2)
C27	5066(2)	2510(5)	7792(3)	28(1)
C28	5541(6)	2093(10)	7527(6)	27(2)
C29	5529(3)	2543(6)	6901(3)	36(1)
C30	5544(3)	881(5)	7505(3)	38(1)
S3	2889(1)	3293(1)	7932(1)	38(1)
C17	2549(2)	3842(4)	8437(2)	41(1)
C18	2226(2)	4695(5)	8189(2)	43(1)
C19	2261(2)	4899(3)	7589(2)	33(1)
S3A	2125(4)	5208(7)	7483(5)	37
C17A	2211(13)	4650(20)	8207(9)	37
C18A	2568(15)	3800(30)	8310(12)	37
C19A	2767(8)	3618(15)	7794(13)	37
C20	2590(1)	4228(2)	7363(1)	26(1)
C21	2715(1)	4166(2)	6758(1)	23(1)
C22	2489(1)	4959(2)	6300(1)	25(1)
C23	2537(1)	4921(2)	5704(1)	22(1)
C24	2303(1)	5858(2)	5273(1)	28(1)
O5	3022(1)	3406(2)	6675(1)	28(1)
O6	2768(1)	4214(1)	5442(1)	23(1)
F7	1988(1)	5528(2)	4711(1)	46(1)
F8	2728(1)	6427(2)	5168(1)	49(1)
F9	1980(1)	6526(2)	5486(1)	50(1)
S2	5365(1)	2883(1)	5211(1)	45(1)
C9	5993(1)	3284(3)	5101(2)	43(1)
C10	6156(1)	4263(3)	5342(2)	42(1)
C11	5772(1)	4726(2)	5640(1)	27(1)
C12	5305(1)	4034(2)	5596(1)	30(1)
C13	4800(1)	4190(2)	5820(1)	28(1)
C14	4758(1)	5132(2)	6153(1)	32(1)
C15	4286(1)	5350(2)	6346(2)	35(1)
C16	4273(1)	6388(3)	6702(2)	48(1)
O3	4423(1)	3464(2)	5702(1)	31(1)
O4	3844(1)	4792(2)	6287(1)	44(1)
F4	4682(1)	7078(2)	6676(1)	60(1)
F5	4340(1)	6175(2)	7309(1)	61(1)
F6	3774(1)	6882(2)	6491(1)	66(1)
S1	3249(1)	3250(1)	3522(1)	28(1)
C1	3425(4)	2959(10)	2853(4)	29(1)
C2	3777(4)	2082(9)	2914(7)	33(2)
C3	3895(4)	1669(7)	3514(6)	36(2)

Table 5.3 Continued:

S1A	3967(2)	1393(3)	3517(3)	28(1)
C1A	3694(9)	2190(20)	2857(13)	31(2)
C2A	3377(9)	3010(20)	2961(9)	32(2)
C3A	3360(7)	2976(12)	3589(9)	34(2)
C4	3643(1)	2195(2)	3917(1)	23(1)
C5	3684(1)	2010(2)	4574(1)	21(1)
C6	4017(1)	1140(2)	4878(1)	27(1)
C7	4108(1)	902(2)	5498(1)	26(1)
C8	4475(2)	-73(3)	5752(2)	41(1)
O1	3412(1)	2635(2)	4838(1)	22(1)
O2	3946(1)	1386(2)	5913(1)	27(1)
F1	4987(1)	226(2)	6088(1)	79(1)
F2	4557(2)	-708(2)	5323(1)	111(1)
F3	4267(1)	-644(2)	6125(1)	93(1)
O7	2754(1)	1819(2)	5702(1)	25(1)

Table 5.4: Bond lengths [Å] and angles [°] for **5.10**.

Eu1-O4	2.326(2)	C28-C29	1.495(16)
Eu1-O2	2.3496(18)	C28-C30	1.521(14)
Eu1-O3	2.360(2)	C29-H29A	0.98
Eu1-O6	2.3675(17)	C29-H29B	0.98
Eu1-O1	2.4014(17)	C29-H29C	0.98
Eu1-O5	2.4232(19)	C30-H30A	0.98
Eu1-O8	2.451(4)	C30-H30B	0.98
Eu1-O7	2.454(2)	C30-H30C	0.98
O8-C26	1.205(12)	S3-C17	1.718(4)
O9-C28	1.445(13)	S3-C20	1.731(3)
O9-H9O	0.69(9)	C17-C18	1.352(5)
C25-C26	1.494(13)	C17-H17	0.95
C25-H25A	0.98	C18-C19	1.386(5)
C25-H25B	0.98	C18-H18	0.95
C25-H25C	0.98	C19-C20	1.353(5)
C26-C27	1.520(16)	C19-H19	0.95
C27-C28	1.532(15)	S3A-C17A	1.719(11)
C27-H27A	0.99	S3A-C20	1.743(10)
C27-H27B	0.99	C17A-C18A	1.354(10)
C17A-H17A	0.95	C18A-H18A	0.95
C18A-C19A	1.386(11)	C19A-C20	1.21(2)

Table 5.4 Continued:

C19A-H19A	0.95	S2-C9	1.695(4)
C20-C21	1.465(4)	S2-C12	1.705(3)
C21-O5	1.257(3)	C9-C10	1.354(5)
C21-C22	1.421(4)	C9-H9	0.95
C22-C23	1.367(4)	C10-C11	1.415(4)
C22-H22	0.95	C10-H10	0.95
C23-O6	1.277(3)	C11-C12	1.414(4)
C23-C24	1.525(4)	C11-H11	0.95
C24-F9	1.325(3)	C12-C13	1.467(4)
C24-F8	1.332(3)	C13-O3	1.267(3)
C24-F7	1.338(3)	C13-C14	1.414(4)
C14-C15	1.364(4)	C16-F4	1.335(4)
C14-H14	0.95	C16-F5	1.343(4)
C15-O4	1.263(4)	S1-C1	1.704(7)
C15-C16	1.530(4)	S1-C4	1.725(3)
C16-F6	1.332(4)	C1-C2	1.379(14)
C1-H1	0.95	S1A-C4	1.681(5)
C2-C3	1.39(2)	S1A-C1A	1.75(3)
C2-H2	0.95	C1A-C2A	1.34(3)
C3-C4	1.388(11)	C1A-H1A	0.95
C3-H3	0.95	C2A-C3A	1.41(3)
C2A-H2A	0.95	C7-O2	1.259(3)
C3A-C4	1.300(14)	C7-C8	1.529(4)
C3A-H3A	0.95	C8-F3	1.302(4)
C4-C5	1.458(4)	C8-F2	1.302(4)
C5-O1	1.272(3)	C8-F1	1.319(4)
C5-C6	1.416(4)	O7-H7A	0.73(4)
C6-C7	1.368(4)	O7-H7B	0.83(4)
C6-H6	0.95		
O4-Eu1-O2	138.46(7)	O2-Eu1-O5	116.79(7)
O4-Eu1-O3	71.50(7)	O3-Eu1-O5	142.62(7)
O2-Eu1-O3	77.41(7)	O6-Eu1-O5	72.39(6)
O4-Eu1-O6	75.20(7)	O1-Eu1-O5	141.54(6)
O2-Eu1-O6	145.18(6)	O4-Eu1-O8	72.44(11)
O3-Eu1-O6	116.87(7)	O2-Eu1-O8	73.21(10)
O4-Eu1-O1	121.08(8)	O3-Eu1-O8	74.55(12)
O2-Eu1-O1	73.84(6)	O6-Eu1-O8	139.51(10)
O3-Eu1-O1	74.10(6)	O1-Eu1-O8	138.42(10)
O6-Eu1-O1	79.86(6)	O5-Eu1-O8	77.15(11)
O4-Eu1-O5	77.04(7)	O4-Eu1-O7	144.58(7)

Table 5.4 Continued:

O2-Eu1-O7	73.24(7)	O6-Eu1-O7	78.79(7)
O3-Eu1-O7	143.05(7)	O1-Eu1-O7	76.53(7)
O5-Eu1-O7	72.42(7)	H25B-C25-H25C	109.5
O8-Eu1-O7	116.50(12)	O8-C26-C25	121.0(12)
C26-O8-Eu1	146.0(7)	O8-C26-C27	120.2(10)
C28-O9-H9O	110(7)	C25-C26-C27	118.8(8)
C26-C25-H25A	109.5	C26-C27-C28	114.3(8)
C26-C25-H25B	109.5	C26-C27-H27A	108.7
H25A-C25-H25B	109.5	C28-C27-H27A	108.7
C26-C25-H25C	109.5	C26-C27-H27B	108.7
H25A-C25-H25C	109.5	C28-C27-H27B	108.7
H27A-C27-H27B	107.6	C29-C28-C27	114.2(10)
O9-C28-C29	109.5(10)	C30-C28-C27	111.4(10)
O9-C28-C30	107.5(9)	C28-C29-H29A	109.5
C29-C28-C30	110.2(7)	C28-C29-H29B	109.5
O9-C28-C27	103.5(7)	H29A-C29-H29B	109.5
C28-C29-H29C	109.5	C28-C30-H30C	109.5
H29A-C29-H29C	109.5	H30A-C30-H30C	109.5
H29B-C29-H29C	109.5	H30B-C30-H30C	109.5
C28-C30-H30A	109.5	C17-S3-C20	91.5(2)
C28-C30-H30B	109.5	C18-C17-S3	112.4(3)
H30A-C30-H30B	109.5	C18-C17-H17	123.8
S3-C17-H17	123.8	C19-C18-H18	124.6
C17-C18-C19	110.9(4)	C20-C19-C18	116.4(4)
C17-C18-H18	124.6	C20-C19-H19	121.8
C18-C19-H19	121.8	C19A-C20-S3A	115.4(12)
C17A-S3A-C20	86.6(9)	C21-C20-S3A	119.3(4)
C18A-C17A-S3A	112.6(13)	O5-C21-C22	123.6(2)
C18A-C17A-H17A	123.7	O5-C21-C20	117.4(2)
S3A-C17A-H17A	123.7	C22-C21-C20	119.0(2)
C17A-C18A-C19A	110.2(14)	C23-C22-C21	123.5(2)
C17A-C18A-H18A	124.9	C23-C22-H22	118.2
C19A-C18A-H18A	124.9	C21-C22-H22	118.2
C20-C19A-C18A	115.1(13)	O6-C23-C22	129.6(2)
C20-C19A-H19A	122.4	O6-C23-C24	112.5(2)
C18A-C19A-H19A	122.4	C22-C23-C24	117.8(2)
C19A-C20-C21	125.2(12)	F9-C24-F8	107.1(2)
C19-C20-C21	132.2(3)	F9-C24-F7	106.8(2)
C19-C20-S3	108.8(2)	F8-C24-F7	105.9(2)
C21-C20-S3	118.9(2)	F9-C24-C23	114.6(2)

Table 5.4 Continued:

F8-C24-C23	110.5(2)	C10-C9-H9	123.6
F7-C24-C23	111.5(2)	S2-C9-H9	123.6
C21-O5-Eu1	132.83(17)	C9-C10-C11	113.5(3)
C23-O6-Eu1	127.72(16)	C9-C10-H10	123.3
C9-S2-C12	91.68(16)	C11-C10-H10	123.3
C10-C9-S2	112.9(3)	C12-C11-C10	110.0(3)
C12-C11-H11	125.0	O3-C13-C14	123.7(3)
C10-C11-H11	125.0	O3-C13-C12	117.6(2)
C11-C12-C13	129.2(3)	C14-C13-C12	118.7(3)
C11-C12-S2	112.0(2)	C15-C14-C13	121.5(3)
C13-C12-S2	118.8(2)	C15-C14-H14	119.2
C13-C14-H14	119.2	F6-C16-F5	106.9(3)
O4-C15-C14	128.9(3)	F4-C16-F5	106.9(3)
O4-C15-C16	112.6(3)	F6-C16-C15	111.2(3)
C14-C15-C16	118.4(3)	F4-C16-C15	113.9(3)
F6-C16-F4	107.8(3)	F5-C16-C15	109.8(3)
C13-O3-Eu1	138.08(18)	C1-C2-H2	124.8
C15-O4-Eu1	135.73(18)	C3-C2-H2	124.8
C1-S1-C4	92.3(5)	C4-C3-C2	115.8(9)
C2-C1-S1	112.8(10)	C4-C3-H3	122.1
C2-C1-H1	123.6	C2-C3-H3	122.1
S1-C1-H1	123.6	C4-S1A-C1A	88.8(11)
C1-C2-C3	110.4(13)	C2A-C1A-S1A	113(2)
C2A-C1A-H1A	123.4	C4-C3A-H3A	122.6
S1A-C1A-H1A	123.4	C2A-C3A-H3A	122.6
C1A-C2A-C3A	109(2)	C3A-C4-C5	124.1(9)
C1A-C2A-H2A	125.5	C3-C4-C5	130.9(5)
C3A-C2A-H2A	125.5	C3A-C4-S1A	114.1(9)
C4-C3A-C2A	114.9(18)	C5-C4-S1A	121.8(3)
C3-C4-S1	108.7(5)	F3-C8-F2	107.5(3)
C5-C4-S1	120.4(2)	F3-C8-F1	105.7(3)
O1-C5-C6	123.8(2)	F2-C8-F1	106.0(3)
O1-C5-C4	118.0(2)	F3-C8-C7	112.6(3)
C6-C5-C4	118.2(2)	F2-C8-C7	114.2(3)
C7-C6-C5	124.2(2)	F1-C8-C7	110.3(3)
C7-C6-H6	117.9	C5-O1-Eu1	131.72(16)
C5-C6-H6	117.9	C7-O2-Eu1	130.97(17)
O2-C7-C6	129.8(2)	Eu1-O7-H7A	118(3)
O2-C7-C8	112.6(2)	Eu1-O7-H7B	125(3)
C6-C7-C8	117.6(3)	H7A-O7-H7B	97(4)

Table 5.5: Anisotropic displacement parameters ($Å^2$ x 10^3) for **5.10**. The anisotropic displacement factor exponent takes the form: $-2\pi^2[h^2 a^{*2} U^{11} + ... + 2 h k a^* b^* U^{12}]$.

	U11	U22	U33	U23	U13	U12
Eu1	19(1)	29(1)	18(1)	-3(1)	3(1)	10(1)
O8	24(2)	35(2)	22(2)	-3(2)	3(2)	6(2)
O9	21(2)	49(3)	18(2)	5(2)	0(2)	-13(2)
C25	25(3)	60(5)	60(5)	23(4)	3(3)	-11(3)
C26	26(3)	36(5)	22(4)	0(3)	7(3)	1(3)
C27	24(2)	39(3)	21(2)	-1(2)	4(2)	-4(2)
C28	18(3)	41(5)	20(4)	-1(3)	1(3)	-6(3)
C29	32(3)	54(4)	20(3)	3(3)	2(2)	-4(3)
C30	33(3)	38(3)	36(4)	0(3)	1(3)	2(3)
S3	51(1)	43(1)	21(1)	3(1)	12(1)	5(1)
C17	50(2)	60(3)	18(2)	-11(2)	17(2)	-12(2)
C18	49(2)	56(3)	31(2)	-16(2)	23(2)	-9(2)
C19	37(2)	33(2)	31(2)	1(2)	13(2)	4(2)
C20	30(1)	26(2)	24(1)	-5(1)	11(1)	-4(1)
C21	27(1)	21(1)	24(1)	-4(1)	11(1)	-3(1)
C22	25(1)	23(1)	31(2)	-1(1)	15(1)	7(1)
C23	16(1)	21(1)	28(1)	2(1)	8(1)	6(1)
C24	28(1)	25(2)	35(2)	6(1)	14(1)	10(1)
O5	36(1)	27(1)	22(1)	2(1)	11(1)	11(1)
O6	22(1)	24(1)	24(1)	1(1)	8(1)	8(1)
F7	52(1)	40(1)	37(1)	13(1)	0(1)	12(1)
F8	43(1)	34(1)	74(1)	23(1)	24(1)	3(1)
F9	62(1)	42(1)	56(1)	17(1)	31(1)	39(1)
S2	39(1)	38(1)	66(1)	-13(1)	26(1)	6(1)
C9	35(2)	49(2)	51(2)	5(2)	20(2)	19(2)
C10	24(2)	57(2)	43(2)	7(2)	6(1)	4(1)
C11	18(1)	30(2)	31(2)	0(1)	3(1)	4(1)
C12	23(1)	30(2)	36(2)	-5(1)	6(1)	8(1)
C13	21(1)	28(2)	33(2)	-6(1)	3(1)	7(1)
C14	24(1)	29(2)	41(2)	-12(1)	4(1)	2(1)
C15	27(2)	33(2)	42(2)	-18(1)	2(1)	8(1)
C16	34(2)	46(2)	58(2)	-25(2)	2(2)	12(2)
O3	22(1)	28(1)	42(1)	-15(1)	6(1)	4(1)
O4	24(1)	49(1)	60(2)	-32(1)	13(1)	3(1)
F4	57(1)	34(1)	84(2)	-29(1)	12(1)	1(1)

Table 5.5 Continued:

F5	57(1)	70(2)	52(1)	-36(1)	9(1)	11(1)
F6	49(1)	57(1)	80(2)	-37(1)	-2(1)	29(1)
S1	29(1)	32(1)	24(1)	2(1)	9(1)	5(1)
C1	31(2)	39(3)	24(3)	2(2)	19(2)	1(2)
C2	38(3)	34(3)	33(3)	0(2)	21(2)	7(3)
C3	42(4)	34(4)	36(3)	-1(3)	17(2)	9(3)
S1A	34(2)	28(2)	26(1)	1(1)	17(1)	7(1)
C1A	39(4)	34(4)	25(4)	6(3)	20(3)	2(4)
C2A	32(4)	36(4)	31(4)	3(4)	14(4)	2(3)
C3A	33(5)	39(5)	31(4)	-1(4)	13(4)	7(4)
C4	20(1)	24(1)	26(1)	-4(1)	9(1)	0(1)
C5	17(1)	23(1)	22(1)	-5(1)	5(1)	-1(1)
C6	28(1)	26(2)	25(1)	-7(1)	4(1)	10(1)
C7	23(1)	21(1)	29(1)	-4(1)	-1(1)	6(1)
C8	54(2)	30(2)	29(2)	-8(1)	-5(1)	22(2)
O1	19(1)	26(1)	20(1)	-3(1)	4(1)	7(1)
O2	28(1)	27(1)	24(1)	1(1)	4(1)	11(1)
F1	49(1)	63(2)	99(2)	-4(1)	-23(1)	32(1)
F2	202(3)	62(2)	44(1)	-16(1)	-10(2)	93(2)
F3	96(2)	66(2)	119(2)	63(2)	33(2)	40(2)
O7	23(1)	29(1)	23(1)	1(1)	7(1)	6(1)

Table 5.6: Hydrogen coordinates (x 10^4) and isotropic displacement parameters ($Å^2$ x 10^3) for **5.10**.

	x	y	z	U(eq)		
H25A	4105	1554	7969	75		
H25B	4271	773	7479	75		
H25C	3719	1519	7259	75		
H27A	5099	2156	8198	34		
H27B	5123	3284	7873	34		
H29A	5536	3324	6924	54		
H29B	5180	2311	6591	54		
H29C	5862	2290	6780	54		
H30A	5864	639	7354	56		
H30B	5185	627	7221	56		
H30C	5586	596	7924	56		
H17	2584	3575	8845	49		
H18	2006	5100	8397	51		
H19	2064	5480	7349	39		
H17A	2029	4906	8503	44		
H18A	2668	3386	8682	44		
H19A	3024	3055	7779	44		
H22	2293	5546	6414	30		
H9	6208	2866	4893	52		
H10	6495	4606	5313	50		
H11	5821	5402	5841	32		
H14	5066	5626	6244	39		
H1	3294	3357	2477	35		
H2	3919	1801	2590	39		
H3	4133	1063	3642	43		
H1A	3764	2060	2464	37		
H2A	3195	3528	2660	38		
H3A	3156	3485	3759	40		
H6	4187	692	4637	33		
H7A	2465(17)		2020(30)		5658(17)	47(12)
H7B	2677(17)		1380(30)		5409(19)	62(13)
H9O	6250(40)		2630(70)		7830(40)	70(30)

Table 5.7: Torsion angles [°] for **5.10**.

Eu1-O8-C26-C25	-18(2)	S3-C17-C18-C19	-0.26(18)
Eu1-O8-C26-C27	163.1(5)	C17-C18-C19-C20	1.0(3)
O8-C26-C27-C28	-76.3(10)	C20-S3A-C17A-C18A	0.04(16)
C25-C26-C27-C28	104.8(16)	S3A-C17A-C18A-C19A	0.1(2)
C26-C27-C28-O9	175.7(8)	C17A-C18A-C19A-C20	-0.2(5)
C26-C27-C28-C29	56.7(10)	C18A-C19A-C20-C21	-176.7(12)
C26-C27-C28-C30	-69.0(10)	C18A-C19A-C20-S3A	0.2(6)
C20-S3-C17-C18	-0.32(13)	C18-C19-C20-C21	177.9(3)
C18-C19-C20-S3	-1.2(3)	C19-C20-C21-O5	-176.6(3)
C17-S3-C20-C19	0.8(2)	S3-C20-C21-O5	2.4(3)
C17-S3-C20-C21	-178.4(3)	S3A-C20-C21-O5	-175.4(4)
C17A-S3A-C20-C19A	-0.2(4)	C19A-C20-C21-C22	-178.3(12)
C17A-S3A-C20-C21	177.0(11)	C19-C20-C21-C22	3.6(5)
C19A-C20-C21-O5	1.5(12)	S3-C20-C21-C22	-177.4(2)
S3A-C20-C21-C22	4.9(5)	O6-C23-C24-F7	48.3(3)
O5-C21-C22-C23	6.3(4)	C22-C23-C24-F7	-133.4(3)
C20-C21-C22-C23	-173.9(3)	C22-C21-O5-Eu1	16.4(4)
C21-C22-C23-O6	1.2(5)	C20-C21-O5-Eu1	-163.35(17)
C21-C22-C23-C24	-176.6(3)	C22-C23-O6-Eu1	-30.1(4)
O6-C23-C24-F9	169.8(2)	C24-C23-O6-Eu1	147.92(18)
C22-C23-C24-F9	-12.0(4)	C12-S2-C9-C10	-0.5(3)
O6-C23-C24-F8	-69.2(3)	S2-C9-C10-C11	1.0(4)
C22-C23-C24-F8	109.1(3)	C9-C10-C11-C12	-1.1(4)
C10-C11-C12-C13	-178.3(3)	C10-C11-C12-S2	0.8(3)
C9-S2-C12-C11	-0.2(2)	C9-S2-C12-C13	178.9(3)
C11-C12-C13-O3	177.3(3)	C13-C14-C15-O4	2.0(6)
S2-C12-C13-O3	-1.7(4)	C13-C14-C15-C16	-179.9(3)
C11-C12-C13-C14	-2.6(5)	O4-C15-C16-F6	-46.6(5)
S2-C12-C13-C14	178.4(2)	C14-C15-C16-F6	135.0(3)
O3-C13-C14-C15	-3.3(5)	O4-C15-C16-F4	-168.6(3)
C12-C13-C14-C15	176.6(3)	C14-C15-C16-F4	13.0(5)
O4-C15-C16-F5	71.5(3)	C4-S1A-C1A-C2A	-0.1(6)
C14-C15-C16-F5	-106.9(4)	S1A-C1A-C2A-C3A	0.0(2)
C14-C13-O3-Eu1	-2.8(5)	C1A-C2A-C3A-C4	0.1(9)
C12-C13-O3-Eu1	177.34(19)	C2A-C3A-C4-C5	179.8(9)
C14-C15-O4-Eu1	5.5(6)	C2A-C3A-C4-S1A	-0.2(14)
C16-C15-O4-Eu1	-172.7(2)	C2-C3-C4-C5	-177.9(5)
C4-S1-C1-C2	-0.2(4)	C2-C3-C4-S1	-0.4(8)
S1-C1-C2-C3	0.0(2)	C1A-S1A-C4-C3A	0.1(11)
C1-C2-C3-C4	0.3(6)	C1A-S1A-C4-C5	-179.9(7)

Table 5.7 Continued:

C1-S1-C4-C3	0.3(6)	S1A-C4-C5-C6	1.3(4)
C1-S1-C4-C5	178.2(4)	S1-C4-C5-C6	-179.4(2)
C3A-C4-C5-O1	2.0(10)	O1-C5-C6-C7	-3.4(4)
C3-C4-C5-O1	178.6(6)	C4-C5-C6-C7	177.3(3)
S1A-C4-C5-O1	-178.0(3)	C5-C6-C7-O2	-2.5(5)
S1-C4-C5-O1	1.3(3)	C5-C6-C7-C8	179.5(3)
C3A-C4-C5-C6	-178.7(9)	O2-C7-C8-F3	44.3(4)
C3-C4-C5-C6	-2.1(7)	C6-C7-C8-F3	-137.4(3)
O2-C7-C8-F2	167.2(3)	C6-C5-O1-Eu1	23.9(4)
C6-C7-C8-F2	-14.4(5)	C4-C5-O1-Eu1	-156.87(17)
O2-C7-C8-F1	-73.5(4)	C6-C7-O2-Eu1	-12.6(4)
C6-C7-C8-F1	104.8(3)	C8-C7-O2-Eu1	165.6(2)

Table 5.8: Hydrogen bonds for **5.10** [Å and °].

D-H...A	d(D-H)	d(H...A)	d(D...A)	<(DHA)
O7-H7A...S1#1	0.73(4)	2.87(4)	3.368(3)	127(3)
O7-H7A...O1#1	0.73(4)	2.16(4)	2.847(3)	157(4)
O7-H7B...O6#1	0.83(4)	2.05(4)	2.825(3)	156(4)
O7-H7B...F7#1	0.83(4)	2.57(4)	3.197(3)	133(3)
O9-H9O...O5#2	0.69(9)	2.06(9)	2.487(5)	121(9)

Symmetry transformations used to generate equivalent atoms:
#1 -x+1/2,-y+1/2,-z+1 #2 -x+1,y,-z+3/2

X-ray Experimental for $(C_{11}H_7N_5I_2)(C_8H_4O_2F_3S)_3Eu$ (**5.11**): Crystals grew as yellow rods by slow evaporation from acetone. The data crystal dimensions were obscured by the protecting oil used and a good estimate of the crystal size was not made. A total of 1404 frames of data were collected using ω-scans with a scan range of 0.5° and a counting time of 40 seconds per frame. The data were collected at 100 K using an Rigaku XStream Cryostream low temperature device. Data reduction were performed

using the Rigaku Americas Corporation's Crystal Clear version 1.40.[39] The structure was solved by direct methods using SIR2004[40] and refined by full-matrix least-squares on F^2 with anisotropic displacement parameters for the non-H atoms using SHELXL-2016/6.[33] Structure analysis was aided by use of the programs PLATON98[34] and WinGX.[35] The hydrogen atoms on carbon were calculated in ideal positions with isotropic displacement parameters set to 1.2 x Ueq of the attached atoms.

Two of the three thiophene groups were disordered. The disorder was typical for terminal thiophene rings and resulted from an approximate 180º rotation about the C-C bond to the ring. The disorder was modeled in the same manner for both rings. The site occupancy for the atoms of one component of the disordered group was assigned to the variable x. The site occupancy factors for the alternate component was assigned to (1 – x). A common isotropic displacement parameter was refined while refining x. The geometry of the two components were restrained to be equivalent to that of the thiophene ring that didn't show signs of disorder. When the value for x converged, the site occupancy factors were fixed and refinement continued by refining the displacement parameters.

The function, $\Sigma w(|F_o|^2 - |F_c|^2)^2$, was minimized, where $w = 1/[(\sigma(F_o))^2 + (0.248*P)^2 + (3.775*P)]$ and $P = (|F_o|^2 + 2|F_c|^2)/3$. $R_w(F^2)$ refined to 0.120, with R(F) equal to 0.0614 and a goodness of fit, S, = 1.03. Definitions used for calculating R(F), $R_w(F^2)$ and the goodness of fit, S, are given below.[36] The data were checked for secondary extinction effects but no correction was necessary. Neutral atom scattering factors and values used to calculate the linear absorption coefficient are from the International Tables for X-ray Crystallography (1992).[37] All figures were generated using SHELXTL/PC.[38]

Table 5.9: Crystal data and structure refinement for **5.11**.

Empirical formula	$C_{35}H_{19}EuF_9I_2N_5O_6S_3$
Formula weight	1278.49
Temperature	100(2) K
Wavelength	0.71073 Å
Crystal system	orthorhombic
Space group	P b a 2
Unit cell dimensions	a = 19.887(3) Å α = 90°
	b = 20.589(3) Å β = 90°
	c = 10.325(2) Å γ = 90°
Volume	4227.6(12) $Å^3$
Z	4
Density (calculated)	2.009 Mg/m^3
Absorption coefficient	3.182 mm^{-1}
F(000)	2440
θ range for data collection	3.011 to 27.484°.
Index ranges	-25<=h<=25, -26<=k<=26, -12<=l<=13
Reflections collected	65460
Independent reflections	9563 [R(int) = 0.1244]
Completeness to θ = 25.242°	99.7 %
Absorption correction	Semi-empirical from equivalents
Max. and min. transmission	1.00 and 0.462
Refinement method	Full-matrix least-squares on F^2
Data / restraints / parameters	9563 / 835 / 644
Goodness-of-fit on F^2	1.083
Final R indices [I>2σ(I)]	R1 = 0.0613, wR2 = 0.1008
R indices (all data)	R1 = 0.0922, wR2 = 0.1122
Absolute structure parameter	0.001(13)
Extinction coefficient	n/a
Largest diff. peak and hole	0.934 and -0.734 $e.Å^{-3}$

Table 5.10 Atomic coordinates (x 10^4) and equivalent isotropic displacement parameters ($Å^2$ x 10^3) for **5.11**. U(eq) is defined as one third of the trace of the orthogonalized U^{ij} tensor.

	x	y	z	U(eq)
C1	5949(7)	3966(6)	1353(15)	29(3)
C2	6367(7)	4459(7)	1801(15)	28(3)
C3	7011(7)	4208(7)	1742(14)	28(3)

Table 5.10 Continued:

C4	7465(6)	3120(7)	1043(14)	24(3)
C5	8121(7)	3250(7)	1287(15)	29(3)
C6	8580(7)	2747(7)	1036(14)	31(3)
C7	8362(6)	2157(6)	635(13)	28(3)
C8	7681(5)	2078(6)	436(15)	23(3)
C9	7746(7)	916(7)	-345(14)	29(3)
C10	7276(7)	514(6)	-844(14)	27(3)
C11	6666(7)	837(6)	-809(13)	23(3)
C12	4787(8)	1059(9)	-2876(17)	45(4)
C13	4973(6)	1238(7)	-1475(15)	32(3)
C14	4678(8)	874(7)	-492(15)	34(4)
C15	4808(7)	1005(7)	834(14)	28(3)
C20	4646(8)	2992(8)	4025(17)	45(4)
C21	5208(6)	2641(6)	3293(15)	29(3)
C22	5668(6)	2326(6)	4052(14)	24(3)
C23	6258(6)	2009(6)	3524(14)	24(3)
C24	6751(6)	1726(6)	4395(12)	25(3)
C25	6750(7)	1607(7)	5682(12)	33(4)
C26	7342(7)	1326(8)	6133(13)	46(4)
C27	7805(7)	1237(8)	5169(13)	48(4)
C28	4524(8)	3785(8)	-1946(15)	39(4)
C29	5159(6)	3397(6)	-1714(15)	28(3)
C30	5684(6)	3463(7)	-2568(16)	35(4)
C31	6312(6)	3126(6)	-2456(15)	29(3)
S3	7631(3)	2930(3)	-3035(7)	39(1)
C32	6852(8)	3267(9)	-3373(18)	37(3)
C33	6864(10)	3569(9)	-4540(20)	41(4)
C34	7483(9)	3537(8)	-5167(17)	45(4)
C35	7950(8)	3202(8)	-4459(16)	41(4)
S3A	6755(9)	3746(9)	-4806(19)	43(3)
C32A	6860(20)	3240(20)	-3470(40)	39(4)
C33A	7520(20)	3080(20)	-3330(40)	39(4)
C34A	7937(15)	3350(20)	-4260(50)	41(4)
C35A	7593(13)	3730(20)	-5140(40)	42(4)
N1	6296(5)	3440(5)	1024(12)	27(3)
N2	6950(5)	3596(5)	1267(11)	26(3)
N3	7221(5)	2544(5)	617(10)	23(3)
N4	7412(5)	1477(5)	-37(11)	24(3)
N5	6733(5)	1432(6)	-307(12)	29(3)
O1	5391(5)	1692(4)	-1413(10)	35(2)
O2	5223(4)	1438(4)	1191(10)	29(2)

Table 5.10 Continued:

O3	5179(4)	2710(5)	2061(9)	27(2)
O4	6384(4)	1994(4)	2327(10)	29(2)
O5	5122(4)	3046(5)	-681(10)	30(2)
O6	6422(4)	2728(4)	-1575(10)	29(2)
F1	4314(6)	616(6)	-2985(10)	75(4)
F2	5331(6)	831(6)	-3496(10)	76(4)
F3	4592(6)	1575(6)	-3548(11)	81(4)
F4	4103(5)	3065(7)	3364(12)	86(4)
F5	4536(4)	2814(4)	5219(11)	56(3)
F6	4847(6)	3644(5)	4173(12)	76(4)
F7	4389(5)	4182(5)	-943(10)	53(3)
F8	3973(4)	3406(5)	-2108(10)	58(3)
F9	4545(5)	4172(5)	-3008(10)	65(3)
S1	4535(4)	855(4)	3416(8)	40(2)
C16	4427(13)	652(12)	1804(17)	34(3)
C17	3979(13)	161(12)	1680(20)	37(4)
C18	3717(12)	-60(11)	2850(20)	37(3)
C19	3974(12)	274(11)	3886(19)	41(4)
S1A	3889(7)	46(7)	1628(14)	35(2)
C16A	4470(20)	653(19)	1930(30)	35(4)
C17A	4500(20)	783(19)	3210(40)	38(4)
C18A	4070(20)	400(20)	3960(30)	40(4)
C19A	3700(20)	-20(19)	3230(20)	37(4)
S2	7506(2)	1486(2)	3708(4)	39(1)
I1	6077(1)	5353(1)	2496(1)	39(1)
I2	7443(1)	-413(1)	-1621(1)	40(1)
Eu1	5885(1)	2314(1)	328(1)	24(1)

Table 5.11: Bond lengths [Å] and angles [°] for **5.11**.

C1-N1	1.329(16)	C4-C5	1.357(18)
C1-C2	1.393(18)	C4-N2	1.436(17)
C1-H1	0.95	C5-C6	1.404(19)
C2-C3	1.382(18)	C5-H5	0.95
C2-I1	2.058(13)	C6-C7	1.356(19)
C3-N2	1.357(17)	C6-H6	0.95
C3-H3	0.95	C7-C8	1.380(16)
C4-N3	1.355(17)	C7-H7	0.95

Table 5.11 Continued:

C8-N3	1.339(15)	C13-O1	1.252(15)
C8-N4	1.433(16)	C13-C14	1.39(2)
C9-C10	1.351(19)	C14-C15	1.419(19)
C9-N4	1.370(17)	C14-H14	0.95
C9-H9	0.95	C15-O2	1.270(16)
C10-C11	1.383(18)	C15-C16	1.45(2)
C10-I2	2.097(14)	C15-C16A	1.50(3)
C11-N5	1.337(18)	C20-F4	1.287(18)
C11-H11	0.95	C20-F5	1.30(2)
C12-F1	1.314(17)	C20-F6	1.41(2)
C12-F3	1.33(2)	C20-C21	1.53(2)
C12-F2	1.342(19)	C21-O3	1.281(17)
C12-C13	1.54(2)	C21-C22	1.368(18)
C22-C23	1.449(18)	C25-H25	0.95
C22-H22	0.95	C26-C27	1.369(15)
C23-O4	1.261(17)	C26-H26	0.95
C23-C24	1.452(16)	C27-S2	1.702(13)
C24-C25	1.351(16)	C27-H27	0.95
C24-S2	1.731(12)	C28-F7	1.345(17)
C25-C26	1.392(17)	C28-F8	1.356(18)
C28-F9	1.357(17)	C28-C29	1.513(19)
C29-O5	1.290(16)	C30-C31	1.434(18)
C29-C30	1.374(18)	C30-H30	0.95
C31-O6	1.244(16)	C34-H34	0.95
C31-C32	1.46(2)	C35-H35	0.95
C31-C32A	1.53(3)	S3A-C35A	1.701(16)
S3-C35	1.697(15)	S3A-C32A	1.733(17)
S3-C32	1.733(15)	C32A-C33A	1.353(19)
C32-C33	1.354(18)	C33A-C34A	1.39(2)
C33-C34	1.395(19)	C33A-H33A	0.95
C33-H33	0.95	C34A-C35A	1.368(17)
C34-C35	1.368(16)	C34A-H34A	0.95
C35A-H35A	0.95	O3-Eu1	2.415(9)
N1-N2	1.364(15)	O4-Eu1	2.384(9)
N1-Eu1	2.559(11)	O5-Eu1	2.378(9)
N3-Eu1	2.715(10)	O6-Eu1	2.394(9)
N4-N5	1.382(14)	S1-C19	1.707(15)
N5-Eu1	2.565(12)	S1-C16	1.729(16)
O1-Eu1	2.417(10)	C16-C17	1.352(18)
O2-Eu1	2.405(9)	C17-C18	1.393(19)

Table 5.11 Continued:

C17-H17	0.95	C16A-C17A	1.352(19)
C18-C19	1.370(16)	C17A-C18A	1.39(2)
C18-H18	0.95	C17A-H17A	0.95
C19-H19	0.95	C18A-C19A	1.371(17)
S1A-C19A	1.700(16)	C18A-H18A	0.95
S1A-C16A	1.731(17)	C19A-H19A	0.95
N1-C1-C2	111.7(12)	N2-C3-C2	106.4(12)
N1-C1-H1	124.2	N2-C3-H3	126.8
C2-C1-H1	124.2	C2-C3-H3	126.8
C3-C2-C1	105.4(12)	N3-C4-C5	125.3(13)
C3-C2-I1	127.6(11)	N3-C4-N2	113.3(11)
C1-C2-I1	126.9(10)	C5-C4-N2	121.4(12)
C4-C5-C6	116.5(13)	C6-C7-H7	121.1
C4-C5-H5	121.8	C8-C7-H7	121.1
C6-C5-H5	121.8	N3-C8-C7	124.4(12)
C7-C6-C5	120.6(12)	N3-C8-N4	114.3(10)
C7-C6-H6	119.7	C7-C8-N4	121.2(11)
C5-C6-H6	119.7	C10-C9-N4	105.7(12)
C6-C7-C8	117.7(12)	C10-C9-H9	127.2
N4-C9-H9	127.2	N5-C11-H11	124.3
C9-C10-C11	107.6(12)	C10-C11-H11	124.3
C9-C10-I2	126.4(10)	F1-C12-F3	107.6(14)
C11-C10-I2	125.9(10)	F1-C12-F2	107.1(14)
N5-C11-C10	111.3(12)	F3-C12-F2	105.4(15)
F1-C12-C13	114.8(14)	F2-C12-C13	109.7(13)
F3-C12-C13	111.7(14)	O1-C13-C14	130.2(15)
O1-C13-C12	112.7(13)	O2-C15-C14	122.2(13)
C14-C13-C12	117.0(13)	O2-C15-C16	119.4(14)
C13-C14-C15	121.6(13)	C14-C15-C16	118.4(14)
C13-C14-H14	119.2	O2-C15-C16A	114.3(15)
C15-C14-H14	119.2	C14-C15-C16A	123.6(16)
F4-C20-F5	113.2(15)	C21-C22-C23	122.7(13)
F4-C20-F6	100.6(14)	C21-C22-H22	118.6
F5-C20-F6	102.3(14)	C23-C22-H22	118.6
F4-C20-C21	113.9(14)	O4-C23-C22	122.7(12)
F5-C20-C21	117.1(13)	O4-C23-C24	117.6(12)
F6-C20-C21	107.2(13)	C22-C23-C24	119.6(12)
O3-C21-C22	130.6(13)	C25-C24-C23	132.9(13)
O3-C21-C20	113.9(12)	C25-C24-S2	110.7(9)
C22-C21-C20	115.5(13)	C23-C24-S2	116.5(10)

Table 5.11 Continued:

C24-C25-C26	113.8(12)	F7-C28-C29	111.4(13)
C24-C25-H25	123.1	F8-C28-C29	112.9(13)
C26-C25-H25	123.1	F9-C28-C29	114.3(13)
C27-C26-C25	112.4(12)	O5-C29-C30	129.0(12)
C27-C26-H26	123.8	O5-C29-C28	112.3(11)
C25-C26-H26	123.8	C30-C29-C28	118.7(13)
C26-C27-S2	111.6(10)	C29-C30-C31	124.3(14)
C26-C27-H27	124.2	C29-C30-H30	117.9
S2-C27-H27	124.2	C31-C30-H30	117.9
F7-C28-F8	106.5(12)	O6-C31-C30	122.1(13)
F7-C28-F9	105.8(12)	O6-C31-C32	118.4(13)
F8-C28-F9	105.3(12)	C30-C31-C32	119.5(13)
O6-C31-C32A	118.7(16)	C32-C33-H33	123.0
C30-C31-C32A	119.2(17)	C34-C33-H33	123.0
C35-S3-C32	91.6(8)	C35-C34-C33	112.0(14)
C33-C32-C31	132.7(16)	C35-C34-H34	124.0
C33-C32-S3	110.4(11)	C33-C34-H34	124.0
C31-C32-S3	116.6(12)	C34-C35-S3	112.1(12)
C32-C33-C34	114.0(14)	C34-C35-H35	124.0
S3-C35-H35	124.0	C35A-C34A-H34A	123.8
C35A-S3A-C32A	91.5(10)	C33A-C34A-H34A	123.8
C33A-C32A-C31	125(3)	C34A-C35A-S3A	111.8(15)
C33A-C32A-S3A	110.6(12)	C34A-C35A-H35A	124.1
C31-C32A-S3A	124(2)	S3A-C35A-H35A	124.1
C32A-C33A-C34A	113.8(16)	C1-N1-N2	104.8(11)
C32A-C33A-H33A	123.1	C1-N1-Eu1	130.1(9)
C34A-C33A-H33A	123.1	N2-N1-Eu1	124.7(8)
C35A-C34A-C33A	112.4(17)	C3-N2-N1	111.7(11)
C3-N2-C4	129.0(11)	C8-N3-C4	115.4(10)
N1-N2-C4	119.3(11)	C8-N3-Eu1	121.9(8)
C4-N3-Eu1	122.6(8)	C23-O4-Eu1	139.4(8)
C9-N4-N5	111.7(11)	C29-O5-Eu1	132.9(8)
C9-N4-C8	128.8(10)	C31-O6-Eu1	139.1(8)
N5-N4-C8	119.5(10)	C19-S1-C16	91.4(8)
C11-N5-N4	103.7(11)	C17-C16-C15	130.8(17)
C11-N5-Eu1	133.1(9)	C17-C16-S1	110.6(11)
N4-N5-Eu1	122.9(8)	C15-C16-S1	118.6(14)
C13-O1-Eu1	134.7(10)	C16-C17-C18	114.2(16)
C15-O2-Eu1	140.8(9)	C16-C17-H17	122.9
C21-O3-Eu1	132.2(8)	C18-C17-H17	122.9

Table 5.11 Continued:

C19-C18-C17	111.9(15)	C16A-C17A-H17A	123.1
C19-C18-H18	124.1	C18A-C17A-H17A	123.1
C17-C18-H18	124.1	C19A-C18A-C17A	112.2(17)
C18-C19-S1	111.9(13)	C19A-C18A-H18A	123.9
C18-C19-H19	124.0	C17A-C18A-H18A	123.9
S1-C19-H19	124.0	C18A-C19A-S1A	111.8(14)
C19A-S1A-C16A	91.5(9)	C18A-C19A-H19A	124.1
C17A-C16A-C15	128(2)	S1A-C19A-H19A	124.1
C17A-C16A-S1A	110.6(12)	C27-S2-C24	91.5(6)
C15-C16A-S1A	121(2)	O5-Eu1-O4	145.2(3)
C16A-C17A-C18A	113.9(16)	O5-Eu1-O6	72.5(3)
O4-Eu1-O6	128.6(3)	O2-Eu1-O3	70.1(3)
O5-Eu1-O2	106.7(3)	O5-Eu1-O1	75.5(3)
O4-Eu1-O2	72.5(3)	O4-Eu1-O1	131.8(3)
O6-Eu1-O2	144.7(3)	O6-Eu1-O1	76.1(3)
O5-Eu1-O3	75.0(3)	O2-Eu1-O1	69.8(3)
O4-Eu1-O3	72.2(3)	O3-Eu1-O1	119.6(3)
O6-Eu1-O3	138.4(3)	O5-Eu1-N1	75.7(3)
O4-Eu1-N1	82.8(3)	O1-Eu1-N5	72.6(3)
O6-Eu1-N1	76.4(4)	N1-Eu1-N5	120.2(3)
O2-Eu1-N1	138.6(4)	O5-Eu1-N3	124.2(3)
O3-Eu1-N1	70.9(3)	O4-Eu1-N3	63.0(3)
O1-Eu1-N1	144.9(4)	O6-Eu1-N3	65.9(3)
O5-Eu1-N5	139.1(4)	O2-Eu1-N3	128.7(3)
O4-Eu1-N5	75.6(3)	O3-Eu1-N3	115.4(3)
O6-Eu1-N5	75.5(3)	O1-Eu1-N3	124.8(3)
O2-Eu1-N5	85.6(3)	N1-Eu1-N3	60.0(3)
O3-Eu1-N5	144.1(3)	N5-Eu1-N3	60.5(3)

Table 5.12: Anisotropic displacement parameters ($Å^2$ x 10^3) for **5.11**. The anisotropic displacement factor exponent takes the form: $-2\pi^2[h^2 a^{*2} U^{11} + ... + 2 h k a^* b^* U^{12}]$.

	U11	U22	U33	U23	U13	U12
C1	20(6)	24(7)	42(8)	-8(6)	1(6)	-2(5)
C2	26(7)	21(7)	38(8)	-5(6)	-1(6)	3(5)
C3	22(6)	29(7)	32(7)	-1(6)	0(6)	-2(6)
C4	15(6)	27(7)	31(7)	1(6)	-5(5)	1(5)
C5	21(6)	26(7)	41(8)	-8(6)	-2(6)	-4(5)
C6	16(6)	36(7)	42(8)	5(6)	-1(6)	-10(6)
C7	25(6)	28(7)	30(8)	3(6)	1(5)	-1(5)
C8	15(5)	30(6)	24(6)	0(6)	4(6)	1(4)
C9	25(7)	33(7)	30(7)	3(6)	2(6)	5(6)
C10	30(7)	21(6)	29(7)	4(6)	1(6)	5(5)
C11	24(6)	25(7)	20(7)	-7(6)	-3(5)	-9(5)
C12	38(8)	54(9)	42(9)	-6(8)	-4(7)	-22(7)
C13	21(6)	36(7)	39(8)	2(7)	-2(6)	-1(6)
C14	38(8)	24(7)	39(8)	-12(6)	-1(7)	-4(6)
C15	24(7)	25(7)	36(8)	-3(6)	-1(6)	2(6)
C20	46(8)	48(9)	41(9)	6(7)	-7(7)	19(7)
C21	27(6)	28(7)	31(7)	-9(7)	-1(6)	1(5)
C22	21(6)	25(7)	27(7)	4(6)	2(5)	-5(5)
C23	24(6)	19(6)	28(7)	4(6)	-5(6)	-8(5)
C24	23(6)	23(7)	27(7)	7(6)	-1(6)	-1(5)
C25	36(7)	33(7)	28(8)	7(6)	4(6)	1(6)
C26	46(8)	59(9)	32(8)	12(7)	1(7)	5(7)
C27	35(7)	59(9)	51(9)	7(8)	-4(7)	15(7)
C28	37(8)	50(8)	30(8)	7(7)	1(6)	10(7)
C29	24(6)	30(7)	31(7)	-2(6)	7(6)	6(5)
C30	25(6)	41(8)	38(8)	9(7)	7(6)	7(6)
C31	27(6)	25(7)	34(7)	1(6)	-4(6)	-10(5)
S3	26(3)	49(3)	43(3)	-1(3)	3(2)	-2(2)
C32	32(6)	43(6)	36(6)	-3(5)	3(5)	-6(5)
C33	35(6)	46(7)	41(6)	-1(6)	4(6)	-3(6)
C34	42(6)	51(7)	41(6)	-2(6)	6(6)	-9(6)
C35	34(6)	49(7)	40(6)	-5(6)	5(5)	-10(5)
S3A	39(5)	49(6)	40(6)	0(5)	8(5)	-8(5)
C32A	33(6)	44(7)	39(7)	-2(6)	3(6)	-5(6)
C33A	33(7)	45(7)	40(7)	-1(6)	3(6)	-5(6)
C34A	34(7)	47(7)	41(7)	-3(6)	6(6)	-6(6)

Table 5.12 Continued:

C35A	39(7)	48(7)	40(7)	-1(6)	7(6)	-8(6)
N1	20(5)	22(6)	40(7)	-3(5)	-5(5)	3(5)
N2	18(5)	32(6)	30(6)	1(5)	-3(5)	-1(5)
N3	24(5)	27(6)	18(6)	7(4)	3(4)	-5(4)
N4	14(5)	27(6)	30(7)	-1(5)	1(4)	-2(4)
N5	17(5)	42(7)	27(6)	4(5)	-1(5)	-4(5)
O1	34(5)	30(5)	40(6)	-10(5)	-5(5)	-7(4)
O2	20(5)	26(5)	40(6)	-2(4)	-1(4)	-5(4)
O3	19(4)	32(5)	31(5)	-4(4)	3(4)	0(4)
O4	21(4)	37(5)	28(5)	5(4)	3(4)	3(4)
O5	18(5)	40(6)	31(5)	4(5)	1(4)	7(4)
O6	21(4)	39(5)	27(5)	5(5)	8(4)	1(4)
F1	77(7)	98(9)	49(7)	-17(6)	-5(5)	-57(7)
F2	71(7)	115(9)	43(7)	-30(6)	9(6)	-20(7)
F3	101(9)	96(9)	47(7)	17(6)	-32(7)	-18(7)
F4	34(5)	154(11)	71(8)	-35(8)	-3(6)	42(6)
F5	56(5)	62(6)	50(6)	7(6)	26(6)	23(4)
F6	102(9)	43(6)	85(9)	5(6)	20(7)	23(6)
F7	47(6)	55(6)	57(7)	-6(5)	9(5)	21(5)
F8	29(5)	81(7)	63(7)	7(5)	-8(4)	13(5)
F9	55(6)	80(7)	62(7)	20(6)	12(5)	38(6)
S1	43(3)	40(3)	37(3)	5(3)	-3(3)	-16(3)
C16	31(6)	31(6)	40(6)	4(5)	-4(5)	-4(5)
C17	35(6)	34(6)	43(6)	5(6)	-5(6)	-4(6)
C18	36(6)	33(6)	41(6)	4(6)	-2(6)	-8(5)
C19	43(6)	40(6)	41(6)	5(6)	-1(6)	-11(6)
S1A	32(4)	29(5)	45(5)	3(4)	-4(4)	-6(4)
C16A	33(6)	32(6)	40(6)	4(6)	-3(6)	-5(6)
C17A	38(6)	37(7)	40(7)	4(6)	-2(6)	-9(6)
C18A	42(6)	38(7)	40(7)	4(6)	-2(6)	-9(6)
C19A	38(6)	34(7)	40(7)	5(6)	-2(6)	-8(6)
S2	24(2)	57(2)	37(3)	8(2)	2(2)	8(2)
I1	34(1)	29(1)	55(1)	-9(1)	2(1)	-1(1)
I2	44(1)	30(1)	45(1)	-6(1)	-2(1)	6(1)
Eu1	15(1)	26(1)	30(1)	-1(1)	0(1)	-1(1)

Table 5.13: Hydrogen coordinates (x 10^4) and isotropic displacement parameters (Å^2 x 10^3) for **5.11**.

x	y	z	U(eq)		x	y	z	U(eq)	
H1	5473	4001	1290	34	H7	8668	1809	497	33
H3	7415	4421	1985	33	H9	8211	828	-231	35
H5	8263	3660	1610	35	H11	6253	658	-1105	27
H6	9048	2822	1148	37	H14	4382	529	-714	40
H22	5598	2315	4962	29	H34A	8409	3284	-4293	49
H25	6379	1706	6228	39	H35A	7797	3950	-5839	51
H26	7415	1208	7012	55	H17	3855	-17	867	45
H27	8240	1058	5300	58	H18	3397	-402	2922	44
H30	5627	3750	-3280	42	H19	3854	191	4762	50
H33	6483	3784	-4893	49	H17A	4796	1102	3566	46
H34	7571	3725	-5990	53	H18A	4039	438	4879	48
H35	8400	3131	-4732	49	H19A	3385	-316	3575	44
H33A	7674	2810	-2652	47					

Table 5.14: Torsion angles [°] for **5.11**.

N1-C1-C2-C3	-0.3(18)	F1-C12-C13-C14	6(2)
N1-C1-C2-I1	-177.3(10)	F3-C12-C13-C14	129.1(15)
C1-C2-C3-N2	0.4(16)	F2-C12-C13-C14	-114.4(15)
I1-C2-C3-N2	177.3(10)	O1-C13-C14-C15	3(3)
N3-C4-C5-C6	2(2)	C12-C13-C14-C15	-179.1(15)
N2-C4-C5-C6	179.7(13)	C13-C14-C15-O2	-3(2)
C4-C5-C6-C7	-3(2)	C13-C14-C15-C16	173.4(18)
C5-C6-C7-C8	3(2)	C13-C14-C15-C16A	176(3)
C6-C7-C8-N3	0(2)	F4-C20-C21-O3	27(2)
C6-C7-C8-N4	177.5(13)	F5-C20-C21-O3	162.7(14)
N4-C9-C10-C11	-0.9(16)	F6-C20-C21-O3	-83.2(15)
N4-C9-C10-I2 1	76.2(9)	F4-C20-C21-C22	-154.8(15)
C9-C10-C11-N5	0.1(17)	F5-C20-C21-C22	-19(2)
I2-C10-C11-N5	-177.0(10)	F6-C20-C21-C22	94.8(15)
F1-C12-C13-O1	-175.4(14)	O3-C21-C22-C23	2(2)
F3-C12-C13-O1	-52.6(18)	C20-C21-C22-C23	-175.5(13)
F2-C12-C13-O1	64.0(18)	C21-C22-C23-O4	-1(2)
C21-C22-C23-C24	175.4(12)	C22-C23-C24-C25	11(2)
O4-C23-C24-C25	-172.7(15)	O4-C23-C24-S2	7.6(16)

Table 5.14 Continued:

C22-C23-C24-S2	-169.0(9)	F9-C28-C29-C30	0(2)
C23-C24-C25-C26	-179.8(15)	O5-C29-C30-C31	1(3)
S2-C24-C25-C26	-0.1(18)	C28-C29-C30-C31	179.7(14)
C24-C25-C26-C27	1(2)	C29-C30-C31-O6	2(2)
C25-C26-C27-S2	-1(2)	C29-C30-C31-C32	-175.9(15)
F7-C28-C29-O5	58.9(17)	C29-C30-C31-C32A	-180(3)
F8-C28-C29-O5	-60.9(16)	O6-C31-C32-C33	166.0(11)
F9-C28-C29-O5	178.8(13)	C30-C31-C32-C33	-16(2)
F7-C28-C29-C30	-120.2(15)	O6-C31-C32-S3	-7(2)
F8-C28-C29-C30	120.1(15)	C30-C31-C32-S3	171.0(12)
C35-S3-C32-C33	0.0(2)	C30-C31-C32A-S3A	-2(5)
C35-S3-C32-C31	174.5(17)	C35A-S3A-C32A-C33A	0.0(2)
C31-C32-C33-C34	-173(2)	C35A-S3A-C32A-C31	168(5)
S3-C32-C33-C34	0.0(3)	C31-C32A-C33A-C34A	-168(5)
C32-C33-C34-C35	0.0(6)	S3A-C32A-C33A-C34A	0.0(3)
C33-C34-C35-S3	0.0(7)	C32A-C33A-C34A-C35A	0.1(6)
C32-S3-C35-C34	0.0(5)	C33A-C34A-C35A-S3A	-0.1(7)
O6-C31-C32A-C33A	-18(4)	C32A-S3A-C35A-C34A	0.0(5)
C30-C31-C32A-C33A	164(2)	C2-C1-N1-N2	0.1(17)
O6-C31-C32A-S3A	176(2)	C2-C1-N1-Eu1	173.7(10)
C2-C3-N2-N1	-0.3(16)	C2-C3-N2-C4	-178.5(13)
C1-N1-N2-C3	0.1(15)	C10-C9-N4-C8	-175.0(13)
Eu1-N1-N2-C3	-173.9(9)	N3-C8-N4-C9	178.5(13)
C1-N1-N2-C4	178.5(12)	C7-C8-N4-C9	0(2)
Eu1-N1-N2-C4	4.5(16)	N3-C8-N4-N5	2.3(18)
N3-C4-N2-C3	177.0(13)	C7-C8-N4-N5	-175.7(12)
C5-C4-N2-C3	-1(2)	C10-C11-N5-N4	0.7(15)
N3-C4-N2-N1	-1.1(18)	C10-C11-N5-Eu1	-173.1(9)
C5-C4-N2-N1	-179.1(13)	C9-N4-N5-C11	-1.3(14)
C7-C8-N3-C4	-1(2)	C8-N4-N5-C11	175.5(12)
N4-C8-N3-C4	-179.0(11)	C9-N4-N5-Eu1	173.3(8)
C7-C8-N3-Eu1	-176.4(11)	C8-N4-N5-Eu1	-9.9(15)
N4-C8-N3-Eu1	5.7(16)	C14-C13-O1-Eu1	-7(2)
C5-C4-N3-C8	0(2)	C12-C13-O1-Eu1	174.8(10)
N2-C4-N3-C8	-177.8(12)	C14-C15-O2-Eu1	9(2)
C5-C4-N3-Eu1	175.5(11)	C16-C15-O2-Eu1	-167.3(15)
N2-C4-N3-Eu1	-2.5(15)	C16A-C15-O2-Eu1	-170(2)
C10-C9-N4-N5	1.4(15)	C22-C21-O3-Eu1	2(2)
C20-C21-O3-Eu1	179.3(9)	C24-C23-O4-Eu1	179.3(9)
C22-C23-O4-Eu1	-4(2)	C30-C29-O5-Eu1	-1(2)

Table 5.14 Continued:

C28-C29-O5-Eu1	179.9(9)	O2-C15-C16A-C17A	7(4)
C30-C31-O6-Eu1	-5(2)	C14-C15-C16A-C17A	-173(2)
C32-C31-O6-Eu1	173.2(11)	O2-C15-C16A-S1A	180(2)
C32A-C31-O6-Eu1	177(2)	C14-C15-C16A-S1A	0(5)
O2-C15-C16-C17	-177.5(14)	C19A-S1A-C16A-C17A	0.0(2)
C14-C15-C16-C17	6(3)	C19A-S1A-C16A-C15	-174(5)
O2-C15-C16-S1	2(3)	C15-C16A-C17A-C18A	174(5)
C14-C15-C16-S1	-174.9(15)	S1A-C16A-C17A-C18A	0.0(3)
C19-S1-C16-C17	0.0(2)	C16A-C17A-C18A-C19A	0.0(6)
C19-S1-C16-C15	-180(3)	C17A-C18A-C19A-S1A	0.0(7)
C15-C16-C17-C18	179(3)	C16A-S1A-C19A-C18A	0.0(5)
S1-C16-C17-C18	0.0(3)	C26-C27-S2-C24	0.9(14)
C16-C17-C18-C19	0.0(6)	C25-C24-S2-C27	-0.5(12)
C17-C18-C19-S1	0.0(7)	C23-C24-S2-C27	179.3(11)
C16-S1-C19-C18	0.0(5)		

X-ray Experimental for $C_{59}H_{48}GdN_5O_7$ (5.12): Crystals grew as yellow prisms by slow evaporation from acetone. The data crystal dimensions were obscured by the protecting oil used and a good estimate of the crystal size was not made. Data collection, unit cell refinement, and data reduction were performed using Rigaku's CrystalClear software.[39] The structure was solved by direct methods using the SIR2014 program[40] and refined by full-matrix least-squares on F^2 with anisotropic displacement parameters for all non-H atoms using SHELXL-2014.[33] The structural analyses were performed using the PLATON98[34] and WinGX[35] programs. The hydrogen atoms were placed in fixed, calculated positions with isotropic displacement parameters set to 1.2 x U_{eq} with respect to the attached atom.

Table 5.15: Crystal data and structure refinement for **5.12**.

Empirical formula	$C_{59}H_{48}GdN_5O_7$	
Formula weight	1096.27	
Temperature	100(2) K	
Wavelength	0.71075 Å	
Crystal system	Triclinic	
Space group	P -1	
Unit cell dimensions	a = 13.357(4) Å	α = 64.548(13)°
	b = 14.642(5) Å	β = 77.01(2)°
	c = 15.561(5) Å	γ = 69.427(18)°
Volume	2562.9(15) $Å^3$	
Z	2	
Density (calculated)	1.421 Mg/m^3	
Absorption coefficient	1.353 mm^{-1}	
F(000)	1114	
Crystal size	0.2000 x 0.2000 x 0.2000 mm^3	
θ range for data collection	2.092 to 25.028°.	
Index ranges	-15<=h<=15, -17<=k<=17, -18<=l<=18	
Reflections collected	33101	
Independent reflections	9026 [R(int) = 0.0973]	
Completeness to θ = 25.028°	99.7 %	
Absorption correction	Semi-empirical from equivalents	
Max. and min. transmission	1.0000 and 0.7095	
Refinement method	Full-matrix least-squares on F^2	
Data / restraints / parameters	9026 / 6 / 651	
Goodness-of-fit on F^2	1.184	
Final R indices [I>2σ(I)]	R1 = 0.0655, wR2 = 0.1379	
R indices (all data)	R1 = 0.0706, wR2 = 0.1409	
Extinction coefficient	n/a	
Largest diff. peak and hole	1.778 and -1.673 e.$Å^{-3}$	

Table 5.16: Atomic coordinates (x 10^4) and equivalent isotropic displacement parameters ($Å^2$x 10^3) for **5.12**. U(eq) is defined as one third of the trace of the orthogonalized U^{ij} tensor.

	x	y	z	U(eq)
C(33)	6836(5)	1165(5)	9268(4)	24(1)
C(11)	8536(5)	-467(6)	5680(4)	30(2)

Table 5.16 Continued:

C(23)	6456(5)	2520(5)	5173(4)	27(1)
C(19)	8700(5)	2262(5)	6436(4)	24(1)
C(38)	6525(5)	-2470(5)	11127(4)	26(1)
C(34)	6441(5)	411(5)	10048(4)	25(1)
C(32)	6437(5)	2322(5)	9136(4)	24(1)
C(36)	6137(5)	-1406(5)	10971(4)	24(1)
C(17)	10489(5)	1803(5)	7050(4)	23(1)
C(25)	5787(5)	3241(5)	4456(5)	28(2)
C(37)	5293(4)	-1066(5)	11602(4)	22(1)
C(16)	11420(5)	988(5)	7405(4)	26(1)
C(3)	11207(5)	-1846(5)	9948(4)	30(2)
C(30)	6815(5)	3056(5)	8318(5)	27(1)
C(40)	6085(5)	-3206(6)	11900(5)	33(2)
C(44)	9055(7)	-5727(6)	8496(6)	48(2)
C(35)	6642(4)	-632(5)	10140(4)	21(1)
C(50)	6532(5)	-1362(6)	7598(4)	29(2)
C(22)	7064(5)	3924(5)	5104(5)	31(2)
C(21)	7108(5)	2843(5)	5512(4)	23(1)
C(49)	7115(5)	-2440(5)	7933(5)	30(2)
C(56)	3699(6)	-353(8)	6135(6)	49(2)
C(48)	8129(5)	-2846(5)	8319(4)	26(1)
C(20)	7842(5)	2016(5)	6279(4)	22(1)
C(2)	10498(5)	-1410(5)	10544(4)	28(2)
C(6)	12278(5)	-3264(6)	7799(5)	35(2)
C(13)	11413(5)	3079(6)	6809(5)	34(2)
C(1)	9484(6)	-1041(5)	10172(4)	29(2)
C(51)	5509(5)	-1035(5)	7118(5)	26(1)
C(31)	5659(6)	2703(6)	9769(5)	36(2)
C(5)	11986(5)	-2938(6)	8553(5)	34(2)
C(7)	11652(5)	-2791(5)	7030(5)	31(2)
C(14)	12342(5)	1226(6)	7437(4)	30(2)
C(39)	4855(5)	-1800(5)	12361(4)	28(2)
C(28)	6427(6)	4134(5)	8126(5)	33(2)
C(46)	8405(7)	-4714(6)	8385(6)	43(2)
C(15)	10485(5)	2855(5)	6761(4)	28(2)
C(8)	10705(5)	-1998(5)	7081(4)	25(1)
C(43)	10490(7)	-5336(6)	8874(6)	46(2)
C(4)	11027(5)	-2141(5)	8532(4)	26(1)
C(12)	12334(5)	2271(5)	7133(5)	31(2)
C(47)	8773(5)	-3985(5)	8502(4)	27(1)
C(41)	5256(5)	-2865(5)	12511(4)	26(1)

Table 5.16 Continued:

C(10)	9221(6)	-881(6)	5021(5)	33(2)
C(24)	6385(6)	4640(5)	4388(5)	36(2)
C(52)	5192(5)	-18(6)	6435(5)	35(2)
C(53)	4886(6)	-1697(6)	7319(6)	43(2)
C(57)	1535(6)	4019(6)	4212(5)	39(2)
C(29)	5267(6)	3779(6)	9588(6)	45(2)
C(27)	5641(6)	4505(6)	8768(6)	45(2)
C(26)	5751(6)	4307(6)	4049(5)	36(2)
C(59)	403(6)	4007(6)	4175(6)	48(2)
C(45)	9823(6)	-4315(6)	8740(5)	42(2)
C(18)	9531(5)	1502(5)	7015(4)	21(1)
C(54)	4291(6)	332(7)	5923(6)	48(2)
C(58)	2402(7)	2989(6)	4392(6)	53(2)
C(42)	10100(7)	-6041(6)	8743(5)	44(2)
C(9)	10139(5)	-1524(5)	5462(4)	28(2)
C(55)	3983(6)	-1359(7)	6821(7)	49(2)
Gd(1)	8297(1)	-457(1)	8058(1)	21(1)
N(3)	10383(4)	-1672(4)	7806(4)	24(1)
N(4)	9989(4)	-1482(4)	6352(4)	24(1)
N(5)	8991(4)	-814(4)	6492(4)	24(1)
N(2)	10640(4)	-1760(4)	9268(4)	22(1)
N(1)	9566(4)	-1251(4)	9399(4)	23(1)
O(1)	9566(3)	535(3)	7501(3)	24(1)
O(2)	7675(3)	1104(3)	6690(3)	23(1)
O(3)	7531(3)	958(3)	8608(3)	24(1)
O(4)	7250(3)	-1007(3)	9521(3)	26(1)
O(5)	8557(3)	-2290(3)	8490(3)	26(1)
O(6)	6796(3)	-611(3)	7597(3)	24(1)
O(7)	1700(5)	4827(4)	4123(4)	55(2)

Table 5.17: Bond lengths [Å] and angles [°] for 5.12.

C(33)-O(3)	1.285(7)	C(23)-C(21)	1.404(8)
C(33)-C(34)	1.393(9)	C(23)-H(28)	0.9500
C(33)-C(32)	1.520(8)	C(19)-C(20)	1.412(8)
C(11)-N(5)	1.342(8)	C(19)-C(18)	1.415(8)
C(11)-C(10)	1.407(9)	C(19)-H(29)	0.9500
C(11)-H(26)	0.9500	C(38)-C(36)	1.385(9)
C(23)-C(25)	1.391(8)	C(38)-C(40)	1.403(9)

Table 5.17 Continued:

C(38)-H(30)	0.9500	C(40)-H(45)	0.9500
C(34)-C(35)	1.403(9)	C(44)-C(46)	1.388(10)
C(34)-H(31)	0.9500	C(44)-C(42)	1.394(11)
C(32)-C(30)	1.396(9)	C(44)-H(46)	0.9500
C(32)-C(31)	1.403(9)	C(35)-O(4)	1.296(7)
C(36)-C(37)	1.419(8)	C(50)-O(6)	1.267(8)
C(36)-C(35)	1.515(8)	C(50)-C(49)	1.407(9)
C(17)-C(16)	1.405(8)	C(50)-C(51)	1.532(8)
C(17)-C(15)	1.405(9)	C(22)-C(24)	1.394(9)
C(17)-C(18)	1.510(8)	C(22)-C(21)	1.414(9)
C(25)-C(26)	1.396(9)	C(22)-H(54)	0.9500
C(25)-H(39)	0.9500	C(21)-C(20)	1.517(7)
C(37)-C(39)	1.390(9)	C(49)-C(48)	1.429(9)
C(37)-H(40)	0.9500	C(49)-H(58)	0.9500
C(16)-C(14)	1.408(9)	C(56)-C(55)	1.375(12)
C(16)-H(41)	0.9500	C(56)-C(54)	1.377(11)
C(3)-C(2)	1.362(9)	C(56)-H(63)	0.9500
C(3)-N(2)	1.373(8)	C(48)-O(5)	1.282(7)
C(3)-H(42)	0.9500	C(48)-C(47)	1.515(8)
C(30)-C(28)	1.392(9)	C(20)-O(2)	1.286(7)
C(30)-H(44)	0.9500	C(2)-C(1)	1.426(9)
C(40)-C(41)	1.389(9)	C(2)-H(67)	0.9500
C(6)-C(5)	1.379(9)	C(39)-C(41)	1.389(9)
C(6)-C(7)	1.394(9)	C(39)-H(87)	0.9500
C(6)-H(68)	0.9500	C(28)-C(27)	1.411(10)
C(13)-C(12)	1.382(9)	C(28)-H(89)	0.9500
C(13)-C(15)	1.414(9)	C(46)-C(47)	1.411(9)
C(13)-H(69)	0.9500	C(46)-H(92)	0.9500
C(1)-N(1)	1.336(8)	C(15)-H(93)	0.9500
C(1)-H(72)	0.9500	C(8)-N(3)	1.337(8)
C(51)-C(53)	1.384(9)	C(8)-N(4)	1.419(8)
C(51)-C(52)	1.388(9)	C(43)-C(45)	1.397(10)
C(31)-C(29)	1.393(10)	C(43)-C(42)	1.409(10)
C(31)-H(78)	0.9500	C(43)-H(95)	0.9500
C(5)-C(4)	1.393(9)	C(4)-N(3)	1.357(8)
C(5)-H(79)	0.9500	C(4)-N(2)	1.405(8)
C(7)-C(8)	1.399(9)	C(12)-H(100)	0.9500
C(7)-H(82)	0.9500	C(47)-C(45)	1.393(9)
C(14)-C(12)	1.391(9)	C(41)-H(105)	0.9500
C(14)-H(85)	0.9500	C(10)-C(9)	1.369(9)

Table 5.17 Continued:

C(10)-H(109)	0.9500	C(58)-H(58C)	0.9800
C(24)-C(26)	1.395(9)	C(42)-H(145)	0.9500
C(24)-H(110)	0.9500	C(9)-N(4)	1.379(7)
C(52)-C(54)	1.411(9)	C(9)-H(147)	0.9500
C(52)-H(114)	0.9500	C(55)-H(148)	0.9500
C(53)-C(55)	1.405(10)	Gd(1)-O(4)	2.359(4)
C(53)-H(115)	0.9500	Gd(1)-O(5)	2.383(4)
C(57)-O(7)	1.223(9)	Gd(1)-O(6)	2.385(4)
C(57)-C(58)	1.500(10)	Gd(1)-O(3)	2.389(4)
C(57)-C(59)	1.533(10)	Gd(1)-O(1)	2.392(4)
C(29)-C(27)	1.390(11)	Gd(1)-O(2)	2.392(4)
C(29)-H(121)	0.9500	Gd(1)-N(1)	2.589(5)
C(27)-H(123)	0.9500	Gd(1)-N(5)	2.610(5)
C(26)-H(124)	0.9500	Gd(1)-N(3)	2.776(5)
C(59)-H(59A)	0.9800	N(4)-N(5)	1.385(7)
C(59)-H(59B)	0.9800	N(2)-N(1)	1.379(7)
C(59)-H(59C)	0.9800	O(3)-C(33)-C(34)	124.0(6)
C(45)-H(134)	0.9500	O(3)-C(33)-C(32)	115.1(5)
C(18)-O(1)	1.276(7)	C(34)-C(33)-C(32)	120.8(6)
C(54)-H(137)	0.9500	N(5)-C(11)-C(10)	112.1(6)
C(58)-H(58A)	0.9800	N(5)-C(11)-H(26)	123.9
C(58)-H(58B)	0.9800		
C(10)-C(11)-H(26)	123.9	C(37)-C(36)-C(35)	121.3(6)
C(25)-C(23)-C(21)	121.0(6)	C(16)-C(17)-C(15)	118.6(6)
C(25)-C(23)-H(28)	119.5	C(16)-C(17)-C(18)	118.2(6)
C(21)-C(23)-H(28)	119.5	C(15)-C(17)-C(18)	123.1(6)
C(20)-C(19)-C(18)	123.4(6)	C(23)-C(25)-C(26)	120.7(6)
C(20)-C(19)-H(29)	118.3	C(23)-C(25)-H(39)	119.6
C(18)-C(19)-H(29)	118.3	C(26)-C(25)-H(39)	119.6
C(36)-C(38)-C(40)	120.4(6)	C(39)-C(37)-C(36)	119.7(6)
C(36)-C(38)-H(30)	119.8	C(39)-C(37)-H(40)	120.2
C(40)-C(38)-H(30)	119.8	C(36)-C(37)-H(40)	120.2
C(33)-C(34)-C(35)	123.9(6)	C(17)-C(16)-C(14)	120.5(6)
C(33)-C(34)-H(31)	118.1	C(17)-C(16)-H(41)	119.8
C(35)-C(34)-H(31)	118.1	C(14)-C(16)-H(41)	119.8
C(30)-C(32)-C(31)	117.8(6)	C(2)-C(3)-N(2)	107.7(6)
C(30)-C(32)-C(33)	118.8(6)	C(2)-C(3)-H(42)	126.2
C(31)-C(32)-C(33)	123.3(6)	N(2)-C(3)-H(42)	126.2
C(38)-C(36)-C(37)	119.5(6)	C(28)-C(30)-C(32)	121.5(6)
C(38)-C(36)-C(35)	119.1(6)	C(28)-C(30)-H(44)	119.3

Table 5.17 Continued:

C(32)-C(30)-H(44)	119.3	C(55)-C(56)-C(54)	121.0(7)
C(41)-C(40)-C(38)	119.7(7)	C(55)-C(56)-H(63)	119.5
C(41)-C(40)-H(45)	120.2	C(54)-C(56)-H(63)	119.5
C(38)-C(40)-H(45)	120.2	O(5)-C(48)-C(49)	123.8(6)
C(46)-C(44)-C(42)	119.1(7)	O(5)-C(48)-C(47)	117.0(6)
C(46)-C(44)-H(46)	120.4	C(49)-C(48)-C(47)	119.2(6)
C(42)-C(44)-H(46)	120.4	O(2)-C(20)-C(19)	124.7(5)
O(4)-C(35)-C(34)	123.3(6)	O(2)-C(20)-C(21)	116.2(5)
O(4)-C(35)-C(36)	114.7(5)	C(19)-C(20)-C(21)	118.9(6)
C(34)-C(35)-C(36)	122.0(6)	C(3)-C(2)-C(1)	105.0(6)
O(6)-C(50)-C(49)	126.8(6)	C(3)-C(2)-H(67)	127.5
O(6)-C(50)-C(51)	115.5(6)	C(1)-C(2)-H(67)	127.5
C(49)-C(50)-C(51)	117.6(6)	C(5)-C(6)-C(7)	121.2(6)
C(24)-C(22)-C(21)	120.3(6)	C(5)-C(6)-H(68)	119.4
C(24)-C(22)-H(54)	119.8	C(7)-C(6)-H(68)	119.4
C(21)-C(22)-H(54)	119.8	C(12)-C(13)-C(15)	120.6(7)
C(23)-C(21)-C(22)	118.1(6)	C(12)-C(13)-H(69)	119.7
C(23)-C(21)-C(20)	118.6(6)	C(15)-C(13)-H(69)	119.7
C(22)-C(21)-C(20)	123.2(6)	N(1)-C(1)-C(2)	111.6(6)
C(50)-C(49)-C(48)	123.7(6)	N(1)-C(1)-H(72)	124.2
C(50)-C(49)-H(58)	118.1	C(2)-C(1)-H(72)	124.2
C(48)-C(49)-H(58)	118.1	C(53)-C(51)-C(52)	118.0(6)
C(53)-C(51)-C(50)	123.9(6)	C(30)-C(28)-H(89)	120.0
C(52)-C(51)-C(50)	118.1(6)	C(27)-C(28)-H(89)	120.0
C(29)-C(31)-C(32)	121.4(7)	C(44)-C(46)-C(47)	122.0(7)
C(29)-C(31)-H(78)	119.3	C(44)-C(46)-H(92)	119.0
C(32)-C(31)-H(78)	119.3	C(47)-C(46)-H(92)	119.0
C(6)-C(5)-C(4)	117.6(6)	C(17)-C(15)-C(13)	120.1(6)
C(6)-C(5)-H(79)	121.2	C(17)-C(15)-H(93)	120.0
C(4)-C(5)-H(79)	121.2	C(13)-C(15)-H(93)	120.0
C(6)-C(7)-C(8)	116.5(6)	N(3)-C(8)-C(7)	124.2(6)
C(6)-C(7)-H(82)	121.8	N(3)-C(8)-N(4)	114.3(5)
C(8)-C(7)-H(82)	121.8	C(7)-C(8)-N(4)	121.5(6)
C(12)-C(14)-C(16)	120.3(6)	C(45)-C(43)-C(42)	119.2(7)
C(12)-C(14)-H(85)	119.9	C(45)-C(43)-H(95)	120.4
C(16)-C(14)-H(85)	119.9	C(42)-C(43)-H(95)	120.4
C(41)-C(39)-C(37)	120.2(6)	N(3)-C(4)-C(5)	123.2(6)
C(41)-C(39)-H(87)	119.9	N(3)-C(4)-N(2)	114.3(5)
C(37)-C(39)-H(87)	119.9	C(5)-C(4)-N(2)	122.5(6)
C(30)-C(28)-C(27)	120.1(7)	C(13)-C(12)-C(14)	119.8(6)

Table 5.17 Continued:

C(13)-C(12)-H(100)	120.1	C(58)-C(57)-C(59)	116.4(7)
C(14)-C(12)-H(100)	120.1	C(27)-C(29)-C(31)	120.5(7)
C(45)-C(47)-C(46)	117.8(6)	C(27)-C(29)-H(121)	119.8
C(45)-C(47)-C(48)	117.9(6)	C(31)-C(29)-H(121)	119.8
C(46)-C(47)-C(48)	124.2(6)	C(29)-C(27)-C(28)	118.8(7)
C(39)-C(41)-C(40)	120.6(6)	C(29)-C(27)-H(123)	120.6
C(39)-C(41)-H(105)	119.7	C(28)-C(27)-H(123)	120.6
C(40)-C(41)-H(105)	119.7	C(24)-C(26)-C(25)	118.8(6)
C(9)-C(10)-C(11)	105.6(6)	C(24)-C(26)-H(124)	120.6
C(9)-C(10)-H(109)	127.2	C(25)-C(26)-H(124)	120.6
C(11)-C(10)-H(109)	127.2	C(57)-C(59)-H(59A)	109.5
C(22)-C(24)-C(26)	121.1(6)	C(57)-C(59)-H(59B)	109.5
C(22)-C(24)-H(110)	119.5	H(59A)-C(59)-H(59B)	109.5
C(26)-C(24)-H(110)	119.5	C(57)-C(59)-H(59C)	109.5
C(51)-C(52)-C(54)	121.8(7)	H(59A)-C(59)-H(59C)	109.5
C(51)-C(52)-H(114)	119.1	H(59B)-C(59)-H(59C)	109.5
C(54)-C(52)-H(114)	119.1	C(47)-C(45)-C(43)	121.6(7)
C(51)-C(53)-C(55)	120.9(8)	C(47)-C(45)-H(134)	119.2
C(51)-C(53)-H(115)	119.6	C(43)-C(45)-H(134)	119.2
C(55)-C(53)-H(115)	119.6	O(1)-C(18)-C(19)	124.6(6)
O(7)-C(57)-C(58)	122.8(8)	O(1)-C(18)-C(17)	115.3(5)
O(7)-C(57)-C(59)	120.8(7)	C(19)-C(18)-C(17)	120.0(6)
C(56)-C(54)-C(52)	118.4(8)	C(56)-C(55)-C(53)	119.8(7)
C(56)-C(54)-H(137)	120.8	C(56)-C(55)-H(148)	120.1
C(52)-C(54)-H(137)	120.8	C(53)-C(55)-H(148)	120.1
C(57)-C(58)-H(58A)	109.5	O(4)-Gd(1)-O(5)	74.14(15)
C(57)-C(58)-H(58B)	109.5	O(4)-Gd(1)-O(6)	77.09(15)
H(58A)-C(58)-H(58B)	109.5	O(5)-Gd(1)-O(6)	72.64(15)
C(57)-C(58)-H(58C)	109.5	O(4)-Gd(1)-O(3)	70.12(14)
H(58A)-C(58)-H(58C)	109.5	O(5)-Gd(1)-O(3)	143.88(14)
H(58B)-C(58)-H(58C)	109.5	O(6)-Gd(1)-O(3)	103.73(14)
C(44)-C(42)-C(43)	120.3(7)	O(4)-Gd(1)-O(1)	132.96(14)
C(44)-C(42)-H(145)	119.8	O(5)-Gd(1)-O(1)	130.57(14)
C(43)-C(42)-H(145)	119.8	O(6)-Gd(1)-O(1)	142.21(14)
C(10)-C(9)-N(4)	106.9(6)	O(3)-Gd(1)-O(1)	74.45(14)
C(10)-C(9)-H(147)	126.6	O(4)-Gd(1)-O(2)	124.50(14)
N(4)-C(9)-H(147)	126.6		
O(5)-Gd(1)-O(2)	134.13(14)	O(1)-Gd(1)-O(2)	70.96(14)
O(6)-Gd(1)-O(2)	72.41(14)	O(4)-Gd(1)-N(1)	73.25(15)
O(3)-Gd(1)-O(2)	73.62(14)	O(5)-Gd(1)-N(1)	80.21(16)

Table 5.17 Continued:

O(6)-Gd(1)-N(1)	144.17(16)	C(8)-N(3)-Gd(1)	121.7(4)
O(3)-Gd(1)-N(1)	84.71(15)	C(4)-N(3)-Gd(1)	119.4(4)
O(1)-Gd(1)-N(1)	73.61(15)	C(9)-N(4)-N(5)	111.4(5)
O(2)-Gd(1)-N(1)	142.21(15)	C(9)-N(4)-C(8)	129.1(5)
O(4)-Gd(1)-N(5)	142.03(16)	N(5)-N(4)-C(8)	119.5(5)
O(5)-Gd(1)-N(5)	73.58(15)	C(11)-N(5)-N(4)	104.0(5)
O(6)-Gd(1)-N(5)	74.65(15)	C(11)-N(5)-Gd(1)	132.1(4)
O(3)-Gd(1)-N(5)	141.45(15)	N(4)-N(5)-Gd(1)	123.9(3)
O(1)-Gd(1)-N(5)	83.99(15)	C(3)-N(2)-N(1)	111.1(5)
O(2)-Gd(1)-N(5)	69.22(15)	C(3)-N(2)-C(4)	127.9(5)
N(1)-Gd(1)-N(5)	119.63(16)	N(1)-N(2)-C(4)	120.9(5)
O(4)-Gd(1)-N(3)	120.51(15)	C(1)-N(1)-N(2)	104.6(5)
O(5)-Gd(1)-N(3)	63.40(15)	C(1)-N(1)-Gd(1)	131.1(4)
O(6)-Gd(1)-N(3)	122.48(14)	N(2)-N(1)-Gd(1)	121.6(4)
O(3)-Gd(1)-N(3)	133.67(15)	C(18)-O(1)-Gd(1)	135.5(4)
O(1)-Gd(1)-N(3)	67.25(15)	C(20)-O(2)-Gd(1)	135.2(4)
O(2)-Gd(1)-N(3)	114.97(14)	C(33)-O(3)-Gd(1)	138.1(4)
N(1)-Gd(1)-N(3)	60.55(15)	C(35)-O(4)-Gd(1)	139.7(4)
N(5)-Gd(1)-N(3)	59.07(15)	C(48)-O(5)-Gd(1)	136.4(4)
C(8)-N(3)-C(4)	117.3(5)	C(50)-O(6)-Gd(1)	135.4(4)

Table 5.18: Anisotropic displacement parameters ($Å^2$ x 10^3) for **5.12**. The anisotropic displacement factor exponent takes the form: $-2\pi^2[h^2 a^{*2}U^{11} + ... + 2 h k a^* b^* U^{12}]$.

	U11	U22	U33	U23	U13	U12
C(33)	19(3)	32(4)	20(3)	-12(3)	-9(3)	-1(3)
C(11)	26(4)	45(4)	21(3)	-16(3)	0(3)	-8(3)
C(23)	28(4)	30(4)	22(3)	-7(3)	-2(3)	-10(3)
C(19)	22(3)	27(3)	20(3)	-7(3)	-4(3)	-7(3)
C(38)	20(3)	32(4)	26(3)	-15(3)	1(3)	-5(3)
C(34)	25(3)	31(4)	21(3)	-15(3)	3(3)	-8(3)
C(32)	24(3)	27(3)	24(3)	-14(3)	-7(3)	-3(3)
C(36)	23(3)	36(4)	16(3)	-12(3)	-3(3)	-10(3)
C(17)	23(3)	36(4)	17(3)	-17(3)	2(3)	-11(3)

Table 5.18 Continued:

C(25)	28(4)	28(3)	31(4)	-9(3)	-7(3)	-11(3)
C(37)	14(3)	31(3)	22(3)	-16(3)	-1(2)	-1(3)
C(16)	25(3)	25(3)	29(3)	-13(3)	-4(3)	-4(3)
C(3)	26(4)	40(4)	25(3)	-14(3)	-6(3)	-7(3)
C(30)	25(3)	30(4)	31(4)	-13(3)	-6(3)	-10(3)
C(40)	37(4)	33(4)	32(4)	-11(3)	-6(3)	-13(3)
C(44)	62(5)	29(4)	59(5)	-20(4)	-18(4)	-9(4)
C(35)	12(3)	29(3)	23(3)	-9(3)	-4(2)	-7(3)
C(50)	26(4)	42(4)	22(3)	-12(3)	3(3)	-17(3)
C(22)	31(4)	29(4)	36(4)	-13(3)	-12(3)	-5(3)
C(21)	13(3)	35(4)	22(3)	-15(3)	2(3)	-4(3)
C(49)	36(4)	31(4)	29(4)	-11(3)	-8(3)	-13(3)
C(56)	21(4)	88(7)	64(6)	-56(5)	-5(4)	-11(4)
C(48)	38(4)	24(3)	19(3)	-9(3)	1(3)	-11(3)
C(20)	17(3)	28(3)	20(3)	-14(3)	3(3)	-3(3)
C(2)	38(4)	31(4)	17(3)	-6(3)	-9(3)	-14(3)
C(6)	21(3)	42(4)	41(4)	-23(3)	-1(3)	-2(3)
C(13)	38(4)	37(4)	34(4)	-14(3)	-8(3)	-16(3)
C(1)	38(4)	30(4)	26(3)	-15(3)	-5(3)	-13(3)
C(51)	18(3)	38(4)	32(4)	-25(3)	3(3)	-8(3)
C(31)	42(4)	38(4)	29(4)	-20(3)	4(3)	-10(3)
C(5)	21(3)	46(4)	33(4)	-22(3)	-3(3)	0(3)
C(7)	23(3)	41(4)	29(4)	-23(3)	2(3)	-2(3)
C(14)	25(3)	40(4)	27(3)	-12(3)	-8(3)	-11(3)
C(39)	19(3)	39(4)	24(3)	-11(3)	4(3)	-13(3)
C(28)	39(4)	26(4)	38(4)	-13(3)	-10(3)	-8(3)
C(46)	52(5)	29(4)	57(5)	-19(4)	-16(4)	-11(4)
C(15)	32(4)	27(3)	30(4)	-12(3)	-9(3)	-11(3)
C(8)	18(3)	32(4)	27(3)	-15(3)	5(3)	-10(3)
C(43)	46(5)	31(4)	58(5)	-18(4)	-8(4)	-4(4)
C(4)	28(4)	29(4)	23(3)	-10(3)	-2(3)	-9(3)
C(12)	28(4)	40(4)	35(4)	-17(3)	-4(3)	-19(3)
C(47)	34(4)	22(3)	25(3)	-8(3)	-4(3)	-9(3)
C(41)	24(3)	36(4)	23(3)	-9(3)	-3(3)	-17(3)
C(10)	39(4)	45(4)	25(3)	-20(3)	0(3)	-17(3)
C(24)	39(4)	21(3)	50(5)	-9(3)	-19(4)	-4(3)
C(52)	28(4)	46(4)	35(4)	-20(3)	0(3)	-12(3)
C(53)	36(4)	47(5)	55(5)	-24(4)	-4(4)	-17(4)
C(57)	53(5)	36(4)	35(4)	-17(3)	-7(4)	-14(4)
C(29)	51(5)	40(4)	45(5)	-25(4)	3(4)	-6(4)

Table 5.18 Continued:

C(27)	56(5)	31(4)	52(5)	-28(4)	-5(4)	-5(4)
C(26)	36(4)	41(4)	30(4)	-9(3)	-13(3)	-10(3)
C(59)	50(5)	42(5)	48(5)	-9(4)	-13(4)	-16(4)
C(45)	47(5)	40(4)	42(4)	-15(4)	-2(4)	-17(4)
C(18)	19(3)	33(4)	16(3)	-15(3)	4(2)	-11(3)
C(54)	24(4)	75(6)	48(5)	-33(5)	-9(4)	-1(4)
C(58)	53(5)	40(5)	57(5)	-16(4)	-3(4)	-7(4)
C(42)	57(5)	23(4)	40(4)	-13(3)	-1(4)	-1(4)
C(9)	32(4)	41(4)	24(3)	-25(3)	6(3)	-15(3)
C(55)	32(4)	62(6)	83(6)	-50(5)	-5(4)	-19(4)
Gd(1)	21(1)	27(1)	19(1)	-12(1)	0(1)	-7(1)
N(3)	24(3)	31(3)	24(3)	-16(2)	-1(2)	-8(2)
N(4)	21(3)	32(3)	23(3)	-16(2)	-1(2)	-6(2)
N(5)	22(3)	29(3)	28(3)	-16(2)	-5(2)	-8(2)
N(2)	17(3)	30(3)	22(3)	-14(2)	-3(2)	-4(2)
N(1)	20(3)	29(3)	26(3)	-15(2)	-4(2)	-6(2)
O(1)	22(2)	28(2)	25(2)	-12(2)	1(2)	-9(2)
O(2)	22(2)	32(2)	22(2)	-18(2)	5(2)	-11(2)
O(3)	26(2)	30(2)	20(2)	-15(2)	5(2)	-11(2)
O(4)	26(2)	33(3)	25(2)	-18(2)	5(2)	-12(2)
O(5)	26(2)	24(2)	27(2)	-14(2)	1(2)	-3(2)
O(6)	19(2)	31(2)	31(2)	-19(2)	-5(2)	-5(2)
O(7)	65(4)	45(3)	60(4)	-18(3)	-13(3)	-21(3)

X-ray Experimental for $(C_{11}H_9N_5)(C_8H_4O_2F_3S)_3Gd$ (5.13): Crystals grew as yellow rhomboidal shaped colorless prisms by slow evaporation from acetone. The data crystal had approximate dimensions 0.16 x 0.09 x 0.05 mm. A total of 754 frames of data were collected using ω-scans with a scan range of 0.5° and a counting time of 45 seconds per frame. Data reduction were performed using the Rigaku Americas Corporation's Crystal Clear version 1.40.[39] The structure was solved by direct methods using SIR2004[40] and refined by full-matrix least-squares on F2 with anisotropic displacement parameters for the non-H atoms using SHELXL-2016/6.[33] Structure analysis was aided by use of the programs PLATON98[34] and WinGX.[35] The hydrogen atoms on carbon

were calculated in ideal positions with isotropic displacement parameters set to 1.2 x Ueq of the attached atoms.

Two of the three thiophene groups were disordered. The disorder was typical for terminal thiophene rings and resulted from an approximate 180º rotation about the C-C bond to the ring. The disorder was modeled in the same manner for both rings. The site occupancy for the atoms of one component of the disordered group was assigned to the variable x. The site occupancy factors for the alternate component was assigned to (1 – x). A common isotropic displacement parameter was refined while refining x. The geometry of the two components were restrained to be equivalent to that of the thiophene ring that didn't show signs of disorder. When the value for x converged, the site occupancy factors were fixed and refinement continued by refining the displacement parameters.

The function, $\Sigma w(|F_o|^2 - |F_c|^2)^2$, was minimized, where $w = 1/[(\sigma(F_o))^2 + (3.775*P)]$ and $P = (|F_o|^2 + 2|F_c|^2)/3$. $R_w(F^2)$ refined to 0.0742, with R(F) equal to 0.0338 and a goodness of fit, S, = 1.09. Definitions used for calculating R(F), $R_w(F^2)$ and the goodness of fit, S, are given below.[36] The data were checked for secondary extinction effects but no correction was necessary. Neutral atom scattering factors and values used to calculate the linear absorption coefficient are from the International Tables for X-ray Crystallography (1992).[37] All figures were generated using SHELXTL/PC.[38]

Table 5.19: Crystal data and structure refinement for **5.13**.

Empirical formula	$C_{35}H_{21}F_9GdN_5O_6S_3$	
Formula weight	1032.00	
Temperature	100(2) K	
Wavelength	0.71075 Å	
Crystal system	triclinic	
Space group	P -1	
Unit cell dimensions	a = 9.8957(6) Å	α = 74.826(3)°
	b = 10.4178(7) Å	β = 80.674(2)°
	c = 19.2714(11) Å	γ = 89.352(2)°
Volume	1891.1(2) $Å^3$	
Z	2	
Density (calculated)	1.812 Mg/m^3	
Absorption coefficient	2.017 mm^{-1}	
F(000)	1014	
Crystal size	0.16 x 0.09 x 0.05 mm^3	
θ range for data collection	3.000 to 27.479°.	
Index ranges	-10<=h<=12, -13<=k<=13, -17<=l<=25	
Reflections collected	16481	
Independent reflections	8655 [R(int) = 0.0355]	
Completeness to θ = 25.242°	99.8 %	
Absorption correction	Semi-empirical from equivalents	
Max. and min. transmission	1.00 and 0.758	
Refinement method	Full-matrix least-squares on F^2	
Data / restraints / parameters	8655 / 642 / 596	
Goodness-of-fit on F^2	1.089	
Final R indices [I>2σ(I)]	R1 = 0.0338, wR2 = 0.0725	
R indices (all data)	R1 = 0.0382, wR2 = 0.0742	
Extinction coefficient	n/a	
Largest diff. peak and hole	0.841 and -1.264 e.$Å^{-3}$	

Table 5.20: Atomic coordinates (x 10^4) and equivalent isotropic displacement parameters ($Å^2$ x 10^3) for **5.13**. U(eq) is defined as one third of the trace of the orthogonalized U^{ij} tensor.

	x	y	z	U(eq)
C1	6606(4)	6149(4)	5933(2)	28(1)
C2	5455(4)	6329(4)	5579(2)	36(1)
C3	4380(4)	6424(4)	6101(2)	34(1)

Table 5.20 Continued:

C4	4177(3)	6330(3)	7425(2)	23(1)
C5	2757(4)	6348(4)	7563(2)	31(1)
C6	2143(4)	6406(4)	8249(2)	34(1)
C7	2943(4)	6438(4)	8774(2)	30(1)
C8	4350(3)	6408(3)	8573(2)	22(1)
C9	4961(4)	6614(4)	9756(2)	31(1)
C10	6184(4)	6653(4)	9993(2)	32(1)
C11	7183(4)	6507(4)	9418(2)	28(1)
C12	10442(4)	3708(4)	6223(2)	36(1)
C13	9937(3)	5007(3)	6390(2)	23(1)
C14	10589(3)	6178(3)	5963(2)	24(1)
C15	10192(3)	7435(3)	6079(2)	22(1)
S1	12237(1)	8707(1)	4910(1)	28(1)
C16	10982(4)	8663(4)	5642(2)	19(1)
C17	10831(6)	9883(7)	5770(3)	33(2)
C18	11732(5)	10885(5)	5278(3)	30(1)
C19	12553(4)	10377(4)	4779(2)	28(1)
S1A	10711(11)	9993(13)	5895(6)	27
C16A	11090(20)	8480(14)	5735(12)	27
C17A	12130(20)	8590(20)	5161(11)	27
C18A	12640(20)	9920(20)	4842(11)	27
C19A	11960(20)	10774(18)	5189(12)	27
C20	10279(4)	9492(4)	8143(2)	30(1)
C21	9085(3)	8971(3)	7864(2)	21(1)
C22	8215(3)	9907(3)	7547(2)	23(1)
C23	7085(3)	9568(3)	7258(2)	19(1)
C24	6172(3)	10619(3)	6948(2)	20(1)
C25	6303(4)	11990(3)	6785(2)	28(1)
C26	5164(4)	12610(4)	6484(2)	38(1)
C27	4228(4)	11718(4)	6430(2)	39(1)
C28	10135(4)	3241(4)	9166(2)	34(1)
C29	8935(3)	3685(4)	8750(2)	23(1)
C30	7918(4)	2742(3)	8828(2)	25(1)
C31	6755(3)	3027(3)	8471(2)	21(1)
S3	4233(2)	2429(2)	8262(1)	31(1)
C32	5702(7)	1975(6)	8602(5)	24(1)
C33	5631(10)	671(8)	8994(5)	41(2)
C34	4350(9)	25(8)	9018(5)	49(2)
C35	3507(8)	872(7)	8642(5)	40(2)
S3A	5713(6)	367(5)	9066(3)	33(1)
C32A	5643(16)	2012(10)	8619(11)	28(3)

Table 5.20 Continued:

C33A	4442(17)	2283(14)	8357(9)	37(3)
C34A	3545(14)	1147(16)	8516(10)	38(2)
C35A	4111(13)	47(14)	8896(10)	41(2)
F1	9499(3)	3136(3)	5965(2)	73(1)
F2	10709(4)	2832(3)	6800(2)	78(1)
F3	11584(3)	3868(2)	5723(1)	48(1)
F4	11471(2)	9425(3)	7712(1)	45(1)
F5	10411(3)	8752(3)	8806(1)	47(1)
F6	10185(3)	10755(2)	8181(2)	45(1)
F7	11319(2)	3412(3)	8712(2)	56(1)
F8	10219(3)	3982(3)	9627(2)	62(1)
F9	10057(3)	1972(2)	9546(1)	49(1)
Gd1	7705(1)	6251(1)	7588(1)	14(1)
N1	6263(3)	6137(3)	6627(2)	22(1)
N2	4887(3)	6297(3)	6732(2)	22(1)
N3	4968(3)	6343(3)	7919(1)	19(1)
N4	5244(3)	6461(3)	9069(2)	22(1)
N5	6614(3)	6389(3)	8854(2)	23(1)
O1	8939(2)	4826(2)	6907(1)	25(1)
O2	9200(2)	7562(2)	6546(1)	24(1)
O3	9085(2)	7732(2)	7957(1)	22(1)
O4	6768(2)	8399(2)	7260(1)	21(1)
O5	9047(2)	4894(2)	8389(1)	22(1)
O6	6561(2)	4135(2)	8058(1)	23(1)
S2	4682(1)	10111(1)	6731(1)	32(1)

Table 5.21: Bond lengths [Å] and angles [°] for **5.13**.

C1-N1	1.323(4)	C1-H1	0.95
C1-C2	1.407(5)	C2-C3	1.363(6)

Table 5.21 Continued:

C2-H2	0.95	C5-C6	1.379(5)
C3-N2	1.364(4)	C5-H5	0.95
C3-H3	0.95	C6-C7	1.388(5)
C4-N3	1.330(4)	C6-H6	0.95
C4-C5	1.387(5)	C7-C8	1.386(5)
C4-N2	1.413(4)	C7-H7	0.95

Table 5.21 Continued:

C8-N3	1.327(4)	C12-F2	1.302(5)
C8-N4	1.414(4)	C12-F1	1.339(5)
C9-N4	1.360(4)	C12-F3	1.342(4)
C9-C10	1.365(5)	C12-C13	1.532(5)
C9-H9	0.95	C13-O1	1.261(4)
C10-C11	1.399(5)	C13-C14	1.379(5)
C10-H10	0.95	C14-C15	1.425(5)
C11-N5	1.335(4)	C14-H14	0.95
C11-H11	0.95	C15-O2	1.251(4)
C15-C16A	1.367(18)	C22-H22	0.95
C15-C16	1.484(5)	C23-O4	1.260(4)
S1-C16	1.713(4)	C23-C24	1.477(4)
S1-C19	1.716(4)	C24-C25	1.382(4)
C16-C17	1.359(6)	C24-S2	1.722(3)
C17-C18	1.419(7)	C25-C26	1.423(5)
C17-H17	0.95	C25-H25	0.95
C18-C19	1.368(5)	C26-C27	1.355(5)
C18-H18	0.95	C26-H26	0.95
C19-H19	0.95	C27-S2	1.704(4)
S1A-C16A	1.709(9)	C27-H27	0.95
S1A-C19A	1.713(8)	C28-F7	1.326(5)
C16A-C17A	1.368(9)	C28-F9	1.330(4)
C17A-C18A	1.424(9)	C28-F8	1.332(5)
C17A-H17A	0.95	C28-C29	1.538(5)
C18A-C19A	1.358(8)	C29-O5	1.266(4)
C18A-H18A	0.95	C29-C30	1.377(5)
C19A-H19A	0.95	C30-C31	1.424(5)
C20-F5	1.334(4)	C30-H30	0.95
C20-F6	1.338(4)	C31-O6	1.252(4)
C20-F4	1.341(4)	C31-C32	1.464(7)
C20-C21	1.534(4)	C31-C32A	1.475(12)
C21-O3	1.256(4)	S3-C32	1.703(6)
C21-C22	1.380(5)	S3-C35	1.708(6)
C22-C23	1.414(4)	C32-C33	1.367(7)
C33-C34	1.431(8)	S3A-C35A	1.722(8)
C33-H33	0.95	C32A-C33A	1.364(9)
C34-C35	1.357(7)	C33A-C34A	1.424(9)
C34-H34	0.95	C33A-H33A	0.95
C35-H35	0.95	C34A-C35A	1.358(8)
S3A-C32A	1.711(9)	C34A-H34A	0.95

Table 5.21 Continued:

C35A-H35A	0.95	Gd1-O1	2.424(2)
Gd1-O5	2.372(2)	Gd1-N1	2.540(3)
Gd1-O6	2.375(2)	Gd1-N5	2.544(3)
Gd1-O4	2.381(2)	Gd1-N3	2.687(3)
Gd1-O3	2.385(2)	N1-N2	1.358(4)
Gd1-O2	2.395(2)	N4-N5	1.359(4)
N1-C1-C2	111.1(3)	C2-C1-H1	124.4
N1-C1-H1	124.4	C3-C2-C1	105.2(3)
C3-C2-H2	127.4	C11-C10-H10	127.3
C1-C2-H2	127.4	N5-C11-C10	111.1(3)
N2-C3-C2	107.2(3)	N5-C11-H11	124.4
N2-C3-H3	126.4	C10-C11-H11	124.4
C2-C3-H3	126.4	F2-C12-F1	106.4(4)
N3-C4-C5	123.7(3)	F2-C12-F3	106.5(3)
N3-C4-N2	115.0(3)	F1-C12-F3	106.2(3)
C5-C4-N2	121.3(3)	F2-C12-C13	112.4(3)
C6-C5-C4	117.7(3)	F1-C12-C13	111.3(3)
C6-C5-H5	121.1	F3-C12-C13	113.6(3)
C4-C5-H5	121.1	O1-C13-C14	129.6(3)
C5-C6-C7	119.9(3)	O1-C13-C12	112.8(3)
C5-C6-H6	120.0	C14-C13-C12	117.6(3)
C7-C6-H6	120.0	C13-C14-C15	121.5(3)
C8-C7-C6	117.2(3)	C13-C14-H14	119.2
C8-C7-H7	121.4	C15-C14-H14	119.2
C6-C7-H7	121.4	O2-C15-C16A	120.4(8)
N3-C8-C7	124.2(3)	O2-C15-C14	122.9(3)
N3-C8-N4	114.9(3)	C16A-C15-C14	115.9(8)
C7-C8-N4	121.0(3)	O2-C15-C16	117.2(3)
N4-C9-C10	107.1(3)	C14-C15-C16	119.9(3)
N4-C9-H9	126.5	C16-S1-C19	91.60(19)
C10-C9-H9	126.5	C17-C16-C15	125.3(4)
C9-C10-C11	105.5(3)	C17-C16-S1	111.2(3)
C9-C10-H10	127.3	C15-C16-S1	123.5(3)
C16-C17-C18	113.8(4)	C18-C19-H19	123.8
C16-C17-H17	123.1	S1-C19-H19	123.8
C18-C17-H17	123.1	C16A-S1A-C19A	91.4(6)
C19-C18-C17	111.0(4)	C15-C16A-C17A	129.2(13)
C19-C18-H18	124.5	C15-C16A-S1A	117.9(12)
C17-C18-H18	124.5	C17A-C16A-S1A	111.6(7)
C18-C19-S1	112.4(3)	C16A-C17A-C18A	113.0(9)

Table 5.21 Continued:

C16A-C17A-H17A	123.5	F5-C20-F6	107.0(3)
C18A-C17A-H17A	123.5	F5-C20-F4	106.0(3)
C19A-C18A-C17A	111.2(9)	F6-C20-F4	106.4(3)
C19A-C18A-H18A	124.4	F5-C20-C21	111.3(3)
C17A-C18A-H18A	124.4	F6-C20-C21	114.8(3)
C18A-C19A-S1A	112.9(8)	F4-C20-C21	110.8(3)
C18A-C19A-H19A	123.6	O3-C21-C22	130.6(3)
S1A-C19A-H19A	123.6	O3-C21-C20	112.7(3)
C22-C21-C20	116.7(3)	O5-C29-C30	130.1(3)
C21-C22-C23	122.6(3)	O5-C29-C28	113.1(3)
C21-C22-H22	118.7	C30-C29-C28	116.8(3)
C23-C22-H22	118.7	C29-C30-C31	122.2(3)
O4-C23-C22	124.2(3)	C29-C30-H30	118.9
O4-C23-C24	116.2(3)	C31-C30-H30	118.9
C22-C23-C24	119.6(3)	O6-C31-C30	124.0(3)
C25-C24-C23	131.1(3)	O6-C31-C32	117.5(4)
C25-C24-S2	111.9(2)	C30-C31-C32	118.6(4)
C23-C24-S2	117.1(2)	O6-C31-C32A	115.9(6)
C24-C25-C26	111.4(3)	C30-C31-C32A	120.0(6)
C24-C25-H25	124.3	C32-S3-C35	91.8(3)
C26-C25-H25	124.3	C33-C32-C31	131.7(6)
C27-C26-C25	112.6(3)	C33-C32-S3	111.6(5)
C27-C26-H26	123.7	C31-C32-S3	116.6(4)
C25-C26-H26	123.7	C32-C33-C34	112.6(7)
C26-C27-S2	113.0(3)	C32-C33-H33	123.7
C26-C27-H27	123.5	C34-C33-H33	123.7
S2-C27-H27	123.5	C35-C34-C33	111.3(6)
F7-C28-F9	106.4(3)	C35-C34-H34	124.4
F7-C28-F8	106.8(4)	C33-C34-H34	124.4
F9-C28-F8	107.7(3)	C34-C35-S3	112.7(5)
F7-C28-C29	111.0(3)	C34-C35-H35	123.7
F9-C28-C29	114.7(3)	S3-C35-H35	123.7
F8-C28-C29	109.9(3)	C32A-S3A-C35A	91.1(5)
C33A-C32A-C31	122.3(10)	C35A-C34A-H34A	124.5
C33A-C32A-S3A	111.6(7)	C33A-C34A-H34A	124.5
C31-C32A-S3A	126.0(9)	C34A-C35A-S3A	113.0(8)
C32A-C33A-C34A	113.5(8)	C34A-C35A-H35A	123.5
C32A-C33A-H33A	123.3	S3A-C35A-H35A	123.5
C34A-C33A-H33A	123.3	O5-Gd1-O6	72.61(8)
C35A-C34A-C33A	110.9(9)	O5-Gd1-O4	143.70(8)

Table 5.21 Continued:

O6-Gd1-O4	129.36(8)	O5-Gd1-O1	74.23(8)
O5-Gd1-O3	73.71(8)	O6-Gd1-O1	74.77(8)
O6-Gd1-O3	139.85(8)	O4-Gd1-O1	134.29(8)
O4-Gd1-O3	72.88(8)	O3-Gd1-O1	115.76(8)
O5-Gd1-O2	108.86(8)	O2-Gd1-O1	69.76(8)
O6-Gd1-O2	142.18(8)	O5-Gd1-N1	141.00(8)
O4-Gd1-O2	72.41(8)	O6-Gd1-N1	76.52(8)
O3-Gd1-O2	70.40(8)	O4-Gd1-N1	75.16(8)
O3-Gd1-N1	142.71(8)	N2-N1-Gd1	121.9(2)
O2-Gd1-N1	82.06(9)	N1-N2-C3	110.9(3)
O1-Gd1-N1	75.12(9)	N1-N2-C4	120.5(3)
O5-Gd1-N5	75.01(8)	C3-N2-C4	128.6(3)
O6-Gd1-N5	78.90(9)	C8-N3-C4	117.4(3)
O4-Gd1-N5	81.42(9)	C8-N3-Gd1	122.0(2)
O3-Gd1-N5	71.80(9)	C4-N3-Gd1	120.7(2)
O2-Gd1-N5	138.80(9)	N5-N4-C9	111.2(3)
O1-Gd1-N5	144.19(9)	N5-N4-C8	118.8(3)
N1-Gd1-N5	121.56(9)	C9-N4-C8	129.9(3)
O5-Gd1-N3	122.67(8)	C11-N5-N4	105.1(3)
O6-Gd1-N3	65.55(8)	C11-N5-Gd1	130.7(2)
O4-Gd1-N3	64.13(8)	N4-N5-Gd1	124.0(2)
O3-Gd1-N3	118.32(8)	C13-O1-Gd1	134.3(2)
O2-Gd1-N3	128.29(8)	C15-O2-Gd1	140.3(2)
O1-Gd1-N3	125.90(8)	C21-O3-Gd1	132.2(2)
N1-Gd1-N3	61.33(9)	C23-O4-Gd1	137.1(2)
N5-Gd1-N3	60.25(8)	C29-O5-Gd1	133.0(2)
C1-N1-N2	105.6(3)	C31-O6-Gd1	138.0(2)
C1-N1-Gd1	131.6(2)	C27-S2-C24	91.17(18)

Table 5.22: Anisotropic displacement parameters ($Å^2$ x 10^3) for **5.13**. The anisotropic displacement factor exponent takes the form: $-2\pi^2[h^2 a^{*2} U^{11} + ... + 2 h k a^* b^* U^{12}]$.

	U11	U22	U33	U23	U13	U12
C1	33(2)	29(2)	22(2)	-6(1)	-6(1)	-4(2)
C2	44(2)	43(2)	24(2)	-7(2)	-16(2)	-5(2)

Table 5.22 Continued:

C3	35(2)	39(2)	32(2)	-4(2)	-22(2)	-1(2)
C4	20(2)	20(2)	27(2)	-2(1)	-7(1)	1(1)
C5	17(2)	37(2)	40(2)	-7(2)	-12(2)	1(1)
C6	11(2)	39(2)	49(2)	-7(2)	-6(2)	1(1)
C7	15(2)	37(2)	33(2)	-4(2)	2(1)	2(1)
C8	13(2)	23(2)	28(2)	-3(1)	-4(1)	2(1)
C9	29(2)	39(2)	22(2)	-9(2)	4(1)	7(2)
C10	32(2)	46(2)	20(2)	-12(2)	-4(2)	4(2)
C11	23(2)	43(2)	16(2)	-7(2)	-5(1)	5(2)
C12	36(2)	32(2)	36(2)	-13(2)	7(2)	2(2)
C13	19(2)	24(2)	27(2)	-10(1)	-4(1)	2(1)
C14	20(2)	28(2)	24(2)	-10(1)	1(1)	1(1)
C15	22(2)	27(2)	16(2)	-6(1)	-4(1)	0(1)
S1	28(1)	25(1)	25(1)	-4(1)	7(1)	-1(1)
C16	19(2)	23(2)	14(2)	-3(2)	-2(2)	5(2)
C17	40(3)	32(3)	24(3)	-7(2)	5(2)	-7(2)
C18	40(3)	24(2)	25(2)	-11(2)	3(2)	-1(2)
C19	29(2)	18(2)	33(2)	-2(2)	3(2)	-5(2)
C20	23(2)	35(2)	37(2)	-16(2)	-11(2)	-1(2)
C21	13(2)	31(2)	20(2)	-11(1)	0(1)	-2(1)
C22	20(2)	24(2)	25(2)	-10(1)	-3(1)	-1(1)
C23	15(2)	22(2)	18(2)	-4(1)	2(1)	1(1)
C24	17(2)	24(2)	19(2)	-5(1)	-1(1)	3(1)
C25	34(2)	31(2)	21(2)	-9(1)	-3(1)	8(2)
C26	46(2)	30(2)	36(2)	-5(2)	-9(2)	12(2)
C27	37(2)	40(2)	42(2)	-8(2)	-18(2)	18(2)
C28	33(2)	33(2)	41(2)	-8(2)	-20(2)	9(2)
C29	20(2)	31(2)	19(2)	-6(1)	-6(1)	9(1)
C30	26(2)	23(2)	22(2)	0(1)	-5(1)	7(1)
C31	21(2)	21(2)	18(2)	-6(1)	2(1)	3(1)
S3	21(1)	42(1)	34(1)	-18(1)	-6(1)	-2(1)
C32	26(3)	27(2)	22(2)	-11(2)	-2(2)	0(2)
C33	38(3)	33(4)	51(3)	-10(3)	-8(3)	-2(3)
C34	51(3)	34(3)	60(4)	-6(3)	-11(3)	-10(3)
C35	38(3)	37(3)	50(3)	-16(3)	-9(2)	-17(2)
S3A	34(2)	20(2)	41(2)	-4(1)	-3(1)	0(1)
C32A	28(4)	28(4)	31(4)	-11(4)	-2(4)	0(4)
C33A	36(4)	37(4)	38(4)	-14(4)	-3(4)	-8(4)
C34A	36(4)	34(4)	45(4)	-11(4)	-7(4)	-8(4)
C35A	42(4)	32(4)	49(4)	-10(4)	-11(4)	-7(4)
F1	52(2)	69(2)	118(3)	-72(2)	7(2)	-12(2)

Table 5.22 Continued:

F2	112(3)	45(2)	57(2)	5(1)	14(2)	43(2)
F3	44(2)	33(1)	61(2)	-22(1)	23(1)	1(1)
F4	19(1)	59(2)	61(2)	-25(1)	-4(1)	-9(1)
F5	54(2)	54(2)	39(1)	-10(1)	-29(1)	-5(1)
F6	43(2)	37(1)	72(2)	-31(1)	-31(1)	4(1)
F7	19(1)	58(2)	85(2)	-4(2)	-14(1)	12(1)
F8	79(2)	62(2)	68(2)	-32(2)	-56(2)	24(2)
F9	49(2)	39(1)	57(2)	5(1)	-32(1)	8(1)
Gd1	11(1)	19(1)	13(1)	-3(1)	-2(1)	1(1)
N1	21(1)	24(2)	19(1)	-2(1)	-6(1)	-1(1)
N2	19(1)	24(2)	26(2)	-3(1)	-12(1)	1(1)
N3	14(1)	22(1)	21(1)	-2(1)	-4(1)	-1(1)
N4	15(1)	31(2)	20(1)	-4(1)	0(1)	3(1)
N5	16(1)	36(2)	16(1)	-6(1)	0(1)	1(1)
O1	26(1)	24(1)	24(1)	-6(1)	0(1)	1(1)
O2	25(1)	22(1)	21(1)	-5(1)	5(1)	0(1)
O3	16(1)	27(1)	24(1)	-8(1)	-5(1)	-1(1)
O4	17(1)	21(1)	25(1)	-5(1)	-5(1)	1(1)
O5	17(1)	25(1)	23(1)	-4(1)	-6(1)	1(1)
O6	18(1)	25(1)	23(1)	1(1)	-5(1)	-2(1)
S2	23(1)	33(1)	39(1)	-6(1)	-12(1)	5(1)

Table 5.23: Hydrogen coordinates (x 10^4) and isotropic displacement parameters ($Å^2$ x 10^3) for **5.13**.

	x	y	z	U(eq)		x	y	z	U(eq)
H1	7511	6049	5704	33	H2	5432	6375	5082	43
H3	3452	6553	6038	41	H19A	12153	11706	5055	32
H5	2227	6322	7198	38	H22	8383	10816	7522	27
H6	1174	6425	8363	40	H25	7058	12458	6863	34
H7	2543	6479	9250	36	H26	5070	13547	6338	45
H9	4079	6682	10022	37	H27	3403	11964	6243	47
H10	6327	6758	10451	39	H30	7994	1872	9130	30
H11	8139	6493	9428	33	H33	6354	241	9225	49
H14	11321	6146	5583	29	H34	4119	-880	9264	59
H17	10180	10050	6154	40	H35	2611	626	8596	48
H18	11762	11788	5294	36	H33A	4224	3145	8094	44
H19	13223	10891	4402	34	H34A	2668	1157	8374	46
H17A	12483	7851	4994	32	H35A	3671	-809	9052	49
H18A	13363	10180	4438	32					

Table 5.24: Torsion angles [°] for **5.13**.

N1-C1-C2-C3	-0.2(5)	C12-C13-C14-C15	-179.9(3)
C1-C2-C3-N2	-0.3(4)	C13-C14-C15-O2	-3.3(5)
N3-C4-C5-C6	1.2(6)	C13-C14-C15-C16A	166.2(13)
N2-C4-C5-C6	-178.8(3)	C13-C14-C15-C16	175.7(3)
C4-C5-C6-C7	-0.3(6)	O2-C15-C16-C17	9.0(4)
C5-C6-C7-C8	0.0(6)	C14-C15-C16-C17	-170.0(3)
C6-C7-C8-N3	-0.4(6)	O2-C15-C16-S1	-172.1(3)
C6-C7-C8-N4	178.8(3)	C14-C15-C16-S1	8.9(5)
N4-C9-C10-C11	-0.4(4)	C19-S1-C16-C17	-0.06(14)
C9-C10-C11-N5	0.3(5)	C19-S1-C16-C15	-179.1(4)
F2-C12-C13-O1	-53.0(5)	C15-C16-C17-C18	178.9(4)
F1-C12-C13-O1	66.2(4)	S1-C16-C17-C18	-0.12(19)
F3-C12-C13-O1	-173.9(3)	C16-C17-C18-C19	0.3(3)
F2-C12-C13-C14	128.2(4)	C17-C18-C19-S1	-0.3(4)
F1-C12-C13-C14	-112.5(4)	C16-S1-C19-C18	0.2(3)
F3-C12-C13-C14	7.3(5)	O2-C15-C16A-C17A	-172.1(11)
O1-C13-C14-C15	1.5(6)	C14-C15-C16A-C17A	18(2)

Table 5.24 Continued:

O2-C15-C16A-S1A	-7(2)	C16A-C17A-C18A-C19A	0.1(4)
C14-C15-C16A-S1A	-176.4(11)	C17A-C18A-C19A-S1A	-0.1(5)
C19A-S1A-C16A-C15	-168(3)	C16A-S1A-C19A-C18A	0.1(4)
C19A-S1A-C16A-C17A	-0.02(16)	F5-C20-C21-O3	-46.5(4)
C15-C16A-C17A-C18A	166(3)	F6-C20-C21-O3	-168.2(3)
S1A-C16A-C17A-C18A	0.0(2)	F4-C20-C21-O3	71.3(4)
F5-C20-C21-C22	134.6(3)	F9-C28-C29-O5	-179.4(3)
F6-C20-C21-C22	12.9(5)	F8-C28-C29-O5	59.2(4)
F4-C20-C21-C22	-107.6(4)	F7-C28-C29-C30	121.8(4)
O3-C21-C22-C23	0.5(6)	F9-C28-C29-C30	1.2(5)
C20-C21-C22-C23	179.2(3)	F8-C28-C29-C30	-120.3(4)
C21-C22-C23-O4	-0.2(5)	O5-C29-C30-C31	0.8(6)
C21-C22-C23-C24	178.1(3)	C28-C29-C30-C31	-179.8(3)
O4-C23-C24-C25	-171.3(3)	C29-C30-C31-O6	0.5(5)
C22-C23-C24-C25	10.3(5)	C29-C30-C31-C32	-178.2(5)
O4-C23-C24-S2	7.7(4)	C29-C30-C31-C32A	-175.1(10)
C22-C23-C24-S2	-170.7(2)	O6-C31-C32-C33	177.2(5)
C23-C24-C25-C26	179.4(3)	C30-C31-C32-C33	-4.0(8)
S2-C24-C25-C26	0.3(4)	O6-C31-C32-S3	-7.3(8)
C24-C25-C26-C27	0.0(5)	C30-C31-C32-S3	171.5(4)
C25-C26-C27-S2	-0.3(5)	C35-S3-C32-C33	0.03(15)
F7-C28-C29-O5	-58.7(4)	C35-S3-C32-C31	-176.3(8)
C31-C32-C33-C34	175.6(11)	C1-N1-N2-C3	-0.7(4)
S3-C32-C33-C34	0.0(2)	Gd1-N1-N2-C3	169.5(2)
C32-C33-C34-C35	0.0(4)	C1-N1-N2-C4	180.0(3)
C33-C34-C35-S3	0.1(4)	Gd1-N1-N2-C4	-9.8(4)
C32-S3-C35-C34	-0.1(3)	C2-C3-N2-N1	0.6(4)
O6-C31-C32A-C33A	-3.6(14)	C2-C3-N2-C4	179.8(3)
C30-C31-C32A-C33A	172.4(7)	N3-C4-N2-N1	7.1(4)
O6-C31-C32A-S3A	171.4(10)	C5-C4-N2-N1	-172.9(3)
C30-C31-C32A-S3A	-12.6(19)	N3-C4-N2-C3	-172.1(3)
C35A-S3A-C32A-C33A	0.01(16)	C5-C4-N2-C3	7.9(6)
C35A-S3A-C32A-C31	-175(2)	C7-C8-N3-C4	1.3(5)
C31-C32A-C33A-C34A	176(2)	N4-C8-N3-C4	-178.1(3)
S3A-C32A-C33A-C34A	0.0(2)	C7-C8-N3-Gd1	-179.1(3)
C32A-C33A-C34A-C35A	-0.1(4)	N4-C8-N3-Gd1	1.6(4)
C33A-C34A-C35A-S3A	0.1(5)	C5-C4-N3-C8	-1.7(5)
C32A-S3A-C35A-C34A	0.0(4)	N2-C4-N3-C8	178.3(3)
C2-C1-N1-N2	0.5(4)	C5-C4-N3-Gd1	178.7(3)
C2-C1-N1-Gd1	-168.3(2)	N2-C4-N3-Gd1	-1.3(4)

Table 5.24 Continued:

C10-C9-N4-N5	0.5(4)	N3-C8-N4-C9	175.4(3)
C10-C9-N4-C8	-177.6(3)	C7-C8-N4-C9	-3.9(6)
N3-C8-N4-N5	-2.5(4)	C10-C11-N5-N4	0.0(4)
C7-C8-N4-N5	178.1(3)	C10-C11-N5-Gd1	175.2(2)
C9-N4-N5-C11	-0.3(4)	C22-C23-O4-Gd1	-5.4(5)
C8-N4-N5-C11	178.1(3)	C24-C23-O4-Gd1	176.2(2)
C9-N4-N5-Gd1	-175.9(2)	C30-C29-O5-Gd1	-3.8(6)
C8-N4-N5-Gd1	2.4(4)	C28-C29-O5-Gd1	176.8(2)
C14-C13-O1-Gd1	-8.9(6)	C30-C31-O6-Gd1	1.4(5)
C12-C13-O1-Gd1	172.5(2)	C32-C31-O6-Gd1	-179.9(5)
C16A-C15-O2-Gd1	-154.8(14)	C32A-C31-O6-Gd1	177.2(10)
C14-C15-O2-Gd1	14.2(5)	C26-C27-S2-C24	0.5(4)
C16-C15-O2-Gd1	-164.8(3)	C25-C24-S2-C27	-0.4(3)
C22-C21-O3-Gd1	4.4(5)	C23-C24-S2-C27	-179.7(3)
C20-C21-O3-Gd1	-174.3(2)		

CHAPTER NOTES AND REFERENCES

(1) Cotton, S. A.; Raithby, P. R. *Coord. Chem. Rev.* **2017**, *340*, 220–231.

(2) Bünzli, J.-C. G. *J. Coord. Chem.* **2014**, *67* (23/24), 3706–3733.

(3) Yang; Jones, R. A. *J. Am. Chem. Soc.* **2005**, *127* (21), 7686–7687.

(4) Yang, X.-P.; Jones, R. A.; Wong, W.-K.; Lynch, V.; Oye, M. M.; Holmes, A. L. *Chem. Commun.* **2006**, No. 17, 1836–1838.

(5) Yang, X.; Rivers, J. H.; McCarty, W. J.; Wiester, M.; Jones, R. A. *New J. Chem.* **2008**, *32* (5), 790–793.

(6) Yang, X.; Schipper, D.; Jones, R. A.; Lytwak, L. A.; Holliday, B. J.; Huang, S. *J. Am. Chem. Soc.* **2013**, *135* (23), 8468–8471.

(7) Halcrow, M. A. *New J. Chem.* **2014**, *38* (5), 1868–1882.

(8) Wang, X.; Chang, H.; Xie, J.; Zhao, B.; Liu, B.; Xu, S.; Pei, W.; Ren, N.; Huang, L.; Huang, W. *Coord. Chem. Rev.* **2014**, *273–274*, 201–212.

(9) Gupta, B. K.; Haranath, D.; Saini, S.; Singh, V. N.; Shanker, V. *Nanotechnology* **2010**, *21* (5), 055607.

(10) Basak, S.; Mohiddon, M. A.; Baumgarten, M.; Müllen, K.; Chandrasekar, R. *Sci. Rep.* **2015**, *5*, 8406.

(11) Chow, C.-F. *J. Fluoresc.* **2012**, *22* (6), 1539–1546.

(12) Meruga, J. M.; Cross, W. M.; May, P. S.; Luu, Q.; Crawford, G. A.; Kellar, J. J. *Nanotechnology* **2012**, *23* (39), 395201.

(13) Binnemans, K. *Chem. Rev.* **2009**, *109* (9), 4283–4374.

(14) Wang, M.; Chen, Z.; Zheng, W.; Zhu, H.; Lu, S.; Ma, E.; Tu, D.; Zhou, S.; Huang, M.; Chen, X. *Nanoscale* **2014**, *6* (14), 8274–8282.

(15) Sessler, J. L.; Dow, W. C.; O'Connor, D.; Harriman, A.; Hemmi, G.; Mody, T. D.; Miller, R. A.; Qing, F.; Springs, S.; Woodburn, K.; Young, S. W. *J. Alloys Compd.* **1997**, *249* (1–2), 146–152.

(16) Jones, R. A.; Gnanam, A. J.; Arambula, J. F.; Jones, J. N.; Swaminathan, J.; Yang, X.; Schipper, D.; Hall, J. W.; DePue, L. J.; Dieye, Y.; Vadivelu, J.; Chandler, D. J.; Marcotte, E. M.; Sessler, J. L.; Ehrlich, L. I. R.; Brown, K. A. *Faraday Discuss.* **2015**, *175* (0), 241–255.

(17) Binnemans, K. *Coord. Chem. Rev.* **2015**, *295*, 1–45.

(18) Horrocks, W. D.; Albin, M. In *Progress in Inorganic Chemistry*; Lippard, S. J., Ed.; John Wiley & Sons, Inc.: Hoboken, NJ, USA, 1984; Vol. 31, pp 1–104.

(19) Weissman, S. I. *J. Chem. Phys.* **1942**, *10* (4), 214–217.

(20) Bünzli, J.-C. G. *Coord. Chem. Rev.* **2015**, *293–294*, 19–47.

(21) Bohnsack, A. M. Novel Multifunctional Porous Coordination Polymers from Pre-Synthetically Modified Organophosphorous Ligands. PhD Dissertation, The University of Texas at Austin: Austin, TX, 2015.

(22) Meshkova, S. B.; Topilova, Z. M.; Bolshoy, D. V.; Beltyukova, S. V.; Tsvirko, M. P.; Venchikov, V. Y. *Acta Phys. Pol. A* **1999**, *95* (6), 983–990.

(23) Ahn, H. S.; Davenport, T. C.; Tilley, T. D. *Chem. Commun.* **2014**, *50* (29), 3834–3837.

(24) Suzuki, H.; Moro-Oka, Y.; Ikawa, T.; Miyajima, T.; Tanaka, I.; Ashida, T. *Chem. Lett.* **1982**, *11* (9), 1369–1370.

(25) Wilkerson, J. M. Luminescent lanthanide-containing materials: from small molecules to conducting metallopolymers, The University of Texas at Austin: Austin, TX, 2012.

(26) Stanley, J. M.; Zhu, X.; Yang, X.; Holliday, B. J. *Inorg. Chem.* **2010**, *49* (5), 2035–2037.

(27) Jameson, D. L.; Goldsby, K. A. *J. Org. Chem.* **1990**, *55* (17), 4992–4994.

(28) Zoppellaro, G.; Baumgarten, M. *Eur. J. Org. Chem.* **2005**, *2005* (14), 2888–2892.

(29) Sager, W. F.; Filipescu, N.; Serafin, F. A. *J. Phys. Chem.* **1965**, *69* (4), 1092–1100.

(30) *FeliX32 Analysis*; Photon Technology International, 2001.

(31) *SAINT V8.27B*; Bruker AXS Inc.: Madison, WI, USA, 2012.

(32) Sheldrick, G. M. *Acta Crystallogr. Sect. A* **2015**, *71* (1), 3–8.

(33) Sheldrick, G. M. *Acta Crystallogr. Sect. C Struct. Chem.* **2015**, *71* (1), 3–8.

(34) Spek, A. L. *PLATON98*; Utrecht University: Padualaan 8, 3584 CH Utrecht, The Netherlands, 1998.

(35) Farrugia, L. J. *J. Appl. Crystallogr.* **1999**, *32* (4), 837–838.

(36) $R_w(F^2) = \{S_w(|F_o|^2 - |F_c|^2)^2/S_w(|F_o|)^4\}^{1/2}$ where w is the weight given each reflection. $R(F) = S(|F_o| - |F_c|)/S|F_o|\}$ for reflections with $F_o > 4(s(F_o))$. $S = [S_w(|F_o|^2 - |F_c|^2)^2/(n - p)]^{1/2}$, where n is the number of reflections and p is the number of refined parameters.

(37) *International Tables for X-ray Crystallography*; Kluwer Academic Press: Boston, MA, USA, 1992; Vol. C.

(38) Sheldrick, G. M. *SHELXLT/PC*; Siemens Analytical X-ray Instruments, Inc.: Madison, WI, USA, 1994.

(39) *CrystalClear*; Rigaku Americas Corporation: The Woodlands, Texas, USA, 2008.

(40) Burla, M. C.; Caliandro, R.; Camalli, M.; Carrozzini, B.; Cascarano, G. L.; De Caro, L.; Giacovazzo, C.; Polidori, G.; Spagna, R. *J. Appl. Crystallogr.* **2005**, *38* (2), 381–388.

Outlook and Future Directions

CHAPTER 2

The synthesis and characterization of the nitro- and amino-bppy derivatives described in Chapter 2 should allow for further expansion of the library of possible ligands with an even larger range of electronic and chemical environments. In addition to serving as versatile synthetic intermediates, characterization of the electronics of these ligands indicate that they offer a means of tuning energy levels and binding strengths of bppy complexes.

CHAPTER 3

The incorporation of amide spacers into a known electropolymerizable ligand has demonstrated disruption of π-conjugation between separate portions of a previously-conjugated molecule, as evidenced by crystallographic and spectroscopic analyses. Spectroscopic and electrochemical evidence gathered in these studies suggests two viable paths for the improvement of highly-emissive electropolymerizable metallopolymers: the substitution of EDOT with electropolymerizable groups which undergo oxidation at lower anodic potentials such as oligothiophene derivatives, as well as the employment of inert, rigid, aliphatic spacers such as bicyclo[2.2.2]octane derivatives to achieve conjugation interruption while avoiding incorporation of possible excited-state quenchers while avoiding the use of high-energy N–H or O–H oscillators.

CHAPTER 4

The establishment of synthetic routes to form both mono- and di-substituted terminal imino-bppy ligands allow for condensation polymerization of bppy-containing materials which avoid the use of expensive metal catalysts.

The synthesis of diazotization and CuAAC products demonstrate the feasibility of diazonium chemistry as a tool for the facile synthetic modification of bppy at the pyrazole 4-position. Additionally, these compounds open up opportunities for the incorporation of bppy in new classes of functional materials, such as azo- dyes, photoswitchable systems, surface-functionalized electronic materials and click polymers.

CHAPTER 5

The spectroscopic analysis of Tb(III), Eu(III) and Sm(III) Ln-PCM-25 materials prove that the zwitterionic framework employed may be used to sensitize Ln(III) luminescence. Though stepwise activation of these materials by evacuation at ambient and elevated temperatures gave little insight into H_2O-dependence of these materials, future studies may be directed toward determining luminescent properties of PCM-25 materials synthesized with the rest of the lanthanide series.

Although a modest number of Ln-tridecker materials were analyzed by absorption and emission spectroscopies, these investigations should be expanded to analogous tridecker complexes incorporating other Ln(III) ions.

Further work should be pursued in reproducing Ln(III) dimers bridged by diacetone-alcohol ligands so as to better understand and utilize this novel lanthanide binding motif in future Ln(III) material synthesis.

Appendix A: Polymorphs of 2-(4-nitropyrazol-1-yl)-6-(pyrazol-1-yl)pyridine

INTRODUCTION

Polymorphism has been shown to be of significant intrigue to the scientific community, especially in the area of pharmaceutical development, where it can dictate important aspects of potential drugs such as solubility, bioavailability and half-life.[1–4] Though it is postulated that there are numerous polymorphs for any given compound,[5,6] the discovery of these has also been described as a "black art."[7]

During the synthesis and subsequent purification of 2-(4-nitropyrazol-1-yl)-6-(pyrazol-1-yl)pyridine (**2.5** in Chapter 2), excellent-quality crystals of the product were obtained by evaporation from dichloromethane solvent; the resulting single-crystal structure was obtained and reported, and was observed to crystallize in the P-1 space group (form **I**).[8] Fortuitously, slow evaporation of solutions of **2.5** from acetone have yielded two additional polymorphs of this species (forms **II** and **III**), reported here.

RESULTS AND DISCUSSION

Whereas crystals of form **I** were rhombohedral in appearance, both forms **II** and **III** grew as fibrous crystals obtained from evaporation of acetone solutions. Though the growth conditions of **II** and **III** appear similar, **II** was allowed to evaporate over a time period of three days and **III** was evaporated for nine. This appears to have been a significant factor in the formation of each polymorph. Though the concentrations of each solution which resulted in forms **II** and **III** were not monitored, this may have also been a factor which gave rise to these different structures. The asymmetric units of forms **I-III** are shown in Figure A.1.

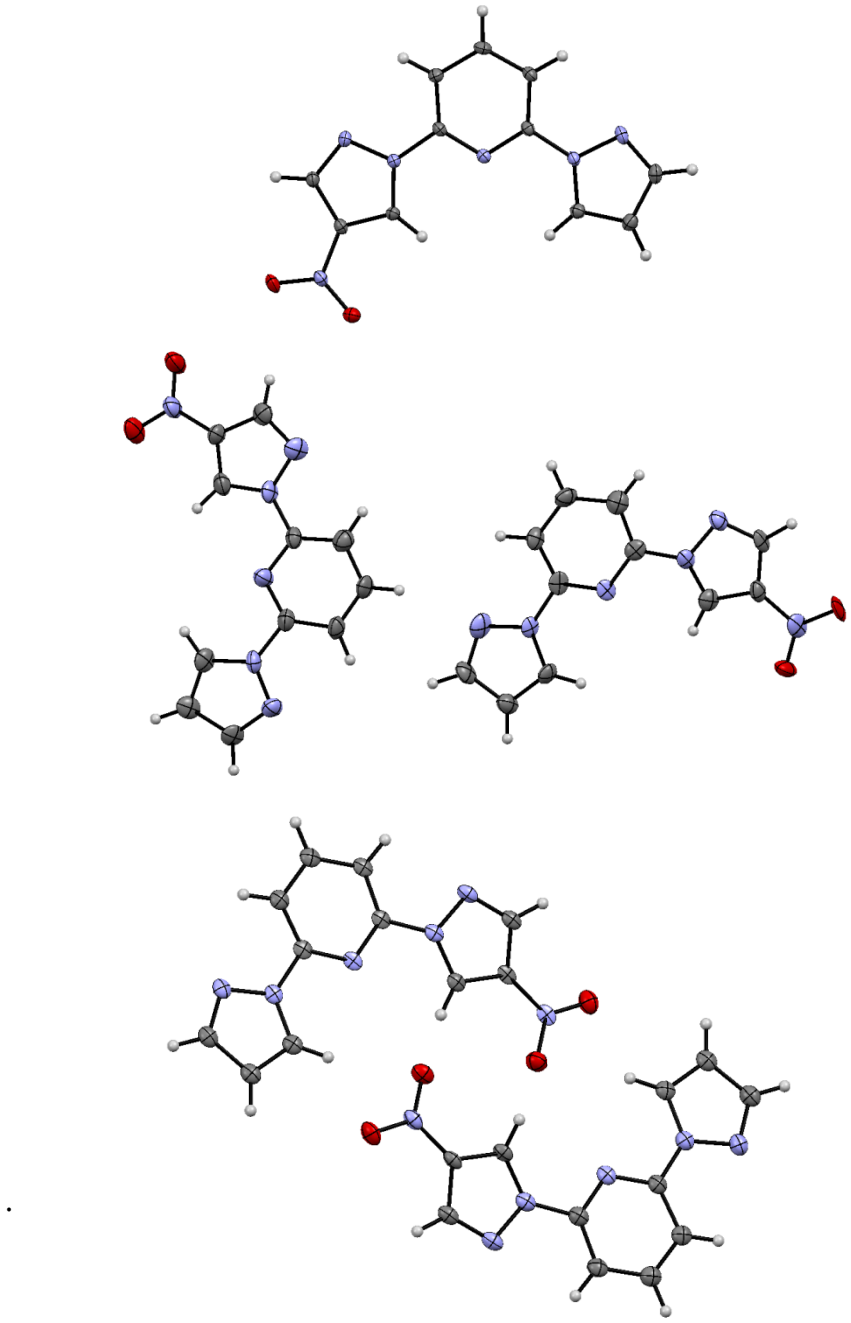

Figure A.1: Asymmetric units of **2.5** polymorphs **I** (top), **II** (middle) and **III** (bottom).

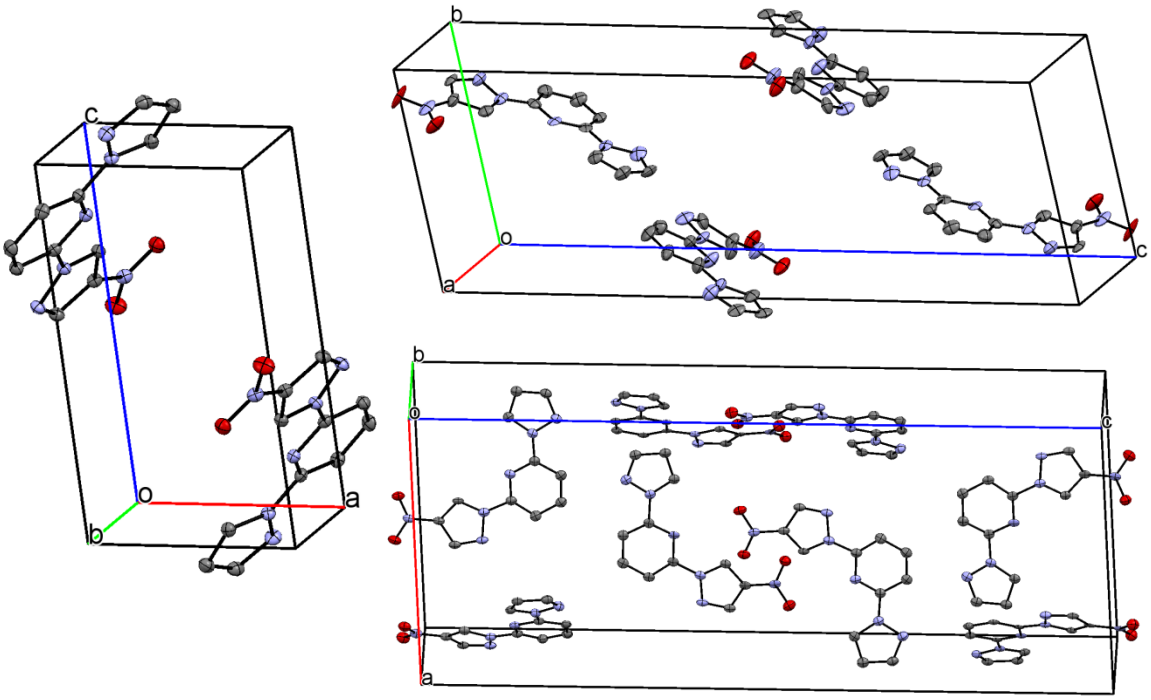

Figure A.2: Unit cells of form **I** (left), **II** (right, top) and **III** (right, bottom). H atoms are omitted for clarity.

Both forms **I** and **II** crystallize in the P-1 space group, whereas form **III** assumes the $Pna2_1$ space group. **II** and **III** both feature two molecules in the asymmetric unit, but orientations differ in both relative positioning and coplanar angles of the adjacent molecules. Unit cells of each form are shown in Figure A.2. All three unit cells exhibit face-on stacking of the molecules; form **II** and **III** differ, however, in the orientation of adjacent molecular stacks (Figure A.3). Form **II** features all molecules packing in one facial orientation with 3.801 Å between stacked molecules. The packing of form **III** features a face-to face stacking motif with 3.704 Å intermolecular stacking distances.

EXPERIMENTAL

Details regarding the synthesis of compound **2.5** and X-ray crystallography of form **I** are reported in Chapter 2. X-ray diffraction data acquisition and analysis were performed by Dr. Vincent M. Lynch.

X -ray Experimental for form II:

Crystals grew as very thin, very long, colorless needles by slow evaporation from acetone. The data crystal was cut from a larger crystal and had approximate dimensions 0.19 x 0.03 x 0.02 mm. The data were collected on an Agilent Technologies SuperNova

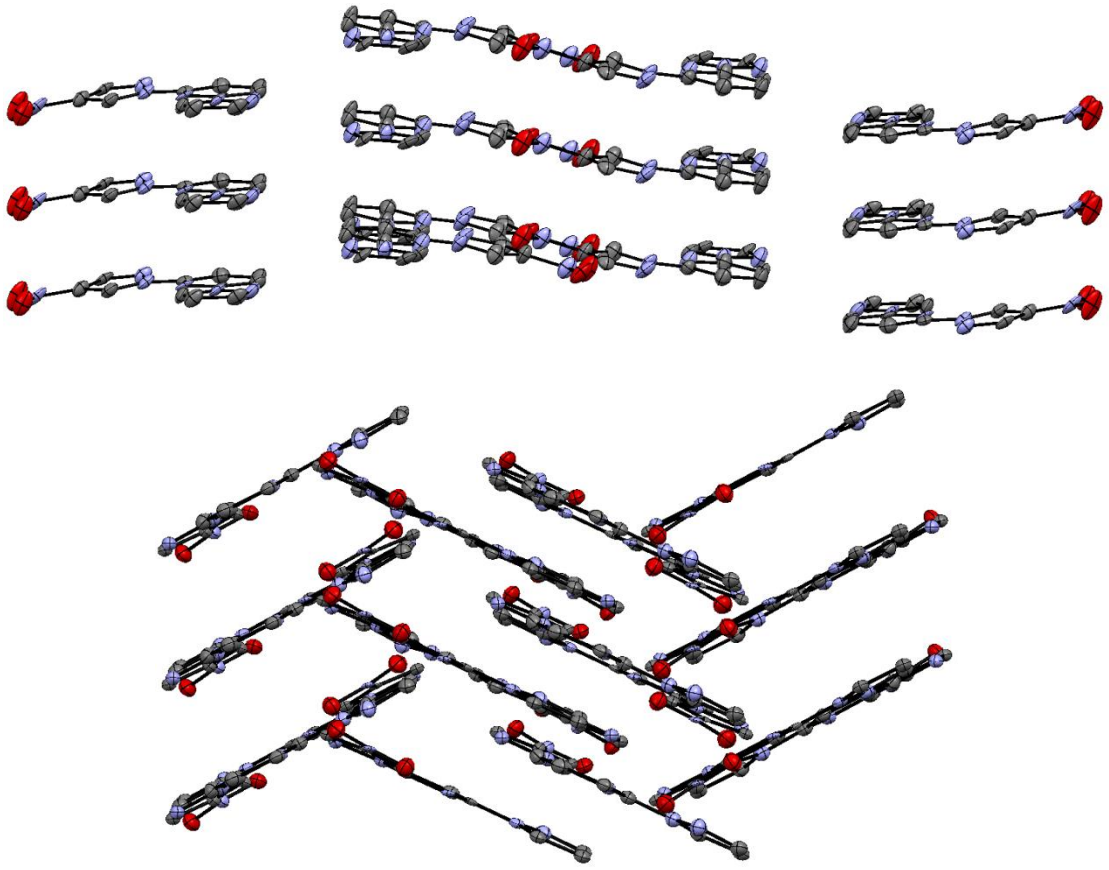

Figure A.3: Edge-on view of packing in form **II** (top) and form **III** (bottom). H atoms are omitted for clarity.

Dual Source diffractometer using a μ-focus Cu Kα radiation source (λ = 1.5418Å) with collimating mirror monochromators. A total of 720 frames of data were collected using ω-scans with a scan range of 1° and a counting time of 23 seconds per frame with a detector offset of +/- 0.0° and 8 seconds per frame with a detector offset of +/- 78.0°. The data were collected at 100 K using an Oxford 700 Cryostream low temperature device. Details of crystal data, data collection and structure refinement are listed in Table A.1. Data collection, unit cell refinement and data reduction were performed using Agilent Technologies CrysAlisPro V 1.171.38.43f.[9] The structure was solved by direct methods using SHELXT[10] and refined by full-matrix least-squares on F2 with anisotropic displacement parameters for the non-H atoms using SHELXL-2016/6.[11] Structure analysis was aided by use of the programs PLATON98[12] and WinGX.[13] The hydrogen atoms were calculated in ideal positions with isotropic displacement parameters set to 1.2xUeq of the attached atom.

The function, $\Sigma w(|F_o|^2 - |F_c|^2)^2$, was minimized, where $w = 1/[(\sigma(F_o))^2 + (0.0816*P)^2 + (1.233*P)]$ and $P = (|F_o|^2 + 2|F_c|^2)/3$. $R_w(F^2)$ refined to 0.375, with R(F) equal to 0.152 and a goodness of fit, S, = 1.21. Definitions used for calculating R(F), $R_w(F^2)$ and the goodness of fit, S, are given below.[14] The data were checked for secondary extinction effects but no correction was necessary. Neutral atom scattering factors and values used to calculate the linear absorption coefficient are from the International Tables for X-ray Crystallography (1992).[15] All figures were generated using SHELXTL/PC.[16] Tables of positional and thermal parameters, bond lengths and angles, torsion angles and figures are found below.

Table A.1: Crystal data and structure refinement for **II**.

Empirical formula	$C_{11}H\ N_6O_2$	
Formula weight	256.23	
Temperature	100(2) K	
Wavelength	1.54184 Å	
Crystal system	triclinic	
Space group	P -1	
Unit cell dimensions	a = 3.8005(9) Å	α = 92.529(14)°
	b = 9.1062(18) Å	β = 91.850(16)°
	c = 32.660(5) Å	γ = 101.838(19)°
Volume	1104.2(4) $Å^3$	
Z	4	
Density (calculated)	1.541 Mg/m^3	
Absorption coefficient	0.956 mm^{-1}	
F(000)	528	
Crystal size	0.19 x 0.03 x 0.02 mm^3	
θ range for data collection	2.711 to 59.758°.	
Index ranges	-4<=h<=4, -10<=k<=10, -35<=l<=35	
Reflections collected	4750	
Independent reflections	4750	
Completeness to θ= 59.758°	95.7 %	
Absorption correction	Semi-empirical from equivalents	
Max. and min. transmission	1.00 and 0.148	
Refinement method	Full-matrix least-squares on F^2	
Data / restraints / parameters	4750 / 228 / 344	
Goodness-of-fit on F^2	1.211	
Final R indices [I>2σ(I)]	R1 = 0.1515, wR2 = 0.3198	
R indices (all data)	R1 = 0.2267, wR2 = 0.3750	
Extinction coefficient	n/a	
Largest diff. peak and hole	0.576 and -0.510 e.$Å^{-3}$	

Table A.2: Atomic coordinates (x 10^4) and equivalent isotropic displacement parameters ($Å^2$ x 10^3) for **II**. U(eq) is defined as one third of the trace of the orthogonalized U^{ij} tensor.

	x	y	z	U(eq)
C1	-5060(30)	2411(14)	9691(4)	30(3)
C2	-6870(30)	1112(14)	9464(4)	28(3)

Table A.2 Continued:

N1	-6300(30)	1169(11)	9075(3)	31(3)
C4	-2810(30)	2994(14)	8662(4)	26(3)
C5	-4140(40)	2127(16)	8308(4)	37(3)
C6	-2940(30)	2737(15)	7937(4)	36(3)
C7	-430(30)	4098(14)	7935(4)	30(3)
C8	680(30)	4800(14)	8312(4)	26(3)
C9	4640(30)	7008(15)	8683(4)	31(3)
C10	7030(30)	8222(15)	8563(4)	36(3)
C11	6920(30)	8094(14)	8132(4)	36(3)
C12	380(30)	7488(15)	5297(4)	33(3)
C13	-1370(30)	6267(16)	5505(4)	35(3)
N7	-280(30)	6382(13)	5898(3)	40(3)
C15	3700(30)	8312(14)	6321(4)	29(3)
C16	2890(40)	7531(16)	6665(4)	39(3)
C17	4510(40)	8163(15)	7037(4)	38(3)
C18	6830(30)	9520(15)	7048(4)	34(3)
C19	7440(30)	10206(15)	6675(4)	36(3)
C20	11060(30)	12341(15)	6327(4)	36(3)
C21	13440(30)	13626(15)	6452(4)	35(3)
C22	13590(30)	13556(15)	6885(4)	34(3)
C3	-3270(30)	3269(15)	9403(4)	32(3)
N2	-3970(20)	2544(11)	9047(3)	26(2)
N3	-380(20)	4305(11)	8664(3)	23(2)
N4	3310(20)	6174(11)	8336(3)	24(2)
N5	4670(30)	6818(14)	7997(3)	40(3)
N6	-5120(30)	2773(13)	10125(3)	39(3)
C14	2490(30)	8457(16)	5578(4)	37(3)
N8	2050(30)	7768(12)	5932(3)	31(3)
N9	6090(30)	9650(12)	6314(3)	37(3)
N10	9970(30)	11625(12)	6664(3)	31(3)
N11	11540(30)	12329(13)	7012(3)	37(3)
N12	-340(30)	7780(13)	4871(3)	39(3)
O1	-3200(20)	3954(10)	10261(3)	44(2)
O2	-7090(20)	1870(11)	10320(3)	54(3)
O3	1550(20)	8868(11)	4730(3)	46(3)
O4	-2510(20)	6834(11)	4671(3)	50(3)

Table A.3: Bond lengths [Å] and angles [°] for **II**.

C1-C3	1.359(17)	C7-C8	1.374(16)
C1-C2	1.406(17)	C7-H7	0.95
C1-N6	1.442(15)	C8-N3	1.299(13)
C2-N1	1.299(13)	C8-N4	1.429(16)
C2-H2	0.95	C9-N4	1.357(14)
N1-N2	1.385(13)	C9-C10	1.359(17)
C4-N3	1.351(16)	C9-H9	0.95
C4-C5	1.391(16)	C10-C11	1.404(16)
C4-N2	1.396(14)	C10-H10	0.95
C5-C6	1.406(17)	C11-N5	1.341(16)
C5-H5	0.95	C11-H11	0.95
C6-C7	1.401(18)	C12-C14	1.360(17)
C6-H6	0.95	C12-C13	1.389(18)
C12-N12	1.458(15)	C13-N7	1.328(15)
C13-H13	0.95	C18-C19	1.398(16)
N7-N8	1.383(14)	C18-H18	0.95
C15-N9	1.364(16)	C19-N9	1.307(14)
C15-C16	1.365(16)	C19-N10	1.447(16)
C15-N8	1.420(15)	C20-N10	1.339(14)
C16-C17	1.389(17)	C20-C21	1.361(18)
C16-H16	0.95	C20-H20	0.95
C17-C18	1.361(18)	C21-C22	1.419(16)
C17-H17	0.95	C21-H21	0.95
C22-N11	1.316(16)	N6-O1	1.225(13)
C22-H22	0.95	C14-N8	1.340(15)
C3-N2	1.303(14)	C14-H14	0.95
C3-H3	0.95	N10-N11	1.339(13)
N4-N5	1.346(13)	N12-O4	1.212(13)
N6-O2	1.212(13)	N12-O3	1.216(13)
C3-C1-C2	103.5(11)	C2-N1-N2	103.4(10)
C3-C1-N6	127.9(12)	N3-C4-C5	124.1(12)
C2-C1-N6	128.7(11)	N3-C4-N2	115.3(11)
N1-C2-C1	112.7(11)	C5-C4-N2	120.7(12)
N1-C2-H2	123.6	C4-C5-C6	115.6(13)
C1-C2-H2	123.6	C4-C5-H5	122.2

Table A.3 Continued:

C6-C5-H5	122.2	C5-C6-H6	119.6
C7-C6-C5	120.8(13)	C8-C7-C6	116.2(12)
C7-C6-H6	119.6	C8-C7-H7	121.9
C6-C7-H7	121.9	C9-C10-C11	105.9(11)
N3-C8-C7	125.7(12)	C9-C10-H10	127.0
N3-C8-N4	114.8(11)	C11-C10-H10	127.0
C7-C8-N4	119.5(11)	N5-C11-C10	110.1(12)
N4-C9-C10	106.8(11)	N5-C11-H11	125.0
N4-C9-H9	126.6	C10-C11-H11	125.0
C10-C9-H9	126.6	C14-C12-C13	107.5(11)
C14-C12-N12	126.1(12)	C18-C17-H17	120.2
C13-C12-N12	125.8(12)	C16-C17-H17	120.2
N7-C13-C12	111.2(12)	C17-C18-C19	116.9(13)
N7-C13-H13	124.4	C17-C18-H18	121.5
C12-C13-H13	124.4	C19-C18-H18	121.5
C13-N7-N8	102.8(11)	N9-C19-C18	126.4(13)
N9-C15-C16	124.6(12)	N9-C19-N10	114.0(11)
N9-C15-N8	114.0(10)	C18-C19-N10	119.5(12)
C16-C15-N8	121.4(12)	N10-C20-C21	107.2(12)
C15-C16-C17	118.0(13)	N10-C20-H20	126.4
C15-C16-H16	121.0	C21-C20-H20	126.4
C17-C16-H16	121.0	C20-C21-C22	103.1(12)
C18-C17-C16	119.6(12)	C20-C21-H21	128.4
C22-C21-H21	128.4	N2-C3-H3	125.7
N11-C22-C21	112.7(12)	C1-C3-H3	125.7
N11-C22-H22	123.6	C3-N2-N1	111.9(10)
C21-C22-H22	123.6	C3-N2-C4	129.0(11)
N2-C3-C1	108.6(12)	N1-N2-C4	119.1(10)
C8-N3-C4	117.5(11)	O2-N6-O1	126.2(11)
N5-N4-C9	111.8(11)	O2-N6-C1	116.3(11)
N5-N4-C8	121.5(10)	O1-N6-C1	117.4(11)
C9-N4-C8	126.6(10)	N8-C14-C12	104.7(12)
C11-N5-N4	105.4(10)	N8-C14-H14	127.6
C12-C14-H14	127.6	N11-N10-C19	120.4(10)
C14-N8-N7	113.7(11)	C20-N10-C19	126.0(11)
C14-N8-C15	127.0(12)	C22-N11-N10	103.3(10)
N7-N8-C15	119.3(10)	O4-N12-O3	124.6(11)
C19-N9-C15	114.3(11)	O4-N12-C12	117.4(11)
N11-N10-C20	113.5(11)	O3-N12-C12	117.5(11)

Table A.4: Anisotropic displacement parameters ($Å^2$ x 10^3) for **II**. The anisotropic displacement factor exponent takes the form: $-2\pi^2[h^2a^{*2}U^{11} + ... + 2\ h\ k\ a^*\ b^*\ U^{12}]$.

	U11	U22	U33	U23	U13	U12
C1	29(6)	31(7)	30(7)	15(5)	1(5)	5(6)
C2	22(6)	25(7)	37(7)	21(5)	-3(5)	6(5)
N1	31(5)	25(6)	35(6)	11(4)	-3(4)	3(5)
C4	22(6)	31(7)	31(6)	3(5)	-3(5)	17(5)
C5	36(7)	39(7)	38(7)	5(6)	2(6)	16(6)
C6	43(7)	36(7)	29(7)	3(5)	-14(5)	8(6)
C7	37(7)	27(7)	29(6)	10(5)	1(5)	15(6)
C8	23(6)	31(7)	32(6)	12(5)	-2(5)	21(5)
C9	39(7)	35(7)	21(6)	7(5)	-9(5)	11(6)
C10	38(7)	28(7)	40(7)	9(6)	-9(6)	3(6)
C11	41(7)	20(7)	46(7)	14(6)	-2(6)	5(6)
C12	37(7)	34(7)	26(6)	10(5)	-6(5)	5(6)
C13	23(6)	47(8)	34(7)	2(6)	8(5)	7(6)
N7	41(6)	36(6)	44(6)	12(5)	-16(5)	13(5)
C15	35(7)	25(7)	28(6)	8(5)	6(5)	9(6)
C16	44(7)	40(8)	33(7)	5(6)	-2(6)	10(6)
C17	50(7)	38(7)	26(6)	16(5)	-6(6)	6(6)
C18	35(7)	42(8)	27(6)	15(6)	-1(5)	7(6)
C19	40(7)	39(7)	27(7)	10(6)	5(6)	5(6)
C20	41(7)	36(7)	35(7)	14(6)	-6(6)	16(6)
C21	34(7)	27(7)	47(7)	10(6)	-11(6)	15(6)
C22	31(6)	35(7)	37(7)	10(6)	-17(5)	12(6)
C3	36(7)	31(7)	33(7)	10(6)	-6(5)	14(6)
N2	21(5)	28(6)	30(6)	12(4)	-8(4)	6(4)
N3	20(5)	22(5)	33(5)	12(4)	-6(4)	13(4)
N4	23(5)	27(6)	26(5)	12(4)	-5(4)	13(4)
N5	43(6)	48(7)	34(6)	16(5)	-9(5)	19(5)
N6	39(6)	38(7)	40(6)	24(5)	-13(5)	8(5)
C14	36(7)	38(7)	35(7)	13(6)	6(5)	0(6)
N8	40(6)	26(6)	30(5)	15(4)	-2(5)	9(5)
N9	41(6)	33(6)	34(6)	11(5)	-13(5)	-3(5)
N10	35(6)	31(6)	27(5)	13(5)	6(5)	7(5)
N11	40(6)	37(6)	30(6)	6(5)	-12(5)	1(5)
N12	42(6)	32(7)	40(6)	16(5)	-5(5)	-4(5)
O1	55(6)	25(5)	42(6)	8(4)	-17(4)	-14(5)
O2	51(6)	53(7)	47(6)	38(5)	-5(5)	-23(5)

Table A.4 Continued:

O3	38(5)	47(6)	53(6)	28(5)	-9(4)	3(5)
O4	45(6)	48(7)	48(6)	20(5)	-11(5)	-13(5)

Table A.5: Hydrogen coordinates (x 10^4) and isotropic displacement parameters (Å^2 x 10^3) for **II**.

	x	y	z	U(eq)		x	y	z	U(eq)
H2	-8344	282	9583	33	H16	1265	6584	6650	46
H5	-5762	1184	8316	44	H17	4001	7650	7282	46
H6	-3845	2221	7684	44	H18	7977	9980	7297	41
H7	457	4513	7688	36	H20	10322	12013	6052	43
H9	4027	6787	8956	38	H21	14692	14386	6289	42
H10	8472	8997	8735	43	H22	15018	14313	7064	40
H11	8250	8807	7962	43	H3	-1767	4235	9452	39
H13	-3108	5454	5382	41	H14	3949	9410	5533	44

Table A.6: Torsion angles [°] for **II**.

C3-C1-C2-N1	-0.8(13)	C6-C7-C8-N3	0.5(17)
N6-C1-C2-N1	178.0(11)	C6-C7-C8-N4	178.5(10)
C1-C2-N1-N2	1.2(13)	N4-C9-C10-C11	2.3(13)
N3-C4-C5-C6	-3.2(17)	C9-C10-C11-N5	-2.5(14)
N2-C4-C5-C6	176.3(10)	C14-C12-C13-N7	-3.8(15)
C4-C5-C6-C7	2.9(17)	N12-C12-C13-N7	-175.2(12)
C5-C6-C7-C8	-1.7(18)	C12-C13-N7-N8	3.4(14)
N9-C15-C16-C17	2.4(19)	C2-C1-C3-N2	0.0(13)
N8-C15-C16-C17	-177.7(12)	N6-C1-C3-N2	-178.8(11)
C15-C16-C17-C18	-0.1(19)	C1-C3-N2-N1	0.7(13)
C16-C17-C18-C19	0.1(19)	C1-C3-N2-C4	178.4(10)
C17-C18-C19-N9	-2(2)	C2-N1-N2-C3	-1.2(12)
C17-C18-C19-N10	-177.9(12)	C2-N1-N2-C4	-179.1(9)
N10-C20-C21-C22	0.5(13)	N3-C4-N2-C3	6.3(16)
C20-C21-C22-N11	0.9(14)	C5-C4-N2-C3	-173.2(12)

Table A.6 Continued:

N3-C4-N2-N1	-176.1(9)	N3-C8-N4-N5	179.6(9)
C5-C4-N2-N1	4.4(15)	C7-C8-N4-N5	1.4(16)
C7-C8-N3-C4	-0.6(16)	N3-C8-N4-C9	-2.6(16)
N4-C8-N3-C4	-178.7(9)	C7-C8-N4-C9	179.2(10)
C5-C4-N3-C8	2.1(17)	C10-C11-N5-N4	1.7(13)
N2-C4-N3-C8	-177.4(8)	C9-N4-N5-C11	-0.2(12)
C10-C9-N4-N5	-1.4(13)	C8-N4-N5-C11	178.0(10)
C10-C9-N4-C8	-179.4(10)	C3-C1-N6-O2	175.5(12)
C2-C1-N6-O2	-3.0(18)	C13-N7-N8-C14	-2.0(14)
C3-C1-N6-O1	-4.5(18)	C13-N7-N8-C15	178.1(10)
C2-C1-N6-O1	176.9(12)	N9-C15-N8-C14	-3.3(18)
C13-C12-C14-N8	2.3(14)	C16-C15-N8-C14	176.7(12)
N12-C12-C14-N8	173.8(12)	N9-C15-N8-N7	176.6(10)
C12-C14-N8-N7	-0.3(14)	C16-C15-N8-N7	-3.3(17)
C12-C14-N8-C15	179.7(12)	C18-C19-N9-C15	4.3(19)
N10-C19-N9-C15	-180.0(11)	C18-C19-N10-C20	173.5(11)
C16-C15-N9-C19	-4.3(19)	C21-C22-N11-N10	-1.9(13)
N8-C15-N9-C19	175.7(10)	C20-N10-N11-C22	2.2(13)
C21-C20-N10-N11	-1.8(14)	C19-N10-N11-C22	-179.5(10)
C21-C20-N10-C19	-179.9(11)	C14-C12-N12-O4	-174.5(13)
N9-C19-N10-N11	179.5(10)	C13-C12-N12-O4	-4.6(19)
C18-C19-N10-N11	-4.5(18)	C14-C12-N12-O3	13.5(19)
N9-C19-N10-C20	-2.5(18)	C13-C12-N12-O3	-176.7(12)

X-ray Experimental for form III:

Crystals grew as long, thin, colorless needles by slow evaporation from acetone. The data crystal was cut from a larger crystal and had approximate dimensions; 0.28 x 0.09 x 0.04 mm. The data were collected on an Agilent Technologies SuperNova Dual Source diffractometer using a μ-focus Cu Kα radiation source (λ = 1.5418Å) with collimating mirror monochromators. A total of 725 frames of data were collected using ω-scans with a scan range of 1° and a counting time of 10 seconds per frame with a detector offset of +/- 41.3° and 40 seconds per frame with a detector offset of +/- 107.4°.

The data were collected at 100 K using an Oxford 700 Cryostream low temperature device. Details of crystal data, data collection and structure refinement are listed in Table A.7. Data collection, unit cell refinement and data reduction were performed using Agilent Technologies CrysAlisPro V 1.171.37.35h.[9] The structure was solved by direct methods using SHELXT[10] and refined by full-matrix least-squares on F2 with anisotropic displacement parameters for the non-H atoms using SHELXL-2016/6.[11] Structure analysis was aided by use of the programs PLATON98[12] and WinGX.[13] The hydrogen atoms were calculated in ideal positions with isotropic displacement parameters set to 1.2xUeq of the attached atom.

The function, $\Sigma w(|F_o|2 - |F_c|^2)^2$, was minimized, where $w = 1/[(\sigma(F_o))^2 + (0.1563*P)^2 + (35.43*P)]$ and $P = (|F_o|^2 + 2|F_c|^2)/3$. $R_w(F^2)$ refined to 0.328, with R(F) equal to 0.101 and a goodness of fit, S, = 0.967. Definitions used for calculating R(F), $R_w(F^2)$ and the goodness of fit, S, are given below.[14] The data were checked for secondary extinction effects but no correction was necessary. Neutral atom scattering factors and values used to calculate the linear absorption coefficient are from the International Tables for X-ray Crystallography (1992).[15] All figures were generated using SHELXTL/PC.[16] Tables of positional and thermal parameters, bond lengths and angles, torsion angles and figures are found below.

Table A.7: Crystallographic Data for **III**.

Empirical formula	$C_{11}H_8N_6O_2$
Formula weight	256.23
Temperature	100(2) K
Wavelength	1.54184 Å
Crystal system	orthorhombic
Space group	$Pna2_1$
Unit cell dimensions	a = 18.0859(12) Å α = 90°. b = 3.7042(3) Å β = 90°. c = 32.592(4) Å γ = 90°.
Volume	2183.5(4) $Å^3$
Z	8
Density (calculated)	1.559 Mg/m^3
Absorption coefficient	0.967 mm^{-1}
F(000)	1056
Crystal size	0.280 x 0.093 x 0.044 mm^3
θ range for data collection	2.711 to 73.583°.
Index ranges	-21<=h<=22, -4<=k<=2, -32<=l<=39
Reflections collected	7941
Independent reflections	3600 [R(int) = 0.0431]
Completeness to θ = 67.684°	99.4 %
Absorption correction	Semi-empirical from equivalents
Max. and min. transmission	1.00 and 0.518
Refinement method	Full-matrix least-squares on F^2
Data/restraints/parameters	3600 / 781 / 343
Goodness-of-fit on F^2	0.967
Final R indices [I>2σ(I)]	R1 = 0.1008, wR2 = 0.3252
R indices (all data)	R1 = 0.1052, wR2 = 0.3283
Absolute structure parameter	0.6(5)
Extinction coefficient	n/a
Largest diff. peak and hole	0.899 and -0.677 e.$Å^{-3}$

Table A.8: Atomic coordinates (x 10^4) and equivalent isotropic displacement parameters ($Å^2$ x 10^3) for **III**. U(eq) is defined as one third of the trace of the orthogonalized U^{ij} tensor.

	x	y	z	U(eq)
C1	4237(7)	13910(40)	3118(4)	23(2)
C2	4220(7)	14240(40)	3548(4)	22(2)
C3	4872(7)	12720(30)	3673(4)	21(2)
C4	5931(6)	9890(30)	3305(4)	17(2)

Table A.8 Continued:

C5	6244(7)	9150(30)	2932(4)	21(2)
C6	6938(7)	7520(30)	2928(4)	21(2)
C7	7278(6)	6710(30)	3300(4)	18(2)
C8	6898(6)	7670(30)	3651(4)	17(2)
C9	6876(6)	7320(30)	4411(4)	18(2)
C10	7373(6)	5910(30)	4693(4)	16(2)
C11	7981(6)	4720(30)	4466(4)	19(2)
C12	8033(7)	-3930(40)	6866(4)	24(2)
C C13	8025(7)	-4260(40)	6439(4)	23(2)
C14	7373(7)	-2760(30)	6320(4)	22(2)
C15	6348(6)	120(30)	6696(4)	20(2)
C16	6030(7)	1080(30)	7077(4)	22(2)
C17	5348(7)	2620(40)	7075(4)	24(2)
C18	4988(7)	3370(30)	6706(4)	24(2)
C19	5357(7)	2500(30)	6353(4)	21(2)
C20	5382(6)	2770(30)	5589(4)	19(2)
21	4886(6)	4010(30)	5308(4)	20(2)
C22	4280(6)	5340(30)	5536(4)	21(2)
N1	4844(6)	12370(30)	2983(3)	21(2)
N2	5225(5)	11640(30)	3328(3)	18(2)
N3	6232(5)	9260(20)	3665(3)	16(2)
N4	7199(5)	6770(30)	4044(3)	18(2)
N5	7885(5)	5200(30)	4071(4)	21(2)
N6	7288(5)	5830(20)	5125(3)	18(2)
N7	7440(6)	-2280(30)	7015(3)	25(2)
N8	7025(6)	-1610(30)	6667(3)	21(2)
N9	6014(5)	910(30)	6338(3)	20(2)
N10	5061(6)	3220(30)	5958(3)	21(2)
N11	4379(5)	4910(30)	5931(4)	22(2)
N12	4971(5)	4070(30)	4876(4)	22(2)
O1	6729(5)	7320(30)	5276(3)	30(2)
O2	7767(5)	4340(30)	5332(3)	30(2)
O3	4481(5)	5590(30)	4672(3)	30(2)
O4	5520(5)	2700(20)	4726(3)	26(2)

Table A.9: Bond lengths [Å] and angles [°] for III.

C1-N1	1.314(17)	C2-C3	1.370(18)
C1-C2	1.406(18)	C2-H2	0.95
C1-H1	0.95	C3-N2	1.355(16)
C3-H3	0.95	C4-N3	1.313(16)

Table A.9 Continued:

C4-C5	1.369(18)	C7-C8	1.382(18)
C4-N2	1.434(14)	C7-H7	0.95
C5-C6	1.395(18)	C8-N3	1.339(15)
C5-H5	0.95	C8-N4	1.431(17)
C6-C7	1.391(19)	C9-N4	1.346(16)
C6-H6	0.95	C9-C10	1.390(17)
C9-H9	0.95	C10-N6	1.416(17)
C10-C11	1.397(17)	C11-N5	1.310(16)
C11-H11	0.95	C16-C17	1.360(18)
C12-N7	1.325(17)	C16-H16	0.95
C12-C13	1.397(19)	C17-C18	1.395(19)
C12-H12	0.95	C17-H17	0.95
C13-C14	1.362(18)	C18-C19	1.367(19)
C13-H13	0.95	C18-H18	0.95
C14-N8	1.363(17)	C19-N9	1.325(16)
C14-H14	0.95	C19-N10	1.422(17)
C15-N9	1.348(16)	C20-N10	1.344(17)
C15-N8	1.385(15)	C20-C21	1.362(17)
C15-C16	1.412(18)	C20-H20	0.95
C21-C22	1.414(17)	C22-H22	0.95
C21-N12	1.415(18)	N1-N2	1.344(14)
C22-N11	1.308(17)	N4-N5	1.371(14)
N6-O2	1.229(13)	N6-O1	1.252(13)
N7-N8	1.382(15)	N12-O4	1.217(13)
N10-N11	1.386(14)	N12-O3	1.243(13)
N1-C1-C2	113.0(12)	C7-C6-H6	120.6
N1-C1-H1	123.5	C5-C6-H6	120.6
C2-C1-H1	123.5	C8-C7-C6	116.5(11)
C3-C2-C1	104.0(12)	C8-C7-H7	121.7
C3-C2-H2	128.0	C6-C7-H7	121.7
C1-C2-H2	128.0	N3-C8-C7	126.0(12)
N2-C3-C2	106.3(12)	N3-C8-N4	114.6(11)
N2-C3-H3	126.9	C7-C8-N4	119.3(11)
C2-C3-H3	126.9	N4-C9-C10	104.5(10)
N3-C4-C5	125.8(11)	N4-C9-H9	127.8
N3-C4-N2	113.8(11)	C10-C9-H9	127.8
C5-C4-N2	120.3(12)	C9-C10-C11	106.0(11)
C4-C5-C6	117.8(12)	C9-C10-N6	126.6(11)
C4-C5-H5	121.1	C11-C10-N6	127.3(10)
C6-C5-H5	121.1	N5-C11-C10	111.9(11)
C7-C6-C5	118.9(12)	N5-C11-H11	124.0

Table A.9 Continued:

C10-C11-H11	124.0	C13-C12-H12	123.3
N7-C12-C13	113.3(12)	C14-C13-C12	104.9(12)
N7-C12-H12	123.3	C14-C13-H13	127.5
C12-C13-H13	127.5	C13-C14-H14	126.5
C13-C14-N8	106.9(12)	N8-C14-H14	126.5
N9-C15-N8	116.0(11)	N8-C15-C16	122.5(12)
N9-C15-C16	121.5(12)	C17-C16-C15	118.1(13)
C17-C16-H16	120.9	C22-C21-N12	127.0(11)
C15-C16-H16	120.9	N11-C22-C21	111.6(11)
C16-C17-C18	120.7(13)	N11-C22-H22	124.2
C16-C17-H17	119.7	C21-C22-H22	124.2
C18-C17-H17	119.7	C1-N1-N2	103.6(10)
C19-C18-C17	116.7(12)	N1-N2-C3	113.2(10)
C19-C18-H18	121.6	N1-N2-C4	120.2(11)
C17-C18-H18	121.6	C3-N2-C4	126.6(11)
N9-C19-C18	125.0(13)	C4-N3-C8	115.0(11)
N9-C19-N10	112.7(11)	C9-N4-N5	113.6(10)
C18-C19-N10	122.3(11)	C9-N4-C8	126.3(10)
N10-C20-C21	106.0(11)	N5-N4-C8	120.1(10)
N10-C20-H20	127.0	C11-N5-N4	104.0(10)
C21-C20-H20	127.0	O2-N6-O1	123.6(11)
C20-C21-C22	105.9(12)	O2-N6-C10	118.5(10)
C20-C21-N12	127.1(11)	O1-N6-C10	118.0(10)
C12-N7-N8	102.9(11)	N7-N8-C15	120.5(11)
C14-N8-N7	111.9(10)	C19-N9-C15	117.8(11)
C14-N8-C15	127.6(11)	C20-N10-N11	112.6(11)
C20-N10-C19	128.6(10)	O4-N12-O3	123.7(12)
N11-N10-C19	118.5(10)	O4-N12-C21	118.7(10)
C22-N11-N10	103.8(10)	O3-N12-C21	117.6(10)

Table A.10: Anisotropic displacement parameters ($Å^2$ x 10^3) for **III**. The anisotropic displacement factor exponent takes the form: $-2\pi^2[h^2a^*2U^{11} + ... + 2\ h\ k\ a^*\ b^*\ U^{12}]$.

	U11	U22	U33	U23	U13	U12
C1	21(3)	15(4)	31(4)	1(3)	-2(3)	-4(3)
C2	21(3)	14(3)	31(4)	2(3)	0(3)	-3(3)

Table A.10 Continued:

C3	22(3)	13(3)	27(4)	2(3)	1(3)	-4(3)
C4	19(3)	7(3)	26(3)	-1(3)	0(3)	-8(3)
C5	22(3)	14(3)	27(4)	0(3)	0(3)	-6(3)
C6	21(3)	15(3)	29(4)	-1(3)	2(3)	-7(3)
C7	17(3)	8(3)	30(3)	-1(3)	1(3)	-6(3)
C8	17(3)	6(3)	27(3)	-2(3)	0(3)	-7(3)
C9	17(3)	10(3)	26(3)	-3(3)	-1(3)	-4(3)
C10	15(3)	4(3)	30(3)	-3(3)	-2(3)	-5(3)
C11	16(3)	10(3)	32(4)	-1(3)	0(3)	-3(3)
C12	24(3)	18(4)	32(4)	3(3)	-1(3)	-1(3)
C13	23(3)	16(4)	31(4)	1(3)	0(3)	-5(3)
C14	22(3)	17(4)	26(4)	0(3)	1(3)	-5(3)
C15	20(3)	15(3)	26(3)	0(3)	0(3)	-4(3)
C16	24(3)	15(4)	27(4)	-1(3)	1(3)	-5(3)
C17	26(4)	19(4)	29(4)	-2(3)	2(3)	-3(3)
C18	22(3)	22(4)	29(4)	-1(3)	2(3)	-4(3)
C19	21(3)	15(3)	28(3)	0(3)	1(3)	-2(3)
C20	17(3)	11(3)	29(3)	0(3)	0(3)	3(3)
C21	14(3)	14(3)	31(3)	1(3)	-1(3)	1(3)
C22	17(3)	12(4)	33(4)	0(3)	1(3)	-1(3)
N1	20(3)	17(3)	27(3)	2(3)	-2(3)	-5(3)
N2	19(3)	9(3)	25(3)	1(3)	-1(3)	-5(2)
N3	17(3)	3(3)	28(3)	-1(3)	0(3)	-3(3)
N4	16(3)	10(3)	28(3)	-2(3)	1(2)	-4(2)
N5	16(3)	13(3)	32(3)	-1(3)	1(3)	1(3)
N6	18(3)	3(3)	32(3)	0(3)	-3(3)	-4(3)
N7	23(3)	23(3)	28(3)	1(3)	-4(3)	0(3)
N8	21(3)	18(3)	25(3)	1(3)	-1(3)	-2(3)
N9	19(3)	13(3)	27(3)	2(3)	0(3)	-3(3)
N10	19(3)	15(3)	29(3)	-1(3)	1(3)	-2(3)
N11	17(3)	14(3)	34(3)	-1(3)	2(3)	0(3)
N12	18(3)	16(3)	33(3)	1(3)	-3(3)	2(3)
O1	26(4)	30(5)	33(5)	-2(4)	1(3)	4(4)
O2	29(4)	28(4)	35(5)	5(4)	-6(4)	1(4)
O3	24(4)	25(4)	40(5)	3(4)	-7(4)	5(4)
O4	24(4)	19(4)	37(5)	-3(4)	0(3)	2(3)

Table A.11: Hydrogen coordinates (x 10^4) and isotropic displacement parameters ($Å^2$ x 10^3) for **III**.

	x	y	z	U(eq)		x	y	z	U(eq)
H1	3850	14718	2944	27	H2	3843	15287	3713	27
H3	5042	12470	3948	25	H6	7176	6964	2676	25
H5	5995	9729	2684	25	H7	7746	5551	3312	22
H9	6413	8436	4464	21	H16	6285	653	7327	26
H11	8412	3681	4583	23	H17	5114	3205	7327	29
H12	8425	-4799	7034	29	H18	4510	4426	6700	29
H13	8394	-5311	6269	28	H20	5858	1787	5536	23
H14	7195	-2550	6047	26	H22	3852	6404	5418	25

Table A.12: Torsion angles [°] for **III**.

N1-C1-C2-C3	-0.7(15)	N4-C9-C10-C11	2.3(12)
C1-C2-C3-N2	0.4(13)	N4-C9-C10-N6	-179.9(10)
N3-C4-C5-C6	1.2(18)	C9-C10-C11-N5	-1.7(13)
N2-C4-C5-C6	178.7(10)	N6-C10-C11-N5	-179.4(10)
C4-C5-C6-C7	0.3(17)	N7-C12-C13-C14	-1.0(16)
C5-C6-C7-C8	-1.3(16)	C12-C13-C14-N8	0.1(14)
C6-C7-C8-N3	1.1(16)	N9-C15-C16-C17	4.4(18)
C6-C7-C8-N4	177.1(10)	N8-C15-C16-C17	-177.2(12)
C15-C16-C17-C18	-2.5(19)	N3-C4-N2-C3	1.8(15)
C16-C17-C18-C19	-0.6(19)	C5-C4-N2-C3	-175.9(11)
C17-C18-C19-N9	2.3(19)	C5-C4-N3-C8	-1.4(16)
C17-C18-C19-N10	-177.9(11)	N2-C4-N3-C8	-179.0(9)
N10-C20-C21-C22	2.4(13)	C7-C8-N3-C4	0.2(16)
N10-C20-C21-N12	-179.5(12)	N4-C8-N3-C4	-175.9(9)
C20-C21-C22-N11	-1.0(14)	C10-C9-N4-N5	-2.2(13)
N12-C21-C22-N11	-179.1(12)	C10-C9-N4-C8	178.4(10)
C2-C1-N1-N2	0.7(14)	N3-C8-N4-C9	0.7(16)
C1-N1-N2-C3	-0.4(13)	C7-C8-N4-C9	-175.7(11)
C1-N1-N2-C4	179.6(10)	N3-C8-N4-N5	-178.6(9)
C2-C3-N2-N1	0.0(13)	C7-C8-N4-N5	5.0(15)
C2-C3-N2-C4	180.0(10)	C10-C11-N5-N4	0.3(13)
N3-C4-N2-N1	-178.2(9)	C9-N4-N5-C11	1.2(13)
C5-C4-N2-N1	4.0(15)	C8-N4-N5-C11	-179.4(10)

Table A.12 Continued:

C9-C10-N6-O2	176.9(11)	C13-C14-N8-N7	0.8(14)
C11-C10-N6-O2	-5.7(16)	C13-C14-N8-C15	179.4(12)
C9-C10-N6-O1	-3.5(16)	C12-N7-N8-C14	-1.4(14)
C11-C10-N6-O1	173.9(11)	C12-N7-N8-C15	179.9(11)
C13-C12-N7-N8	1.5(15)	N9-C15-N8-C14	-3.7(18)
C16-C15-N8-C14	177.8(12)	C18-C19-N9-C15	-0.5(18)
N9-C15-N8-N7	174.8(10)	N10-C19-N9-C15	179.7(10)
C16-C15-N8-N7	-3.8(17)	N8-C15-N9-C19	178.6(11)
C16-C15-N9-C19	-2.9(17)	C21-C20-N10-N11	-3.2(14)
C21-C20-N10-C19	-177.2(12)	C20-N10-N11-C22	2.5(13)
N9-C19-N10-C20	-5.6(18)	C19-N10-N11-C22	177.3(10)
C18-C19-N10-C20	174.6(12)	C20-C21-N12-O4	4.7(19)
N9-C19-N10-N11	-179.4(10)	C22-C21-N12-O4	-177.6(12)
C18-C19-N10-N11	0.8(17)	C20-C21-N12-O3	-174.1(12)
C21-C22-N11-N10	-0.9(13)		

Appendix Notes and References

(1) Higashi, K.; Ueda, K.; Moribe, K. *Adv. Drug Deliv. Rev.*

(2) Rodrigues, M. A.; Tiago, J. M.; Duarte, A.; Geraldes, V.; Matos, H. A.; Gomes Azevedo, E. *Cryst. Growth Des.* **2016**, *16* (11), 6222–6229.

(3) Morissette, S. L.; Almarsson, Ö.; Peterson, M. L.; Remenar, J. F.; Read, M. J.; Lemmo, A. V.; Ellis, S.; Cima, M. J.; Gardner, C. R. *Adv. Drug Deliv. Rev.* **2004**, *56* (3), 275–300.

(4) Schultheiss, N.; Newman, A. *Cryst. Growth Des.* **2009**, *9* (6), 2950.

(5) Kuhnert-Brandstätter, M. *Pharm. Unserer Zeit* **1975**, *4* (5), 131–137.

(6) Fox, D.; Labes, M. M.; Weissberger, A. *Physics and Chemistry of the Organic Solid State*; Wiley Interscience: New York, 1965; Vol. 2.

(7) Bernstein, J. *Cryst. Growth Des.* **2011**, *11* (3), 632–650.

(8) Strohecker, D. J.; Lynch, V. M.; Holliday, B. J.; Jones, R. A. *Dalton Trans.*

(9) *CrysAlisPro*; Agilent Technologies UK Ltd.: Oxford, UK, 2013.

(10) Sheldrick, G. M. *Acta Crystallogr. Sect. A* **2015**, *71* (1), 3–8.

(11) Sheldrick, G. M. *Acta Crystallogr. Sect. C Struct. Chem.* **2015**, *71* (1), 3–8.

(12) Spek, A. L. *PLATON98*; Utrecht University: Padualaan 8, 3584 CH Utrecht, The Netherlands, 1998.

(13) Farrugia, L. J. *J. Appl. Crystallogr.* **1999**, *32* (4), 837–838.

(14) $R_w(F^2) = \{S_w(|F_o|^2 - |F_c|^2)^2/S_w(|F_o|)^4\}^{1/2}$ where w is the weight given each reflection. $R(F) = S(|F_o| - |F_c|)/S|F_o|\}$ for reflections with $F_o > 4(s(F_o))$. $S = [S_w(|F_o|^2 - |F_c|^2)^2/(n - p)]^{1/2}$, where n is the number of reflections and p is the number of refined parameters.

(15) *International Tables for X-ray Crystallography*; Kluwer Academic Press: Boston, MA, USA, 1992; Vol. C.

(16) Sheldrick, G. M. *SHELXLT/PC*; Siemens Analytical X-ray Instruments, Inc.: Madison, WI, USA, 1994.

References

CHAPTER 1

(1) Jameson, D. L.; Blaho, J. K.; Kruger, K. T.; Goldsby, K. A. Inorg. Chem. 1989, 28 (24), 4312–4314.

(2) Jameson, D. L.; Goldsby, K. A. J. Org. Chem. 1990, 55 (17), 4992–4994.

(3) Halcrow, M. A. New J. Chem. 2014, 38 (5), 1868–1882.

(4) Brien, K. A.; Garner, C. M.; Pinney, K. G. Tetrahedron 2006, 62 (15), 3663–3666.

(5) Christenson, D. L.; Tokar, C. J.; Tolman, W. B. Organometallics 1995, 14 (5), 2148–2150.

(6) Watson, A. A.; House, D. A.; Steel, P. J. J. Org. Chem. 1991, 56 (12), 4072–4074.

(7) Sun; Yu; Wu; Xiao, W.-J. Organometallics 2005, 24 (12), 2959–2963.

(8) Wang, L.; Liu, N.; Dai, B.; Hu, H. Eur. J. Org. Chem. 2014, 2014 (29), 6493–6500.

(9) Duncan, N. C.; Garner, C. M.; Nguyen, T.; Hung, F.; Klausmeyer, K. Tetrahedron Lett. 2008, 49 (40), 5766–5769.

(10) Vermonden, T.; Branowska, D.; Marcelis, A. T. M.; Sudhölter, E. J. R. Tetrahedron 2003, 59 (27), 5039–5045.

(11) Rajadurai, C.; Schramm, F.; Brink, S.; Fuhr, O.; Ghafari, M.; Kruk, R.; Ruben, M. Inorg. Chem. 2006, 45 (25), 10019–10021.

(12) Elhaïk, J.; Pask, C. M.; Kilner, C. A.; Halcrow, M. A. Tetrahedron 2007, 63 (2), 291–298.

(13) Basak, S.; Hui, P.; Chandrasekar, R. Synthesis 2009, 2009 (23), 4042–4048.

(14) Mohammed, R.; Chastanet, G.; Tuna, F.; Malkin, T. L.; Barrett, S. A.; Kilner, C. A.; Létard, J.-F.; Halcrow, M. A. Eur. J. Inorg. Chem. 2013, 2013 (5–6), 819–831.

(15) Du, W.; Wang, Q.; Wang, L.; Yu, Z. Organometallics 2014, 33 (4), 974–982.

(16) Zoppellaro, G.; Baumgarten, M. Eur. J. Org. Chem. 2005, 2005 (14), 2888–2892.

(17) Grimmett, M.; Iddon, B. Heterocycles 1994, 37 (3), 2087–2147.

(18) Pritchard, R.; Lazar, H.; Barrett, S. A.; Kilner, C. A.; Asthana, S.; Carbonera, C.; Létard, J.-F.; Halcrow, M. A. Dalton Trans. 2009, No. 33, 6656–6666.

(19) Stanley, J. M.; Zhu, X.; Yang, X.; Holliday, B. J. Inorg. Chem. 2010, 49 (5), 2035–2037.

(20) Zhu, X. J.; Holliday, B. J. Macromol. Rapid Commun. 2010, 31 (9–10), 904–909.

(21) Basak, S.; Narayana, Y. S. L. V.; Baumgarten, M.; Müllen, K.; Chandrasekar, R. Macromolecules 2013, 46 (2), 362–369.

(22) Narayana, Y. S. L. V.; Venkatakrishnarao, D.; Biswas, A.; Mohiddon, M. A.; Viswanathan, N.; Chandrasekar, R. ACS Appl. Mater. Interfaces 2016, 8 (1), 952–958.

(23) Narayana, Y. S. L. V.; Basak, S.; Baumgarten, M.; Müllen, K.; Chandrasekar, R. Adv. Funct. Mater. 2013, 23 (47), 5875–5880.

(24) Basak, S.; Hui, P.; Boodida, S.; Chandrasekar, R. J. Org. Chem. 2012, 77 (7), 3620–3626.

(25) Pritchard, R.; Kilner, C. A.; Barrett, S. A.; Halcrow, M. A. Inorganica Chim. Acta 2009, 362 (12), 4365–4371.

(26) Strohecker, D. J.; Lynch, V. M.; Holliday, B. J.; Jones, R. A. Dalton Trans., submitted.

(27) Halcrow, M. A. Coord. Chem. Rev. 2009, 253 (21–22), 2493–2514.

(28) Halcrow, M. A. Coord. Chem. Rev. 2005, 249 (24), 2880–2908.

(29) Jo, D.-H.; Yeo, H.-J. Bull. Korean Chem. Soc. 1993, 14 (6), 682–686.

(30) Karam, A. R.; Catarí, E. L.; López-Linares, F.; Agrifoglio, G.; Albano, C. L.; Díaz-Barrios, A.; Lehmann, T. E.; Pekerar, S. V.; Albornoz, L. A.; Atencio, R.; González, T.; Ortega, H. B.; Joskowics, P. Appl. Catal. Gen. 2005, 280 (2), 165–173.

(31) Gong, D.; Jia, X.; Wang, B.; Zhang, X.; Jiang, L. J. Organomet. Chem. 2012, 702, 10–18.

(32) Nyamato, G. S.; Alam, M. G.; Ojwach, S. O.; Akerman, M. P. Appl. Organomet. Chem. 2016, 30 (2), 89–94.

(33) Gong, D.; Jia, X.; Wang, B.; Zhang, X.; Huang, K.-W. J. Organomet. Chem. 2014, 766, 79–85.

(34) Jones, G. D.; Martin, J. L.; McFarland, C.; Allen, O. R.; Hall, R. E.; Haley, A. D.; Brandon, R. J.; Konovalova, T.; Desrochers, P. J.; Pulay, P.; Vicic, D. A. J. Am. Chem. Soc. 2006, 128 (40), 13175–13183.

(35) Smith, S. W.; Fu, G. C. Angew. Chem. Int. Ed. 2008, 47 (48), 9334–9336.

(36) Arendt, K. M.; Doyle, A. G. Angew. Chem. Int. Ed. 2015, 54 (34), 9876–9880.

(37) Erickson, L. W.; Lucas, E. L.; Tollefson, E. J.; Jarvo, E. R. J. Am. Chem. Soc. 2016, 138 (42), 14006–14011.

(38) Li, Y.-T.; Liao, B.-S.; Chen, H.-P.; Liu, S.-T. Synthesis 2011, 2011 (16), 2639–2643.

(39) Zikode, M.; Ojwach, S. O.; Akerman, M. P. Appl. Organomet. Chem. 2017, 31 (2), n/a-n/a.

(40) Magubane, M. N.; Nyamato, G. S.; Ojwach, S. O.; Munro, O. Q. RSC Adv. 2016, 6 (69), 65205–65221.

(41) Ghoochany, L. T.; Farsadpour, S.; Sun, Y.; Thiel, W. R. Eur. J. Inorg. Chem. 2011, 2011 (23), 3421–3424.

(42) Jin, W.; Wang, L.; Yu, Z. Organometallics 2012, 31 (15), 5664–5667.

(43) Liu, S.; Zeng, X.; Xu, B. Tetrahedron Lett. 2016, 57 (33), 3706–3710.

(44) Shin, M. S.; Oh, B. J.; Ryu, J. Y.; Park, M. H.; Kim, M.; Lee, J.; Kim, Y. Polyhedron 2017, 125, 101–106.

(45) König, E.; Madeja, K. Chem. Commun. Lond. 1966, No. 3, 61–62.

(46) Kershaw Cook, L. J.; Mohammed, R.; Sherborne, G.; Roberts, T. D.; Alvarez, S.; Halcrow, M. A. Coord. Chem. Rev. 2015, 289–290, 2–12.

(47) Craig, G. A.; Roubeau, O.; Aromí, G. Coord. Chem. Rev. 2014, 269, 13–31.

(48) Holland, J. M.; McAllister, J. A.; Lu, Z.; Kilner, C. A.; Thornton-Pett, M.; Halcrow, M. A. Chem. Commun. 2001, No. 6, 577–578.

(49) Scudder, M. L.; Goodwin, H. A.; Dance, I. G. New J. Chem. 1999, 23 (7), 695–705.

(50) Pritchard, R.; Kilner, C. A.; Halcrow, M. A. Chem. Commun. 2007, No. 6, 577–579.

(51) Elhaïk, J.; Evans, D. J.; Kilner, C. A.; Halcrow, M. A. Dalton Trans. 2005, No. 9, 1693–1700.

(52) Pelascini, F.; Wesolek, M.; Peruch, F.; Cian, A. D.; Kyritsakas, N.; Lutz, P. J.; Kress, J. Polyhedron 2004, 23 (18), 3193–3199.

(53) Money, V. A.; Carbonera, C.; Elhaïk, J.; Halcrow, M. A.; Howard, J. A. K.; Létard, J.-F. Chem. – Eur. J. 2007, 13 (19), 5503–5514.

(54) Schramm, F.; Chandrasekar, R.; Zevaco, T. A.; Rudolph, M.; Görls, H.; Poppitz, W.; Ruben, M. Eur. J. Inorg. Chem. 2009, 2009 (1), 53–61.

(55) Willison, S. A.; Jude, H.; Antonelli, R. M.; Rennekamp, J. M.; Eckert, N. A.; Krause Bauer, J. A.; Connick, W. B. Inorg. Chem. 2004, 43 (8), 2548–2555.

(56) Stock, J. T. J. Chem. Educ. 1991, 68 (10), 801.

(57) Pimentel, G. C.; Spratley, R. D. Understanding Chemistry; Holden-Day, Inc.: San Francisco, CA, USA, 1971.

(58) Cirera, B.; Björk, J.; Otero, R.; Gallego, J. M.; Miranda, R.; Ecija, D. J. Phys. Chem. C 2017, 121 (14), 8033–8041.

(59) Dochain, S.; Vetica, F.; Puttreddy, R.; Rissanen, K.; Enders, D. Angew. Chem. Int. Ed. 2016, 55 (52), 16153–16155.

(60) Chen, D.; Yu, L.; Wang, P. G. Tetrahedron Lett. 1996, 37 (26), 4467–4470.

(61) Yu, L.; Chen, D.; Wang, P. G. Tetrahedron Lett. 1996, 37 (13), 2169–2172.

(62) Kobayashi, S.; Hachiya, I.; Takahori, T.; Araki, M.; Ishitani, H. Tetrahedron Lett. 1992, 33 (45), 6815–6818.

(63) Dissanayake, P.; Allen, M. J. J. Am. Chem. Soc. 2009, 131 (18), 6342–6343.

(64) Wu, P.; Wang, J.; Li, Y.; He, C.; Xie, Z.; Duan, C. Adv. Funct. Mater. 2011, 21 (14), 2788–2794.

(65) Ward, B. D.; Gade, L. H. Chem. Commun. 2012, 48 (86), 10587–10599.

(66) Ende, B. M. van der; Aarts, L.; Meijerink, A. Phys. Chem. Chem. Phys. 2009, 11 (47), 11081–11095.

(67) Méndez-Blas, A.; López-Cruz, E.; Palestino, G.; Calixto, M. E. MRS Adv. 2017, 2 (3), 147–152.

(68) Jeng, J.-T.; Li, Y.-L. J. Vac. Sci. Technol. B Nanotechnol. Microelectron. Mater. Process. Meas. Phenom. 2017, 35 (2), 022203.

(69) Bethencourt, M.; Botana, F. J.; Calvino, J. J.; Marcos, M.; RodrÍguez-Chacón, M. A. Corros. Sci. 1998, 40 (11), 1803–1819.

(70) Tiwari, B.; Ram, S.; Banerji, P. MRS Adv. 2017, 2 (3), 141–146.

(71) Bomberger, C. C.; Lewis, M. R. J. Vac. Sci. Technol. B Nanotechnol. Microelectron. Mater. Process. Meas. Phenom. 2017, 35 (3), 030801.

(72) Chow, C.-F. J. Fluoresc. 2012, 22 (6), 1539–1546.

(73) Sessler, J. L.; Dow, W. C.; O'Connor, D.; Harriman, A.; Hemmi, G.; Mody, T. D.; Miller, R. A.; Qing, F.; Springs, S.; Woodburn, K.; Young, S. W. J. Alloys Compd. 1997, 249 (1–2), 146–152.

(74) Rocha, J.; Carlos, L. D.; Paz, F. A. A.; Ananias, D. Chem. Soc. Rev. 2011, 40 (2), 926–940.

(75) Wang, Y.-F.; Liu, G.-Y.; Sun, L.-D.; Xiao, J.-W.; Zhou, J.-C.; Yan, C.-H. ACS Nano 2013, 7 (8), 7200–7206.

(76) Hanaoka, K.; Kikuchi, K.; Kojima, H.; Urano, Y.; Nagano, T. J. Am. Chem. Soc. 2004, 126 (39), 12470–12476.

(77) Liu, Y.; Tu, D.; Zhu, H.; Chen, X. Chem. Soc. Rev. 2013, 42 (16), 6924–6958.

(78) Cheng, L.; Yang, K.; Li, Y.; Chen, J.; Wang, C.; Shao, M.; Lee, S.-T.; Liu, Z. Angew. Chem. Int. Ed. 2011, 50 (32), 7385–7390.

(79) Wang, M.; Chen, Z.; Zheng, W.; Zhu, H.; Lu, S.; Ma, E.; Tu, D.; Zhou, S.; Huang, M.; Chen, X. Nanoscale 2014, 6 (14), 8274–8282.

(80) Moore, E. G.; Samuel, A. P. S.; Raymond, K. N. Acc. Chem. Res. 2009, 42 (4), 542–552.

(81) Binnemans, K. Chem. Rev. 2009, 109 (9), 4283–4374.

(82) Basak, S.; Mohiddon, M. A.; Baumgarten, M.; Müllen, K.; Chandrasekar, R. Sci. Rep. 2015, 5, 8406.

(83) Chen, X.-Y.; Yang, X.; Holliday, B. J. J. Am. Chem. Soc. 2008, 130 (5), 1546–1547.

(84) de Hatten, X.; Asil, D.; Friend, R. H.; Nitschke, J. R. J. Am. Chem. Soc. 2012, 134 (46), 19170–19178.

(85) Hasegawa, Y.; Kawai, H.; Nakamura, K.; Yasuda, N.; Wada, Y.; Yanagida, S. J. Alloys Compd. 2006, 408–412, 669–674.

(86) Carlos, L. D.; Ferreira, R. A. S.; Bermudez, V. de Z.; Ribeiro, S. J. L. Adv. Mater. 2009, 21 (5), 509–534.

(87) Ma, M.-L.; Ji, C.; Zang, S.-Q. Dalton Trans. 2013, 42 (29), 10579–10586.

(88) Armelao, L.; Quici, S.; Barigelletti, F.; Accorsi, G.; Bottaro, G.; Cavazzini, M.; Tondello, E. Coord. Chem. Rev. 2010, 254 (5–6), 487–505.

(89) Carlos, L. D.; Ferreira, R. A. S.; Bermudez, V. de Z.; Julián-López, B.; Escribano, P. Chem. Soc. Rev. 2011, 40 (2), 536–549.

(90) Bettencourt-Dias, A. de. Dalton Trans. 2007, No. 22, 2229–2241.

(91) Aime, S.; Botta, M.; Fasano, M.; Terreno, E. Chem. Soc. Rev. 1998, 27 (1), 19–29.

(92) Peters, J. A.; Huskens, J.; Raber, D. J. Prog. Nucl. Magn. Reson. Spectrosc. 1996, 28 (3–4), 283–350.

(93) Aspinall, H. C. Chem. Rev. 2002, 102 (6), 1807–1850.

(94) Aime, S.; Barge, A.; Delli Castelli, D.; Fedeli, F.; Mortillaro, A.; Nielsen, F. U.; Terreno, E. Magn. Reson. Med. 2002, 47 (4), 639–648.

(95) Aime, S.; Castelli, D. D.; Crich, S. G.; Gianolio, E.; Terreno, E. Acc. Chem. Res. 2009, 42 (7), 822–831.

(96) Wenzel, T. J.; Zaia, J. J. Org. Chem. 1985, 50 (8), 1322–1324.

(97) Bünzli, J.-C. G. J. Coord. Chem. 2014, 67 (23/24), 3706–3733.

(98) D'Aléo, A.; Pointillart, F.; Ouahab, L.; Andraud, C.; Maury, O. Coord. Chem. Rev. 2012, 256 (15–16), 1604–1620.

(99) Bünzli, J.-C. G.; Piguet, C. Chem. Soc. Rev. 2005, 34 (12), 1048–1077.

(100) Vleck, J. H. V. J. Phys. Chem. 1937, 41 (1), 67–80.

(101) Weissman, S. I. J. Chem. Phys. 1942, 10 (4), 214–217.

(102) Latva, M.; Takalo, H.; Mukkala, V.-M.; Matachescu, C.; Rodríguez-Ubis, J. C.; Kankare, J. J. Lumin. 1997, 75 (2), 149–169.

(103) Fu, L.-M.; Ai, X.-C.; Li, M.-Y.; Wen, X.-F.; Hao, R.; Wu, Y.-S.; Wang, Y.; Zhang, J.-P. J. Phys. Chem. A 2010, 114 (13), 4494–4500.

(104) Narayana, Y. S. L. V.; Chandrasekar, R. ChemPhysChem 2011, 12 (13), 2391–2396.

(105) Bünzli, J.-C. G. Coord. Chem. Rev. 2015, 293–294, 19–47.

(106) Sato, S.; Wada, M. Bull. Chem. Soc. Jpn. 1970, 43 (7), 1955–1962.

(107) Whan, R. E.; Crosby, G. A. J. Mol. Spectrosc. 1962, 8 (1), 315–327.

(108) Binnemans, K. Coord. Chem. Rev. 2015, 295, 1–45.

(109) Haas, Y.; Stein, G. J. Phys. Chem. 1971, 75 (24), 3677–3681.

(110) Haas, Y.; Stein, G. J. Phys. Chem. 1971, 75 (24), 3668–3677.

(111) Supkowski, R. M.; Horrocks Jr., W. D. Inorganica Chim. Acta 2002, 340, 44–48.

(112) Werts, M. H. V.; Jukes, R. T. F.; Verhoeven, J. W. Phys. Chem. Chem. Phys. 2002, 4 (9), 1542–1548.

(113) Remuiñán, M. J.; Román, H.; Alonso, M. T.; Rodríguez-Ubis, J. C. J. Chem. Soc. Perkin Trans. 2 1993, No. 6, 1099–1102.

(114) Brunet, E.; Juanes, O.; Sedano, R.; Rodríguez-Ubis, J.-C. Photochem. Photobiol. Sci. 2002, 1 (8), 613–618.

(115) Kadjane, P.; Starck, M.; Camerel, F.; Hill, D.; Hildebrandt, N.; Ziessel, R.; Charbonnière, L. J. Inorg. Chem. 2009, 48 (11), 4601–4603.

(116) Starck, M.; Kadjane, P.; Bois, E.; Darbouret, B.; Incamps, A.; Ziessel, R.; Charbonnière, L. J. Chem. – Eur. J. 2011, 17 (33), 9164–9179.

(117) Sager, W. F.; Filipescu, N.; Serafin, F. A. J. Phys. Chem. 1965, 69 (4), 1092–1100.

(118) Pereira, C. C. L.; Coutinho, J. T.; Pereira, L. C. J.; Leal, J. P.; Laia, C. A. T.; Monteiro, B. Polyhedron 2015, 91, 42–46.

(119) Martins, J. P.; Martín-Ramos, P.; Coya, C.; Álvarez, A. L.; Pereira, L. C.; Díaz, R.; Martín-Gil, J.; Ramos Silva, M. Mater. Chem. Phys. 2014, 147 (3), 1157–1164.

(120) Binnemans, K.; Bex, C.; Venard, A.; De Leebeeck, H.; Görller-Walrand, C. J. Mol. Liq. 1999, 83 (1–3), 283–294.

(121) Wilkerson, J. M. Luminescent lanthanide-containing materials: from small molecules to conducting metallopolymers, The University of Texas at Austin: Austin, TX, 2012.

CHAPTER 2

(1) Halcrow, M. A. *Coord. Chem. Rev.* **2009**, *253* (21–22), 2493–2514.

(2) Carlos, L. D.; Ferreira, R. A. S.; Bermudez, V. de Z.; Ribeiro, S. J. L. *Adv. Mater.* **2009**, *21* (5), 509–534.

(3) Wang, X.; Chang, H.; Xie, J.; Zhao, B.; Liu, B.; Xu, S.; Pei, W.; Ren, N.; Huang, L.; Huang, W. *Coord. Chem. Rev.* **2014**, *273–274*, 201–212.

(4) Fernández-Moreira, V.; Song, B.; Sivagnanam, V.; Chauvin, A.-S.; Vandevyver, C. D. B.; Gijs, M.; Hemmilä, I.; Lehr, H.-A.; Bünzli, J.-C. G. *Analyst* **2009**, *135* (1), 42–52.

(5) Jameson, D. L.; Blaho, J. K.; Kruger, K. T.; Goldsby, K. A. *Inorg. Chem.* **1989**, *28* (24), 4312–4314.

(6) Halcrow, M. A. *New J. Chem.* **2014**, *38* (5), 1868–1882.

(7) Zoppellaro, G.; Baumgarten, M. *Eur. J. Org. Chem.* **2005**, *2005* (14), 2888–2892.

(8) Zhu, X. J.; Holliday, B. J. *Macromol. Rapid Commun.* **2010**, *31* (9–10), 904–909.

(9) Basak, S.; Hui, P.; Chandrasekar, R. *Synthesis* **2009**, *2009* (23), 4042–4048.

(10) Basak, S.; Narayana, Y. S. L. V.; Baumgarten, M.; Müllen, K.; Chandrasekar, R. *Macromolecules* **2013**, *46* (2), 362–369.

(11) Narayana, Y. S. L. V.; Venkatakrishnarao, D.; Biswas, A.; Mohiddon, M. A.; Viswanathan, N.; Chandrasekar, R. *ACS Appl. Mater. Interfaces* **2016**, *8* (1), 952–958.

(12) Narayana, Y. S. L. V.; Basak, S.; Baumgarten, M.; Müllen, K.; Chandrasekar, R. *Adv. Funct. Mater.* **2013**, *23* (47), 5875–5880.

(13) Narayana, Y. S. L. V.; Baumgarten, M.; Müllen, K.; Chandrasekar, R. *Macromolecules* **2015**, *48* (14), 4801–4812.

(14) Basak, S.; Hui, P.; Boodida, S.; Chandrasekar, R. *J. Org. Chem.* **2012**, *77* (7), 3620–3626.

(15) Pritchard, R.; Kilner, C. A.; Barrett, S. A.; Halcrow, M. A. *Inorganica Chim. Acta* **2009**, *362* (12), 4365–4371.

(16) Mohammed, R.; Chastanet, G.; Tuna, F.; Malkin, T. L.; Barrett, S. A.; Kilner, C. A.; Létard, J.-F.; Halcrow, M. A. *Eur. J. Inorg. Chem.* **2013**, *2013* (5–6), 819–831.

(17) Govor, E. V.; Lysenko, A. B.; Quiñonero, D.; Rusanov, E. B.; Chernega, A. N.; Moellmer, J.; Staudt, R.; Krautscheid, H.; Frontera, A.; Domasevitch, K. V. *Chem. Commun.* **2011**, *47* (6), 1764–1766.

(18) Cardona, C. M.; Li, W.; Kaifer, A. E.; Stockdale, D.; Bazan, G. C. *Adv. Mater.* **2011**, *23* (20), 2367–2371.

(19) Huang, Y.; Zhang, M.; Ye, L.; Guo, X.; Han, C. C.; Li, Y.; Hou, J. *J. Mater. Chem.* **2012**, *22* (12), 5700–5705.

(20) Krumova, K.; Cosa, G. *J. Am. Chem. Soc.* **2010**, *132* (49), 17560–17569.

(21) Al-Anber, M.; Milde, B.; Alhalasah, W.; Lang, H.; Holze, R. *Electrochimica Acta* **2008**, *53* (20), 6038–6047.

(22) Wilkerson, J. M. Luminescent lanthanide-containing materials: from small molecules to conducting metallopolymers, The University of Texas at Austin: Austin, TX, 2012.

(23) Binnemans, K. *Coord. Chem. Rev.* **2015**, *295*, 1–45.

(24) Werts, M. H. V.; Jukes, R. T. F.; Verhoeven, J. W. *Phys. Chem. Chem. Phys.* **2002**, *4* (9), 1542–1548.

(25) Bünzli, J.-C. G. *Coord. Chem. Rev.* **2015**, *293–294*, 19–47.

(26) Tallec, A.; Hazard, R.; SuwiNski, J.; Wagner, P. *Pol. J. Chem.* **2000**, *47* (8), 1177–1183.

(27) Cuadrado, P.; González-Nogal, A. M.; Martínez, S. *Tetrahedron* **1997**, *53* (25), 8585–8598.

(28) Suwiński, J.; Wagner, P. *Pol. J. Chem.* **2000**, *74* (11), 1575–1580.

(29) Yin, P.; Zhang, J.; Parrish, D. A.; Shreeve, J. M. *Chem. - Eur. J.* **2014**, *20* (50), 16529–16536.

(30) Fevig, J. M.; Cacciola, J.; Buriak Jr., J.; Rossi, K. A.; Knabb, R. M.; Luettgen, J. M.; Wong, P. C.; Bai, S. A.; Wexler, R. R.; Lam, P. Y. S. *Bioorg. Med. Chem. Lett.* **2006**, *16* (14), 3755–3760.

(31) Kumar, R.; Joshi, Y. C.; Joshi, P. *Heterocycl. Commun.* **2005**, *11* (3–4), 361–364.

(32) De Sio, F. *Heterocycles* **1984**, *22* (10), 2309–2311.

(33) Wolf, M. O. *Adv. Mater.* **2001**, *13* (8), 545–553.

(34) de Hatten, X.; Asil, D.; Friend, R. H.; Nitschke, J. R. *J. Am. Chem. Soc.* **2012**, *134* (46), 19170–19178.

(35) Chow, C.-F. *J. Fluoresc.* **2012**, *22* (6), 1539–1546.

(36) Tennyson, A. G.; Norris, B.; Bielawski, C. W. *Macromolecules* **2010**, *43* (17), 6923–6935.

(37) De Silva, C. R.; Maeyer, J. R.; Wang, R.; Nichol, G. S.; Zheng, Z. *Inorganica Chim. Acta* **2007**, *360* (11), 3543–3552.

(38) Kumar, K. S.; Schäfer, B.; Lebedkin, S.; Karmazin, L.; Kappes, M. M.; Ruben, M. *Dalton Trans.* **2015**, *44* (35), 15611–15619.

(39) Horrocks, W. D.; Albin, M. In *Progress in Inorganic Chemistry*; Lippard, S. J., Ed.; John Wiley & Sons, Inc.: Hoboken, NJ, USA, 1984; Vol. 31, pp 1–104.

(40) *CrystalClear*; Rigaku Americas Corporation: The Woodlands, Texas, USA, 2008.

(41) Burla, M. C.; Caliandro, R.; Camalli, M.; Carrozzini, B.; Cascarano, G. L.; De Caro, L.; Giacovazzo, C.; Polidori, G.; Spagna, R. *J. Appl. Crystallogr.* **2005**, *38* (2), 381–388.

(42) Sheldrick, G. M. *Acta Crystallogr. Sect. C Struct. Chem.* **2015**, *71* (1), 3–8.

(43) Spek, A. L. *PLATON98*; Utrecht University: Padualaan 8, 3584 CH Utrecht, The Netherlands, 1998.

(44) Farrugia, L. J. *J. Appl. Crystallogr.* **1999**, *32* (4), 837–838.

(45) $R_w(F^2) = \{S_w(|F_o|^2 - |F_c|^2)^2/S_w(|F_o|)^4\}^{1/2}$ where w is the weight given each reflection. $R(F) = S(|F_o| - |F_c|)/S|F_o|\}$ for reflections with $F_o > 4(s(F_o))$. $S = [S_w(|F_o|^2 - |F_c|^2)^2/(n - p)]^{1/2}$, where n is the number of reflections and p is the number of refined parameters.

(46) *International Tables for X-ray Crystallography*; Kluwer Academic Press: Boston, MA, USA, 1992; Vol. C.

(47) Sheldrick, G. M. *SHELXLT/PC*; Siemens Analytical X-ray Instruments, Inc.: Madison, WI, USA, 1994.

(48) *CrysAlisPro*; Agilent Technologies UK Ltd.: Oxford, UK, 2013.

(49) Sheldrick, G. M. *Acta Crystallogr. Sect. A* **2015**, *71* (1), 3–8.

CHAPTER 3

(1) Fernández-Moreira, V.; Song, B.; Sivagnanam, V.; Chauvin, A.-S.; Vandevyver, C. D. B.; Gijs, M.; Hemmilä, I.; Lehr, H.-A.; Bünzli, J.-C. G. *Analyst* **2009**, *135* (1), 42–52.

(2) Wang, X.; Chang, H.; Xie, J.; Zhao, B.; Liu, B.; Xu, S.; Pei, W.; Ren, N.; Huang, L.; Huang, W. *Coord. Chem. Rev.* **2014**, *273–274*, 201–212.

(3) Terai, T.; Kikuchi, K.; Iwasawa, S.; Kawabe, T.; Hirata, Y.; Urano, Y.; Nagano, T. *J. Am. Chem. Soc.* **2006**, *128* (21), 6938–6946.

(4) Park, Y. I.; Kim, H. M.; Kim, J. H.; Moon, K. C.; Yoo, B.; Lee, K. T.; Lee, N.; Choi, Y.; Park, W.; Ling, D.; Na, K.; Moon, W. K.; Choi, S. H.; Park, H. S.; Yoon, S.-Y.; Suh, Y. D.; Lee, S. H.; Hyeon, T. *Adv. Mater.* **2012**, *24* (42), 5755–5761.

(5) Kanazawa, K.; Nakamura, K.; Kobayashi, N. *Jpn. J. Appl. Phys.* **2013**, *52* (5S1), 05DA14.

(6) Carlos, L. D.; Ferreira, R. A. S.; Bermudez, V. de Z.; Ribeiro, S. J. L. *Adv. Mater.* **2009**, *21* (5), 509–534.

(7) Qiao, Y.; Lin, Y.; Zhang, S.; Huang, J. *Chem. – Eur. J.* **2011**, *17* (18), 5180–5187.

(8) Bünzli, J.-C. G. *Coord. Chem. Rev.* **2015**, *293–294*, 19–47.

(9) Ma, M.-L.; Ji, C.; Zang, S.-Q. *Dalton Trans.* **2013**, *42* (29), 10579–10586.

(10) Meruga, J. M.; Cross, W. M.; May, P. S.; Luu, Q.; Crawford, G. A.; Kellar, J. J. *Nanotechnology* **2012**, *23* (39), 395201.

(11) Gupta, B. K.; Haranath, D.; Saini, S.; Singh, V. N.; Shanker, V. *Nanotechnology* **2010**, *21* (5), 055607.

(12) Sessler, J. L.; Dow, W. C.; O'Connor, D.; Harriman, A.; Hemmi, G.; Mody, T. D.; Miller, R. A.; Qing, F.; Springs, S.; Woodburn, K.; Young, S. W. *J. Alloys Compd.* **1997**, *249* (1–2), 146–152.

(13) Wang, M.; Chen, Z.; Zheng, W.; Zhu, H.; Lu, S.; Ma, E.; Tu, D.; Zhou, S.; Huang, M.; Chen, X. *Nanoscale* **2014**, *6* (14), 8274–8282.

(14) Rogin, P.; Hulliger, J. *J. Cryst. Growth* **1997**, *172* (1–2), 200–208.

(15) Hasegawa, Y.; Kawai, H.; Nakamura, K.; Yasuda, N.; Wada, Y.; Yanagida, S. *J. Alloys Compd.* **2006**, *408–412*, 669–674.

(16) Weissman, S. I. *J. Chem. Phys.* **1942**, *10* (4), 214–217.

(17) Wilkerson, J. M. Luminescent lanthanide-containing materials: from small molecules to conducting metallopolymers, The University of Texas at Austin: Austin, TX, 2012.

(18) Jameson, D. L.; Goldsby, K. A. *J. Org. Chem.* **1990**, *55* (17), 4992–4994.

(19) Halcrow, M. A. *New J. Chem.* **2014**, *38* (5), 1868–1882.

(20) Zoppellaro, G.; Baumgarten, M. *Eur. J. Org. Chem.* **2005**, *2005* (14), 2888–2892.

(21) Basak, S.; Mohiddon, M. A.; Baumgarten, M.; Müllen, K.; Chandrasekar, R. *Sci. Rep.* **2015**, *5*, 8406.

(22) Basak, S.; Hui, P.; Boodida, S.; Chandrasekar, R. *J. Org. Chem.* **2012**, *77* (7), 3620–3626.

(23) Narayana, Y. S. L. V.; Baumgarten, M.; Müllen, K.; Chandrasekar, R. *Macromolecules* **2015**, *48* (14), 4801–4812.

(24) Narayana, Y. S. L. V.; Venkatakrishnarao, D.; Biswas, A.; Mohiddon, M. A.; Viswanathan, N.; Chandrasekar, R. *ACS Appl. Mater. Interfaces* **2016**, *8* (1), 952–958.

(25) Narayana, Y. S. L. V.; Basak, S.; Baumgarten, M.; Müllen, K.; Chandrasekar, R. *Adv. Funct. Mater.* **2013**, *23* (47), 5875–5880.

(26) Basak, S.; Narayana, Y. S. L. V.; Baumgarten, M.; Müllen, K.; Chandrasekar, R. *Macromolecules* **2013**, *46* (2), 362–369.

(27) Stanley, J. M.; Zhu, X.; Yang, X.; Holliday, B. J. *Inorg. Chem.* **2010**, *49* (5), 2035–2037.

(28) Chen, X.-Y.; Yang, X.; Holliday, B. J. *J. Am. Chem. Soc.* **2008**, *130* (5), 1546–1547.

(29) Zhu, X. J.; Holliday, B. J. *Macromol. Rapid Commun.* **2010**, *31* (9–10), 904–909.

(30) Milum, K. M.; Kim, Y. N.; Holliday, B. J. *Chem. Mater.* **2010**, *22* (8), 2414–2416.

(31) Friebe, C.; Görls, H.; Jäger, M.; Schubert, U. S. *Eur. J. Inorg. Chem.* **2013**, *2013* (24), 4191–4202.

(32) Caraway, J. D.; Nguyen, M. T.; Mitchell, L. A.; Holliday, B. J. *Macromol. Rapid Commun.* **2015**, *36* (7), 665–670.

(33) Wolf, M. O. *J. Inorg. Organomet. Polym. Mater.* **2006**, *16* (3), 189–199.

(34) Stanley, J. M.; Holliday, B. J. *Coord. Chem. Rev.* **2012**, *256* (15–16), 1520–1530.

(35) Grutzmacher, H.-F. *Eur. Mass Spectrom.* **1998**, *4* (5), 349–357.

(36) Tagle, L. H.; Terraza, C. A.; Ortiz, P.; Rodríguez, M. J.; Tundidor-Camba, A.; Leiva, A.; González-Henríquez, C.; Cabrera, A. L.; Volkmann, U. G.; Ramos-Moore, E. *J. Macromol. Sci. Part A* **2012**, *49* (7), 562–570.

(37) Strohecker, D. J.; Lynch, V. M.; Holliday, B. J.; Jones, R. A. *Dalton Trans.*

(38) Sato, S.; Wada, M. *Bull. Chem. Soc. Jpn.* **1970**, *43* (7), 1955–1962.

(39) Latva, M.; Takalo, H.; Mukkala, V.-M.; Matachescu, C.; Rodríguez-Ubis, J. C.; Kankare, J. *J. Lumin.* **1997**, *75* (2), 149–169.

(40) Chen, J. H.; Dai, C.-A.; Chiu, W.-Y. *J. Polym. Sci. Part Polym. Chem.* **2008**, *46* (5), 1662–1673.

(41) Golub, T.; Becker, J. Y. *Org. Biomol. Chem.* **2012**, *10* (19), 3906–3912.

(42) Xu, H.-C.; Campbell, J. M.; Moeller, K. D. *J. Org. Chem.* **2014**, *79* (1), 379–391.

(43) Zimmerman, H. E.; McKelvey, R. D. *J. Am. Chem. Soc.* **1971**, *93* (15), 3638–3645.

(44) Vives, G.; Gonzalez, A.; Jaud, J.; Launay, J.-P.; Rapenne, G. *Chem. – Eur. J.* **2007**, *13* (19), 5622–5631.

(45) *Rev. Sci. Instrum.* **1996**, *67* (10), 3722–3731.

(46) Pepitone, M. F.; Hardaker, S. S.; Gregory, R. V. *Chem. Mater.* **2003**, *15* (2), 557–563.

(47) De Silva, C. R.; Maeyer, J. R.; Wang, R.; Nichol, G. S.; Zheng, Z. *Inorganica Chim. Acta* **2007**, *360* (11), 3543–3552.

(48) Horrocks, W. D.; Albin, M. In *Progress in Inorganic Chemistry*; Lippard, S. J., Ed.; John Wiley & Sons, Inc.: Hoboken, NJ, USA, 1984; Vol. 31, pp 1–104.

(49) *CrystalClear*; Rigaku Americas Corporation: The Woodlands, Texas, USA, 2008.

(50) *CrysAlisPro*; Agilent Technologies UK Ltd.: Oxford, UK, 2013.

(51) Altomare, A.; Burla, M. C.; Camalli, M.; Cascarano, G. L.; Giacovazzo, C.; Guagliardi, A.; Moliterni, A. G. G.; Polidori, G.; Spagna, R. *J. Appl. Crystallogr.* **1999**, *32* (1), 115–119.

(52) Sheldrick, G. M. *Acta Crystallogr. Sect. A* **2008**, *64* (1), 112–122.

(53) Spek, A. L. *J. Appl. Crystallogr.* **2003**, *36* (1), 7–13.

(54) Farrugia, L. J. *J. Appl. Crystallogr.* **1999**, *32* (4), 837–838.

CHAPTER 4

(1) Jameson, D. L.; Blaho, J. K.; Kruger, K. T.; Goldsby, K. A. *Inorg. Chem.* **1989**, *28* (24), 4312–4314.

(2) Halcrow, M. A. *New J. Chem.* **2014**, *38* (5), 1868–1882.

(3) Zoppellaro, G.; Baumgarten, M. *Eur. J. Org. Chem.* **2005**, *2005* (14), 2888–2892.

(4) Zhu, X. J.; Holliday, B. J. *Macromol. Rapid Commun.* **2010**, *31* (9–10), 904–909.

(5) Basak, S.; Hui, P.; Chandrasekar, R. *Synthesis* **2009**, *2009* (23), 4042–4048.

(6) Basak, S.; Narayana, Y. S. L. V.; Baumgarten, M.; Müllen, K.; Chandrasekar, R. *Macromolecules* **2013**, *46* (2), 362–369.

(7) Narayana, Y. S. L. V.; Venkatakrishnarao, D.; Biswas, A.; Mohiddon, M. A.; Viswanathan, N.; Chandrasekar, R. *ACS Appl. Mater. Interfaces* **2016**, *8* (1), 952–958.

(8) Narayana, Y. S. L. V.; Basak, S.; Baumgarten, M.; Müllen, K.; Chandrasekar, R. *Adv. Funct. Mater.* **2013**, *23* (47), 5875–5880.

(9) Narayana, Y. S. L. V.; Baumgarten, M.; Müllen, K.; Chandrasekar, R. *Macromolecules* **2015**, *48* (14), 4801–4812.

(10) Basak, S.; Hui, P.; Boodida, S.; Chandrasekar, R. *J. Org. Chem.* **2012**, *77* (7), 3620–3626.

(11) Pritchard, R.; Kilner, C. A.; Barrett, S. A.; Halcrow, M. A. *Inorganica Chim. Acta* **2009**, *362* (12), 4365–4371.

(12) Tallec, A.; Hazard, R.; SuwiNski, J.; Wagner, P. *Pol. J. Chem.* **2000**, *47* (8), 1177–1183.

(13) Cuadrado, P.; González-Nogal, A. M.; Martínez, S. *Tetrahedron* **1997**, *53* (25), 8585–8598.

(14) Suwiński, J.; Wagner, P. *Pol. J. Chem.* **2000**, *74* (11), 1575–1580.

(15) Yin, P.; Zhang, J.; Parrish, D. A.; Shreeve, J. M. *Chem. - Eur. J.* **2014**, *20* (50), 16529–16536.

(16) Fevig, J. M.; Cacciola, J.; Buriak Jr., J.; Rossi, K. A.; Knabb, R. M.; Luettgen, J. M.; Wong, P. C.; Bai, S. A.; Wexler, R. R.; Lam, P. Y. S. *Bioorg. Med. Chem. Lett.* **2006**, *16* (14), 3755–3760.

(17) Kumar, R.; Joshi, Y. C.; Joshi, P. *Heterocycl. Commun.* **2005**, *11* (3–4), 361–364.

(18) De Sio, F. *Heterocycles* **1984**, *22* (10), 2309–2311.

(19) Strohecker, D. J.; Lynch, V. M.; Holliday, B. J.; Jones, R. A. *Dalton Trans.*, submitted.

(20) Wolf, M. O. *Adv. Mater.* **2001**, *13* (8), 545–553.

(21) Frischmann, P. D.; MacLachlan, M. J. *Chem. Commun.* **2007**, No. 43, 4480–4482.

(22) Nagymihály, Z.; Kollár, L. *Tetrahedron* **2015**, *71* (17), 2555–2560.

(23) Tennyson, A. G.; Norris, B.; Bielawski, C. W. *Macromolecules* **2010**, *43* (17), 6923–6935.

(24) Chen, L.; Chen, Z.; Li, X.; Huang, W.; Li, X.; Liu, X. *Polymer* **2013**, *54* (7), 1739–1745.

(25) Huang, W.; Jiang, Y.; Li, X.; Li, X.; Wang, J.; Wu, Q.; Liu, X. *ACS Appl. Mater. Interfaces* **2013**, *5* (18), 8845–8849.

(26) Davis, T. unpublished work.

(27) Deadman, B. J.; Collins, S. G.; Maguire, A. R. *Chem. – Eur. J.* **2015**, *21* (6), 2298–2308.

(28) Mahouche-Chergui, S.; Gam-Derouich, S.; Mangeney, C.; Chehimi, M. M. *Chem. Soc. Rev.* **2011**, *40* (7), 4143–4166.

(29) Miras; C, M.; Acevedo, D. F.; Monge, N.; Frontera, E.; Rivarola, C. R.; Barbero, C. A. *Open Macromol. J.* **2008**, *2* (1).

(30) Yildiz, E.; Boztepe, H. *Turk. J. Chem.* **2002**, *26* (6), 897.

(31) Huisgen, R. *Angew. Chem. Int. Ed. Engl.* **1963**, *2* (10), 565–598.

(32) Zheng, Z.-J.; Wang, D.; Xu, Z.; Xu, L.-W. *Beilstein J. Org. Chem.* **2015**, *11* (1), 2557–2576.

(33) Rostovtsev, V. V.; Green, L. G.; Fokin, V. V.; Sharpless, K. B. *Angew. Chem. Int. Ed.* **2002**, *41* (14), 2596–2599.

(34) Zhang, L.; Chen, X.; Xue, P.; Sun, H. H. Y.; Williams, I. D.; Sharpless, K. B.; Fokin, V. V.; Jia, G. *J. Am. Chem. Soc.* **2005**, *127* (46), 15998–15999.

(35) Kumar, K.; Konar, D.; Goyal, S.; Gangar, M.; Chouhan, M.; Rawal, R. K.; Nair, V. A. *J. Org. Chem.* **2016**, *81* (20), 9757–9764.

(36) Zikode, M.; Ojwach, S. O.; Akerman, M. P. *Appl. Organomet. Chem.* **2017**, *31* (2), n/a-n/a.

(37) Christenson, D. L.; Tokar, C. J.; Tolman, W. B. *Organometallics* **1995**, *14* (5), 2148–2150.

(38) Hussain, G.; Ather, M.; Khan, M. U. A.; Saeed, A.; Saleem, R.; Shabir, G.; Channar, P. A. *Dyes Pigments* **2016**, *130*, 90–98.

(39) Watson, A. A.; House, D. A.; Steel, P. J. *J. Org. Chem.* **1991**, *56* (12), 4072–4074.

(40) LeCloux, D. D.; Tolman, W. B. *J. Am. Chem. Soc.* **1993**, *115* (3), 1153–1154.

(41) Kowalczyk, R.; Skarżewski, J. *Tetrahedron* **2005**, *61* (3), 623–628.

(42) Kashima, C.; Shibata, S.; Yokoyama, H.; Nishio, T. *J. Heterocycl. Chem.* **2003**, *40* (5), 773–782.

(43) Zhang, L.; Chen, X.; Xue, P.; Sun, H. H. Y.; Williams, I. D.; Sharpless, K. B.; Fokin, V. V.; Jia, G. *J. Am. Chem. Soc.* **2005**, *127* (46), 15998–15999.

(44) Orlandi, M.; Tosi, F.; Bonsignore, M.; Benaglia, M. *Org. Lett.* **2015**, *17* (16), 3941–3943.

(45) Cabral, B. J. C. *Chem. Phys. Lett.* **2017**, *667*, 332–336.

(45) Zhou, Y.; Liu, B.; Wang, X. *Polymer* **2017**, *111*, 229–238.

(47) Delaire, J. A.; Nakatani, K. *Chem. Rev.* **2000**, *100* (5), 1817–1846.

(48) Liu, Y.; Kim, J.; Seo, H.; Park, S.; Chae, J. *Adv. Synth. Catal.* **2015**, *357* (10), 2205–2212.

(49) Wolf, M. O. *J. Inorg. Organomet. Polym. Mater.* **2006**, *16* (3), 189–199.

(50) de Hatten, X.; Asil, D.; Friend, R. H.; Nitschke, J. R. *J. Am. Chem. Soc.* **2012**, *134* (46), 19170–19178.

(51) Chow, C.-F. *J. Fluoresc.* **2012**, *22* (6), 1539–1546.

(52) Wang, M.; Funabiki, K.; Matsui, M. *Dyes Pigments* **2003**, *57* (1), 77–86.

(53) Travieso-Puente, R.; Budzak, S.; Chen, J.; Stacko, P.; Jastrzebski, J. T. B. H.; Jacquemin, D.; Otten, E. *J. Am. Chem. Soc.* **2017**, *139* (9), 3328–3331.

(54) Weston, C. E.; Richardson, R. D.; Fuchter, M. J. *Chem. Commun.* **2016**, *52* (24), 4521–4524.

(55) Morgan, G. T.; Ackerman, I. *J. Chem. Soc., Trans.* **1923**, *123* (0), 1308–1318.

CHAPTER 5

(1) Cotton, S. A.; Raithby, P. R. *Coord. Chem. Rev.* **2017**, *340*, 220–231.

(2) Bünzli, J.-C. G. *J. Coord. Chem.* **2014**, *67* (23/24), 3706–3733.

(3) Yang; Jones, R. A. *J. Am. Chem. Soc.* **2005**, *127* (21), 7686–7687.

(4) Yang, X.-P.; Jones, R. A.; Wong, W.-K.; Lynch, V.; Oye, M. M.; Holmes, A. L. *Chem. Commun.* **2006**, No. 17, 1836–1838.

(5) Yang, X.; Rivers, J. H.; McCarty, W. J.; Wiester, M.; Jones, R. A. *New J. Chem.* **2008**, *32* (5), 790–793.

(6) Yang, X.; Schipper, D.; Jones, R. A.; Lytwak, L. A.; Holliday, B. J.; Huang, S. *J. Am. Chem. Soc.* **2013**, *135* (23), 8468–8471.

(7) Halcrow, M. A. *New J. Chem.* **2014**, *38* (5), 1868–1882.

(8) Wang, X.; Chang, H.; Xie, J.; Zhao, B.; Liu, B.; Xu, S.; Pei, W.; Ren, N.; Huang, L.; Huang, W. *Coord. Chem. Rev.* **2014**, *273–274*, 201–212.

(9) Gupta, B. K.; Haranath, D.; Saini, S.; Singh, V. N.; Shanker, V. *Nanotechnology* **2010**, *21* (5), 055607.

(10) Basak, S.; Mohiddon, M. A.; Baumgarten, M.; Müllen, K.; Chandrasekar, R. *Sci. Rep.* **2015**, *5*, 8406.

(11) Chow, C.-F. *J. Fluoresc.* **2012**, *22* (6), 1539–1546.

(12) Meruga, J. M.; Cross, W. M.; May, P. S.; Luu, Q.; Crawford, G. A.; Kellar, J. J. *Nanotechnology* **2012**, *23* (39), 395201.

(13) Binnemans, K. *Chem. Rev.* **2009**, *109* (9), 4283–4374.

(14) Wang, M.; Chen, Z.; Zheng, W.; Zhu, H.; Lu, S.; Ma, E.; Tu, D.; Zhou, S.; Huang, M.; Chen, X. *Nanoscale* **2014**, *6* (14), 8274–8282.

(15) Sessler, J. L.; Dow, W. C.; O'Connor, D.; Harriman, A.; Hemmi, G.; Mody, T. D.; Miller, R. A.; Qing, F.; Springs, S.; Woodburn, K.; Young, S. W. *J. Alloys Compd.* **1997**, *249* (1–2), 146–152.

(16) Jones, R. A.; Gnanam, A. J.; Arambula, J. F.; Jones, J. N.; Swaminathan, J.; Yang, X.; Schipper, D.; Hall, J. W.; DePue, L. J.; Dieye, Y.; Vadivelu, J.; Chandler, D. J.; Marcotte, E. M.; Sessler, J. L.; Ehrlich, L. I. R.; Brown, K. A. *Faraday Discuss.* **2015**, *175* (0), 241–255.

(17) Binnemans, K. *Coord. Chem. Rev.* **2015**, *295*, 1–45.

(18) Horrocks, W. D.; Albin, M. In *Progress in Inorganic Chemistry*; Lippard, S. J., Ed.; John Wiley & Sons, Inc.: Hoboken, NJ, USA, 1984; Vol. 31, pp 1–104.

(19) Weissman, S. I. *J. Chem. Phys.* **1942**, *10* (4), 214–217.

(20) Bünzli, J.-C. G. *Coord. Chem. Rev.* **2015**, *293–294*, 19–47.

(21) Bohnsack, A. M. Novel Multifunctional Porous Coordination Polymers from Pre-Synthetically Modified Organophosphorous Ligands. PhD Dissertation, The University of Texas at Austin: Austin, TX, 2015.

(22) Meshkova, S. B.; Topilova, Z. M.; Bolshoy, D. V.; Beltyukova, S. V.; Tsvirko, M. P.; Venchikov, V. Y. *Acta Phys. Pol. A* **1999**, *95* (6), 983–990.

(23) Ahn, H. S.; Davenport, T. C.; Tilley, T. D. *Chem. Commun.* **2014**, *50* (29), 3834–3837.

(24) Suzuki, H.; Moro-Oka, Y.; Ikawa, T.; Miyajima, T.; Tanaka, I.; Ashida, T. *Chem. Lett.* **1982**, *11* (9), 1369–1370.

(25) Wilkerson, J. M. Luminescent lanthanide-containing materials: from small molecules to conducting metallopolymers, The University of Texas at Austin: Austin, TX, 2012.

(26) Stanley, J. M.; Zhu, X.; Yang, X.; Holliday, B. J. *Inorg. Chem.* **2010**, *49* (5), 2035–2037.

(27) Jameson, D. L.; Goldsby, K. A. *J. Org. Chem.* **1990**, *55* (17), 4992–4994.

(28) Zoppellaro, G.; Baumgarten, M. *Eur. J. Org. Chem.* **2005**, *2005* (14), 2888–2892.

(29) Sager, W. F.; Filipescu, N.; Serafin, F. A. *J. Phys. Chem.* **1965**, *69* (4), 1092–1100.

(30) *FeliX32 Analysis*; Photon Technology International, 2001.

(31) *SAINT V8.27B*; Bruker AXS Inc.: Madison, WI, USA, 2012.

(32) Sheldrick, G. M. *Acta Crystallogr. Sect. A* **2015**, *71* (1), 3–8.

(33) Sheldrick, G. M. *Acta Crystallogr. Sect. C Struct. Chem.* **2015**, *71* (1), 3–8.

(34) Spek, A. L. *PLATON98*; Utrecht University: Padualaan 8, 3584 CH Utrecht, The Netherlands, 1998.

(35) Farrugia, L. J. *J. Appl. Crystallogr.* **1999**, *32* (4), 837–838.

(36) $R_w(F^2) = \{S_w(|F_o|^2 - |F_c|^2)^2/S_w(|F_o|)^4\}^{1/2}$ where w is the weight given each reflection. $R(F) = S(|F_o| - |F_c|)/S|F_o|\}$ for reflections with $F_o > 4(s(F_o))$. $S = [S_w(|F_o|^2 - |F_c|^2)^2/(n - p)]^{1/2}$, where n is the number of reflections and p is the number of refined parameters.

(37) *International Tables for X-ray Crystallography*; Kluwer Academic Press: Boston, MA, USA, 1992; Vol. C.

(38) Sheldrick, G. M. *SHELXLT/PC*; Siemens Analytical X-ray Instruments, Inc.: Madison, WI, USA, 1994.

(39) *CrystalClear*; Rigaku Americas Corporation: The Woodlands, Texas, USA, 2008.

(40) Burla, M. C.; Caliandro, R.; Camalli, M.; Carrozzini, B.; Cascarano, G. L.; De Caro, L.; Giacovazzo, C.; Polidori, G.; Spagna, R. *J. Appl. Crystallogr.* **2005**, *38* (2), 381–388.

APPENDIX A

(1) Higashi, K.; Ueda, K.; Moribe, K. *Adv. Drug Deliv. Rev.*

(2) Rodrigues, M. A.; Tiago, J. M.; Duarte, A.; Geraldes, V.; Matos, H. A.; Gomes Azevedo, E. *Cryst. Growth Des.* **2016**, *16* (11), 6222–6229.

(3) Morissette, S. L.; Almarsson, Ö.; Peterson, M. L.; Remenar, J. F.; Read, M. J.; Lemmo, A. V.; Ellis, S.; Cima, M. J.; Gardner, C. R. *Adv. Drug Deliv. Rev.* **2004**, *56* (3), 275–300.

(4) Schultheiss, N.; Newman, A. *Cryst. Growth Des.* **2009**, *9* (6), 2950.

(5) Kuhnert-Brandstätter, M. *Pharm. Unserer Zeit* **1975**, *4* (5), 131–137.

(6) Fox, D.; Labes, M. M.; Weissberger, A. *Physics and Chemistry of the Organic Solid State*; Wiley Interscience: New York, 1965; Vol. 2.

(7) Bernstein, J. *Cryst. Growth Des.* **2011**, *11* (3), 632–650.

(8) Strohecker, D. J.; Lynch, V. M.; Holliday, B. J.; Jones, R. A. *Dalton Trans.*

(9) *CrysAlisPro*; Agilent Technologies UK Ltd.: Oxford, UK, 2013.

(10) Sheldrick, G. M. *Acta Crystallogr. Sect. A* **2015**, *71* (1), 3–8.

(11) Sheldrick, G. M. *Acta Crystallogr. Sect. C Struct. Chem.* **2015**, *71* (1), 3–8.

(12) Spek, A. L. *PLATON98*; Utrecht University: Padualaan 8, 3584 CH Utrecht, The Netherlands, 1998.

(13) Farrugia, L. J. *J. Appl. Crystallogr.* **1999**, *32* (4), 837–838.

(14) $R_w(F^2) = \{S_w(|F_o|^2 - |F_c|^2)^2/S_w(|F_o|)^4\}^{1/2}$ where w is the weight given each reflection. $R(F) = S(|F_o| - |F_c|)/S|F_o|\}$ for reflections with $F_o > 4(s(F_o))$. $S = [S_w(|F_o|^2 - |F_c|^2)^2/(n - p)]^{1/2}$, where n is the number of reflections and p is the number of refined parameters.

(15) *International Tables for X-ray Crystallography*; Kluwer Academic Press: Boston, MA, USA, 1992; Vol. C.

(16) Sheldrick, G. M. *SHELXLT/PC*; Siemens Analytical X-ray Instruments, Inc.: Madison, WI, USA, 1994.